

**For Reference**

---

**NOT TO BE TAKEN FROM THIS ROOM**



# For Reference

NOT TO BE TAKEN FROM THIS ROOM

Ex LIBRIS  
UNIVERSITATIS  
ALBERTAENSIS









THE UNIVERSITY OF ALBERTA

PRECAMBRIAN GEOLOGY AND GEOCHRONOLOGY OF THE  
YELLOWKNIFE AREA, N.W.T.

by

DAVID CHRISTOPHER GREEN B.Sc., (Hons.) M.Sc.



A THESIS

SUBMITTED TO THE FACULTY OF GRADUATE STUDIES  
IN PARTIAL FULFILMENT OF THE REQUIREMENTS FOR THE DEGREE  
OF DOCTOR OF PHILOSOPHY

DEPARTMENT OF GEOLOGY

EDMONTON, ALBERTA

April, 1968







UNIVERSITY OF ALBERTA

FACULTY OF GRADUATE STUDIES

The undersigned certify that they have read, and recommend to the Faculty of Graduate Studies for acceptance, a thesis entitled "Precambrian Geology and Geochronology of the Yellowknife Area, N.W.T." submitted by David Christopher Green, B.Sc., (Hons.) M.Sc., in partial fulfilment of the requirements for the degree of Doctor of Philosophy.







## ABSTRACT

U-Pb, Rb-Sr and K-Ar geochronology of several Archaean rock units in the Slave Province establishes a sequence of events which may be treated as a single tectonic cycle. The oldest rocks ( $\approx 2650$  m.y.) are calc-alkaline to tholeiitic basic pillow lavas, which pass upwards into intermediate lavas and pyroclastics in two cycles to give a total thickness of 7000 to 40,000 feet. They were probably extruded on oceanic-type crust as there is no isotopic evidence for pre-existing sialic segments. Unconformably overlying the volcanics are polymictic conglomerates and quartz greywackes with turbidite characteristics.

Since the  $^{87}\text{Sr}/^{86}\text{Sr}$  initial ratios of the volcanics and syn-kinematic Kenoran intrusives are similar, the basalt-dacite association is probably the early extrusive expression of the subcrustal processes which led to the intrusion of calc-alkaline batholiths into the deforming volcanic-sedimentary pile.

Concordant ages of 2620-2640 m.y. are recorded for the syn-kinematic quartz diorite batholiths and 2590-2610 m.y. for the major late kinematic bodies. Pegmatitic adamellites ( $\approx 2575$  m.y.) are the youngest plutonic units and may be the product of partial anatexis of the Yellowknife Group metasediments. Regional metamorphism of the andalusite-sillimanite facies reflects the relative unimportance of load pressure in the thin-crustal Kenoran deformation.

Comparison of the results obtained by the three radiometric methods indicates that an interval of over 100 m.y. may elapse between the time of emplacement of a given rock unit and the subsequent closure of the K-Ar system. The sequence of apparent K-Ar mineral dates is in accord with the relative argon retentivities of the various minerals.





## ACKNOWLEDGMENTS

The writer is indebted especially to Dr. H. Baadsgaard who introduced him to the research techniques which made this thesis possible. His enthusiastic supervision and assistance is much appreciated. Dr. R. E. Folinsbee visited the writer in the field and gave freely of his considerable knowledge of the area. Dr. Baadsgaard and Mr. J. Henderson (John Hopkins University) also assisted in the somewhat arduous task of collecting suitable samples. Capable field assistance was given by Mr. T. Folinsbee (1966) and Mr. R. Mann (1967).

Mass spectrometer facilities were made available by the Department of Physics through the courtesy of Drs. G. L. Cumming and H. R. Krouse and were maintained by Mr. H. Langer of the Department of Physics.

Other material assistance was rendered by Messrs. R. Thorpe (Geological Survey of Canada), K. Polk and J. Kelly (Giant Yellowknife Mines) and D. Comba (Echo Bay Mines). Messrs. A. Stelmach and G. Bonnet assisted in the chemical laboratory. Thin sections were prepared by Mrs. E. Vincze. Mr. R. K. O'Nions read the first draft of the manuscript.

Fruitful discussions with faculty members (particularly Dr. R. A. Burwash), graduate students and distinguished visitors to the Department of Geology are also gratefully acknowledged.

Field expenses were met by a generous grant from the Boreal Institute, University of Alberta. Maintenance during the project was provided by the award of Graduate Teaching Assistantships and a National Research Council Studentship for 1966 to 1968. This work was carried out at the University of Alberta within the isotope geology program which is supported by a National Research Council grant.

The thesis was typed by Mrs. M. Wylie.





## TABLE OF CONTENTS

|   | Page |
|---|------|
| ABSTRACT .. .. .  | i    |
| ACKNOWLEDGMENTS .. .. .   | ii   |
| <u>CHAPTER I</u> - INTRODUCTION .. .. .                             | 1    |
| Location, Geography and Access .. .. .                              | 1    |
| Methods .. .. .   | 3    |
| Previous Geochronology .. .. .                                      | 5    |
| <u>CHAPTER II</u> - REGIONAL GEOLOGY .. .. .                        | 8    |
| Geologic Provinces of the Canadian Shield .. .. .                   | 9    |
| Slave Province .. .. .  | 12   |
| Geology of the Yellowknife and Ross - Redout Lake Districts .. .. . | 12   |
| Yellowknife District .. .. .  | 15   |
| Ross Lake-Redout Lake District .. .. .                              | 16   |
| Yellowknife Group .. .. .   | 17   |
| Division A .. .. .  | 17   |
| Division B .. .. .  | 21   |
| Unclassified Conglomerates .. .. .                                  | 23   |
| Early Mafic Intrusives .. .. .                                      | 27   |
| Yellowknife Bay area .. .. .  | 27   |
| Cameron River area .. .. .  | 31   |
| Plutonic Intrusives .. .. .   | 32   |
| Western granodiorite .. .. .  | 32   |
| Contaminated (hybrid) rocks .. .. .                                 | 36   |
| Stock Lake stock .. .. .  | 38   |
| South-east granodiorite .. .. .                                     | 39   |
| Ross Lake granodiorite .. .. .                                      | 42   |





|  |    |    |     |
|--|----|----|-----|
| Redout Lake granite and associated pegmatites  | .. | .. | 45  |
| Prosperous Lake granite and associated pegmatites                                    | .. | .. | 46  |
| Quartz Feldspar Porphyries   | .. | .. | 49  |
| Proterozoic Diabase Dykes  | .. | .. | 50  |
| Structure  | .. | .. | 51  |
| Metamorphism   | .. | .. | 55  |
| Economic Geology   | .. | .. | 61  |
| <u>CHAPTER III - GEOCHRONOLOGY OF THE YELLOWKNIFE AREA</u>                           | .. | .. | 64  |
| Sample Preparation   | .. | .. | 64  |
| Radiometric Methods  | .. | .. | 65  |
| Potassium-argon method   | .. | .. | 67  |
| Rubidium-strontium whole rock method   | .. | .. | 73  |
| Uranium-lead method  | .. | .. | 78  |
| Results  | .. | .. | 85  |
| <u>CHAPTER IV - INTERPRETATION OF RADIOMETRIC DATA</u>                               | .. | .. | 102 |
| <u>CHAPTER V - CORRELATION WITH OTHER AREAS</u>                                      | .. | .. | 127 |
| <u>CHAPTER VI - TECTONIC HISTORY OF THE YELLOWKNIFE DISTRICT</u>                     | .. | .. | 132 |
| Outline  | .. | .. | 132 |
| Nature of the volcanic sequence  | .. | .. | 135 |
| Character of the "unclassified conglomerate" and Division B sediments                | .. | .. | 136 |
| Island arc formation and determination of the age of the Yellowknife Group volcanics | .. | .. | 138 |
| A possible model for derivation of the calc-alkaline suite                           | .. | .. | 139 |
| Onset of plutonism within the Kenoran orogeny  | .. | .. | 142 |
| Strontium isotope initial ratios   | .. | .. | 143 |
| Late kinematic granites and pegmatites   | .. | .. | 144 |
| Final stages of the tectonic cycle   | .. | .. | 146 |
| General comments on the tectonic cycle   | .. | .. | 147 |





|                         |    |    |    |    |    |    |     |
|-------------------------|----|----|----|----|----|----|-----|
| SUMMARY AND CONCLUSIONS | .. | .. | .. | .. | .. | .. | 148 |
| REFERENCES CITED        | .. | .. | .. | .. | .. | .. | 152 |

## APPENDICES

|                                      |    |    |    |    |    |        |
|--------------------------------------|----|----|----|----|----|--------|
| 1. Petrography of dated samples      | .. | .. | .. | .. | .. | A1-14  |
| 2. Sample locality index             | .. | .. | .. | .. | .. | A15-23 |
| 3. Chemical procedures               | .. | .. | .. | .. | .. | A24-28 |
| 4. K-Ar, Rb-Sr and U-Pb calculations | .. | .. | .. | .. | .. | A29-39 |
| 5. Computer programmes               | .. | .. | .. | .. | .. | A40-45 |
| 6. Error analysis                    | .. | .. | .. | .. | .. | A46-50 |





## LIST OF FIGURES

|            |   |    |    |    |    | Page |
|------------|---|----|----|----|----|------|
| Figure 1.  | Location map of thesis area   | .. | .. | .. |    | 2    |
| Figure 2.  | Structural Provinces of the Canadian Shield   |    |    | .. |    | 10   |
| Figure 3.  | Regional geology, Yellowknife area, Northwest Territories (after Boyle, 1961)                 | .. | .. | .. |    | 14   |
| Figure 4.  | Regional geology, Cameron River - Redout Lake area (after Henderson, 1941, and Fortier, 1947) |    |    | .. |    | 20   |
| Figure 5.  | Metamorphic "isograds" in the Cameron River volcanic belt (after Edie, 1949)                  | .. | .. | .. |    | 58   |
| Figure 6.  | Radioactive decay scheme, $^{40}\text{K}$   | .. | .. | .. |    | 68   |
| Figure 7.  | Zircon concordia and continuous Pb diffusion plots  | .. | .. | .. | .. | 80   |
| Figure 8.  | Rb-Sr whole rock isochron plot, Yellowknife (meta-) volcanics                                 | .. | .. | .. | .. | 102  |
| Figure 9.  | Rb-Sr whole rock isochron plot, Cameron River (meta-) volcanics                               | .. | .. | .. | .. | 103  |
| Figure 10. | Rb-Sr whole rock isochron plot, Yellowknife Group (meta-) sediments                           | .. | .. | .. | .. | 104  |
| Figure 11. | Rb-Sr whole rock isochron plot, South-east granodiorite                                       | .. | .. | .. | .. | 105  |
| Figure 12. | Rb-Sr whole rock isochron plot, Western granodiorite  | .. | .. | .. | .. | 106  |
| Figure 13. | Rb-Sr whole rock isochron plot, Ross Lake granodiorite  | .. | .. | .. | .. | 107  |
| Figure 14. | Rb-Sr mineral isochron plot, Prosperous Lake granite  | .. | .. | .. | .. | 108  |
| Figure 15. | K-Ar dates, Yellowknife subprovince   |    |    | .. | .. | 109  |
| Figure 16. | K-Ar dates, Yellowknife subprovince, in terms of rock units                                   | .. | .. | .. | .. | 110  |
| Figure 17. | Concordia plot of zircons from six rock units, Yellowknife area                               | .. | .. | .. | .. | 121  |





# LIST OF TABLES

|           |  |    |    |    |    | Page   |
|-----------|--|----|----|----|----|--------|
| Table 1.  | Radioactive systems used in this thesis  | .. | .. |    |    | 3      |
| Table 2.  | Time-stratigraphic classification for the Canadian Shield (after Wanless et al., 1967) |    | .. |    |    | 11     |
| Table 3.  | Table of formations (Precambrian), Yellowknife area (after Boyle, 1961)                | .. | .. | .. | .. | 13     |
| Table 4.  | Analyses of early mafic intrusives   | .. | .. |    |    | 29     |
| Table 5.  | Modal analyses of rocks from the Western granodiorite                                  | .. | .. | .. | .. | 33     |
| Table 6.  | Analyses, Western granodiorite   | .. | .. | .. |    | 34     |
| Table 7.  | Analyses of hybrid rocks and an associated quartz diorite                              | .. | .. | .. | .. | 37     |
| Table 8.  | Modal analyses, Stock Lake stock   | .. | .. | .. |    | 39     |
| Table 9.  | Analyses, South-east granodiorite  | .. | .. | .. |    | 41     |
| Table 10. | Analyses, Ross Lake granodiorite   | .. | .. | .. |    | 43     |
| Table 11. | Analyses, Prosperous Lake granite  | .. | .. | .. |    | 47     |
| Table 12. | Modal analyses, Prosperous Lake granite and a nearby stock                             | .. | .. | .. | .. | 48     |
| Table 13. | Isotopic abundances of K and Ar nuclides   | .. | .. |    |    | 68     |
| Table 14. | Isotopic abundances of common strontium and rubidium                                   | .. | .. | .. | .. | 74     |
| Table 15. | Calibration of 12 inch mass spectrometer with N.B.S. and Broken Hill leads             | .. | .. | .. |    | 85     |
| Table 16. | Summary of K-Ar data   | .. | .. | .. | .. | 87, 88 |
| Table 17. | K-Ar dates grouped in terms of rock units  | .. | .. |    |    | 89     |
| Table 18. | Rb-Sr analytical data, Yellowknife (meta-) volcanics                                   | .. | .. | .. | .. | 91     |
| Table 19. | Rb-Sr analytical data, Cameron River (meta-) volcanics                                 | .. | .. | .. | .. | 92     |
| Table 20. | Rb-Sr analytical data, Yellowknife Group (meta-) sediments                             | .. | .. | .. | .. | 93     |





|           |   |          |
|-----------|---|----------|
| Table 21. | Rb-Sr analytical data, South-east grano-<br>diorite .. .. . | 94       |
| Table 22. | Rb-Sr analytical data, Western granodiorite ..              | 95       |
| Table 23. | Rb-Sr analytical data, Ross Lake grano-<br>diorite .. .. .  | 96       |
| Table 24. | Rb-Sr analytical data, Prosperous Lake granite ..           | 97       |
| Table 25. | Lead isotope analytical data, zircons .. ..                 | 98, 99   |
| Table 26. | Uranium-lead data and radiometric dates .. ..               | 100      |
| Table 27. | K-Ar computation sheet .. .. .                              | A30, A31 |
| Table 28. | Rb-Sr computation sheet .. .. .                             | A32-A34  |
| Table 29. | U-Pb computation sheet .. .. .                              | A35-A38  |

## LIST OF PLATES

|          |             |    |
|----------|-------------|----|
| Plate 1. | opposite p. | 18 |
| Plate 2. | "           | 23 |
| Plate 3. | "           | 32 |
| Plate 4. | "           | 35 |
| Plate 5. | "           | 36 |
| Plate 6. | "           | 38 |
| Plate 7. | "           | 82 |





## CHAPTER I

### INTRODUCTION

Application of the radiometric methods of isotope geology to a relatively well-studied area of the western Canadian Precambrian Shield may be expected to yield a more complete picture of the geological evolution of the area than that obtained by previous field and laboratory studies.

This thesis presents the results, interpretations and conclusions of a geochronometric study of two critical areas within the Archaean Yellowknife subprovince. Selected samples were collected during three months field work in order to obtain radiometric results which may be interpreted within the framework of previous geological work.

The initial problems posed at the outset of the investigation were determination of the age of the Yellowknife Group and of the plutons which intrude it and clarification of the time-stratigraphic position of the "unclassified conglomerate" horizon. Results from the investigation bear on the larger problems of the tectonic evolution of the area and the concept of orogenic cycles.

#### Location, Geography and Access

Yellowknife is situated on the north shore of Great Slave Lake (see Fig. 1) approximately 700 miles north of Edmonton, Alberta. The areas in which field work was carried out are shown in greater detail in Figs. 3 and 4.

The country is almost flat when viewed from the air, but





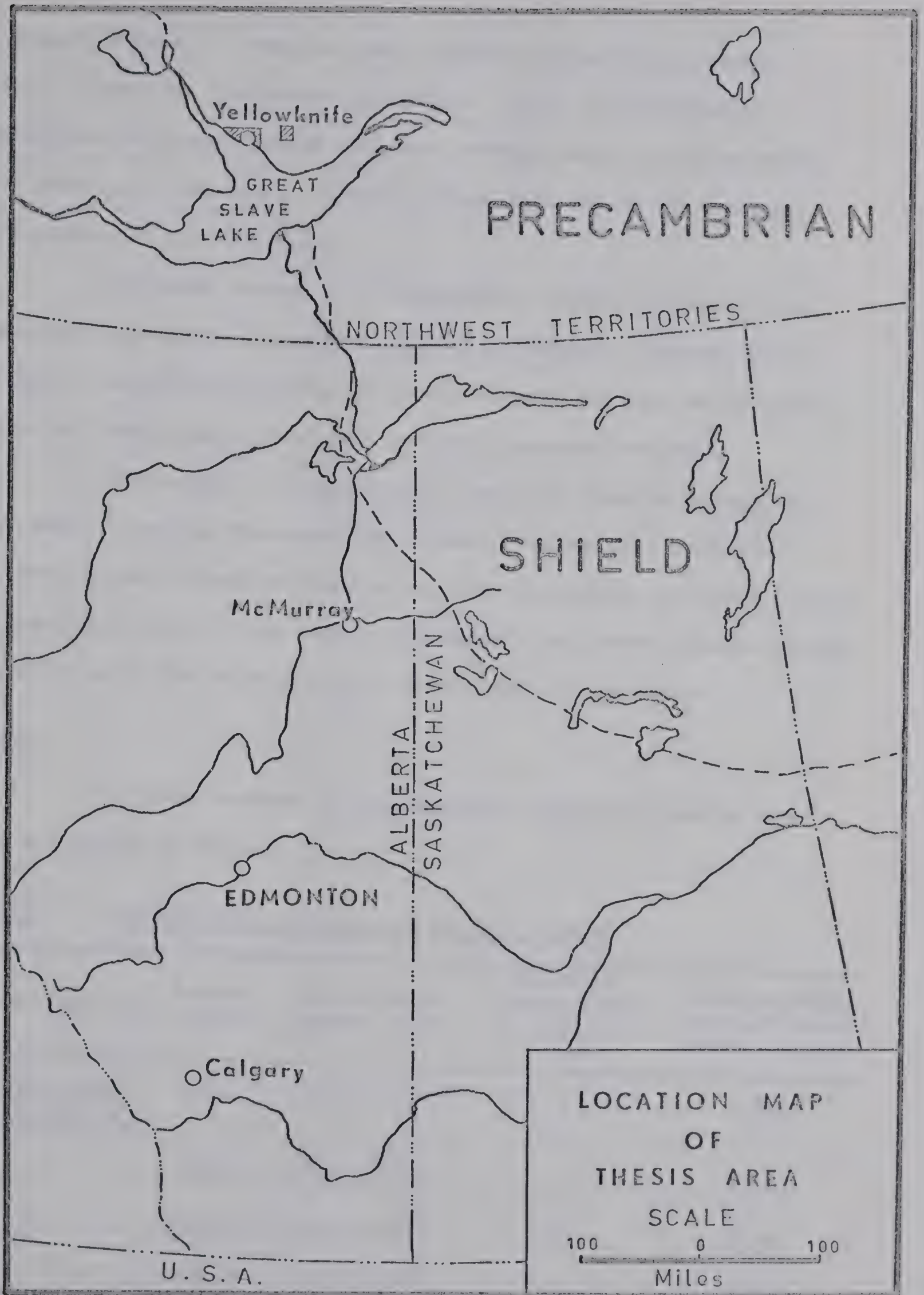


Fig. 1. Location map of thesis area





is rugged in detail. Numerous lakes reflect the youthful drainage pattern imposed by Pleistocene glaciation. Drift is sporadically distributed as ground moraine boulders, perched blocks, modified esker sand plains and lake clays. Glacial striae indicate an ice movement from north-east to south-west.

Although outcrop is of exceptional quality, musket-filled depressions may obscure important structural features. Diabase dykes and faults are often recognised as lineal depressions from aerial photographs and identified on the basis of a few scattered outcrops.

Yellowknife is accessible by road from Edmonton except for a few weeks at spring "break-up" and autumn "freeze-up". Commercial air services have a regular schedule into an all-weather air strip located on a sand plain west of the town of Yellowknife and charter planes operate from Yellowknife Bay using floats in summer and skis in winter.

### Methods

The decay schemes of the radioactive isotopes used in this study are listed in Table 1.

Table 1.      Radioactive systems used in this thesis

| Daughter nuclide  | Parent nuclide   | Half-life of parent, years                           | Probable uncertainty in half-life, percent | Isotope abundance of parent, atomic percent |
|---|------------------|--|--|---|
| $^{40}\text{Ca}$ ( $\beta$ decay)<br>$^{40}\text{Ar}$ ( $K_{e^-}$ -capture) | $^{40}\text{K}$  | $1.306 \times 10^9$                                  | 5  | 0.0119                                      |
| $^{87}\text{Sr}$  | $^{87}\text{Rb}$ | $5.0 \times 10^{10}$ *<br>( $4.7 \times 10^{10}$ )** | 5  | 27.60                                       |
| $^{207}\text{Pb}$   | $^{235}\text{U}$ | $7.13 \times 10^8$                                   | 1  | 0.720                                       |
| $^{206}\text{Pb}$   | $^{238}\text{U}$ | $4.51 \times 10^9$                                   | 0.5  | 99.27                                       |

\* Aldrich et al. (1956)

\*\* McMullen et al. (1966)





Geochronology is based on the primary premise that if the amount and rate of decay of the radioactive parent nuclide and the amount of the radiogenic daughter nuclide can be determined, the time taken to accumulate the radiogenic daughter nuclide may be calculated using the fundamental decay equation representing a process of the first order.

$$-\frac{dN}{dt} = \lambda N \quad (\text{where } N \text{ is the no. of atoms of the original parent nuclide remaining after time } t.)$$

Integrating,  $N = N_0 e^{-\lambda t}$  (where  $N_0$  is the original number of atoms of the parent nuclide and  $\lambda$  is the decay constant.)

$$\text{thus } \frac{N}{N_0} = e^{-\lambda t}$$

Since geological time is measured backwards from the present and

$$N_0^D - N^P = N^D \quad (\text{where } D \text{ and } P \text{ are superscripts representing daughter and parent nuclide respectively.})$$

$$\text{thus } N^D = N^P (e^{\lambda t} - 1)$$

$$\text{and } \frac{N^D}{N^P} = e^{\lambda t} - 1$$

$$\text{solving for } t, \quad t = \frac{1}{\lambda} \ln \left( 1 + \frac{N^D}{N^P} \right)$$

Because of the dual decay scheme for  $^{40}\text{K}$ , the previous equation becomes:

$$t = \frac{1}{\lambda_{e^-} + \lambda_{\beta}} \ln \left( 1 + \frac{\lambda_{e^-} + \lambda_{\beta}}{\lambda_{e^-}} \frac{{}^{40}\text{Ar}}{{}^{40}\text{K}} \right)$$

The half-life of the parent nuclide is related to the decay constant in the following manner:

$$\text{if } N^D = N^P \quad \text{or} \quad N^P = \frac{1}{2} N_0^P$$

$$\text{then } t_{\frac{1}{2}} = \frac{\ln 2}{\lambda}$$

The  $t$  calculated from the decay equation will be the age of the phase being measured provided the phase has been a closed system since its formation. Five other criteria are listed by Rankama (1954, p. 110). The rate of decay of the radioactive nuclide must be known, and of a favourable magnitude, the sample measured must be representative



of a known geological phase and analytical methods must be accurate. The amount of daughter product incorporated in the phase at the time of formation should be known and nonequilibrium amounts of any radionuclides intermediate in the decay scheme should be absent. The isotopic composition of the parent nuclide should be known and constant through time and through the range of materials studied if the abundance ratio is used in calculating the amount of parent nuclide.

The development of geochronology from the first publication by Boltwood (1907) has been reviewed by many authors (e.g. Faul, 1954 and Hamilton, 1965) and will not be repeated here. Important contributions were made by Holmes (1913, 1929 and 1931), Aston (1933) and Nier (1938) in the pre-World War II period. The rapid development of potassium-argon and rubidium-strontium methods immediately after the War came as a consequence of greatly improved mass spectrometer instrumentation.

The individual methods of U-Pb, Rb-Sr and K-Ar geochronometry and their specific application to the problem at hand are described in Chapter III.

### Previous Geochronology

The first age determination carried out in the Yellowknife district was that of Keevil, Jolliffe and Larsen (1942), who used the helium method to date a whole rock sample of the South-east granodiorite. Helium leakage is thought to be responsible for a too young age of 1200 m.y. In 1952, Larsen, Keevil and Harrison reported a lead-alpha activity age of 904 m.y. on a zircon concentrate separated from a marginal phase of the South-east granodiorite. Folinsbee (1955) applied the radiation dosage method of Hurley and Fairbairn (1953) to the same sample of zircon





and obtained an age of "2380 m.y. with a rather high probable error". Russell and Cumming (1955) revised the lead model dates on galena samples reported by Russell et al. in 1954 to an average value of 2255 m.y. Subsequent lead model data by Robertson (1966) on galena and pyrite samples from veins in the greenstone belt yield a much older date of 2860 m.y.

K-Ar age determinations made by Folinsbee and his co-workers (Folinsbee et al., 1956) led to the conclusion that there was no significant difference in age between the "older" hornblende diorites and "younger" muscovite granites. The K-Ar biotite dates reported by Folinsbee are 2330 and 2340 m.y. (approximately 2290 m.y. if the presently accepted decay constants are used).

The extensive program of K-Ar dating carried out by the Geological Survey of Canada was the next contribution to the geochronology of the Slave Province. Twenty nine K-Ar dates on micas and hornblende are recorded in G.S.C. Papers 60-17 to 65-17, though only three dates are recorded from the area immediately around Yellowknife (2490, 2540 and 2615 m.y.).

Mica K-Ar dates (including those presented in this thesis) from the area around Yellowknife are tightly grouped around the mean values collated by Stockwell (1964) for the Kenoran orogeny in the Slave province (MM2393, M2473, MP2552 m.y.) and correlate well with the Kenoran of the Superior province.

With the foregoing background of K-Ar dating, the Rb-Sr method was introduced in 1963. The first data are those of Van Breeman (1965). In the course of experimental work on the thermally-induced relocation of Sr and Rb in a block of the South-east granodiorite,





Van Breeman determined a mineral isochron age of 2460 m.y.  $\pm$  40 m.y.  
( $\lambda^{87}\text{Rb} = 1.47 \times 10^{-11} \text{ year}^{-1}$ ). The biotite separated from the grano-  
diorite gave a K-Ar date of 2390 m.y.



## CHAPTER II

### REGIONAL GEOLOGY

The Canadian Precambrian Shield forms over half the surface area of mainland Canada, i.e. about 1.6 million square miles. This immense expanse of metasedimentary, metavolcanic and plutonic rocks was first mapped geologically in 1845 by Sir William Logan, the founder of the Geological Survey of Canada. Reconnaissance of the western part of the Shield and more detailed stratigraphic work in southern Ontario and western Quebec led to the early development of a two fold classification of the rock units involved. The Archaean (older) rocks were seen to be separated by a major unconformity from the Proterozoic (younger) rocks.

Names such as Keewatin, Timiskaming, Yellowknife (Archaean) and Huronian, Great Slave and Snare (Proterozoic) have been applied to rock-stratigraphic units in local areas. However, the desire for correlation led to an association of stratigraphic time with the rock stratigraphic terms. As a result names were applied far from the type locality purely on the basis of lithological similarity.

Only in recent years have radiometric determinations of geologic age begun to establish a basis for a Precambrian stratigraphic timetable. Because the early methods of age determination were restricted to minerals from pegmatites and granitic rocks, it was necessary to bracket ages of metasedimentary and metavolcanic sequences by determinations on the associated intrusive rocks and on the underlying basement. Recently developed methods, including Rb-Sr whole rock geochrometry, have greatly enlarged the scope and applicability of isotope geology such that





large regions may be characterised by geological evolution within a given time span.

### Geologic Provinces of the Canadian Shield

Subdivision of the Shield into a number of provinces based on their lithological similarity and relative age of folding was first attempted by M. E. Wilson (1939, 1941). Gill (1948, 1949) proposed names for the structural provinces and classified subprovinces in terms of mountains, plains and belted plains (Gill, 1949, p. 63). These terms are used in a palaeogeographic rather than topographic sense. J. T. Wilson (1949a, 1949b) brought forward a similar division of the Shield based on geophysical properties and the trends of foliations and major lineations. Using the limited number of radiometric dates available at the time, Wilson explained the distribution of provinces in terms of a continental accretion hypothesis.

Reconnaissance K-Ar geochronology by the Geological Survey of Canada firmly established the regional subdivision of the Shield on a basis of ages of folding, major igneous events and accompanying metamorphism (Stockwell, 1964). Maxima in the distribution of K-Ar ages indicate three main orogenic periods, the Kenoran (circa. 2500 m.y.), Hudsonian (circa. 1700 m.y.) and Grenville (circa. 950 m.y.).

In general, a province is characterised by K-Ar dates representing the youngest orogenic event. However, an increasing body of evidence from geological and Rb-Sr and U-Pb radiometric methods indicates the presence of multiple orogenic events in parts of the Superior, Churchill and Grenville provinces.

Fig. 2 shows the major structural provinces of the Canadian





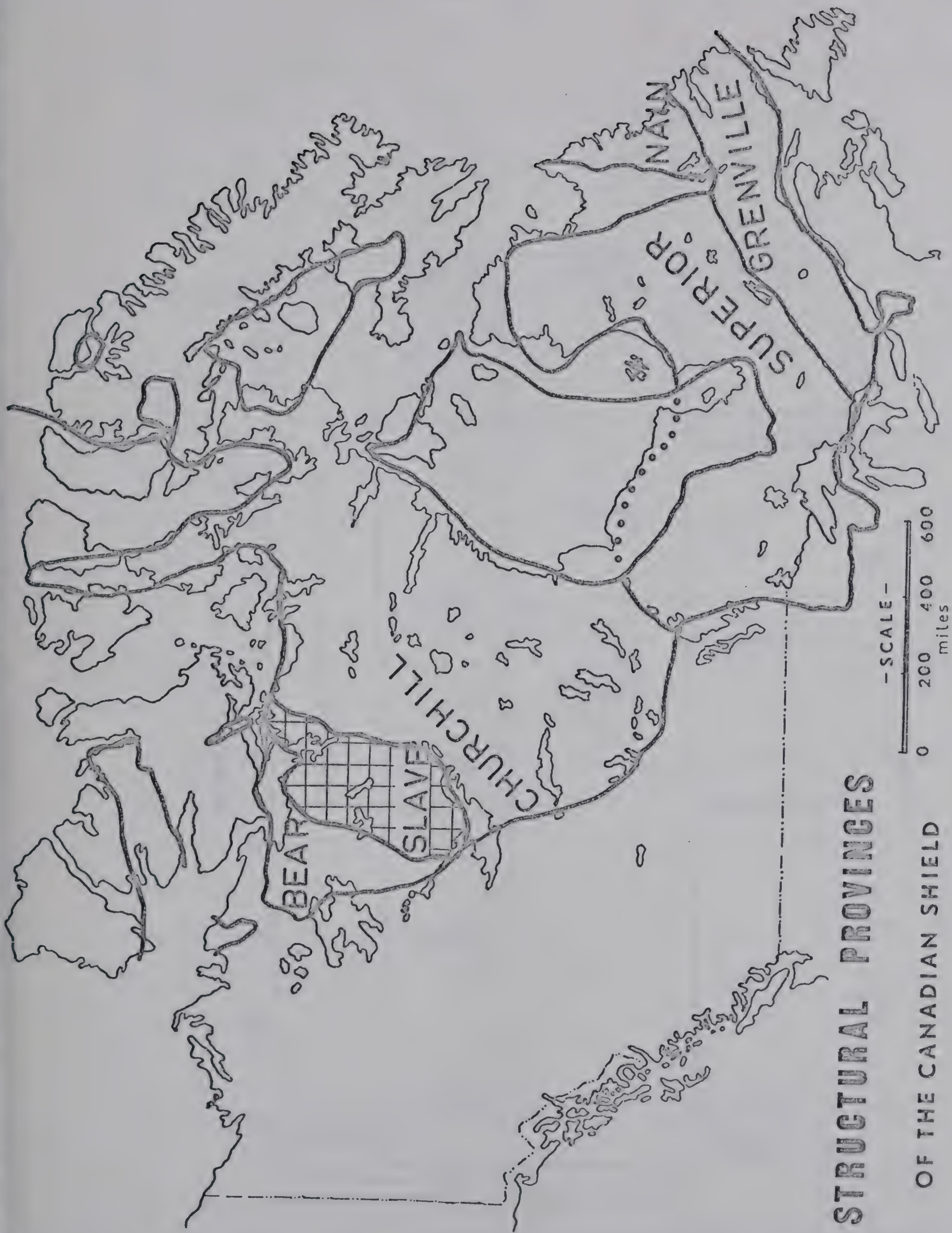


Fig. 2. Structural Provinces of the Canadian Shield



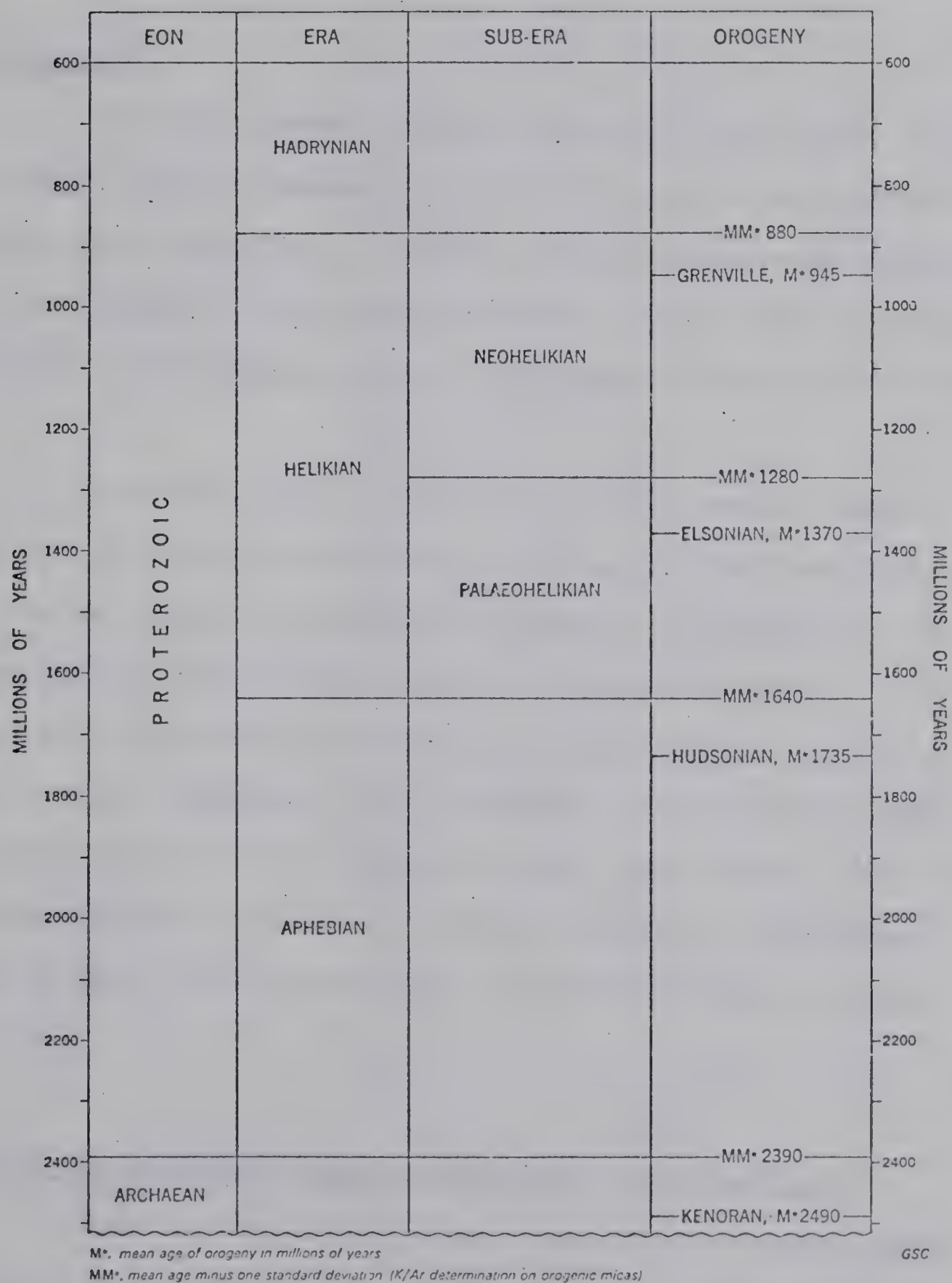


Table 2. Time - stratigraphic classification for the Canadian Shield showing standard MM (mean minus one standard deviation) horizons for K-Ar mica dates related to the main orogenic episodes. (from Wanless et al., 1967, based on Stockwell, 1964)





Shield. The boundaries are based on the most recent compilation of K-Ar ages (Wanless et al. 1967, Fig. 1). The Precambrian time scale and division of rock stratigraphic units proposed by Stockwell (1964, table III) is reproduced as Table 2.

### Slave Province

The Slave Province was first defined by Gill (1948, 1949). The original southern boundary was placed at the north shore of Lake Athabasca (Gill, 1949, Fig. 3). Modern usage of the term is restricted to an area bounded by Gill's Snare Mountains and Slave Lake Mountains. J. T. Wilson (1949) retained the term Yellowknife Province for a similar area.

Jolliffe (1952, p. 142) introduced the term Yellowknife subprovince to include the territory extending north of Great Slave Lake for 200 miles. Because of gold mineralization, the Yellowknife subprovince has been geologically mapped in considerable detail. Among the most important references are Geological Survey of Canada reports by Jolliffe (1936), Henderson (1939), Henderson and Brown (1949, 1952), Lord (1942), Fortier (1947), Folinsbee (1947), Moore (1956), Boyle (1961), and Baragar (1966). A detailed structural analysis of the boundary between the Slave and Bear Provinces is provided by Ross and McGlynn (1963, 1965).

### Geology of the Yellowknife and Ross Lake-Redout Lake districts

There are many similarities between the two districts and the table of formations reproduced below (Table 3) may be applied to either area with little modification. Figs. 3 and 4 show the geology





## TABLE OF FORMATIONS

Table 3.

(Precambrian) - extensively modified from Boyle, 1961





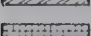
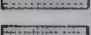
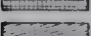

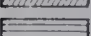
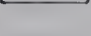
| Age          | Formation                                       | Description  | Remarks  |
|--------------|---|--|--|
| PROTEROZOIC  |   | Diabase dykes  |  |
|              |   | Granite, granodiorite  | (Hudsonian)  |
|              |   | Nepheline-sodalite syenite   |  |
|              |   | Diabase, picrite-gabbro dykes  | (see Leech, 1966)                                  |
|              | Snare Group                                     | Finely bedded, alternating siltstone and shale and metamorphic equivalents. Dolomite, arkose   | (see Lord, 1942, Ross and McGlynn, 1963)           |
| UNCONFORMITY |   |  |  |
| ARCHAEAN     |   | Redout Lake, Prosperous Lake granites and associated pegmatites  |  |
|              |   | Western granodiorite (?Ross Lake granodiorite)   |  |
|              |   | Stock Lake stock, aplites (?South-east granodiorite)   |  |
|              |   | Quartz feldspar porphyries   |  |
|              |   | Second phase of metadiorite and metagabbro intrusion   |  |
|              | Yellowknife Group Division B                    | Greywacke, argillite, phyllite quartzite, etc. and their metamorphic equivalents. Dacite, trachyte, rhyolite, quartz porphyry, pyroclastics and their metamorphic equivalents. | (Overlie Div. A with apparent regional conformity) |
|              | Unclassified (Stratigraphic position uncertain) | Conglomerate and quartzite   |  |
|              |   | Local Unconformity (?South-east granodiorite)  | (Folinsbee et al. 1968)                            |
|              |   | First phase of metadiorite and metagabbro intrusion  |  |
|              | Yellowknife Group Division A                    | Basalt, andesite, dacite rhyolite, cherty tuff and their metamorphic equivalents   |  |
|              |   | (?Ross Lake granodiorite)  | (Baragar, 1966)                                    |





# REGIONAL GEOLOGY, YELLOWKNIFE AREA Northwest Territories

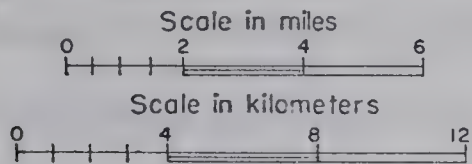
## Legend:

-  Diabase, Gabbro
-  Prosperous Lake Granite
-  Western Granodiorite, Southeast Granodiorite
-  Diorite
-  Graywacke, Argillite, Quartzite, Slate, Phyllite
-  Nodular Quartz-Mica Schist and Hornfels
-  Dacite, Trachyte, Rhyolite, Qtz-Porphyry and Tuff
-  Andesite, Basalt, Metagabbro
-  Conglomerate and Quartzite
-  Drift-covered area

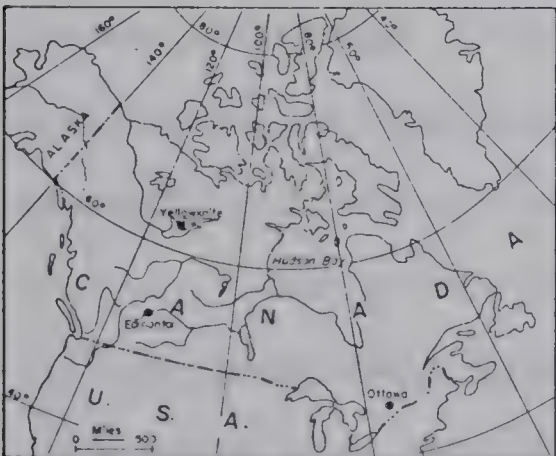
 Fault

### SAMPLE LOCATIONS

● = K/Ar    ▲ = Rb/Sr    X = U/Pb



### Location Map



MAP ADAPTED FROM BOYLE, 1961, FIG.1.

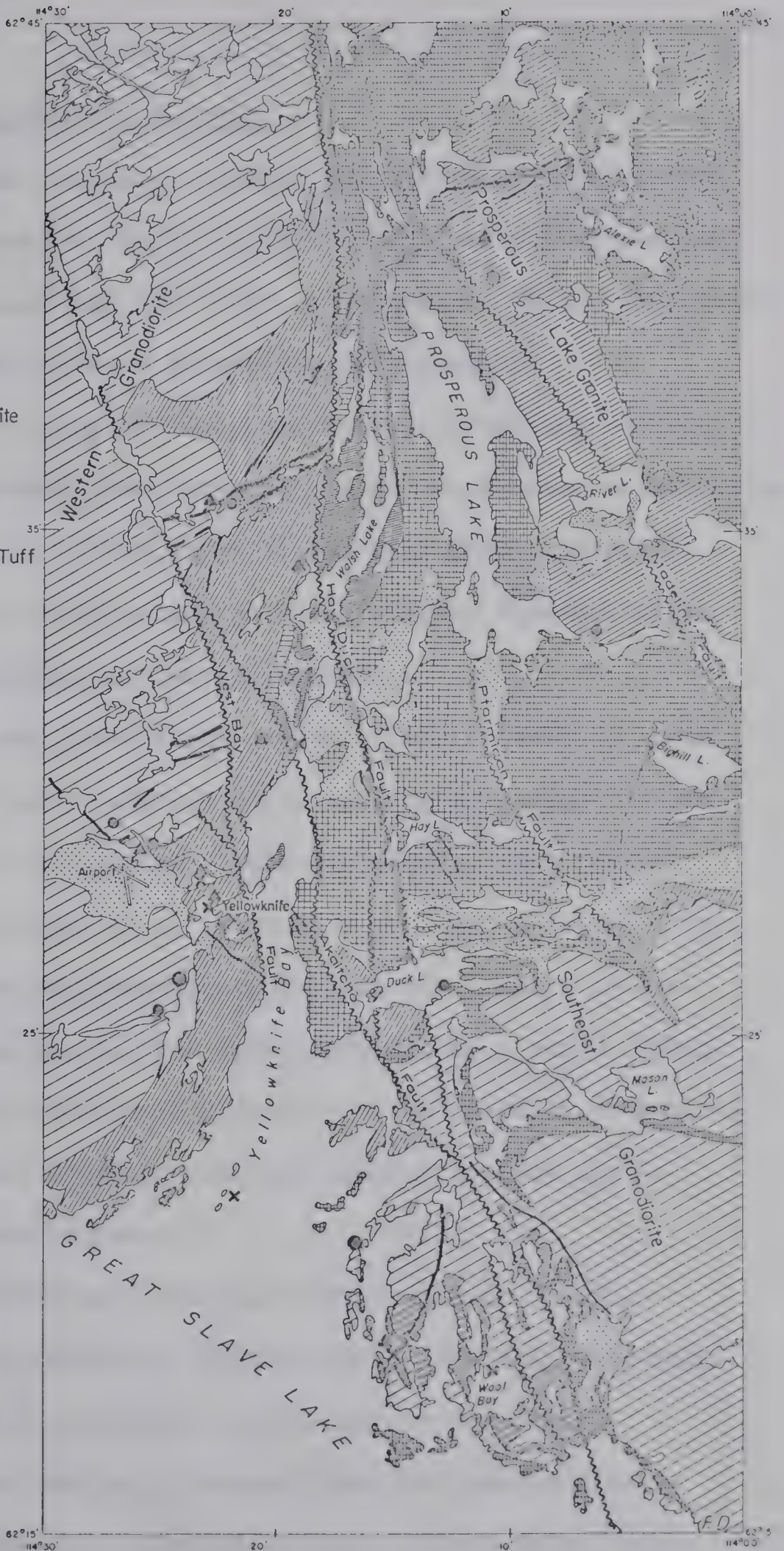


Fig. 3. Regional geology, Yellowknife area, Northwest Territories (after Boyle, 1961)





of the respective districts.

### Yellowknife district

The oldest rocks presently exposed are the Yellowknife Group metavolcanics and metasediments. Boyle (1961, p. 172) has postulated that a large mass of sediments once lay below the metavolcanics of the Yellowknife Group but there is no field evidence to support this concept.

The Yellowknife Group is divided into two divisions; Division A includes metabasalts, meta-andesites, metadacites and associated pyroclastics while Division B includes greywackes, argillites, quartzites, arkoses, tuffs and conglomerates and their metamorphic equivalents together with intermediate and acid metavolcanics and pyroclastics.

Conglomerates and quartzites (unclassified in Table 3) occur along the contact of Divisions A and B. Their stratigraphic position is controversial, but they are cut by the oldest diabase dyke set (Set 1, Leech, 1966) for which K-Ar ages of at least 2100 m.y. are obtained. The contact of the unclassified conglomerates with Division A rocks is distinctly unconformable while the contact between Divisions A and B, though obscure, is thought to be regionally conformable. The presence of granite boulders in the conglomerate suggests that the Kenoran orogeny may be preceded by an earlier orogenic event.

Mafic sills, dykes and irregular masses intrude Division A but are rarely found in the sediments of Division B. The acid volcanics of Division B are intruded by irregular hornblende diorite sills.

Plutonic masses ranging in composition from quartz diorite to muscovite granite intrude the Yellowknife Group. Three major bodies occur in the Yellowknife district; the South-east granodiorite on the





east side of Yellowknife Bay, the Western granodiorite flanking the metavolcanics on the west side of Yellowknife Bay and the Prosperous Lake Granite on the east side of Prosperous Lake. A wide contact aureole surrounds the Prosperous Lake granite and evidence of assimilation of basic volcanics marks the borders of the other bodies. The Stock Lake stock (Kelly, 1964) and smaller offshoots at Pud Lake and in the underground workings of the Con mine are considered to be satellites of the Western granodiorite. A small stock east of the north end of Walsh Lake carries abundant disseminated arsenopyrite.

Quartz feldspar porphyries cut the metavolcanics and carry angular fragments of the metavolcanics and the Western granodiorite.

A composite picrite-gabbro sheet along the line of the Hay-Duck fault (see Fig. 3) and three sets of diabase dykes (Wilson, 1949, Leech, 1966) are the only post-Kenoran Precambrian rocks in the Yellowknife district.

#### Ross Lake - Redout Lake district

In this area there is also controversy as to which are the oldest rocks. Both Fortier (1947) and Henderson (1941) thought that the gneissic granodiorite to the east of the Yellowknife Group was intrusive into that Group. Baragar (1966, p. 13) suggests that the gneissic granodiorite may be older than the metavolcanic rocks of the Yellowknife Group. The field evidence bearing on this problem is discussed in the section "Cameron River area".

Overlying the metavolcanics at the south end of Ross Lake is a narrow belt of conglomerate (with calcareous lenses) which appears to be structurally conformable with the underlying metavolcanics. North



of Ross Lake no conglomerate is found and the volcanic sequence passes without apparent break into the greywackes, slates, quartzites and metamorphic equivalents of the Yellowknife Group (Division B).

Swarms of hornblende gabbro dykes intrude the metavolcanics and the gneissic granodiorite. Their strike is consistently slightly west of south, essentially parallel to the foliation in the granodiorite. The interbanded complex of granodiorite and dykes is intruded by the Redout Lake granite and its associated pegmatites. Two sets of diabase dykes cut all previous rock units.

### Yellowknife Group

The term Yellowknife Group was first used in its presently accepted sense by Henderson (1939). It includes volcanic and sedimentary divisions which are older than the Kenoran granitic intrusive rocks. Bell (1929, p. 18) had applied the term "Yellowknife series" to the rocks exposed near the outlet of the Yellowknife River.

### Division A

In describing intermediate to basic rocks in the Canadian Shield, it has been customary to apply the terms andesite and basalt on a basis of colour with an implicit inference that more exact terminology would class them as meta-andesite and meta-basalt. Many grey or light green lavas have been mapped as andesites when they are pale in colour because of the development of epidote, amphibole, chlorite or carbonate minerals during metamorphism. For example, Brown (1949, p. 16) classified the metavolcanic sequence in the Yellowknife area as 96% andesite on the basis of modal minerals whereas



PLATE 1



(a) Pillows in Yellowknife Group, Division A meta-volcanics, near Giant Yellowknife mine office.  
NOTE: Undeformed pillows, in greenschist facies, tops towards the top of the picture.



(b) Deformed pillows in Yellowknife Group, Division A. metavolcanics, northeast of Long Lake.  
NOTE: Amphibolite facies, selvages replaced by quartz and K-feldspar, some pods of introduced calcite.



(c) Acid pyroclastic unit, Yellowknife Group, Division A, 400 yds west of B shaft, Giant Yellowknife property.  
NOTE: This is referred to as the Brock horizon; other units are massive, porphyritic dacites.

a classification on the basis of normative minerals shows basalt 49% quartz basalt 6%, andesite 27%, latite 3%, dacite 8%, and quartz latite 7%, (Baragar, 1966). Any attempt to classify ancient lavas in terms of a chemical classification based on unmetamorphosed flows involves the assumption of isochemical metamorphism.

Exposures of metavolcanic rocks in the area west of Yellowknife Bay form one of the thickest, continuous sections in the Canadian Shield. Henderson and Brown (1952) record at least 22,000 feet of nearly vertical flows and Baragar (1966, p. 12) reports over 40,000 feet of section including gabbro sills. The base of the section is cut off by the Western granodiorite.

Massive and pillowed flows which generally face south east and dip steeply east form most of the volcanic sequence. Original structures are often perfectly preserved. Pillows averaging 1 foot to 2 feet in maximum diameter are particularly well preserved (Plate 1). Flow contacts are commonly marked by a layer of flow breccia and irregular top surfaces may be filled by an overlying tuff band. Pillows have  $\frac{1}{2}$  inch to 3 inches of darker-coloured, fine grained rim with a structureless, slightly coarser-grained centre. Massive flows are coarser-grained than the pillowed flows and are difficult to distinguish from the sills which intrude the volcanic sequence.

Variolitic pillow lavas are valuable marker horizons. Spherules from these flows may reach a diameter of one inch and weather as white resistant nodules in the dark green pillows. The four most continuous variolitic horizons are the Yellowrex flows, Negus flows, Fox flows and the Stock flows. Each of these is described in detail by Henderson and Brown (1952) and in unpublished mining company reports.







In thin section the basic flows are composed of a preponderance of secondary minerals. Hornblende and chlorite form more than 50% of the rock, plagioclase and epidote form approximately 30 to 40% and accessories include carbonates (calcite and ankerite), sericite, biotite, apatite, magnetite and quartz. Where it is possible to determine the composition of the original plagioclase, it is andesine to labradorite.

Dacites are well exposed along the Giant road approximately  $\frac{1}{4}$  mile N.W. of the new Yellowknife town site. These were sampled in detail because of their expected favourable Rb/Sr ratio. The dacites have been termed the Townsite or Brock flows. The total thickness of this horizon (lower acidic layer of Baragar, 1966) is over 1,200 feet, but the section is interrupted by a thick metagabbro sill. The more acid flows are markedly porphyritic with a particularly fine-grained matrix.

On the outcrop described previously (near the new town site) the most acid rocks are only slightly altered. Thin sections show fresh phenocrysts of plagioclase ( $An_{40}$ ) and occasional quartz. The groundmass is a fine-grained recrystallised mixture of plagioclase, quartz, biotite, chlorite with minor carbonate, sericite, epidote, apatite, magnetite, pyrite and zircon.

The lower part of the Townsite series of flows is more basic and at least one horizon shows pillow structures.

Pyroclastic rocks occur mainly in the upper part of the volcanic pile. Breccias and agglomerates may be as much as several hundred feet thick (e.g., between Jackson and Vee Lakes), but average 5 to 10 feet in thickness. Tuffs range from crystal tuffs to cherty tuffs and commonly show graded bedding. Although most tuff beds are





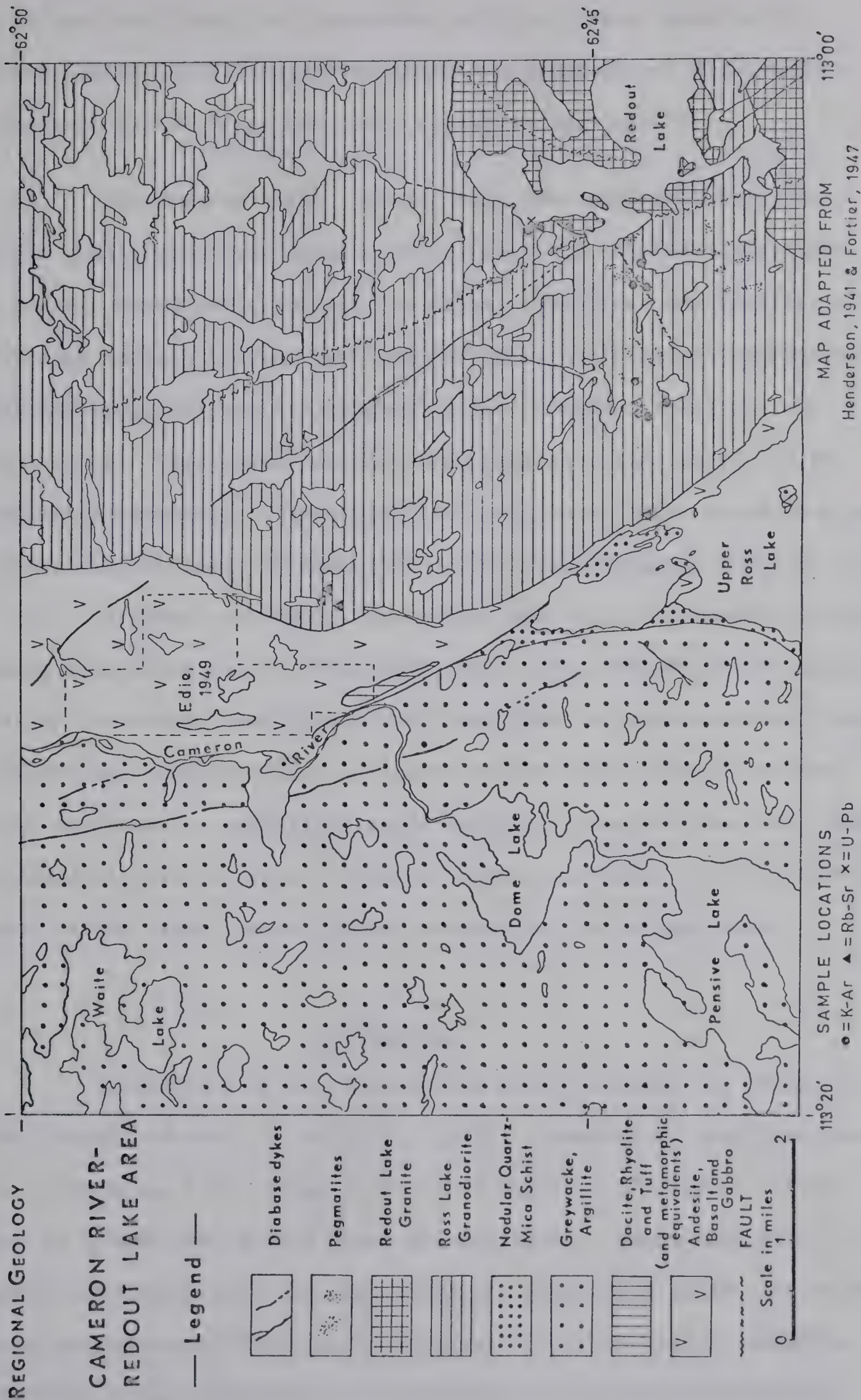


Fig. 4. Geological map of the Cameron River - Redout Lake area (after Henderson, 1941 and Fortier, 1947)





thin (1 inch to 2 feet) and concordant with the lavas, some larger bodies of cherty tuff form irregular masses which appear to transgress the regional strike (e.g. near the Crestaurum mine shaft).

The Cameron River volcanic belt runs northwest from Ross Lake and then follows the Cameron River (Fig. 4). It ranges in width from a few hundred yards to over two miles. The flows are vertical or dip steeply southeast, but they face northwest and thus are overturned. A striking ridge of rhyolite (quartz latite) trends parallel to the Cameron River. This discontinuous layer occurs in the upper part of the volcanic sequence. Intermediate and acid rocks comprise as much as 1,400 feet of the total thickness of 7,000+ feet (Baragar, 1966, p. 13).

Although pillowed flows occur, they are less common and more deformed than those in the Yellowknife area. The effects of metamorphism are also more severe, and Edie (1949) describes the basic rocks as andesine or oligoclase - amphibolites. A review of the thin sections prepared by Edie confirms the crystalloblastic texture of many of the basic rocks. Some recrystallised tuffs are thought to have contained pelitic material because of the large amount of biotite produced on metamorphism.

#### Division B

Division B of the Yellowknife Group includes two series of rocks (Divisions B and C of Jolliffe, 1942). Immediately overlying the lavas of Division A is a thin (2,000 to 6,000 feet, Folinsbee, 1942) series of interbanded acidic flows and sediments. These pass with apparent conformity into the argillites and greywackes which make up the greater proportion of Division B. The relatively unaltered sediments of Division B pass abruptly into assemblages of quartz-mica schists,





commonly knotted, around the Prosperous Lake Granite. Graded bedding (Plate 2) is a distinctive feature of the greywackes.

An unconformity is developed locally along the boundary separating the rocks of Division A from the rest of the Yellowknife Group. On a regional scale the contact appears to be conformable. In most exposures bedding in the basal conglomerate and overlying arkosic quartzite departs less than  $15^{\circ}$  from the strikes of the flow contacts in the overlying lavas.

The evidence for local unconformity rests largely on the position of the unclassified conglomerate described in the next section. It is the author's opinion that the conglomerate forms the base of Division B but evidence to the contrary is presented by Henderson and Brown, 1952. In order to simplify the description of Division B, it will be assumed that the unclassified conglomerate and immediately overlying beds are correctly placed at the base of Division B.

Acid volcanics overlies the basal conglomerate and quartzite. These are mylonitized and are extensively altered to carbonates. Along the southern shores of Walsh Lake, porphyritic hornblende diorite ?sills intrude the acid flows. The basin (and northern extremity) of Walsh Lake are marked by soft argillites which are probably younger than the acid volcanics on either side. Shearing along the Walsh and Hay-Duck faults is responsible for the extensive alteration of this series.

The upper part of the Yellowknife Group consists of a great thickness of interbedded greywacke, argillite and slate. The greywacke weathers grey or buff, is fine to medium grained and individual beds vary from a few inches to as much as 5 feet in thickness. Quartz is

PLATE 2



(a) Quartz greywacke beds, Yellowknife Group, Division B, near Burwash Point, east side of Yellowknife Bay. NOTE: Graded bedding (tops to the left of the picture), vertical attitude.



(b) Detail of erosional sole-structures at the base of graded beds. Although the vertical disposition does not allow a 3-dimensional view, it is likely that the groove casts are accentuated by load casting.



the predominant mineral but chlorite, sericite, feldspars and carbonates are important constituents. Groove casts are common sole markings and some show the effects of load casting giving rise to delicate flame structures. Commonly a single bed grades from greywacke to argillite without evidence of a break in sedimentation. Some greywackes have included fragments of the underlying argillite beds. Argillites are dark in colour, very fine grained and range up to six inches in thickness.

The relatively unaltered sediments pass gradually into quartz mica schists as the sharply-defined nodular zone is approached. Biotite is developed in place of chlorite.

The first appearance of andalusite knots marks the outer limits of the nodular zone. Knots, strictly porphyroblastic minerals, are most abundant in the finer grained argillaceous tops of graded beds. Other porphyroblasts include andalusite (commonly chiastolite), garnet, poikiloblastic cordierite, staurolite and sillimanite. Folinsbee (1942) suggests that the type of porphyroblast depends on the composition of the host rock rather than on relative proximity to the intrusive body. A retrograde thermal episode has reduced many of the porphyroblasts to micaceous aggregates pseudomorphing the outline of the original minerals and so permitting their identification.

#### Unclassified Conglomerates

Conglomerates of controversial origin occur in both Yellowknife and Ross Lake areas. It should be noted that a similar problem exists in the Superior Province (Bass, 1961, Boutcher et al., 1966) and in Finland (Sederholm, 1931, Eskola, 1941).

The controversy centres around the presence of "granite"





pebbles in the conglomerate. If the "granite" pebbles come from an older terrain (perhaps equivalent to the Laurentian granites of the Minnesota region) then there is no objection to the placement of the unclassified conglomerates and associated quartzites at the base of Division B of the Yellowknife Group. However, the evidence for unconformity at the base of the predominantly sedimentary section is confined to limited areas such as at the south end of Walsh Lake, at the head of Yellowknife Bay and possibly east of Ross Lake. Other exposures of unclassified conglomerates occur on the Sub Islands and the west section of Jolliffe Island.

Henderson and Brown (1952, p. 19) base their conclusion that the conglomerates are post Yellowknife Group on: (1) the contrasting lithology (i.e. quartzite with cross bedding versus greywacke with graded bedding), (2) contrasting structural relations with the underlying rocks, and (3) relations with metagabbro dykes and sills. Each line of evidence will be considered in turn.

(1) The lithology of the unclassified conglomerates is distinctive. On the Sub Islands, well rounded pebbles and cobbles of metavolcanics, metagabbros, porphyries, chert, sodic granite, argillite, slate, ferruginous carbonate, jasper and vein quartz make up as much as 70% of the exposed surface of the conglomerate horizons. Exposures on Jolliffe Island are similar except that the matrix is schistose and elongation of the softer pebbles is noticeable. The proportion of granite cobbles decreases to the north and the amount of elongation becomes more extreme.

Just north of the head of Yellowknife Bay the conglomerate varies from 10 to 200 feet in thickness and contains "stretched" cobbles





up to two feet in length. Here the maximum elongation is nearly vertical and as much as 8 times the intermediate dimension which trends approximately north. The average trend of the minimum dimension is east - west and the length of this axis is approximately one third or one half the intermediate axial dimension.

Examination of 11 thin sections from cobbles thought to be granitic in the field showed only three which could be clearly recognised as plutonic acid or intermediate rocks. The remainder were acid porphyries. At the south end of Jackson Lake, a diligent search failed to locate any "granite" pebbles or cobbles.

Immediately overlying the conglomerates are quartzites with well developed cross-bedding. When returned to the horizontal from their present almost vertical orientation, the cross-bedding in the quartzites indicates a source to the south.

Henderson and Brown argue that the contrasting lithology of the unclassified rocks and Division B indicates "entirely different conditions of deposition and, hence, probably different periods of deposition". The lithology of the unclassified rocks is not dissimilar from that of the Snare Group although limestone is the basal member in most Snare Group exposures (Ross and McGlynn, 1963). The possibility that the unclassified conglomerates were an outlier of infolded Snare Group rocks was entertained briefly but discarded for the following reasons: (a) the unclassified rocks are folded and metamorphosed and there is no radiometric evidence for a Hudsonian event corresponding to the deformation of Snare Group rocks in the Yellowknife Bay area, (b) the unclassified conglomerates and quartzites are cut by the oldest diabase dyke set on the west side of Banting Lake (114°17'35"E, 62°37'N).





(2) Henderson and Brown state that "it seems unlikely that sedimentary rocks of the same age, in areas within less than a mile of each other, would exhibit entirely different structural relations to an old erosion surface". Comparision with younger suites suggests that a parallel situation is found in some young "eugeosynclines" (Kay, 1951) which are thought to be geanticlinal volcanic island arcs rather than geosynclinal basins. Minor unconformities and conglomerates of local provenance are characteristic of such an environment and the angular magnitude of an unconformity is not a reliable criterion of its geographic or temporal extent.

(3) The third argument used by Henderson and Brown is based on contemporaneity of metagabbro and metadiorite sills and dykes. Although the unclassified conglomerates rest with marked unconformity on some of the metagabbro dykes and sills, there is no reason for rejecting the possibility of a second, post conglomerate, phase of basic intrusion. Folded mafic intrusions are not as common in Division B as they are in the Division A metavolcanics. The most striking example is that at Tibbitt Lake, 7 miles S.S.W. of Ross Lake (Fortier, 1947). Since at least three phases of diabase dykes were emplaced during the Proterozoic (Leech, 1966) it is reasonable to allow at least two phases during the Archaean.

The weight of evidence favours placement of the "unclassified conglomerate" in Division B of the Yellowknife Group and probably at the base of that unit.





## Early Mafic Intrusives

### Yellowknife Bay area

Early mafic intrusives may be divided into two types: (a) sills and irregular intrusions and (b) dykes. Irregular intrusions are more common in the lower part of Division A, while the dykes cut the sills, irregular intrusions and the lavas. The dykes appear to post-date the first phase of folding suffered by the Yellowknife Group. Baragar (1966, p. 13) regards the sills as "basaltic flows out of stratigraphic position". Dykes, on the other hand, do not appear to be feeders to the flows (Henderson and Brown, 1952, p. 20) but are of similar composition.

Two groups of sills are most important, the Kam group and the Townsite group. The largest Kam sill shows textural banding and is slightly differentiated (Baragar, 1966, p. 17). Other sills are difficult to distinguish from medium to coarse-grained massive lavas particularly in view of the commonly poor development of chilled contact zones. Although the Kam sills are practically confined to the area southwest of the West Bay fault, it is possible that the sills near the old townsite are their faulted continuation. In these sills, as in the stratigraphically lower Townsite sills and some of the irregular bodies, the emplacement appears to have been permissive.

The three Townsite sills are well exposed just north of the present townsite. They intrude dacites of the Brock horizon and are coarse-grained, massive rocks with rather diffuse chilled edges. The central sill is porphyritic and the northernmost (lower) sill is more extensively weathered than the upper sills. Across the West Bay fault, the sills are again restricted to the Brock horizon. Detailed mapping





by Giant Yellowknife Mines Ltd. around Vee Lake confirms the suggestion made by Henderson and Brown (1952, p. 21) that these sills are displaced by the Akaitcho fault and extend through Vee Lake where they are associated with pyroclastics equivalent to the Brock horizon.

In thin section the sills are similar to the massive flows. Hornblende, plagioclase and epidote are the chief constituents. There is no trace of any original pyroxene in the form of unaltered cores or relict euhedra in any of the thin sections studied.

Irregular intrusions are generally restricted to the lower half of Division A. They are often cut by metagabbro and metadiorite dykes although their margins are sharply chilled. It is probable that there are at least two ages of irregular intrusions. The younger group are well exposed on the west side of Shadow and Daigle Lakes in the form of coarse-grained, transgressive bodies up to 500 feet wide. Although the rocks appear fresh on the exposed surface, thin sections show extensive uranitization of hornblende while the plagioclase (An<sub>55</sub>) appears relatively fresh. Epidote forms granular patches.

The presence of labradorite and hornblende as primary constituents of the early mafic intrusions makes classification of the rocks difficult. They lie between diorite and gabbro in terms of modal minerals and colour index after allowance is made for subsequent low grade regional metamorphism. However, the term hornblende gabbro is preferred because of the tholeiitic normative composition (Table 4). Crystallisation of hornblende rather than pyroxene, the typical mafic constituent of gabbros, is a reasonable possibility in a hydrous environment.



Table 4. Analyses of early mafic intrusives  
(from Baragar, 1966, Boyle, 1961 and Nockolds, 1954)

|                                | Composite of<br>metadiorite<br>and metagabbro<br>dykes<br>%                  | Chilled<br>margin<br>Kam Pt.<br>sill<br>% | Gabbro peg-<br>matite Kam<br>Pt. sill<br>% | Average<br>tholeiitic<br>olivine<br>basalt<br>(Nockolds)<br>% |
|--------------------------------|--|---|--|---|
| SiO <sub>2</sub>               | 48.76  | 48.0                                      | 48.4                                       | 47.9  |
| TiO <sub>2</sub>               | 0.89   | 0.78                                      | 1.60                                       | 1.7   |
| Al <sub>2</sub> O <sub>3</sub> | 14.63  | 14.7                                      | 12.3                                       | 11.8  |
| Fe <sub>2</sub> O <sub>3</sub> | 1.67   | 1.9                                       | 3.6  | 2.3   |
| FeO                            | 9.87   | 9.2                                       | 11.7                                       | 9.8   |
| MnO                            | 0.24   | 0.14                                      | 0.19                                       | 0.2   |
| MgO                            | 8.08   | 7.2                                       | 4.7  | 14.1  |
| CaO                            | 9.94   | 9.5                                       | 8.9  | 9.3   |
| Na <sub>2</sub> O              | 2.13   | 2.6                                       | 2.1  | 1.7   |
| K <sub>2</sub> O               | 0.58   | 0.4                                       | 0.1  | 0.5   |
| H <sub>2</sub> O <sup>+</sup>  | 2.43   | n.d.                                      | n.d.                                       | n.d.  |
| H <sub>2</sub> O <sup>-</sup>  | 0.12   | "   | "  | "   |
| P <sub>2</sub> O <sub>5</sub>  | 0.08   | "   | "  | "   |
| CO <sub>2</sub>                | 0.18   | "   | "  | "   |
| Total                          | <u>99.84</u> (includes<br>0.24% S, Cr <sub>2</sub> O <sub>3</sub><br>Cl & C) | <u>94.42</u>                              | <u>93.57</u>                               | <u>100.1</u>  |
| less O = S, Cl                 | 0.05   | -   | -  | -   |
| Net Total                      | <u>99.79</u>   | <u>94.42</u>                              | <u>93.59</u>                               | <u>100.1</u>  |
| S.G.                           | 2.97   | -   | -  | -   |

Analyst: J. A. Maxwell

Geol. Surv. Canada

C.I.P.W. Norms

|                  |              |              |              |             |
|------------------|--------------|--------------|--------------|-------------|
| Qz               | 0.0          | 0.0          | 6.74         | 0.0         |
| Or               | 3.43         | 2.36         | 0.59         | 2.8         |
| Ab               | 18.01        | 21.99        | 17.76        | 14.1        |
| An               | 28.65        | 27.26        | 23.84        | 23.4        |
| (wo              | 7.93         | 8.29         | 8.48         | )           |
| Di (en           | 4.30         | 4.46         | 3.56         | 18.9)       |
| (fs              | 3.36         | 3.56         | 4.94         | )           |
| Hy (en           | 12.66        | 9.43         | 8.14         | 18.6)       |
| (fs              | 9.89         | 7.52         | 11.28        | )           |
| Ol (fo           | 2.21         | 2.83         | -            | 14.7)       |
| (fa              | 1.91         | 2.48         | -            | )           |
| Mt               | 2.42         | 2.75         | 5.22         | 3.3         |
| Il               | 1.69         | 1.48         | 3.04         | 3.2         |
| Ap               | 0.19         | -            | -            | 0.4         |
| Ca               | 0.41         | -            | -            | -           |
| H <sub>2</sub> O | <u>2.55</u>  | <u>-</u>     | <u>-</u>     | <u>-</u>    |
| Total            | <u>99.61</u> | <u>94.42</u> | <u>93.59</u> | <u>99.4</u> |





It is suggested by Henderson and Brown (1952, p. 23) that some of the irregular metagabbro and metadiorite bodies cannot be explained in terms of injection in magmatic form because the flow contacts, pillowed layers and cherty tuffs are not disturbed by the intrusion. Boyle (1961, p. 172-173) further suggests that the metadiorite masses and dykes may represent mafic material expelled during the formation of the Western granodiorite by granitization. Detailed mapping carried out by the writer during 1967 produced evidence to support both the magmatic and dioritization hypotheses, and the problem remains unresolved. Where the metagabbros are in contact with cherty tuffs (e.g. Joe Lake, Daigle Lake) it is suggested that the cherts may have behaved in an incompetent manner during subsequent deformation and the true relationships are obscured. Such incompetent behaviour in recrystallised cherts is a feature of geosynclinal-volcanic assemblages in the Phanerozoic (e.g. Franciscan Group, California, Davis, 1918, p. 241 and Neranleigh-Fernvale Group, Queensland, Bryan and Jones, 1962).

Both sills and early irregular intrusions were folded at the same time as the Yellowknife Group. Metagabbro and metadiorite (hornblende gabbro) dykes and the later irregular intrusions post-date the first deformation of the Yellowknife Group volcanics.

Dykes make up as much as 10% of the greenstone belt in the area west of the West Bay fault. In this area they strike north to northwest and dip to the west at  $60^{\circ}$  or less. Across the West Bay fault the dykes strike north to northeast and dip east at  $40^{\circ}$  to  $60^{\circ}$ . This remarkable difference in attitude across the West Bay fault led Henderson and Brown (1952, p. 24) to argue that the dykes were related to the early schistosity which shows a similar disparity across the West Bay fault.





This implies that the West Bay fault (normally regarded as a post-diabase or late fault) must have an earlier component.

The dykes range in width up to 300 feet, but are commonly 5 to 30 feet wide. They weather green or buff-green, are dark green when fresh and may be particularly porphyritic. Microscopically, the rocks have a poikilitic texture with subhedral hornblende (40-70%) enclosing lath-like plagioclase (40-60%,  $An_{60-45}$ ). Both major components are commonly altered to epidote, chlorite and sericite. All dykes have distinctive chilled contacts.

#### Cameron River area

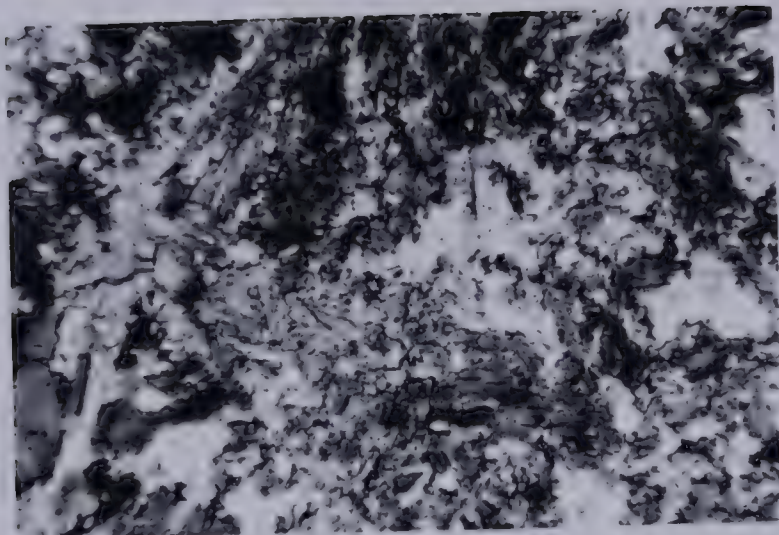
It is necessary to consider the early mafic intrusions of this area in some detail in order to evaluate the evidence offered by Baragar (1966, p. 13) to support the possibility that the granitic gneisses east of the Cameron River are older than the Cameron River volcanics.

The assumption on which Baragar's argument rests is that the "mafic dykes are assumed to be related to the Cameron River flows, which seems reasonable since they are roughly coincident in space and evidently about the same age ---". While there is no doubt that the sills within the Cameron River volcanic sequence are closely related in time to the flows, it is not necessarily true that the dykes have a similarly close temporal relationship with the flows. The following evidence suggests that the dykes post-date the main deformational phase affecting the Yellowknife Group and the concurrent intrusion of the Ross Lake granodiorite.

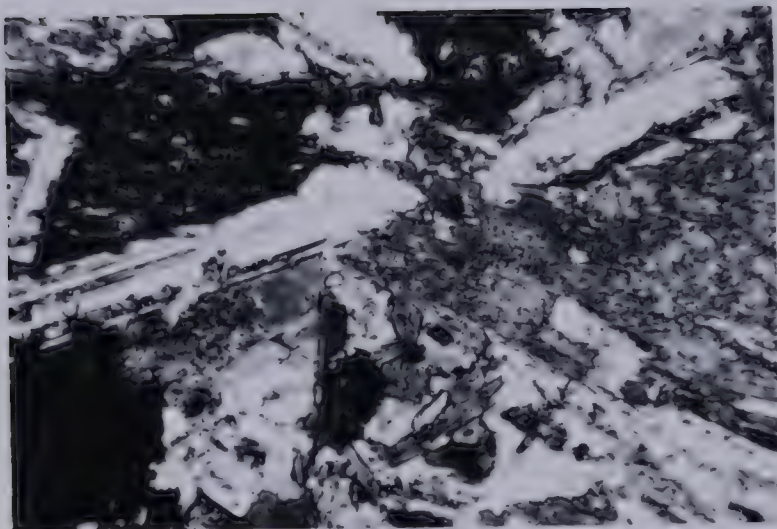
(1) The flows and sills are metamorphosed to at least upper albite epidote hornfels facies, and the contact aureole is related to the



PLATE 3



- (a) Metamorphosed basic sill, Cameron River volcanic belt, unit 1K of Edie, 1949.  
NOTE: Crystalloblastic texture, granular plagioclase (grey), quartz (white), biotite, opaque oxides, and chlorite (pale grey). Plain light, X 64. DCG 153.



- (b) Centre of basic dyke, cuts Ross Lake granodiorite,  $1\frac{1}{2}$  miles north of N. end, Ross Lake.  
NOTE: Plagioclase ( $An_{45}-An_{55}$ ), hornblende (dark grey), minor biotite, opaque oxides and chlorite.  
X nicols, X 64. DCG 160A



- (c) Bent albite twin lamellae; Oligoclase from margin of Ross Lake granodiorite. Thin section E1 (Edie, 1949).  
X nicols, X 64.



margin of the older gneissic granodiorite (Edie, 1949, p. 40). Thin sections of intrusives within the volcanic sequence have crystalloblastic textures, contain abundant sodic hornblende with ragged terminations, completely recrystallised and untwinned granular plagioclase, biotite and quartz. Epidote and chlorite are relatively uncommon, chlorite is a retrogressive phase (Plate 3a).

(2) Dykes within the gneissic granodiorite are fresh, have distinct chilled borders and are unfolded. Such metamorphic effects as are observed are related to the Redout Lake granite and associated pegmatites. Thin sections of a typical dyke some 5 miles west of the Redout Lake granite border but approximately 1 mile inside the western margin of the gneissic granodiorite have a distinctive igneous texture. Plate 3b shows fresh, sharply twinned plagioclase ( $An_{45-55}$ ) and hornblende in the form of large poikilitic plates which are occasionally twinned together with biotite, opaque oxides, quartz and epidote. Chlorite is again a retrogressive phase.

For these reasons, the writer retains the interpretation of Fortier (1947) and Henderson (1941). Isotope data presented in Chapter III is consistent with such a view.

### Plutonic Intrusives

#### Western Granodiorite

This mass extends from the contact with the greenstones west of Yellowknife Bay for over 50 miles to the Stagg River (which runs into the western end of Great Slave Lake). It is a massive, relatively homogeneous body ranging in composition from quartz diorite to adamellite (Table 5). The grain size is generally less than  $\frac{1}{4}$  inch, but porphyritic





Table 5.

## Modal Analyses of Rocks from the Western Granodiorite

|                | G48                    | G44                    | G33                    | G3                     | G18                    | G11                    | G5              | G32                 | G8          |
|----------------|------------------------|------------------------|------------------------|------------------------|------------------------|------------------------|-----------------|---------------------|-------------|
|                | Quartz<br>diorite<br>% | Grano-<br>diorite<br>% | Quartz<br>diorite<br>% | Quartz<br>diorite<br>% | Grano-<br>diorite<br>% | Grano-<br>diorite<br>% | Adamellite<br>% | Hybrid<br>rock<br>% | Aplite<br>% |
| Quartz         | 26.4                   | 38.6                   | 33.4                   | 31.1                   | 26.6                   | 26.6                   | 21.5            | 1.2                 | 36.3        |
| K-feldspar     | 5.2                    | 11.2                   | 5.7                    | 5.4                    | 13.4                   | 11.0                   | 34.6            | 1.6                 | 41.5        |
| Plagioclase    | 57.6                   | 42.6                   | 52.4                   | 46.6                   | 42.6                   | 53.0                   | 34.4            | 17.2                | 15.3        |
| Biotite        | 8.5                    | 5.0                    | 5.9                    | 6.7                    | 3.2                    | 6.8                    | 8.6             | 10.4                | -           |
| Chlorite       | 2.1                    | 1.2                    | 0.1                    | -                      | -                      | -                      | tr              | 3.0                 | 1.0         |
| Muscovite      | 1.0                    | 0.4                    | 1.0                    | -                      | -                      | 0.8                    | -               | -                   | 4.7         |
| Hornblende     | -                      | -                      | -                      | 6.5                    | 13.2                   | -                      | -               | 44.2                | -           |
| Opaque oxides  | 0.6                    | 0.6                    | 1.0                    | 1.6                    | 0.4                    | 0.9                    | 0.5             | 0.6                 | 1.1         |
| Apatite        | 0.4                    | 0.4                    | 0.2                    | 0.2                    | 0.6                    | tr                     | 0.4             | 1.6                 | 0.1         |
| Zircon         | tr                     | tr                     | tr                     | tr                     | tr                     | tr                     | tr              | -                   | tr          |
| Sphene         | 0.2                    | -                      | 0.3                    | 0.1                    | -                      | 0.1                    | -               | 2.2                 | -           |
| Epidote        | tr                     | -                      | -                      | 1.5                    | -                      | 0.8                    | tr              | 18.0                | -           |
| Garnet         | -                      | -                      | -                      | 0.3                    | -                      | -                      | -               | -                   | -           |
| Other minerals | zoisite,<br>pyrite     |                        |                        |                        |                        |                        |                 | sulphides           |             |
|                | 100.0                  | 100.0                  | 100.0                  | 100.0                  | 100.0                  | 100.0                  | 100.0           | 100.0               | 100.0       |





Table 6. Analyses, Western granodiorite  
(from Boyle, 1961)

|                                | Composite of<br>Western grano-<br>diorite in con-<br>tact zone<br>%        | Composite of<br>Western grano-<br>diorite 2 miles<br>from contact zone<br>% | Aplite (cuts grani-<br>tized amphibolite,<br>Ryan Lake)<br>% |
|--------------------------------|--|---|--|
| SiO <sub>2</sub>               | 72.95  | 75.92   | 78.80  |
| TiO <sub>2</sub>               | 0.19   | 0.07  | 0.31   |
| Al <sub>2</sub> O <sub>3</sub> | 14.11  | 13.46   | 10.73  |
| Fe <sub>2</sub> O <sub>3</sub> | 0.37   | 0.11  | 1.78   |
| FeO                            | 1.89   | 1.51  | 0.39   |
| MnO                            | 0.06   | 0.08  | 0.06   |
| MgO                            | 0.56   | 0.21  | 0.62   |
| CaO                            | 1.46   | 1.34  | 1.63   |
| Na <sub>2</sub> O              | 4.29   | 2.14  | 2.10   |
| K <sub>2</sub> O               | 2.80   | 4.17  | 2.43   |
| H <sub>2</sub> O <sup>-</sup>  | 0.69   | 0.69  | 0.27   |
| H <sub>2</sub> O <sup>+</sup>  | 0.06   | 0.08  | 0.26   |
| P <sub>2</sub> O <sub>5</sub>  | 0.06   | 0.10  | 0.15   |
| CO <sub>2</sub>                | 0.14   | tr  | tr   |
| Total                          | <u>99.68</u> (includes<br>0.05% Cl,<br>Cr <sub>2</sub> O <sub>3</sub> & S) | <u>99.92</u> (includes<br>0.04% S)  | <u>99.69</u> (includes<br>0.16% S)                           |
| less O = S, Cl                 | 0.01   | 0.02  | 0.06   |
| Net Total                      | <u>99.67</u>   | <u>99.90</u>  | <u>99.63</u>   |
| S.G.                           | 2.66   | 2.65  | 2.65   |
| Analyst:                       | J. A. Maxwell  | J. A. Maxwell   | J. A. Maxwell  |

C.I.P.W. Norms

|                  |              |              |              |
|------------------|--------------|--------------|--------------|
| Qz               | 32.54        | 43.39        | 53.30        |
| Or               | 16.54        | 24.64        | 14.36        |
| Ab               | 36.28        | 18.10        | 17.76        |
| An               | 5.96         | 5.99         | 7.11         |
| Co               | 1.84         | 3.23         | 2.04         |
| Hy (en           | 1.39         | 0.52         | 1.54)        |
| (fs              | 2.96         | 2.71         | - )          |
| Mt               | 0.54         | 0.16         | 0.55         |
| He               | -            | -            | 1.40         |
| Il               | 0.36         | 0.13         | 0.59         |
| Ap               | 0.14         | 0.24         | 0.36         |
| Ca               | 0.32         | -            | -            |
| H <sub>2</sub> O | <u>0.75</u>  | <u>0.77</u>  | <u>0.53</u>  |
| Total            | <u>99.63</u> | <u>99.89</u> | <u>99.54</u> |

PLATE 4



(a) Included angular blocks of metavolcanics (greenstone) in the marginal phase of the Western granodiorite. Kam Lake, 2 miles S.S.W. of Yellowknife.



(b) Inclusions of metavolcanics in the marginal phase of the Western granodiorite. Both units are cut, in turn, by an aplite dyke and a minor fault.



phases are developed locally. Aplite dykes up to 20 feet in thickness are relatively common near contacts with the Yellowknife Group. Pegmatites are rare.

In the southern part of the area, contacts with the Yellowknife Group are sharp. To the north, the contacts become more diffuse. The contact zone ranges from  $\frac{1}{2}$  mile to a few feet in width, and it is marked by many included blocks of greenstone (Plate 4) up to as much as 500 feet in size. Around Kam Lake the inclusions are angular, and show no evidence of reaction with the intruding magma, but on the shore of the west arm of Long Lake and west of Ryan Lake, evidence of assimilation is widespread.

A fresh surface is light grey or pale pink in colour, weathering red or white. Away from the contact zone there is little evidence of foliation although a very weak foliation trending north-northeast and dipping steeply west is occasionally observed in road cuttings along the Yellowknife Highway.

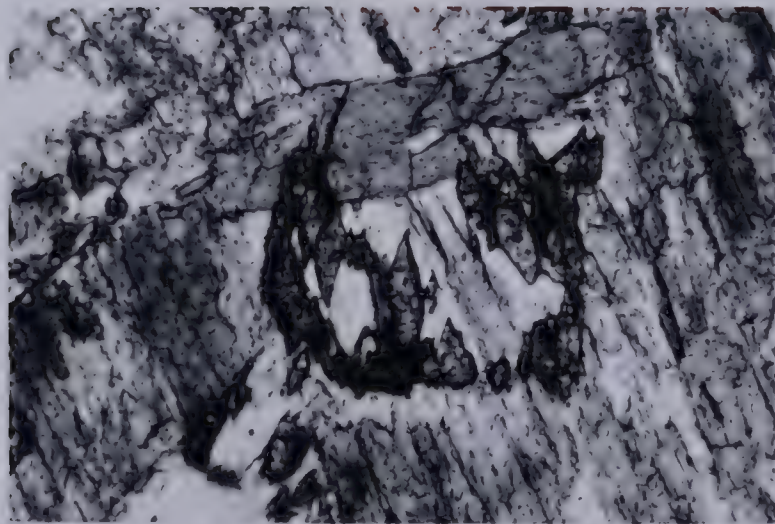
Modal analyses of typical rocks from this unit are presented in Table 5, and petrographic descriptions of the rocks used for dating may be found in Appendix 1. Analyses quoted by Boyle (1961, p. 71) are reproduced as Table 6. The nomenclature of these rocks poses a problem as the term granodiorite transgresses the silica - percentage boundary (66%) set up to separate acid from intermediate rocks in the classical scheme. Lindgren's (1900) original definition of granodiorite where K-feldspar forms between an eighth and one third of the total feldspar has been adopted as this corresponds to current North American usage. Where K-feldspar forms less than one eighth of the total feldspar and quartz more than 10%, the term quartz diorite is used, adamellites contain K-feldspar to the extent of between one third and two thirds of the total



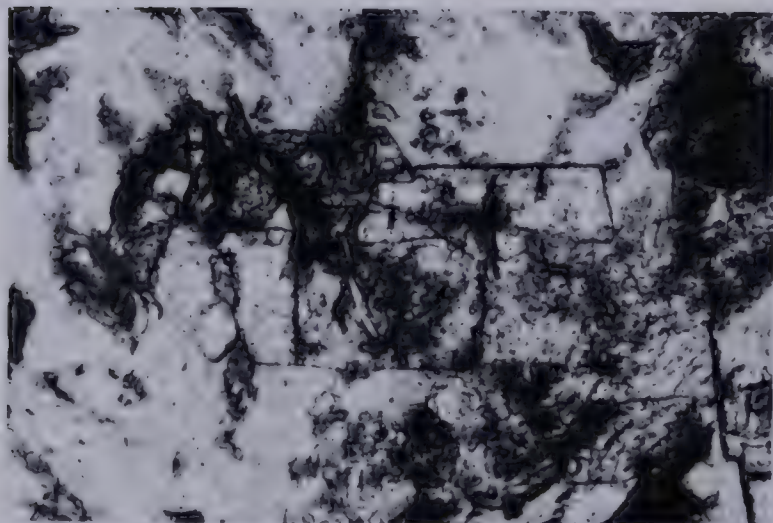
PLATE 5



(a) Rounded inclusions of contaminated wallrock in the marginal phase of the Western granodiorite, 400 yds. from west shore, Ryan Lake.  
NOTE: Development of K<sub>2</sub> feldspar porphyroblasts.



(b) Idiomorphic sphene in biotite. Contaminated hybrid rock, 500 yds. from west shore, Ryan Lake.  
Plain light, X 100, DCG 222.



(c) Epidote porphyroblast in chlorite (with minor opaque oxides). Contaminated hybrid rock, 500 yds. from west shore, Ryan Lake.  
Plain light, X 100, DCG 222.



feldspar. Other definitions of granodiorite are given by Knopf, 1957, p. 91.

Biotite and hornblende are common mafic minerals, and both were used for K-Ar dating. Biotite is often slightly chloritised, but hornblende is consistently fresh.

#### Contaminated (hybrid) rocks

West of Ryan Lake and in several other localities there is much evidence for contamination of the granodiorite with the greenstones. Boyle (1961, p. 72) describes the area near Ryan Lake as granitized and briefly discusses the chemical changes involved in the transformation of amphibolite to granite. This area contains a large pod of hybrid rock (DCG 32) which is cut by later phases of the Western granodiorite (DCG 33). Smaller pods of contaminated rocks show development of feldspar porphyroblasts (Plate 5a).

Six thin sections were examined in order to trace the progress of the reciprocal reaction between the granodiorite and amphibolite wall rocks. The most prominent feature is conversion of basic plagioclase ( $An_{55}$ ) to oligoclase ( $An_{25}$ ) with concomitant separation of prismatic, yellow epidote which forms subhedral crystals as much as 3 mms. in length. Hornblende with the usual pleochroic scheme  $\alpha$  = pale yellow-brown,  $\beta$  = yellow-green,  $\gamma$  = olive green is altered to a form with blue-green Z pleochroism. This is partially replaced by biotite and pale epidote. Opaque oxides are rimmed with granular sphene, which is also scattered through the ground-mass (Plate 5b). Apatite is unusually plentiful as acicular prisms, and the most advanced stages of contamination show introduction of nests of quartz. Plagioclase is partly altered to sericite. There is no development





Table 7. Analyses of hybrid rocks and an associated quartz diorite, Ryan Lake (from Boyle, 1961)

|                                | Amphibolite<br>%                    | Granitized<br>amphibolite<br>%      | Grey "granite"<br>(cf. DCG 33)<br>% |
|--------------------------------|-------------------------------------|-------------------------------------|-------------------------------------|
| SiO <sub>2</sub>               | 50.41                               | 52.87                               | 74.80                               |
| TiO <sub>2</sub>               | 0.79                                | 0.74                                | 0.36                                |
| Al <sub>2</sub> O <sub>3</sub> | 15.21                               | 13.02                               | 12.98                               |
| Fe <sub>2</sub> O <sub>3</sub> | 0.63                                | 1.30                                | 0.62                                |
| FeO                            | 11.65                               | 8.54                                | 1.40                                |
| MnO                            | 0.23                                | 0.19                                | 0.09                                |
| MgO                            | 7.02                                | 9.35                                | 0.06                                |
| CaO                            | 9.48                                | 8.65                                | 1.96                                |
| Na <sub>2</sub> O              | 1.64                                | 1.80                                | 2.85                                |
| K <sub>2</sub> O               | 0.74                                | 1.12                                | 3.17                                |
| H <sub>2</sub> O <sup>+</sup>  | 2.56                                | 1.89                                | 0.79                                |
| H <sub>2</sub> O <sup>-</sup>  | 0.05                                | 0.03                                | 0.08                                |
| P <sub>2</sub> O <sub>5</sub>  | 0.09                                | 0.20                                | 0.08                                |
| CO <sub>2</sub>                | 0.02                                | 0.35                                | 0.93                                |
| Total                          | <u>100.60</u><br>(includes 0.08% S) | <u>100.25</u><br>(includes 0.20% S) | <u>100.20</u><br>(includes 0.03% S) |
| less O = S                     | 0.03                                | 0.07                                | 0.01                                |
| Net total                      | <u>100.57</u>                       | <u>100.18</u>                       | <u>100.19</u>                       |
| S.G.                           | 2.95                                | 2.80                                | 2.70                                |
| Analyst:                       | R. J. C. Fabry                      | R. J. C. Fabry                      | R. J. C. Fabry                      |

C.I.P.W. Norms

|                  |               |               |               |
|------------------|---------------|---------------|---------------|
| Qz               | 1.59          | 4.22          | 43.83         |
| Or               | 4.37          | 6.62          | 18.73         |
| Ab               | 13.87         | 15.22         | 24.10         |
| An               | 31.96         | 24.14         | 3.32          |
| Co               | -             | -             | 3.65          |
| (wo              | 5.99          | 6.37          | - )           |
| Di (en           | 2.77          | 3.80          | - )           |
| (fs              | 3.17          | 2.24          | - )           |
| Hy (en           | 14.71         | 19.48         | 0.15)         |
| (fs              | 16.83         | 11.50         | 1.63)         |
| Mt               | 0.91          | 1.88          | 0.90          |
| Il               | 1.50          | 1.41          | 0.68          |
| Ap               | 0.21          | 0.47          | 0.19          |
| Ca               | 0.05          | 0.08          | 2.12          |
| H <sub>2</sub> O | <u>2.61</u>   | <u>1.92</u>   | <u>0.87</u>   |
| Total            | <u>100.53</u> | <u>100.06</u> | <u>100.17</u> |

PLATE 6



(a) Screens of amphibolitized volcanics and gabbros invaded by Western granodiorite. North shore, Long Lake.



(b) Polymictic conglomerate, Sub Islands, Yellowknife Bay. View is slightly oblique to the bedding plane which dips steeply east (Specks of orange lichen suggest a small amount of calcareous matrix).



(c) View southwest from Bush Pilots monument. Yellowknife Group metavolcanics in foreground, Yellowknife Bay in middle distance (right) and new town of Yellowknife in far distance.



of K-feldspar until the conversion of hornblende to biotite is complete. This usually occurs within a few inches of the contact. Complementary evidence of reaction lies in the decreased K-feldspar content of the granodiorites adjacent to the mixed zone and the presence of ragged xenocrysts of biotite.

The reactions described in the previous paragraph bear a remarkable similarity to those found in the classical locality of Lake Manipouri, New Zealand (Turner, 1937) and the border of the Coast Range batholith (Waters, 1938). Similar rocks (appinites) have also been investigated by Deer (1950) who favours a hybrid origin for marginal diorites because of the presence of two varieties of hornblende (the second of which is in equilibrium with acid plagioclase) and textural inhomogeneity.

Analyses of the amphibolite country rock, contaminated (granitized) amphibolite and granodiorites quoted by Boyle (1961, p. 72) are reproduced as Table 7 where they show clearly the effects of introduction of silica, alkalies and phosphorous into the amphibolite.

Additional field evidence for marginal contamination of the Western granodiorite is seen on the northwestern shore of Long Lake. Here granodiorite is intruded along the prominent northerly striking foliation in the amphibolites (Plate 6). This zone of intrusion is about 50 yards wide and persists inland for 200 yards. The mixed zone is replaced along strike by a zone of biotite - hornblende rich pods within the granodiorite.

#### Stock Lake stock

This body is ovoid in shape, 5,000 feet by 2,000 feet in size





and thought to be an apophysis of the Western granodiorite. The stock has been described in detail by Kelly (1964) and the following description is a summary of his work. Stock Lake stock intrudes Division A of the Yellowknife Group approximately  $1\frac{1}{2}$  miles north of the town of Yellowknife.

Modal analyses from over 100 samples indicate a compositional range from quartz diorite to quartz monzonite (adamellite). A slight gap exists between the two extreme modal compositions. Contact effects are minimal as the stock intrudes the contact zone (almandine-amphibolite facies) of the Yellowknife Group metavolcanics.

Modal analyses of three typical rocks are reproduced as Table 8.

Table 8. Modal analyses, Stock Lake stock

|                | K77            | K182         | DGG 50                           |
|----------------|----------------|--------------|----------------------------------|
| Quartz         | 32.2%          | 26.2%        | 36.6%                            |
| K-feldspar     | 4.2            | 12.6         | 34.0                             |
| Plagioclase    | 56.0           | 58.0         | 27.0                             |
| Biotite        | 3.2            | 3.0          | 1.0                              |
| Sericite       | 1.0            | 0.1          | 0.6                              |
| Opaque oxides  | 0.2            | 0.1          | 0.6                              |
| Apatite        | -              | -            | 0.2                              |
| Other minerals | 3.2            | -            | -                                |
|                | 100.0          | 100.0        | 100.0                            |
|                | Quartz diorite | Granodiorite | Quartz monzonite<br>(Adamellite) |

#### South-east granodiorite

This body occurs on the east side of Yellowknife Bay, is some 40 miles in maximum width and intrudes the volcanics and sediments of the Yellowknife Group. The western section has the composition of a quartz diorite and contains many metavolcanic xenoliths, but the greater part of





the mass is a biotite-bearing granodiorite.

Van Breeman (1965) used a block of typical biotite granodiorite for Rb-Sr thermal migration experiments. An accurate mode made by Van Breeman from 11 thin sections is reported below together with a mode of a more basic phase. Analyses of the two rocks are also recorded (Folinsbee et al., 1968).

The analyses are noteworthy for their high soda content and are more akin to trondhjemites than normal granodiorites. There is, however, no justification for adopting the generic name as the colour index is somewhat higher than that usually assigned to trondhjemites ( $< 10\%$ ). The term tonalite is avoided in this thesis because of the very different restrictions on composition placed on this term by various authors. The original tonalite (Monte Tonale) contains quartz as an essential, but minor modal constituent ( $< 10\%$ ), Johannsen (1931), however, does not restrict the amount of quartz and stresses the near absence of K-feldspar.

Because of the generally concordant nature of the contacts, with sediments and volcanic rocks dipping steeply away from the granodiorite, Buddington (1959, p. 705) interpreted this body as a pluton of the mesozone. As such, the South-east granodiorite was thought to have been emplaced into both the volcanics and sediments of the Yellowknife Group. It has recently been suggested (Folinsbee et al., 1968) that the sodic granodiorites were emplaced and unroofed before deposition of the unclassified conglomerate horizon. There is no doubt that boulders of the South-east granodiorite form a substantial part of the clastic fraction of the conglomerate horizon in the Sub Islands. If these outcrops are stratigraphically equivalent to those at the north end of Yellowknife Bay, it must be concluded that the South-east granodiorite predates at least part of the Yellowknife Group.



Table 9. Analyses, South-east granddiorite

|                                |        |                      | C.I.P.W. Norms   |        |       |
|--------------------------------|--------|----------------------|------------------|--------|-------|
| (a) DCG 120                    |        | (b) O.V.B.<br>(1965) |                  |        |       |
|                                |        |                      | (a)              | (b)    |       |
| SiO <sub>2</sub>               | 59.45% | 65.90%               | Qz               | 8.92   | 20.34 |
| TiO <sub>2</sub>               | 0.80   | 0.51                 | Or               | 9.69   | 18.91 |
| Al <sub>2</sub> O <sub>3</sub> | 19.02  | 16.34                | Ab               | 38.91  | 33.83 |
| Fe <sub>2</sub> O <sub>3</sub> | 0.78   | 0.44                 | An               | 26.41  | 12.67 |
| FeO                            | 4.56   | 4.01                 | Co               | -      | -     |
| MnO                            | 0.08   | 0.04                 |                  | ( 0.22 | - )   |
| MgO                            | 2.02   | 1.18                 | Di               | ( 0.09 | - )   |
| CaO                            | 5.69   | 2.87                 |                  | ( 0.12 | - )   |
| Na <sub>2</sub> O              | 4.60   | 4.00                 | Hy               | ( 4.94 | 2.94  |
| K <sub>2</sub> O               | 1.64   | 3.20                 |                  | ( 6.43 | 6.23  |
| H <sub>2</sub> O <sup>+</sup>  | 0.82   | 1.08                 | Mt               | 1.13   | 0.64  |
| H <sub>2</sub> O <sup>-</sup>  | 0.06   | 0.06                 | Il               | 1.52   | 0.97  |
| P <sub>2</sub> O <sub>5</sub>  | 0.14   | 0.24                 | Ap               | 0.33   | 0.57  |
| CO <sub>2</sub>                | 0.06   | n.d.                 | Cal              | 0.14   | -     |
| Cl                             | 0.04   | n.d.                 | H <sub>2</sub> O | 0.88   | 1.14  |
| S                              | 0.03   | n.d.                 |                  |        |       |
| Total                          | 99.79  | 99.87                | Total            | 99.73  | 99.88 |
| - O = S, Cl                    | .02    | -                    |                  |        |       |
|                                | 99.77  | 99.87                |                  |        |       |

Analysts: D. Thaemlitz (University of Minnesota), O. Van Breeman (University of Alberta).

| Modes         | (b)           | (a)            |
|---------------|---------------|----------------|
| Quartz        | 28.39         | 12.0           |
| K-feldspar    | 2.58          | 0.6            |
| Plagioclase   | 53.57         | 56.8           |
|               | (sericitized) |                |
| Biotite       | 13.67         | 11.6           |
| Chlorite      | 0.10          | -              |
| Hornblende    | -             | 15.2           |
| Opaque oxides | 0.18          | 1.1            |
| Apatite       | 0.23          | 0.5            |
| Zircon        | 0.06          | 0.05           |
| Sphene        | 0.51          | -              |
| Epidote       | 0.54          | 2.2            |
|               |               | (clinozoisite) |
| Calcite       | 0.15          | -              |
| Pyrite        | 0.02          | -              |
|               | 100.00        | 100.05         |





The intrusive relationships on the western side of the South-east granodiorite may therefore be more apparent than real. Buddington (op. cit. p. 706) makes particular note of the discordant boundary zone of metamorphism which appears unrelated to the early granodiorite mass.

The conclusions offered in the previous paragraph are supported by evidence from radiometric dating but require study in the field to establish their validity.

#### Ross Lake granodiorite

Prior to 1937, the two granitic bodies in this area, approximately 45 miles east-northeast of Yellowknife, were not distinguished. Henderson (1941) classified the older rock as biotite granodiorite and the younger (Redout Lake granite) as muscovite granite. Field evidence of the relationship between the Ross Lake granodiorite and the Redout Lake granite is best exposed between Ross and Redout Lakes (see Fig. 4) where hundreds of north-westerly trending basic dykes (which intrude the older body) are intersected by rare element-bearing pegmatites and the main mass of younger muscovite granite.

The Ross Lake granodiorite has a distinctive gneissic structure which varies in degree of development but is nowhere absent. For reasons given previously, this body probably intrudes the Cameron River volcanics and at least the basal part of the Yellowknife Group sediments although the contact is poorly exposed. The western margin near the northern extremity of Ross Lake contains large metasedimentary schist inclusions as well as the characteristic hornblende-biotite schist inclusions which Fortier (1947) regarded as a product of contamination by the basic flows. The north-westerly trending basic dykes strike approximately parallel to





Table 10. Analyses, Ross Lake granodiorite

|                                | <u>%</u>     |                  | <u>C.I.P.W. Norm</u> |
|--------------------------------|--------------|------------------|----------------------|
| SiO <sub>2</sub>               | 71.15        | Qz               | 47.94%               |
| TiO <sub>2</sub>               | 0.28         | Or               | 16.48                |
| Al <sub>2</sub> O <sub>3</sub> | 14.92        | Ab               | 37.89                |
| Fe <sub>2</sub> O <sub>3</sub> | 0.31         | An               | 6.01                 |
| FeO                            | 1.99         | Co               | 2.33                 |
| MnO                            | 0.05         | Hy (En           | 2.54)                |
| MgO                            | 1.02         | (Fs              | 3.03)                |
| CaO                            | 1.70         | Mt               | 0.45                 |
| Na <sub>2</sub> O              | 4.48         | Il               | 0.53                 |
| K <sub>2</sub> O               | 2.79         | Ap               | 0.19                 |
| H <sub>2</sub> O <sup>+</sup>  | 0.68         | Ca               | 0.68                 |
| H <sub>2</sub> O <sup>-</sup>  | 0.04         | H <sub>2</sub> O | 0.72                 |
| P <sub>2</sub> O <sub>5</sub>  | 0.08         |                  |                      |
| CO <sub>2</sub>                | <u>0.30</u>  |                  |                      |
| Total                          | <u>99.79</u> | Total            | <u>99.79</u>         |

Analyst: Eileen H. Kane

|                   | <u>Mode</u>  |
|-------------------|--------------|
| Sodic plagioclase | 47.9%        |
| K-feldspar        | 9.5          |
| Quartz            | 29.1         |
| Biotite           | 7.8          |
| Sericite          | 5.5          |
| Chlorite          | <u>0.2</u>   |
| Total             | <u>100.0</u> |



the trend of schist inclusions in the granodiorite.

Edie (1949) described the granodiorite near the contact between the metavolcanics and the granodiorite as a gneissic sodaclase granodiorite. Re-examination of the rock specimen (E1) described by Edie does not support the use of the term sodaclase (in the sense of Johannsen, 1931- Ab<sub>100</sub> to Ab<sub>90</sub>) although primary plagioclase phenocrysts are normally zoned towards albite at the perimeter. A series of careful extinction angle measurements in the zone normal to a suggests a plagioclase composition of An<sub>27</sub> to An<sub>13</sub>, the  $n_p$  refractive index of the calcic cores is slightly greater than the Lakeside mounting medium ( $n = 1.54$ ) and comparable with  $n_w$  of adjoining quartz grains.

Table 10 shows an analysis, C.I.P.W. norm and mode of the rock analysed by Edie (1949).

To the east of the contact, the granitic rocks become more potassic and are classified as adamellite and granite (DCG 259). In this property they are similar to the Western granodiorite of the Yellowknife area which also shows an increase in K<sub>2</sub>O/Na<sub>2</sub>O ratio with increasing distance from the metavolcanic - granodiorite boundary.

Although an attempt was made to avoid specimens showing evidence of hydrothermal alteration from the later pegmatite-forming event, a study of the thin sections shows that this is difficult. In particular, two lines of evidence support the probability that there has been a substantial contribution of potassium. Plagioclase is extensively sericitized and recrystallisation of the sericite forms muscovite porphyroblasts within the altered plagioclase. In addition, some K-feldspar porphyroblasts contain rounded inclusions of sodic plagioclase. Adjacent to Redout Lake, the effects of potash introduction are





megascopically visible in the form of microcline porphyroblasts near pegmatite bodies. However, sample DCG 259 was collected over half a mile north of the nearest outcrop of Redout Lake granite, and the microcline in this specimen is believed to be original.

#### Redout Lake granite and associated pegmatites

The Redout Lake granite forms a large stock which is completely surrounded by the older Ross Lake granodiorite. In the field, this rock is uniform in appearance and consists of a pink coloured, medium grained, holocrystalline muscovite-bearing adamellite. Thin sections indicate that approximately equal amounts of fresh oligoclase (zoned  $An_{22}$  to  $An_3$ ) and microcline microperthite are present, belying the immediate field impression of a true granite. Hamilton (1948) records the following mode for a typical specimen of this body. Quartz 21%, microcline microperthite 31%, oligoclase-albite 38%, biotite 8% and muscovite 2%. These proportions differ only slightly from the specimen examined in this study (DCG 258).

Most attention was paid to the spectacular pegmatite bodies for which Hutchinson (1955) demonstrates a genetic relationship with the Redout Lake granite. The pegmatites are spatially zoned around the younger granite mass with simple replacement pegmatites near the Redout Lake granite and discordant rare element-bearing pegmatites in successive zones outward from the central granite. In general, lithium-bearing pegmatites are farthest removed, followed by columbium and tantalum-bearing bodies with beryllium rich pegmatites closest to the parent granite.

Hutchinson (1955) suggests that the "original differentiate --- may have been an alkali-bearing aqueous solution rich only in potassium, the volatiles and the rare elements. This solution affected the wholesale





reorganisation of the country rocks to form giant pegmatites by replacement near the batholith. Sodium, displaced from the plagioclase of the original rock by potassium, as well as silicon and aluminium were added to the migrating pegmatitic emanations. These emanations continued to move outward and eventually formed the fluid emplaced pegmatites, farthest from the batholith".

Such a scheme explains the prevalence of sodium in the form of cleavelandite in the later-formed pegmatites. There is considerable evidence for the reprecipitation of calcium as tremolite, epidote and sphene (especially DCG 253-255) after its initial displacement by the addition of potassium to the wallrocks. However, the zonation of plagioclase composition can also be simply explained in terms of Bowen's reaction series for crystallisation of a silicate melt under conditions of falling temperature.

Very satisfactory samples of biotite and muscovite for K-Ar dating were obtained from blasted pits where pegmatites have been tested for columbite-tantalite, tapiolite, beryl and spodumene. An extensive collection of columbite-tantalite and tapiolite specimens was also made for future U-Pb dating.

#### Prosperous Lake granite and associated pegmatites

This mass is part of an area of over 1,000 square miles underlain by a fine to medium-grained pink "granite" and associated pegmatites. The country rocks are metasediments of the Yellowknife Group, Division B. Again the term "granite" cannot be applied in the strict sense as modal analyses show approximately equivalent amounts of K-feldspar and oligoclase. Boyle (1961, p. 71) reports between 30 to 35% quartz,



Table 11. Analyses, Prosperous Lake granite

|                                | 1. Baadsgaard<br>(pers. comm.)<br>% | 2. Folinsbee<br>et al. (1968)<br>%     | Composite sample,<br>Boyle, 1961<br>% |
|--------------------------------|-------------------------------------|--|---------------------------------------|
| SiO <sub>2</sub>               | 74.09                               | 73.86                                  | 74.28                                 |
| TiO <sub>2</sub>               | 0.14                                | 0.11                                   | 0.07                                  |
| Al <sub>2</sub> O <sub>3</sub> | 14.30                               | 14.57                                  | 14.38                                 |
| Fe <sub>2</sub> O <sub>3</sub> | 0.18                                | 0.29                                   | 0.32                                  |
| FeO                            | 0.99                                | 0.83                                   | 0.77                                  |
| MnO                            | 0.02                                | 0.04                                   | 0.04                                  |
| MgO                            | 0.31                                | 0.30                                   | 0.16                                  |
| CaO                            | 0.82                                | 0.66                                   | 0.60                                  |
| Na <sub>2</sub> O              | 3.61                                | 3.50                                   | 4.18                                  |
| K <sub>2</sub> O               | 5.08                                | 4.88                                   | 4.15                                  |
| P <sub>2</sub> O <sub>5</sub>  | 0.26                                | 0.27                                   | 0.11                                  |
| H <sub>2</sub> O <sup>+</sup>  | 0.23                                | 0.47                                   | 0.42                                  |
| H <sub>2</sub> O <sup>-</sup>  | 0.04                                | 0.02                                   | 0.01                                  |
| CO <sub>2</sub>                | n.d.                                | 0.04                                   | 0.18                                  |
| Total                          | <u>100.07</u>                       | <u>99.94</u><br>(includes 0.10% F, Cl) | <u>99.69</u><br>(includes 0.02% Cl)   |
| less O = F, Cl, S              | -                                   | 0.04                                   | -                                     |
| Net Total                      | <u>100.07</u>                       | <u>99.94</u>                           | <u>99.69</u>                          |

Analysts: L. R. Campbell, A. Rich D. Thaemlitz J. A. Maxwell  
and L. Yopik, U. of A.

C.I.P.W. Norms

|                  |               |              |              |
|------------------|---------------|--------------|--------------|
| Qz               | 31.51         | 33.32        | 32.88        |
| Or               | 30.01         | 28.83        | 24.52        |
| Ab               | 30.53         | 29.60        | 35.35        |
| An               | 2.37          | 1.26         | 1.12         |
| Co               | 2.00          | 3.07         | 2.60         |
| Hy (En           | 2.25          | 0.75         | 0.40)        |
| (Fs              |               | 1.18         | 1.11)        |
| Mt               | 0.26          | 0.42         | 0.46         |
| Il               | 0.27          | 0.21         | 0.13         |
| Ap               | 0.62          | 0.64         | 0.26         |
| Ca               | -             | 0.09         | 0.41         |
| H <sub>2</sub> O | 0.27          | 0.49         | 0.43         |
| Total            | <u>100.09</u> | <u>99.86</u> | <u>99.68</u> |





25 to 30% microcline, 20 to 25% oligoclase, 5 to 10% muscovite and 5 to 10% biotite. A sample selected for thermal migration experiments by Dr. H. Baadsgaard has been analysed in triplicate and the analysis, C.I.P.W. norm and mode are recorded in Tables 11 and 12. Analyses quoted by Folinsbee et al., (1968) and Boyle (1961) are also quoted.

Table 12.

| Mode of analysed Prosperous Lake<br>granite sample used in thermal<br>migration experiments |       | Mode of small stock on west side of<br>Prosperous Lake |       |
|---|-------|--|-------|
| Quartz  | 37.4% | Quartz   | 29.8% |
| K-feldspar  | 25.9  | K-feldspar   | 14.4  |
| Plagioclase (An <sub>13</sub> )   | 21.7  | Plagioclase (An <sub>30</sub> -An <sub>25</sub> )      | 36.0  |
| Biotite   | 1.7   | Biotite  | 16.8  |
| Muscovite   | 12.5  | Chlorite   | 0.6   |
| Opaque oxides   | 0.3   | Sericite   | 0.2   |
| Apatite   | 0.2   | Opaque oxides  | 1.1   |
| Garnet (almandine)  | 0.3   | (including pyrrhotite and<br>arsenopyrite)             |       |
|   |       | Haematite  | 0.4   |
|   |       | Sphene   | 0.2   |
| TOTAL   | 100.0 | TOTAL  | 100.0 |

The similarity of these three analyses from different areas is striking. For this reason, it has not been possible to use the whole rock isochron method to date this body as there is insufficient Rb/Sr variation in the whole rock samples. Almandine garnets are ubiquitous and appear to be similar to those described by Folinsbee (1942) from the metasediments. Together with the diffuse nature of the contacts with the country rock there is some evidence that partial anatexis of the Yellowknife Group sediments contributed to the formation of the Prosperous Lake granite. This interpretation is consistent with the initial  $^{87}\text{Sr}/^{86}\text{Sr}$  ratio reported for this body in Chapter III.

Pegmatites form almost half of the Prosperous Lake granite





mass, and they are concentrated near the margin. Many are dyke-like in form and have relatively sharp contact with the granite. Most pegmatites are simple and contain quartz, microcline (near maximum microcline, Baadsgaard et al., 1961), cleavelandite, muscovite, tourmaline and garnet. A few complex pegmatites contain beryl, spodumene, amblygonite, scheelite and columbo-tantalites. The complex pegmatites tend to be clustered immediately outside the margin of the main body.

It is difficult to obtain clean biotite concentrates for K-Ar work from this mass as there is a slight pervasive chloritization which has affected each sample to some degree.

A small stock occurs on the west side of Prosperous Lake. This body has been tentatively grouped with the Prosperous Lake granite but is more calcic in character (see mode, Table 12) and is particularly rich in pyrrhotite and arsenopyrite.

#### Quartz Feldspar Porphyries

Fresh specimens of the quartz feldspar porphyries contain quartz and plagioclase (approx. An<sub>23</sub>) phenocrysts in a fine grained ground-mass of quartz, sericite, carbonates and chloritized biotite flakes. Sulphides are relatively common and other accessory minerals include apatite, epidote and rare zircon. They form dykes and small irregular masses, but are often continuous for up to a mile (e.g. north of Daigle Lake to Walsh Lake). Although they do not appear to cut the Western granodiorite, they carry angular fragments of the metavolcanics and in one instance an altered fragment of granitoid composition. They appear to post-date the first main folding phase but are extensively sheared by the transecting shear zones carrying the gold mineralization. Boyle





(1961, p. 74) notes the similarity in soda to potash ratio between a composite sample of the quartz feldspar porphyries and the marginal part of the Western granodiorite.

#### Proterozoic Diabase Dykes and Differentiated Picrite Sill

Mafic dykes are a common post orogenic feature of every major Precambrian shield area. Those in the Yellowknife area are but a segment of a tholeiitic swarm which may be extended through the Ungava Peninsula, south Greenland and northwestern Scotland (Payne et al., 1965) to give possible independent confirmation of the hypothesis of continental drift.

Four sets of dykes within the Slave Province were established by Burwash et al., (1963) during preliminary K-Ar dating. Set I consists of large (100-200 feet wide) dykes striking N 70°E to E - W, Sets II and IV are less important, striking N - S to N 30°W and N 45°W - N 60°W respectively and Set III forms dyke swarms striking N 10°W to N 30°W. Set III are the youngest on structural grounds and have been related to the Keewanawan extrusives of Ontario and northern Minnesota. Burwash et al. dated Set III as between 1,000 and 1,100 m.y., Set II as 1,400-1,600 m.y. and Set I as 1,800-2,000 and 2,220-2,400 m.y. Leech (1966) extended this work and found three periods of diabase dyke intrusion, viz. 2,200-2,400 m.y., 1,100-1,200 m.y. and 600-700 m.y. The youngest set of dykes (Set III) are not represented in the Yellowknife district. There is considerable scatter in the 66 dates recorded by Leech, and it is not yet established why the K-Ar mineral dates are consistently 300 to 400 m.y. older than the dates given by some whole rock samples from the older dyke sets. Post dyke faulting is widespread, and it is possible





that some of the dates represent reflections of younger thermal events. In addition, error limits imposed by potassium determinations are considerable at low K contents (see Appendix 6).

The mineralogy of the diabase dykes is uniform and simple. Plagioclase (An<sub>80</sub>-An<sub>55</sub>) and pyroxene (augite-pigeonite) form over 80% of the rock, commonly in an ophitic or subophitic texture. Some samples are particularly fresh, but olivine (approx. 10%) is rather commonly altered to mesh-like antigorite + magnetite. An interstitial granophyric intergrowth contains quartz, alkali feldspar and opaque oxides. Apatite, haematite, leucoxene and carbonates are accessory minerals.

The Yellowknife differentiated sill is described by Hill (1940) and Leech (1966). This body consists of olivine gabbro (picrite) and quartz gabbro segments separated by a fault zone. Dates range from 1,490 to 2,090 m.y. (on biotite from the contact zone), and the differentiated body is possibly related to the dykes forming Sets II and IV.

### Structure

Yellowknife Group metavolcanics and metasediments occupy complexly folded structural basins bordered by granitic intrusives. The original structural relationships are largely obscured by later folding and at least two periods of faulting. The metavolcanic rocks dip steeply away from the bordering granitic masses to form nearly homoclinal successions broken only by early shear zones and late transcurrent faults. The metasedimentary rocks form a series of refolded isoclinal folds expressed as domes and canoe-shaped synclines. This difference in folding style is probably the result of the competent nature of the massive volcanic horizons as opposed to the incompetent character of the





argillites and slates of the Division B sediments.

The complex pattern of faulting and fracturing has been discussed exhaustively by Boyle (1961) and others. Only a brief summary is given here as the geochronology programme was planned to avoid faulted and sheared areas. Two major periods of faulting were first distinguished by Henderson and Brown (1950). The early shear zones range from those which are parallel to the flow boundaries to those which transect the flows at angles of up to  $45^{\circ}$ . The shear zones vary from highly altered schist zones up to hundreds of feet wide to breccia-filled zones in more massive rocks. The shear zone systems which transect the flow boundaries are most important from an economic viewpoint as they contain most of the gold mineralization (e.g. Con, Negus-Rycon and Giant-Campbell systems). Boyle (op. cit. p. 31) concludes that the early shear zones were produced during thrust faulting which occurred simultaneously with the emplacement of the Western granodiorite. The shear zones are also controlled by an axial plane cleavage which is generally near vertical in attitude. Since some early shear zones cut the granodiorite-metavolcanic contact, the shearing continued after the emplacement of the granodiorite.

Early fracturing in the sedimentary rocks takes the form of fracturing parallel to the contorted bedding planes, along axial portions of folds and as saddle reefs (e.g. Ptarmigan and Camlaren systems).

Major late faults are concentrated in the Yellowknife Bay area (Brown, 1955). They are narrow fractures, rarely more than a few feet wide along which horizontal movements of over three miles have taken place. The strike of seven major faults in the Yellowknife area is between  $N 10^{\circ}W$  and  $N 40^{\circ}W$ . Their dip is generally vertical. Many





secondary faults link the major faults and almost all have a left hand sense of movement.

Since the strike separations of variously dipping marker horizons such as late diabase dykes, tuff bands and early mafic intrusives are similar, the net slip movement is very nearly horizontal. The net slip along part of the West Bay fault was calculated by Campbell (1948) as west side south 16,140 feet and down 1,570 feet relative to the east side. Brown (1955) obtained similar results using different marker horizons. Both Brown and Badgely (1965) have attempted to analyse the pattern of late faulting; Brown used the concept of stress-strain ellipsoids and Badgely applied the McKinstry (1953) stress reorientation model. Their conclusions are consistent and show the maximum principal stress lying in a horizontal plane and trending NW, the minimum principal stress is at right angles and also in a horizontal plane while the mean principal stress lies in the vertical plane.

Although Badgely (op. cit., p. 274) discusses the work of R. W. Boyle (1961) in a section entitled "Relationship of strike-slip faults to igneous activity and to ore mineralization", there is no economic mineralization associated with the late strike-slip faults. Rather, the dilatant ore zones described by Boyle are associated with the early west-dipping reverse dip-slip (thrust) faults. The ore shoots are localized in shear zone junctions, flexures or rolls in the wall zones and in dragfolded axial zones.

It is difficult to determine the age relations between the faults and diabase dykes unequivocally, but it is possible that the faulting could be approximately contemporaneous with the NW trending diabase dykes (Set IV, Burwash et al., 1963, Leech, 1966). These dykes





tend to run along the late fault zones and may be either sheared by, or chilled against fault gouge. Burwash et al., (op. cit.) dated Set II dykes, thought to be a conjugate to Set IV, at approximately 1,100 m.y. but Leech (op. cit.) recorded dates as old as 2,000 m.y. from Set IV.

The western margin of the Western granodiorite intrudes west-facing basic metavolcanics and conformably overlying paraconglomerates, feldspathic greywackes and shales. The total thickness of the Yellowknife Group in this area varies from over 20,000 feet near Arseno Lake to less than 4,000 feet further north (McGlynn and Ross, 1963). Lord (1942) found no trace of pre-Yellowknife Group boulders in the paraconglomerate horizon.

In this area, the Yellowknife Group is intruded by granodiorite and adamellite plutons belonging to both Archaean and Proterozoic orogenic episodes. In general, the granitic rocks east of the Emile River are Archaean, and those to the west are Proterozoic, but they are only able to be differentiated where their contact relations with the Proterozoic Snare Group have been determined. The detailed structural analysis by Ross and McGlynn (1963, 1965), which has thrown considerable light on the problem, need not be considered further as the critical areas are north of the area of interest. However, it does serve to emphasize the encroachment onto the western margin of the Slave Province by the Hudsonian orogeny of the Bear Province.





## Metamorphism

The most complete treatment of the metamorphic history of the Yellowknife area is that of Folinsbee (1942). Boyle (1961) has described the metamorphic facies within the Yellowknife metavolcanic belt, and Edie (1949) deals with the Cameron River metavolcanics. Three major metamorphic episodes are distinguished by Folinsbee (op. cit.); (a) an early regional metamorphism, followed closely by (b) a thermal event and (c) a later hydrothermal, retrograde metamorphism.

Because of the varying terminology relating to the metamorphic facies represented in the area it has been necessary to adopt a single facies classification. That of Winkler (1965) has been used since it is a readily available compilation of the most recent developments in the concept of metamorphic facies.

In areas well removed from the plutonic intrusives, the metavolcanics and metasediments may be assigned to the quartz - albite - muscovite - chlorite subfacies of the greenschist facies. The occurrence of chloritoid suggests that the low grade regional assemblage belongs to a Barrovian type facies series. However, the higher grade metamorphic rocks cannot be interpreted in terms of the standard Barrovian sequence because of the presence of cordierite as the most common metacrysts in the massive knotted rocks. The characteristic presence of andalusite and the absence of kyanite in the higher grade rocks suggests that the metamorphism passes into the andalusite - sillimanite or Abukuma-type facies proposed by Miyashiro (1961). This supposition is supported by the comparative absence of almandine in the metamorphosed basic rocks while it is relatively common in the high grade pelitic assemblages. Since the subfacies of Abukuma type closely resemble the subfacies of





contact metamorphism, the highest grade knotted schists and metavolcanics may be placed in either the sillimanite - cordierite - muscovite - almandine subfacies or the upper part of the hornblende - hornfels facies.

Sillimanite is present in the inner part of the thermal aureole surrounding the Prosperous Lake granite, where it coexists with muscovite rather than the orthoclase of the pyroxene hornfels facies. It is suggested, therefore, that the operating pressure was intermediate between that which results in the classic Barrovian sequence and the low pressures of contact metamorphism. This conclusion follows from the negative slope of the andalusite - sillimanite phase boundary and demonstrates the near identity of deep-seated contact metamorphism and low pressure regional metamorphism. Recent experimental work suggests that the pressure required for such an assemblage could be as low as 4 kb., supporting the contention of Folinsbee (op. cit.) that the Prosperous Lake granite was emplaced under conditions of low pressure. Similar assemblages in K-poor, Al-rich pelites are recorded by Read (1952, Buchan type) and Zwart, (1962, Bosost type).

Boyle (1961, p. 66) shows that the metavolcanics adjacent to the Western granodiorite display three regional metamorphic facies. The facies are apparently used in the sense of Eskola (1939). A narrow zone of almandine - amphibolite facies (staurolite - almandine subfacies?) parallels the margin of the granodiorite. Characterised by the stable occurrence of andesine + epidote + blue-green hornblende, this assemblage is typical of regional rather than contact metamorphism because epidote does not persist into the hornblende - hornfels facies. This narrow zone passes rapidly into a broad zone called the epidote amphibolite facies by Boyle.





The epidote amphibolite facies was renamed the quartz - albite - epidote - almandine subfacies by Fyfe et al., (1958) and included in the greenschist facies as the highest temperature member because oligoclase is not yet a stable phase. For this reason, the reported stable occurrence of oligoclase and actinolite in the epidote-actinolite zone is anomalous. Turner and Verhoogen (1960) also define the boundary of the greenschist and almandine - amphibolite facies in terms of the albite ( $< \text{An}_7$ ) - oligoclase ( $> \text{An}_{15}$ ) transition and the disappearance of chlorite in the higher temperature facies. Hornblende is already a stable phase in the uppermost greenschist facies, and it is impossible to interpret the assemblages reported by Boyle (op. cit.) in terms of the Barrovian-type facies series. The stable actinolite + epidote + oligoclase + chlorite + quartz assemblage reported by Boyle may be attributed to the quartz - andalusite - plagioclase - chlorite subfacies of the upper part of the greenschist facies in the Abukuma-type series. This supposition rests on the adequate identification of oligoclase in the metavolcanics and metagabbros. A limited number of refractive index measurements on untwinned plagioclases from thin-sections tend to confirm Boyle's identification. Very little of the metavolcanic sequence falls in the lower greenschist facies.

Edie (1949) interprets the Cameron River metavolcanics in terms of the classic Barrovian zones of Tilley (1924). His conclusions are similar to those already reached. On the basis of "isograds"\* expressing the ratio of hornblende to total hornblende + chlorite, he found a rather striking degree of correspondence between the "isograd"\* boundaries and the outer limit of the Ross Lake granodiorite (Fig. 5).

---

\* quotation marks added by the present author to indicate that the terms are used in a generalized sense.





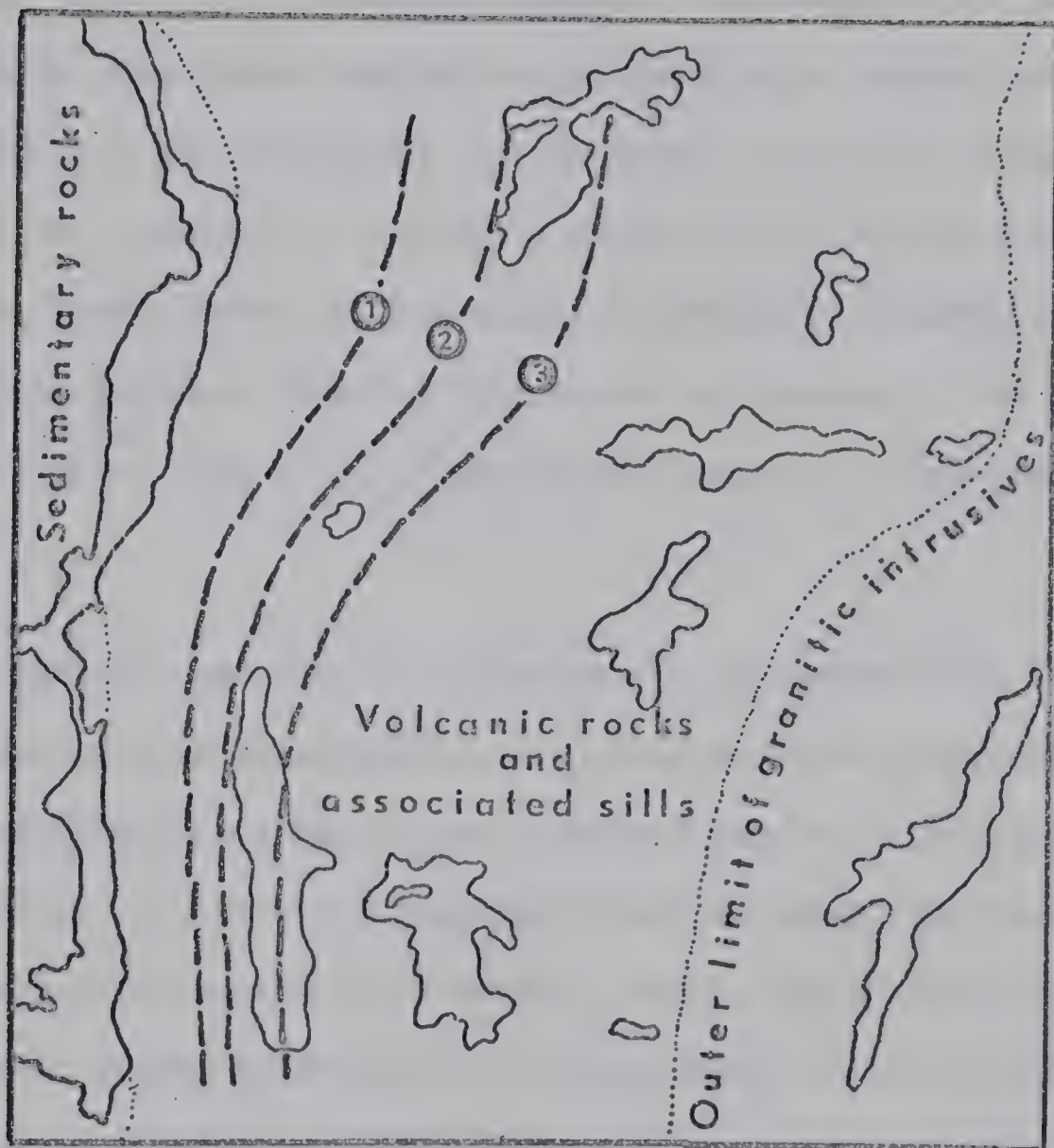


Fig. 5. Metamorphic "isograds" in the Cameron River volcanic belt as shown by the ratio of hornblende to combined hornblende and chlorite (from Edie, 1949): ①=0.0, ②=0.5, ③=1.0.

Note: The term "isograd" is used in a general sense as hornblende has a wide range of compositions, not necessarily related to the grade of metamorphism. For this reason, the definition of isograd by Tilley (1924) cannot be applied.



This reinterpretation of the available data reinforces the opinion offered by Folinsbee (1942) that the metamorphism was dominantly thermal in character and explains some of the apparent anomalies which led Folinsbee to place more emphasis on variabilities of bulk composition than on an orderly sequence of metamorphic zones. For example, the outer limit of the nodular zone (where cordierite and andalusite appear together) marks the appearance of the andalusite - cordierite - muscovite subfacies. Within this zone, the presence of staurolite depends on a suitable bulk composition of the parent rocks (high alumina,  $\text{FeO} \gg \text{MgO}$ ). Staurolite would be unstable in a higher pressure (Barrovian) environment. The area deserves further study in the light of recent developments in experimental petrology.

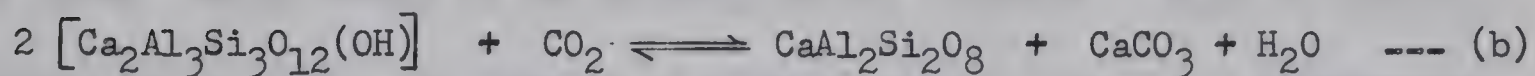
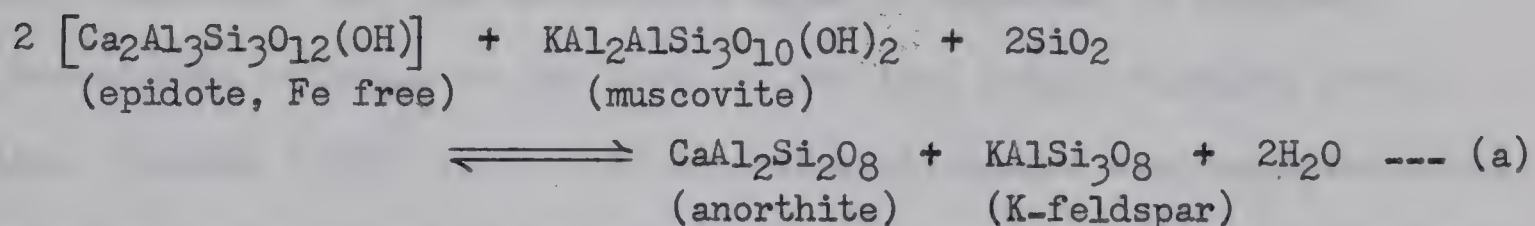
It is readily seen that it is impossible to separate the first two metamorphic episodes proposed previously. They could be interpreted in terms of a gradually increasing thermal gradient and/or a lessening of tectonic pressures. The third metamorphic event is clearly distinguishable and has considerable economic importance. Boyle (1961) refers to the "chlorite-carbonate schist facies" which is superimposed on the regional metamorphic zones, and Folinsbee (1942) discusses the apparent zonal inversion which results from hydrothermal alteration. Many of the porphyroblasts in the metasediments are degraded to sericite and chlorite pseudomorphs and make the task of establishing upper limits of metamorphic zones difficult. Folinsbee (op. cit.) found that the zone of maximum hydrothermal alteration coincided approximately with the outer border of the nodular zone. On that basis he recommended that this limited area warranted careful prospecting.





Boyle (op. cit.) suggests that the thermal structure established in the country rocks during the formation of the granodiorite bodies (?granitization) resulted in migration of water, carbon dioxide, sulphur and some chalcophile elements towards the cooler parts of the metamorphic belt. When thrust faulting occurred towards the end of the orogenic episode, the shear zones acted as passageways and low pressure dilatant zones with the result that mobile components were lost to the surface.

Consideration of the following equations (Kretz, 1963)



shows that it may be predicted that the establishment of a  $\text{P}_{\text{H}_2\text{O}}$  gradient on a regional basis (approximately a closed system) leads to a situation where the formation of epidote and sericite is favoured by release of  $\text{CO}_2$  when local strong decrements in pressure are experienced. Ramberg (1952, p. 195) points out that decreasing pressures alone will not cause minerals to precipitate along the flow path of a liquid "hydrothermal" solution. If, however, the watery solution contains both calcite and an excess of dissolved  $\text{CO}_2$ , loss of  $\text{CO}_2$  will cause precipitation of  $\text{CaCO}_3$  because a decreased content of  $\text{CO}_2$  in solution decreases the solubility of calcite.

The equilibria in these and similar equations was evidently severely displaced in dilatant zones with the result that the walls of shear zones were extensively carbonatized and hydrated. Many of these reactions release large amounts of silica. Boyle (op. cit.) disposes of the excess silica by upward migration and dispersal at the surface.





axial zones of isoclinal folds (e.g. Hump mine, Camlaren). Quartz veins bearing gold are occasionally found cutting the bedding of the sediments (Ptarmigan mine). Small amounts of pyrite, chalcopyrite, galena, sphalerite and carbonates are associated with free gold in the less metamorphosed sediments, but gold-bearing quartz veins inside the nodular zone also contain pyrrhotite and tourmaline.

Wide zones of wallrock alteration containing ankerite, calcite, sericite and chlorite are characteristic of mesothermal deposits. Early workers suggested that the Yellowknife deposits belonged to Lindgren's low mesothermal category on the basis of the lead sulphantimonide association. Coleman (1957) found that the sulphantimonides were representative of a later, cooler stage in the mineralization sequence. There is textural evidence for at least two periods of mineralization, the first represented by a comparatively simple assemblage of deformed, granulated gold-bearing pyrite and arsenopyrite and the second by an extensive suite of sulpho-salts dominated by the tetrahedrite series. Aurostibite ( $\text{AuSb}_2$ ) generally occurs as a coating on the gold, indicating reaction of antimonial solutions with gold in the solid state.

For these reasons the period of gold mineralization extends over a range of temperatures (Boyle lists four definite ages) and may be more accurately placed in Buddington's (1935) xenothermal category. This observation is in accord with the metamorphic history developed in the previous section and the geothermometry data of Coleman (op. cit., p. 420-422). The occurrence of scheelite in the Con - Rycon veins supports the suggestion that the early gold mineralization is indicative of a relatively high temperature.

Supergene minerals are not extensive and are chiefly the



alteration products of exposed mineral zones.

The two presently productive mines, Giant Yellowknife and Con-Rycon, mill approximately 1,500 tons of ore per day of an average grade of between 0.7 and 0.8 oz. per ton. Expansion of the Yellowknife mining camp is largely contingent on a substantial increase in the price of gold.





### CHAPTER III

#### GEOCHRONOLOGY OF THE YELLOWKNIFE AREA

##### Sample Preparation

Samples were collected from fresh, glaciated outcrops and blasted roadcuts where possible. The weathered surface was removed in the field, and samples were individually wrapped to prevent contamination. Whole rock samples were carefully trimmed to avoid epidote and calcite veins. These samples commonly weighed over 10 lbs. and care was taken to insure they were valid representatives of chosen rock types. Samples for K-Ar mineral separation were chosen from approximately 200 rock specimens. The main criteria employed in their selection were geological importance and freedom from visible chlorite.

Samples from which zircons were expected were collected in large quantities, between 50 and 400 lbs. in every case. Some of the zircon samples had been collected in previous years by Drs. Folinsbee and Baadsgaard and by Mr. O. Van Breeman. Simple panning of a ground specimen was found to be of considerable value in determining whether a rock was sufficiently rich in zircon to warrant separation.

Sample localities are recorded in Appendix 2. Approximately  $1\frac{1}{2}$  tons of samples were collected during two short field seasons.

In the laboratory the samples were washed free of the pervasive dust which had accumulated during transportation from Yellowknife. Large samples were reduced in size with an hydraulic rock splitter and a sledge hammer. At this stage thin sections were prepared from hand specimens. Selected samples were then reduced to 2 inch fragments and crushed to less than  $\frac{1}{2}$  inch with a jaw crusher. A Bico Braun plate mill reduced





the rock powder to less than 35 mesh size (U.S. Standard) and this powder was bagged for further treatment. A whole rock sample was withdrawn at this point and crushed to 270 mesh in a Bleuler rotary swing mill.

If micas and hornblende for K-Ar work were required, the crushed powder was dry sieved to ascertain the fraction from which clean separates could be obtained and a suitable fraction (generally 60 to 120 mesh) carefully washed with acetone to remove adhering rock dust. For zircon separation a Wilfley table was used and in this case suitably washed fractions of biotite, muscovite and hornblende were readily obtained as a byproduct.

Mineral separations were performed with standard heavy liquid techniques involving the use of tetrabromoethane, methylene iodide and Clerici solution. Preliminary separation was carried out with the Frantz isodynamic separator. Pyrite impurities were removed from zircon concentrates by froth flotation and hand-picking was only found to be necessary in a few cases. A "float-sink" procedure using heated Clerici solution was particularly effective in zircon purification. All mineral separates were washed in distilled water. Zircons were heated in 1:1  $\text{HNO}_3$  for two hours and washed with lead-free water.

A representative fraction of each final mineral separation was mounted in Permunt and the purity estimated by a rapid grain count. All zircon concentrates were of better than 99% purity. The purity of minerals used for K-Ar dating is recorded in Appendix 1.

#### Radiometric Methods

In this section, the problems which are capable of solution



by K-Ar, Rb-Sr and U-Pb radiometric methods are discussed, and a brief description of the equipment and procedures used is given. Details of the routine chemical procedures are given in appendices. Sufficient data relating to the instrumentation is provided so that the analytical procedures may be evaluated.

Since the major analytical technique is mass spectrometry and the final data depends on the quality of the mass spectrometer results, a brief, generalised description is given. The following summary is based on Hamilton (1965), from which references to the technical literature may be obtained.

In general, a mass spectrometer consists of the following components:-

- (1) A sample system by which the sample is introduced into the mass spectrometer.
- (2) An ion source to produce ions characteristic of the sample.
- (3) A system of slits through which the ion beam passes, is accelerated by an electrical field and is collimated. The ion beam may be focussed for direction and velocity.
- (4) An analyser (magnet) in which the beam is resolved.
- (5) A final slit system through which the separated ion beam passes.
- (6) A detector system, generally an electrometer.
- (7) A recorder system, e.g. recording voltmeter.

Ideally, the intensity of the ion current produced by a given isotope is proportional to its concentration. Peaks are monitored on a chart recorder.

To prevent ion scattering and consequent "tailing" of peaks, the path of the ion beam must be in a region of low gas pressure. The





required low pressures are provided by a combination of mechanical, vapour diffusion and ion getter pumps.

All the instruments possessed adequate resolution of the mass range for which they were used, although correction occasionally was necessary for slight "tailing" on unspiked Sr spectra where very precise measurement of the  $^{87}\text{Sr}$  peaks is required. Lead spectra were completely resolved.

#### Potassium-argon method

Because of the widespread occurrence of potassium-bearing minerals in the earth's crust, the K-Ar method has been applied to many geochronological problems over the past 15 years. Recent developments in our understanding of the limitations of this method have lead to a more optimistic view than that of a few years ago, when it seemed probable that all that could reasonably be derived from the method was a minimum date representing the last metamorphic event.

As no correction is possible for initial isotopically pure  $^{40}\text{Ar}$  contamination, it is necessary to assume that essentially complete fractionation takes place between the parent and inert daughter nuclides at the time of mineral formation. This assumption appears to be valid for phases rich in potassium but remains controversial in potassium-deficient minerals. Clear evidence for an excess of  $^{40}\text{Ar}$  in cyclo-silicates and some framework silicates is recorded (Damon and Kulp, 1958; Hart and Dodd, 1962 and McDougall and Green, 1964), and it is probable that a small, finite amount of initial  $^{40}\text{Ar}$  is present in all mineral phases of deep seated environments.

One of the most commonly used minerals, hornblende, has been





reported to contain excess  $^{40}\text{Ar}$  (Hunt, 1962), but the consensus is that the apparent excellent argon retention in hornblende compared with that of micas is a function of the higher activation energy (110-200 kcal/mole) rather than a result of excess  $^{40}\text{Ar}$  (Hart, 1961, Gerling et al., 1965). There are no other demonstrated instances where an amphibole age is clearly in excess of the true age.

The decay scheme and isotopic abundances of K and Ar are shown in Fig. 6 and Table 13.

Figure 6

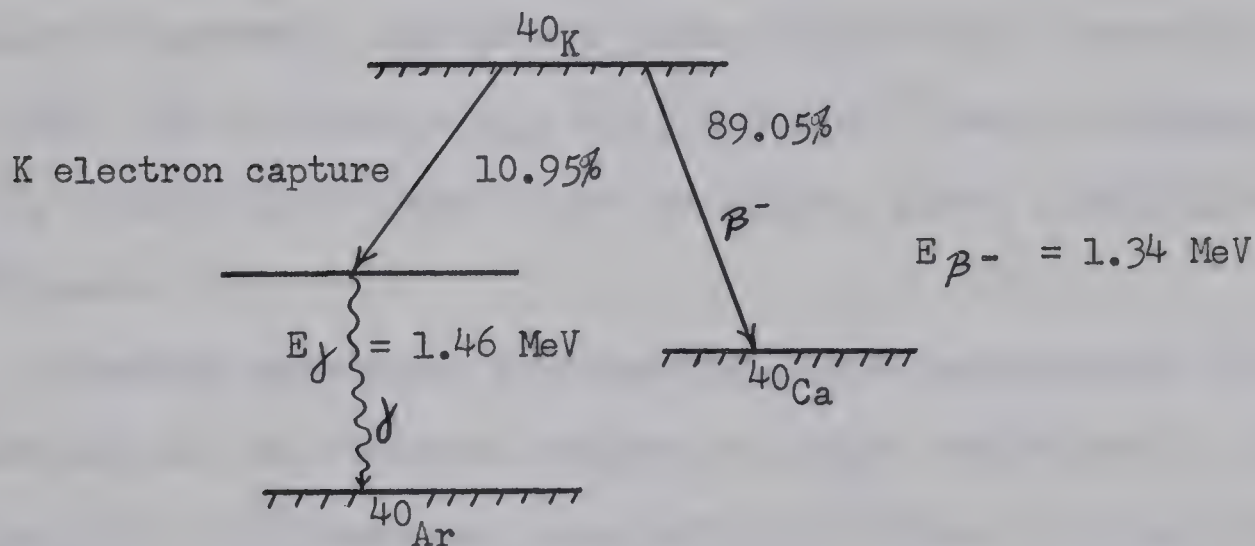


Table 13. Isotopic abundances of K and Ar nuclides

|           |                  |                      |   |   |              |
|-----------|------------------|----------------------|---|---|--------------|
| Potassium | $^{39}\text{K}$  | 93.08 atomic percent |   |   |              |
|           | $^{40}\text{K}$  | 0.0119               | " | " | (Nier, 1950) |
|           | $^{41}\text{K}$  | 6.91                 | " | " |              |
| Argon     | $^{36}\text{Ar}$ | 0.337                | " | " |              |
|           | $^{38}\text{Ar}$ | 0.063                | " | " | (Nier, 1950) |
|           | $^{40}\text{Ar}$ | 99.600               | " | " |              |



Radioactive decay of  $^{40}\text{K}$  produces the stable isotope  $^{40}\text{Ca}$  by emission of a  $\beta^-$  particle, and  $^{40}\text{Ar}$  by K- electron capture followed by emission of  $\gamma$  radiation to reach the ground state. The half life is related to the sum of the two partial decay constants,  $\lambda_\beta$  and  $\lambda_e$ , and is determined by counting the relatively high energy  $\beta$  decay activity. The ratio of the two partial decay constants is termed the branching ratio (R), where  $R = \frac{\lambda_e}{\lambda_\beta}$

The branching ratio and half life can also be determined by measurement of total potassium and radiogenic argon from minerals whose age is known by means of concordant uranium-lead ages on cogenetic minerals. In this manner, Wasserburg, Hayden and Jensen (1956) found a branching ratio of 0.118. If a value of  $\lambda_\beta = 4.7 \pm 0.5 \times 10^{-10}/\text{year}$  is assumed, a value of  $\lambda_e = 5.57 \times 10^{-11}/\text{year}$  can be calculated, giving a half life of  $1.32 \times 10^9$  years.

Counting experiments give somewhat higher measurements of  $\lambda_e$ . Most workers now use the constants adopted by Aldrich and Wetherill, 1958; vis.  $\lambda_e = 5.85 \times 10^{-11}/\text{year}$  and  $\lambda_\beta = 4.72 \times 10^{-10}/\text{year}$ ,  $R = 0.124$  and  $T_{1/2} = 1.306 \times 10^9$  years. For Archaean minerals an error of 10% in either  $\lambda_e$  or  $\lambda_\beta$  will result in an error of approximately 5% in the calculated age. Common practice is to neglect possible errors in the decay constants and quote the precision of the analyses in terms of the analytical errors involved in K and Ar determinations (see Appendix 6).

Although mica K-Ar dates are easily affected by low temperature metamorphic events, the micas do not lose argon spontaneously once below the "blocking temperature" (MacIntyre et al., 1967). Because continuous diffusion of radiogenic argon is thought to take place at depths of as little as 10,000 feet (Hurley et al., 1962) in orogenic belts, Harper





(1967, p. 128) suggests that K-Ar dates from Precambrian terrains may have no relation to times of metamorphic recrystallisation and orogenesis. Instead, they may represent chelogenic processes (as defined by Sutton, 1963) related to the uplift and subsequent stabilization of continental blocks. Some of the basement cores studied by Burwash et al. (1962) come from wells where bottom-hole temperatures in excess of 80°C are recorded, so that the "blocking temperature" must lie above this lower limit. Moorbath (1967) discusses this problem in some detail.

For the reasons given above there is no reason why the mean of a number of K-Ar mica dates should be correlated with the peak of an orogenic episode. Rather, such a peak on a histogram represents the termination of a diffusion episode. This simple picture is complicated by the differences in relative argon retentivity of hornblendes and coarse-grained micas resulting in a spectrum of apparent ages lying between the limits of the mineral-forming event and subsequent thermal closure. A similar spectrum may be produced by argon loss during a later metamorphic episode, either from thermal events or from processes of dynamic metamorphism.

In order to define a crystallisation episode within a basement complex, a few dates by Rb-Sr whole rock or U-Pb methods may be more valuable than a large number of K-Ar mica dates. On the other hand, a sharp thermal event is often defined by the K-Ar method.

The technique used in extracting and purifying argon is similar to that described by Goldich et al. (1961). The apparatus used for this work does not differ from that described by Peterman (1962) except that the magnesium perchlorate water trap has been replaced by a second cold trap.





Mass spectrometry was carried out with the Associated Electrical Industries Ltd. MS-10 mass spectrometer described by Farrar et al. (1964). This is a single focussing, 2 inch radius,  $180^\circ$  deflection instrument with an electron impact ion source. Vacuum requirements are met by a water cooled oil diffusion pump and a Varian Associates VacIon ion getter pump. Ion currents are recorded by a single collection system. They are amplified by an Applied Physics Corporation Cary vibrating reed electrometer. Scanning is carried out by varying the accelerating voltage. The residual pressure after complete baking of the system is in the vicinity of  $1 \times 10^{-9}$  mm Hg. Measurements are made dynamically, maintaining a constant argon pressure of around  $2 \times 10^{-7}$  mm Hg through a molecular leak into the spectrometer tube.

Determination of the amount of  $^{40}\text{Ar}$  is made by isotope dilution. A known amount of 99.9% pure  $^{38}\text{Ar}$  is added to the extracted argon, prior to final purification. Calibrated  $^{38}\text{Ar}$  tracers (spikes) had been prepared previously by Dr. H. Baadsgaard.

Mass discrimination is monitored before and after sample measurements by determining the  $^{40}\text{Ar}/^{36}\text{Ar}$  ratio of purified air argon under the same pressure conditions as that prevailing during measurement of the isotopic ratios of samples. Over a period of three months, values of the  $^{40}\text{Ar}/^{36}\text{Ar}$  standard varied over the small range 305.2 to 306.8. Sample measurements were normalized to the standard Nier  $^{40}\text{Ar}/^{36}\text{Ar}$  value of 295.5 for air argon.

Since all minerals contain some occluded nonradiogenic  $^{40}\text{Ar}$  ("air argon") it is necessary to subtract this amount from the total amount of  $^{40}\text{Ar}$  determined by mass spectrometry. For this purpose the  $^{36}\text{Ar}$  peak is measured as accurately as possible and a correction made on the





basis of the composition of present day air argon.

Potassium is determined by two methods. After a double leach following dissolution with HF and H<sub>2</sub>SO<sub>4</sub> and ignition, potassium is precipitated with sodium tetraphenylboron solution (biotites) or determined by flame photometry (hornblendes). Correction is made for a small amount of coprecipitated rubidium tetraphenylboron in the first procedure.

Replicate analyses by the author and Mr. R. K. O'Nions suggest that the precision of the tetraphenylboron method is approximately 1% of the potassium content of micas and the precision of flame photometric determinations on hornblendes is approximately 3%. Details of the procedure are well established in the laboratory and are recorded in several previous theses (Peterman, 1962, Leech, 1965).

Argon peaks are corrected in the manner shown in Table 27.

$$^{40}\text{Ar}^* = ^{40}\text{Ar}_{\text{total}} - (^{40}\text{Ar}_{\text{spike}} + ^{40}\text{Ar}_{\text{air}} + ^{40}\text{Ar}_{\text{residual}})$$

$$^{38}\text{Ar}_{\text{spike}} = ^{38}\text{Ar}_{\text{total}} = ^{38}\text{Ar}_{\text{residual}} \quad (^{38}\text{Ar} \text{ from the air is almost always negligible for Precambrian samples})$$

$$^{36}\text{Ar}_{\text{air}} = ^{36}\text{Ar}_{\text{total}} - (^{36}\text{Ar}_{\text{residual}} + ^{36}\text{Ar}_{\text{spike}})$$

Since the volume of <sup>38</sup>Ar in the previously calibrated spike is known, the amount of <sup>40</sup>Ar may be calculated after correction for mass discrimination:-

$$\text{vol } ^{40}\text{Ar}^* = \frac{\text{vol } ^{38}\text{Ar}}{\text{sample weight} \times (^{38}\text{Ar}_{\text{spike}} / ^{40}\text{Ar}) \text{ corrected}}$$

Interlaboratory comparison of a standard muscovite sample (P-207) indicates that the analytical data from this laboratory compares favourably with determinations from other major laboratories (Lanphere and Dalrymple (1967)).

The volume of <sup>40</sup>Ar is converted to parts per million and the percentage K<sub>2</sub>O to p.p.m. <sup>40</sup>K. The ratio of these quantities is substituted into the general equation developed previously to give the date of the





sample. In the most practical form this equation is expressed as:-

$$t = 4.341 \times 10^9 \cdot \log \left( 1 + \frac{{}^{40}\text{Ar}(9.068)}{{}^{40}\text{K}} \right) \text{ million years.}$$

#### Rubidium-strontium whole rock method

This method is perhaps the most powerful single tool available to the geochronologist, because a closed chemical system may usually be approximated using a sample of the size of a large hand specimen. Analysis of a series of cogenetic samples with diverse Rb/Sr ratios provides a test of closed system behaviour (Compston et al., 1960), and the resulting linear trend is known as an isochron (Nicolaysen, 1961).

Rubidium forms no minerals of its own, but is readily admitted into the lattices of potassium minerals. It occurs as two isotopes of mass 85 and 87.  ${}^{85}\text{Rb}$  is stable, but  ${}^{87}\text{Rb}$  decays by  $\beta^-$  particle emission to  ${}^{87}\text{Sr}$ . Measurement of the absolute specific activity of  ${}^{87}\text{Rb}$  is difficult because of the large number of low energy  $\beta^-$  particles in the energy spectrum. For this reason controversy surrounds the value of the  ${}^{87}\text{Rb}$  decay constant.

Flynn and Glendenin (1959) counted the specific activity of natural rubidium by dissolving an organic Rb-salt in a liquid scintillator and determined a decay constant of  $\lambda = 1.47 \times 10^{-11}/\text{year}$ . Since this experiment, at least 7 values of  $\lambda {}^{87}\text{Rb}$  have been determined (Leutz et al., 1962), ranging from  $\lambda = 1.19$  to  $1.47 \times 10^{-11}/\text{year}$ . Aldrich et al. (1958) determined a value of  $\lambda {}^{87}\text{Rb} = 1.39 \times 10^{-11}/\text{year}$  by comparison of  ${}^{87}\text{Rb}/{}^{87}\text{Sr}$  ratios of pegmatitic minerals with concordant U-Pb ages of cogenetic uraninites. Dr. W. Compston (pers. comm.) finds that  $\lambda {}^{87}\text{Rb} = 1.39 \times 10^{-11}/\text{year}$  is more compatible with K-Ar and K-Ca ages obtained on the same minerals.





Recent experience in this laboratory supports the use of this decay constant. However, a recent direct determination by McMullen et al., (1966) favours the  $\lambda = 1.47 \times 10^{-11}$ /year decay constant.

The  $\lambda^{87}\text{Rb} = 1.39 \times 10^{-11}$ /year decay constant has been adopted, notwithstanding the fact that dates derived using this constant should check with U-Pb dates since this constant is derived by comparison with U-Pb data. If it is necessary to compare these data with those obtained using the alternative decay constant, it is necessary to subtract  $\approx 6\%$  from the dates quoted in this thesis.

Although applicable to many of the same minerals used for K-Ar determination, the Rb-Sr method is limited in its scope by the very long half life and the presence of common strontium in most rocks and minerals. The whole rock method is particularly useful in Precambrian rocks although exceptionally favourable proportions of rubidium to common strontium allow minerals as young as 12 m.y. to be dated (Jager, 1966).

Table 14. Isotopic abundances of common strontium and rubidium

| <u>Isotope</u>   | <u>Abundance<br/>atomic percent</u> |                             |
|------------------|-------------------------------------|-----------------------------|
| $^{87}\text{Rb}$ | 27.85 )                             | (Nier, 1950)                |
| $^{85}\text{Rb}$ | 72.15 )                             |                             |
| $^{88}\text{Sr}$ | 82.56 )                             | (Bainbridge and Nier, 1950) |
| $^{87}\text{Sr}$ | 7.02 )                              |                             |
| $^{86}\text{Sr}$ | 9.86 )                              |                             |
| $^{84}\text{Sr}$ | 0.56 )                              |                             |

The theoretical basis on which an isochron is based is as follows (adapted from Baadsgaard, 1965):-

Let the subscript o denote the time at which a rock or mineral



first became a closed system and  $p$  denote the present time.

Since  $^{87}\text{Rb}_o = ^{87}\text{Rb}_p e^{\lambda t}$ ,

and  $^{87}\text{Rb}_o - ^{87}\text{Rb}_p = ^{87}\text{Sr}_p^*$  (radiogenic daughter nuclide),

then  $^{87}\text{Rb}_p (e^{\lambda t} - 1) = ^{87}\text{Sr}_p^*$ . (1)

But  $^{87}\text{Sr}_p = ^{87}\text{Sr}_o + ^{87}\text{Sr}_p^*$ .

Substituting in (1)

$$^{87}\text{Sr}_p = ^{87}\text{Sr}_o + ^{87}\text{Rb}_p (e^{\lambda t} - 1).$$

Dividing through by  $^{86}\text{Sr}$ , an invariant quantity, and rearranging,

$$\left( \frac{^{87}\text{Sr}}{^{86}\text{Sr}} \right)_p - \left( \frac{^{87}\text{Sr}}{^{86}\text{Sr}} \right)_o = \left( \frac{^{87}\text{Rb}}{^{86}\text{Sr}} \right)_p (e^{\lambda t} - 1)$$

If values of  $(^{87}\text{Sr}/^{86}\text{Sr})_p$  and  $(^{87}\text{Rb}/^{86}\text{Sr})_p$  are plotted and fall on a straight line, then the time which has elapsed between closure of the Rb-Sr system and the present is given by solving the equation involving the slope of the line.

$$\text{slope} = e^{\lambda t} - 1$$

In addition to the application of the whole rock Rb- Sr isochron method to plutonic rock units which may reasonably have a common age and initial  $^{87}\text{Sr}/^{86}\text{Sr}$  ratio, the method has also been applied to sediments (Compston and Pidgeon, 1962, Whitney and Hurley, 1964) where these conditions are less obvious. Although complicated by the uncertainty introduced by inherited radiogenic strontium in the detrital fraction of the rock and selective removal of either strontium or rubidium during transportation and diagenesis, the method has been successfully employed by Fairbairn et al. (1967) on metasediments in the Canadian shield.

The reason for successful dating of Precambrian metasediments probably lies in a relatively simple isotopic provenance and the relatively short time interval between the time of formation of the source rocks and subsequent weathering, transportation and sedimentation.





Strontium isotopic ratios have been applied to petrogenetic problems as well. Here the initial  $^{87}\text{Sr}/^{86}\text{Sr}$  ratio is of most interest, as the initial ratio is generally characteristic of the source.

Initial  $^{87}\text{Sr}/^{86}\text{Sr}$  ratios from rocks thought to originate in the upper mantle (e.g. oceanic basalts) are generally low, ranging from 0.700 to 0.705 (Faure and Hurley, 1963; Hedge and Walthall, 1963; Heier et al. 1965). There has been a slight increase in the  $^{87}\text{Sr}/^{86}\text{Sr}$  ratio in such rocks with the passage of time, approximately along the line joining Gast's achondritic meteorite value (0.698) to the values obtained from modern oceanic basalts. The slope of the line suggests an average Rb/Sr ratio of 0.021 in the upper mantle. An increasing body of precise evidence (Gast, 1965, Compston et al. 1968) suggests that regional variation of Rb/Sr in mantle source regions may cause the observed variations in  $^{87}\text{Sr}/^{86}\text{Sr}$  ratios. In general, basalt series characterised by high  $\text{K}_2\text{O}$  contents such as alkaline olivine basalts and quartz tholeiites have the highest  $^{87}\text{Sr}/^{86}\text{Sr}$  ratios and the lowest ratios are found in oceanic tholeiites and olivine basalts.

Significantly higher initial ratios ( $^{87}\text{Sr}/^{86}\text{Sr} > 0.710$ ) commonly are restricted to acid rocks. In many cases it may be demonstrated that granitic rocks have been at least partly derived from a source with a higher Rb/Sr ratio such as underlying sialic crust (Moorbath and Bell, 1965). The most puzzling problem at present is that concerning the continental tholeiites and their differentiates. These often contain radiogenic strontium in excess of that which can be produced by radioactive decay in situ. Hamilton (1965) shows isotopic evidence for contamination of the Skaergaard acid granophyres by partial assimilation of country rock. Compston et al. (op. cit.) emphasise that





the high initial ratios of the Tasmanian and Antarctic dolerites are incompatible with simple crustal assimilation because of the low K/Rb ratio ( $\approx 210$ ) and the remarkable uniformity of these rocks over what is now described as a major magmatic province. It is necessary to postulate selective diffusion or partial melting of the lower crust on a regional scale to explain the regional occurrence of these rocks unless gross compositional variations occur in the upper part of the mantle.

In view of these problems, the initial  $^{87}\text{Sr}/^{86}\text{Sr}$  ratio is seen to be a potent, though complex, indicator of petrogenetic history.

Samples for Rb-Sr whole rock determinations are selected on the basis of thin section study and X-ray fluorescence assays for approximate Rb and Sr content. Optimum amounts of sample which would yield  $^{88}\text{Sr}/^{86}\text{Sr}$  and  $^{87}\text{Rb}/^{85}\text{Rb}$  ratios of approximately 2.0 after combination with individual spike solutions are calculated from the preliminary X-ray fluorescence data. An unspiked sample containing approximately 20 micrograms of Sr is also prepared from a homogeneous sample split. Strontium is separated with cation exchange resin (Dowex 50W-X8, 200-400 mesh) and loaded as the chloride onto oxidised tantalum filaments where it is glowed in air before preliminary vacuum heating to remove rubidium. Rubidium is extracted and loaded as the sulphate. A detailed description of the Rb-Sr chemistry is found in Appendix 3.

Mass spectrometry was performed on a 6 inch radius, solid source, single-filament instrument with  $60^\circ$ -sector magnetic deflection (designed and built by Dr. G. Cumming). Isotope dilution analysis was used for both rubidium and strontium determination. Most strontium analyses were recorded using a Dymec integrating digital voltmeter with a Hewlett Packard digital printer on line from an Electronic Instrument Ltd.





vibrating reed electrometer. Peak switching was accomplished by changing the magnet current with a variable shunt network.

In spiked strontium analyses, use is made of the augmented  $^{84}\text{Sr}/^{86}\text{Sr}$  ratio to calculate the mass discrimination of individual analyses. An iterative procedure which is necessary for calculation of  $^{87}\text{Sr}$  using a mixed  $^{84}\text{Sr}/^{86}\text{Sr}$  spike is described in Appendix 4, as are calculations required to determine the  $^{87}\text{Sr}/^{86}\text{Sr}$  and  $^{87}\text{Rb}/^{86}\text{Sr}$  ratios.

An original computer program was written in Fortran IV in order to facilitate calculation of Sr isotope ratios.

#### Uranium - lead method

Of the several naturally radioactive decay schemes used in geochronology, the chemical similarity of parent and daughter nuclides in the U-Pb system produces the most favourable conditions for comparison of apparent dates. As a general rule, pegmatitic uraninite is the only mineral from which concordant U-Pb dates are obtained. Zircon is the most commonly used mineral for U-Pb geochronology because of its widespread occurrence as an accessory mineral. While individual  $^{207}\text{Pb}/^{235}\text{U}$  and  $^{206}\text{Pb}/^{235}\text{U}$  dates are usually discordant, valid interpretations may be deduced from a suite of zircons using the "concordia" approach of Wetherill (1956) and Silver, et al. (1963) or the "discordia" theory of Tilton (1960) and Wasserburg (1963). No apparent dates demonstrably in excess of estimated true ages have been obtained, so that U-Pb ages on zircons are reliable minimum estimates of a zircon-forming process.

The decay schemes (abbreviated) of the two U-Pb systems used in this study are as follows:-





| Nuclide          | Stable decay products   |
|------------------|---|
| $^{238}\text{U}$ | $^{206}\text{Pb} + 8\ ^4\text{He} \quad (\lambda_1 = 1.54 \times 10^{-10}/\text{year})$ |
| $^{235}\text{U}$ | $^{207}\text{Pb} + 7\ ^4\text{He} \quad (\lambda_2 = 9.72 \times 10^{-10}/\text{year})$ |

The decay constants are known to a precision of less than 1% (Banks and Silver, 1966).

From the decay equations,

$$^{206}\text{Pb}_{\text{rad}} = ^{238}\text{U} (e^{\lambda_1 t} - 1)$$

$$^{207}\text{Pb}_{\text{rad}} = ^{235}\text{U} (e^{\lambda_2 t} - 1)$$

three dates may be calculated, the first two in the conventional manner and a third, the so-called "lead - lead" date from the relationship:

$$\frac{^{207}\text{Pb}}{^{206}\text{Pb}} = \frac{(e^{\lambda_1 t} - 1)}{137.8 (e^{\lambda_2 t} - 1)}$$

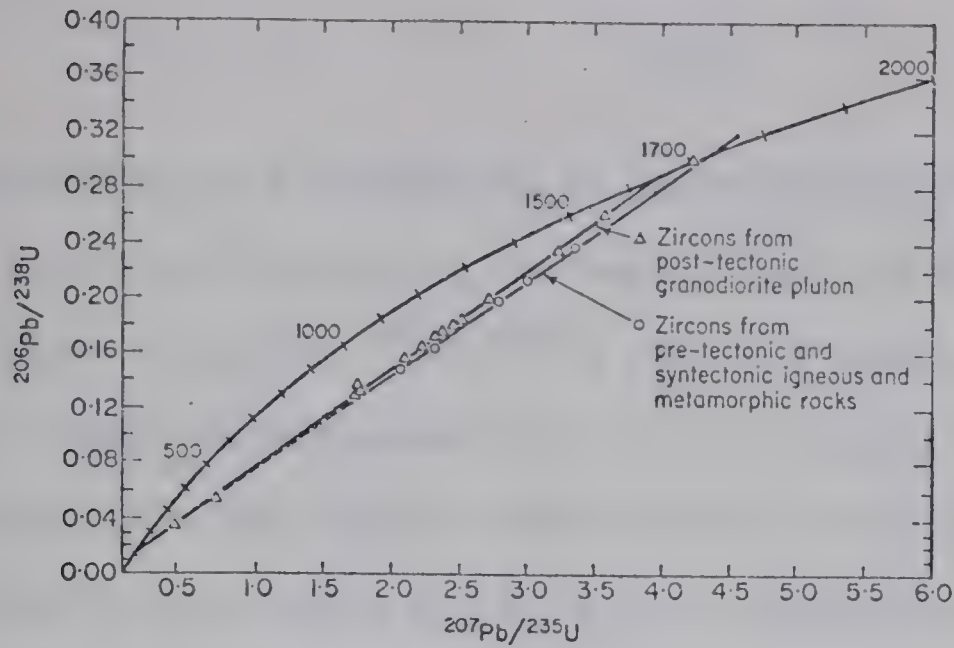
The "lead-lead" date is not an independent determination but is valuable in that it is relatively insensitive to lead loss after the first closure of the system. When U-Pb dates are discordant, the  $^{207}\text{Pb}/^{206}\text{Pb}$  date generally agrees most closely with Rb-Sr and K-Ar dates on cogenetic minerals.

Analyses used in a "concordia" plot (see Fig. 7) must be corrected for any initial non-radiogenic lead (common lead) present in the sample and for contaminant lead introduced during chemical dissolution of the zircon and subsequent extraction of lead. Pending the determination of common or least radiogenic lead in associated feldspar phases, it has been assumed that the composition of common lead is that of conformable lead (on the Russell - Farquhar model, Kanasewich, 1962) of the same age as that of the sample. This calculation requires an iterative procedure which is described in Appendix 4. The convergence is very rapid and may readily be computed on a desk calculator. A computer program in APL was

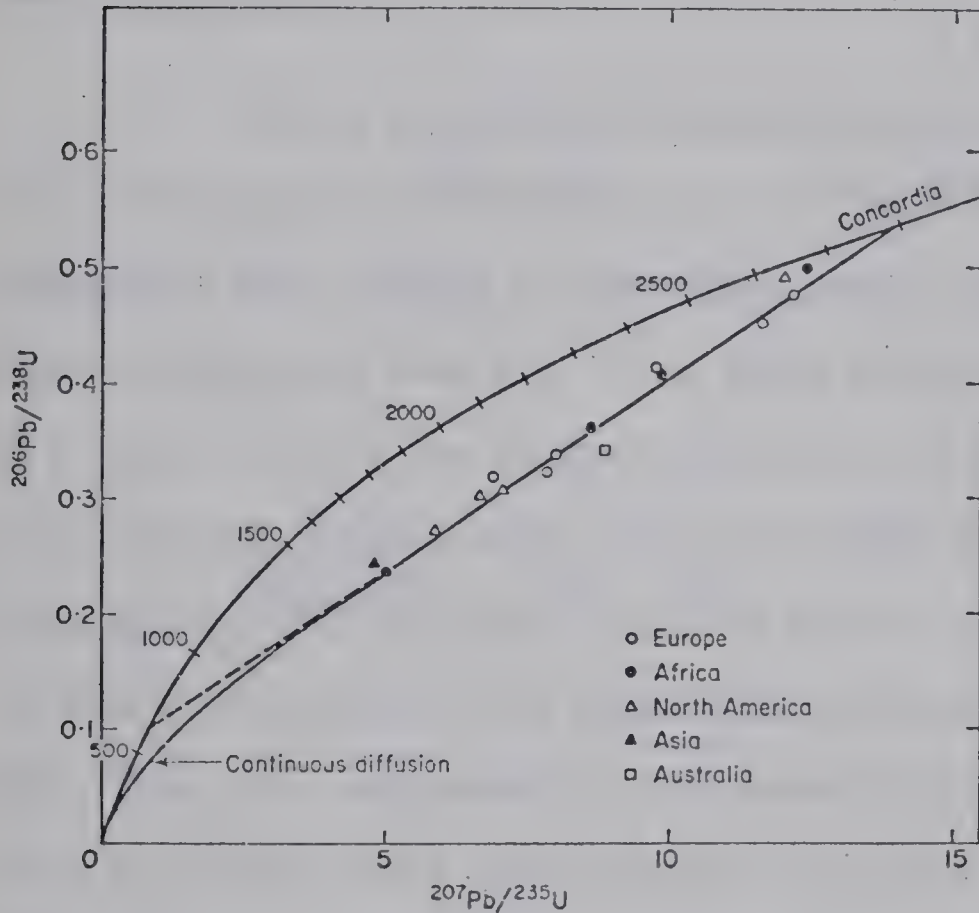




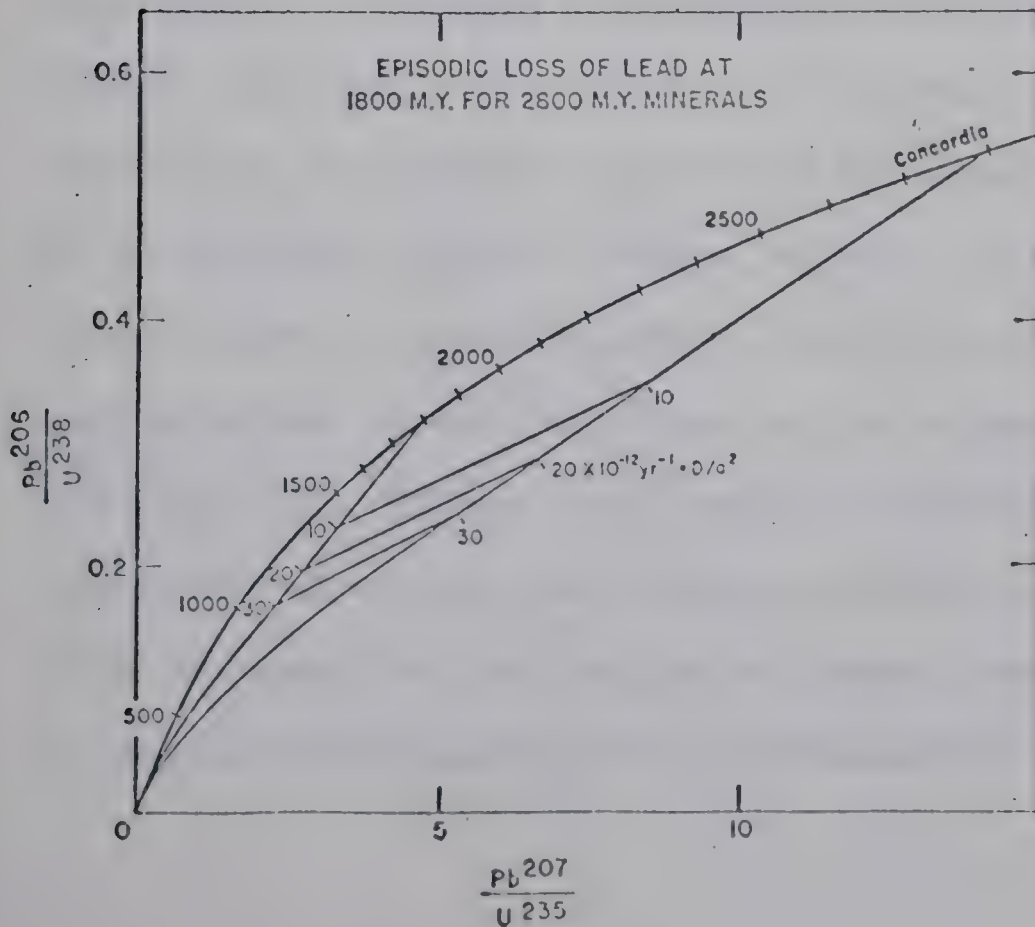
Fig.7.



(a) Zircon-uranium-lead system for Precambrian rocks of the Dragoon Quadrangle, Cochise Co., Arizona. (from Silver, 1963)



(b) Parent-daughter ratios for minerals having  $^{207}\text{Pb}/^{206}\text{Pb}$  ages of 2300-2800 million years. The curve represents calculated values for lead loss by continuous diffusion. (from Tilton, 1960)



(c) Parent-daughter ratios resulting from episodic loss of lead 1800 m.y. ago superimposed on continuous loss of lead by diffusion for hypothetical minerals having an age of 2800 m.y. (from Tilton, 1960)

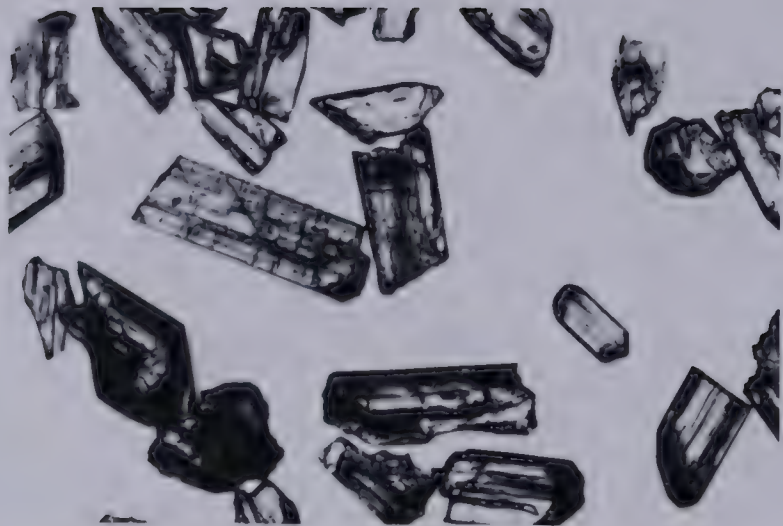


written by Dr. H. Baadsgaard to check the manually computed values. The composition of laboratory contaminant lead was determined independently. Because of the high  $^{206}\text{Pb}/^{204}\text{Pb}$  ratios of most of the zircons, the corrections for common and contaminant lead are not usually critical. In general, zircons with the highest uranium content are most likely to give a greater degree of discordance and may have an increased relative amount of common lead contaminant.

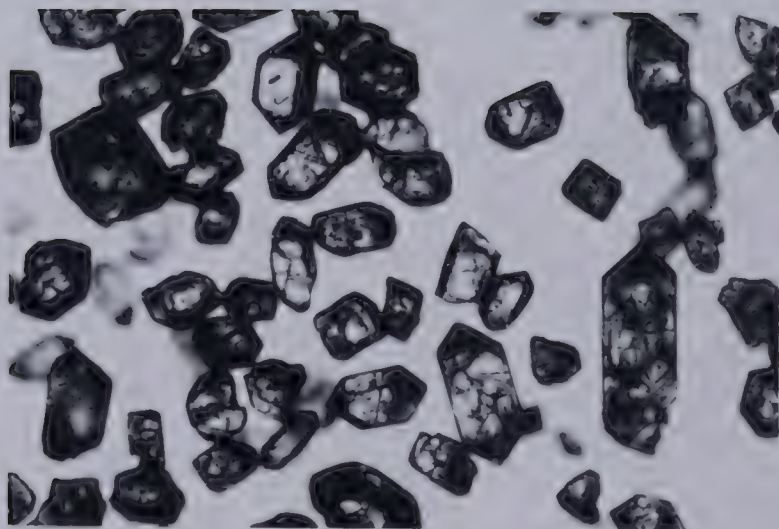
Zircon discordance patterns usually follow the sequence  $^{207}\text{Pb}/^{206}\text{Pb}$  date  $>$   $^{207}\text{Pb}/^{235}\text{U}$  date  $>$   $^{206}\text{Pb}/^{238}\text{U}$  date. Wetherill (1956) interpreted this pattern to indicate episodic lead loss and developed a graphical solution (see Fig. 7) in which the upper and lower intersections of a chord with the "concordia" yield the time of formation and the time of disturbance respectively. The "concordia" curve is the locus of points along which  $^{206}\text{Pb}/^{238}\text{U}$  and  $^{207}\text{Pb}/^{235}\text{U}$  systems give the same date. While the episodic loss model has been applied successfully by Silver et al. (1961, 1963) (Fig. 7a), many examples have been found where there is no evidence for a geological event corresponding to the lower intersection on the "concordia". To explain this problem, Tilton (1960) proposed that lead may diffuse continuously from crystals at a rate governed by a diffusion coefficient, the effective radius and the concentration gradient. Solution of the diffusion equation (Tilton, op. cit., p. 2936) leads to a model which follows the episodic pattern over the upper part of the "concordia" plot but curves towards the origin at low values of  $^{206}\text{Pb}/^{238}\text{U}$  and  $^{207}\text{Pb}/^{235}\text{U}$  (Fig. 7b). Tilton (1960) shows the complexity which results from a combination of episodic and continuous diffusion lead loss patterns (Fig. 7c). It is fortunate that most suites of zircons from cogenetic rock phases plot on well defined straight lines on a "concordia" diagram.



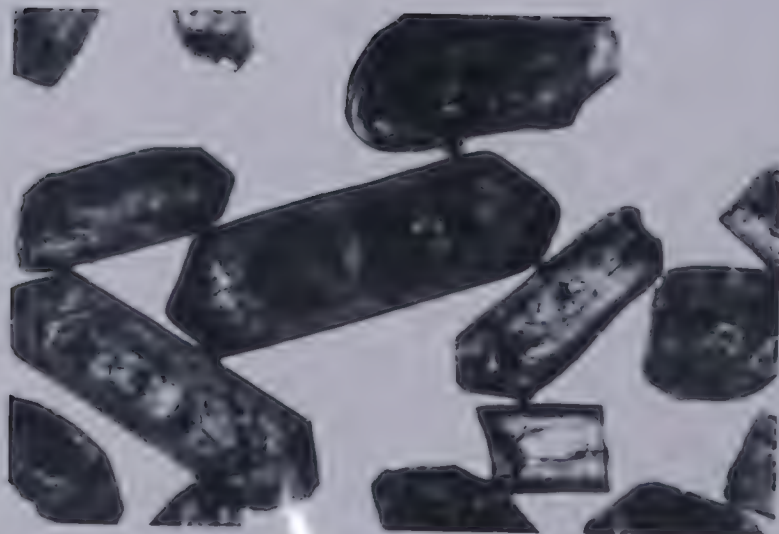
PLATE 7



(a) Zircons from South-east granodiorite (DCG 120)  
Plain light, X 64.



(b) Zircons from granodiorite boulder, Sub Is. conglomerate (DCG 116).  
Plain light, X 100.



(c) Zircons from Yellowknife metavolcanics, dacite (Brock) horizon.  
(DCG 75-206)  
Plain light, X 100.

The zircons studied in this thesis range from pale blue-green, through pale purple or pink to pale brown in colour. All could be classified as hyacinths on the basis of high birefringence and colour. Those from the South-east granodiorite are elongated (Folinsbee, 1955, reports an elongation index approaching 32), are well crystallised with good development of both 111 and 331 pyramidal faces and are almost free from inclusions. The zircons from the Yellowknife volcanics are relatively large (.5 to 2 mms.) pale brown hyacinths, well crystallised and slightly zoned. Their elongation ratio varies between 2 and 4. Those from the Western granodiorite are distinctive in that they are slightly dusty, pale purple or pale brown in colour and well crystallised but with 111 pyramidal terminations alone. A slight haematite staining is crystallographically controlled. The Ross Lake granodiorite zircons are similar to those from the Western Granodiorite. They range from clear pale brown hyacinths to dusty forms and are somewhat less angular.

Zircons from conglomerate boulders are entirely comparable with those of the South-east granodiorite. In the sediments approximately 80% of the zircons show some evidence of rounding. Although a large sample of the Redout Lake granite was collected, only a few zircons were separated. These appeared to be of a normal type, similar to those described by Folinsbee (op. cit.) from the Prosperous Lake granite, which is also very deficient in zircon.

The zircon populations are very similar to those described from around Lake Superior by Tyler et al. (1940) where hyacinths are dominant in the pre-Huronian granites, particularly the pre-Knife Lake Group granites of Minnesota.

The analytical procedures employed for determination of Pb







and U are similar to those described by Tilton et al. (1955). While it was not possible to work with filtered air, all reagents were made up with redistilled lead-free reagents and the cleaned apparatus covered with Parafilm until required for use. The laboratory blank for solution of the total sample is about 1 microgram of total lead under normal working conditions.

Zircons are fused in a deep platinum crucible with between 6 and 10 times their weight of purified sodium tetraborate. Most fusions are complete in 3 hours at a temperature of 1,000°F. The fused sample is then dissolved in about 75 ml. of redistilled 6N HCl diluted 1:3 with water. With constant stirring no silica residue comes out of solution. The solution is made up to 100 or 250 ml. and stored in cleaned volumetric flasks. Aliquots are withdrawn from the stock solution for spiked and unspiked lead determinations and for spiked uranium determinations.

Lead is extracted with a 0.01% solution of dithizone in chloroform from an alkaline ( $\text{pH} = 9$ ) aqueous phase of the sample solution containing saturated ammonium citrate. The extract is then filtered and back extracted with 2%  $\text{HNO}_3$ . To the aqueous phase is added 5 - 10 ml. of 2% KCN and a few ml. of dil.  $\text{NH}_4\text{OH}$  solution, and the dithizone extraction is repeated with 0.001% dithizone solution. The lead dithizonate is back-extracted with 2%  $\text{HNO}_3$  and washed with purified chloroform. The aqueous phase is transferred to a centrifuge tube, adjusted to pH 4.5 and PbS precipitated by passing  $\text{H}_2\text{S}$  through the solution. The precipitate is centrifuged and transferred to an oxidised Ta filament for mass spectrometry. It is necessary to load a small portion of the supernatant liquid with the sulphide and decompose this on the heated filament to ensure the most stable emission. Spiked determinations are made in the same manner,





the  $^{208}\text{Pb}$  spike solution being added to the sample aliquot before the first dithizone extraction.

A preliminary purification of uranium is made by coprecipitation with zirconium hydroxide from a hot solution by passing  $\text{NH}_3$  gas through the combined  $^{235}\text{U}$  spike and sample solutions. The precipitate is centrifuged, washed, and dissolved in a drop or two of 6N  $\text{HNO}_3$  plus saturated  $\text{Al}(\text{NO}_3)_3$ -solution. Uranium is extracted with 25 ml. of hexone (methyl isobutyl ketone) and the aqueous phase discarded. The hexone solution is then filtered through qualitative grade filter paper and stripped with water. The aqueous phase is evaporated to near dryness, taken up with 2 or 3 drops of conc.  $\text{HNO}_3$  and saturated  $\text{NH}_4\text{NO}_3$  solution is added. A second extraction with hexone follows after which the uranium is extracted with water and the aqueous phase evaporated to dryness. The residue is picked up in a drop of 0.01M.  $\text{HNO}_3$  and loaded onto an oxidised Ta filament for the mass spectrometry.

Uranium mass spectrometry was performed on the 6 inch instrument previously described in the section on Rb-Sr geochronology. Uranium aliquots were spiked so that the  $^{235}\text{U}/^{238}\text{U}$  ratio was close to unity and the results have a precision of  $\pm 0.5\%$ .

Isotope analyses for lead were carried out on a 12 inch radius,  $60^\circ$  sector, single focussing, single filament, solid source mass spectrometer designed and built by Dr. G. L. Cumming of the Department of Physics, University of Alberta. The calibration of the instrument has been compared with N.B.S. standard reference sample 982 ("equal atom lead") and with Broken Hill galena. The results are tabulated below:





Table 15. Calibration of 12 inch mass spectrometer  
with N.B.S. 982 and Broken Hill leads

|         | <u>N. B. S. 982</u>       | Standard values (Catanzaro et. al., 1968)    |
|---------|---------------------------|--|
|         | U. of A.                  |  |
| 208/206 | 1.0001 $\pm$ 0.0005       | 1.0002                                       |
| 207/206 | 0.4671 $\pm$ 0.0002       | 0.4671                                       |
| 204/206 | 0.02717 $\pm$ 0.00003     | 0.02722                                      |
|         | <u>Broken Hill galena</u> | Ulrych (1967, pers. comm. Dr. H. Baadsgaard) |
| 208/206 | 2.2282 $\pm$ 0.0010       | 2.2283                                       |
| 207/206 | 0.9616 $\pm$ 0.0010       | 0.9620                                       |
| 204/206 | 0.06239 $\pm$ 0.00004     | 0.06248                                      |

The precision of individual measurements on samples ranges between 0.3 and 1.5% for 204/206 measurements and less than 0.1% for 207/206 and 208/206 measurements. Reproducibility errors are probably no more than 0.3% for 207/206 and 208/206 measurements.

### Results

In this section, results from the three radiometric methods are tabulated. Interpretation of the results is deferred until Chapter IV, and a detailed evaluation of the error limits is made in Appendix 6. In order to evaluate the results, some mention must be made of the principal error sources involved in the analytical procedures. Sample inhomogeneity, variable blank contamination and inaccurate isotopic measurements are the chief sources of analytical error.

Sample inhomogeneity is likely to be a source of error in the Rb-Sr method as different portions were taken for spiked Sr, unspiked Sr and spiked Rb determinations. To minimise this possibility, each sample





was ground for 4 minutes in a swing mill and thoroughly mixed before aliquots for spiked and unspiked determinations were removed. De la Cruz (1967) suggests that the sample be brought into solution and aliquots for spiked Sr, unspiked Sr and Rb determinations withdrawn when necessary. Such a procedure is necessary if micas are an important component of the sample. Variable blank contamination is difficult to avoid but is reduced by using redistilled and "lead clean" reagents and by conducting evaporations under a hood through which passes filtered air at slightly above atmospheric pressure.

Most isotopic measurements for Pb and Sr were recorded on an integrating digital voltmeter and are precise to better than 2 parts per 1,000. With stable emission, the precision is better than 1 part per 1,000. Rubidium and U isotopic measurements are considered to be within  $\pm 0.5\%$  of the true value,  $^{40}\text{Ar}$  measurements within  $\pm 1\%$  (Baadsgaard, 1965) and  $^{40}\text{K}$  measurements to within  $\pm 3\%$  (hornblendes) or  $\pm 1\%$  (micas). Error limits on analytical results are quoted as plus or minus 1 standard deviation.

Results which consistently fall outside these limits may be attributed to geological variation and require a geological interpretation.

#### K-Ar Data

Potassium-argon dates and analytical data are reported in Table 16. Appendix 2 gives the precise location of the analysed specimens and for convenience the dates are grouped in terms of rock units in Table 17. Other recent dates by Burwash and Baadsgaard (1962), the Geological Survey of Canada (Lowden, 1961 et seq.) and Green et al. (1968) are also tabulated here.

Eight pairs of dates were obtained on coexisting biotite +



Table 16.

## Summary of K/Ar data

| Run No. | AK No. | Field No. | Mineral** | $^{40}\text{K}$<br>ppm | $^{40}\text{Ar}/^{40}\text{K}$<br>% | Radiogenic Argon<br>% | Date<br>m.y.* |
|---------|--------|-----------|-----------|------------------------|-------------------------------------|-----------------------|---------------|
| 726     | 703    | 59        | B         | 6.493                  | 0.2962                              | 99.9                  | $2460 \pm 28$ |
| 727     | 708    | 124       | B         | 6.910                  | 0.3123                              | 99.9                  | $2530 \pm 28$ |
| 742     | 712    | 127       | M         | 9.163                  | 0.3133                              | 99.8                  | $2540 \pm 28$ |
| 743     | 711    | 120       | B         | 5.412                  | 0.3016                              | 99.9                  | $2480 \pm 28$ |
| 744     | 707    | 44        | B         | 8.204                  | 0.2695                              | 99.8                  | $2330 \pm 27$ |
| 745     | 704    | 3         | B         | 7.165                  | 0.2771                              | 99.6                  | $2370 \pm 27$ |
| 752     | 705    | 33        | B         | 7.229                  | 0.2420                              | 99.0                  | $2190 \pm 26$ |
| 753     | 709    | 129       | B         | 8.235                  | 0.2841                              | 99.7                  | $2400 \pm 27$ |
| 754     | 706    | 48        | B         | 7.868                  | 0.2774                              | 99.5                  | $2370 \pm 27$ |
| 755     | 710    | 118       | B         | 6.005                  | 0.3016                              | 99.7                  | $2480 \pm 28$ |
| 756     | 714    | 124       | H         | 0.414                  | 0.3128                              | 97.9                  | $2530 \pm 56$ |
| 757     | 713    | 55        | H         | 0.798                  | 0.3077                              | 97.5                  | $2510 \pm 56$ |
| 758     | 715    | 3         | H         | 1.637                  | 0.3071                              | 98.9                  | $2510 \pm 56$ |
| 759     | 716    | 120       | H         | 0.515                  | 0.3343                              | 98.4                  | $2630 \pm 57$ |
| 760     | 717    | 5         | H         | 1.334                  | 0.3135                              | 98.6                  | $2540 \pm 56$ |
| 761     | 718    | 118       | H         | 0.697                  | 0.1330                              | 91.6                  | $1490 \pm 41$ |
| 770     | 774    | 246       | B         | 4.770                  | 0.2790                              | 99.4                  | $2380 \pm 27$ |
| 771     | 775    | 244       | B         | 7.054                  | 0.2769                              | 99.6                  | $2370 \pm 27$ |
| 772     | 776    | 254       | B         | 7.438                  | 0.3027                              | 99.5                  | $2490 \pm 28$ |
| 773     | 778    | 257       | M         | 9.853                  | 0.2968                              | 98.3                  | $2460 \pm 28$ |
| 774     | 777    | 253       | B         | 7.852                  | 0.2943                              | 99.6                  | $2450 \pm 27$ |





Table 16 contd.

| Run No. | AK No. | Field No. | Mineral** | $^{40}\text{K}$<br>ppm | $^{40}\text{Ar}/^{40}\text{K}$ | Radiogenic Argon<br>% | Date<br>m.y.* |
|---------|--------|-----------|-----------|------------------------|--------------------------------|-----------------------|---------------|
| 775     | 779    | 244       | M         | 10.258                 | 0.3022                         | 98.3                  | 2480 $\pm$ 28 |
| 776     | 780    | 246       | M         | 10.106                 | 0.3164                         | 98.7                  | 2550 $\pm$ 28 |
| 777     | 782    | 259       | B         | 8.631                  | 0.2765                         | 99.4                  | 2370 $\pm$ 27 |
| 778     | 781    | 258       | B         | 8.024                  | 0.2959                         | 99.9                  | 2460 $\pm$ 28 |
| 779     | 784    | 204       | B         | 4.406                  | 0.2437                         | 99.8                  | 2200 $\pm$ 26 |
| 780     | 785    | 233       | M         | 10.106                 | 0.2420                         | 99.3                  | 2190 $\pm$ 28 |
| 781     | 783    | 204       | M         | 10.187                 | 0.3094                         | 99.6                  | 2520 $\pm$ 28 |
| 782     | 787    | 245       | B         | 8.044                  | 0.3044                         | 99.9                  | 2500 $\pm$ 28 |
| 783     | 786    | 233       | B         | 4.063                  | 0.2040                         | 97.5                  | 1970 $\pm$ 25 |
| 784     | 789    | 256       | M         | 10.258                 | 0.3158                         | 99.5                  | 2550 $\pm$ 28 |
| 785     | 788    | 307       | B         | 6.175                  | 0.2782                         | 99.8                  | 2370 $\pm$ 27 |

\* Constants used:-  $\lambda_e = 0.585 \times 10^{-10}/\text{yr.}$

$\lambda_\beta = 4.72 \times 10^{-10}/\text{yr.}$

$^{40}\text{K}/\text{K} = 0.000119$  (Nier, 1950)

\*\* Minerals:- B = Biotite

M = Muscovite

H = Hornblende

Note: Ages are rounded to nearest 10 m.y.





Table 17.

## K-Ar dates grouped in terms of rock units

| Western granodiorite<br>m.y.             | South-east granodiorite<br>m.y. | Ross Lake granodiorite<br>m.y.           | Prosperous Lake granite<br>(and associated pegmatites)<br>m.y.  | Redout Lake granite<br>pegmatites)<br>m.y. |
|--|---------------------------------|--|---|--|
| (1970 (B)<br>(2190 (M)                   | 2370 (B)                        | 2370 (B)                                 | (2200 (B)<br>(2520 (M)  | (2370 (B)<br>(2480 (M)                     |
| 2190 (B)                                 | (2480 (B)<br>(1490 (H)*         | 2500 (B)                                 | -----<br>2400 (B) (Stock on west<br>side of Prosperous<br>Lake) | (2380 (B)<br>(2550 (M)                     |
| 2330 (B)                                 | (2480 (B)<br>(2630 (H)          | 2450 (B) Burwash and<br>Baadsgaard, 1962 | -----   | 2450 (B)                                   |
| 2370 (B)                                 | (2530 (B)<br>(2530 (H)          | -----                                    | -----   | 2460 (B)                                   |
| (2370 (B)<br>(2510 (H)                   | 2540 (M)                        |  | 2540 (M) G.S.C. 60-49   | 2460 (M)                                   |
| 2460 (B)                                 | -----                           |  | -----   | 2490 (B)                                   |
| 2510 (H)                                 | 2615 (B) G.S.C. 61-66           |  | 2530 (M) Burwash and<br>Baadsgaard, 1962                        | 2550 (M)                                   |
| 2540 (H)                                 | -----                           |  | -----   | -----                                      |
| -----                                    |                                 |  | 2410 (B) Green et al.<br>1968                                   | 2495 (M) G.S.C. 61-67                      |
| 2490 (B) G.S.C. 61-64                    |                                 |  | 2420 (B)  | 2500 (B) Burwash and<br>Baadsgaard, 1962   |
| -----                                    |                                 |  | 2520 (M)  | -----                                      |
| 2440 (B) Burwash and<br>Baadsgaard, 1962 |                                 |  | -----   |  |
| -----                                    |                                 |  |   |  |



muscovite or hornblende assemblages. Examination of Table 17 shows that in only one case is the biotite date greater than that of the coexisting mineral. A check of the  $K_2O$  determination on hornblende in this sample (\*, - Table 17) revealed no significant error and the low date is inexplicable at the present time. In one case biotite and hornblende gave the same date but in six cases, biotite is significantly younger.

### Rb-Sr Data

Tables 18 to 24 show the analytical data on which Rb-Sr isochrons are based. Isochrons have been fitted to the analytical data with the aid of computer programmes which allow for non-uniform variance in  $^{87}Sr/^{86}Sr$  ratios and incorporate prior estimates of the experimental precision for both coordinates (McIntyre et al. 1966, York, 1966). Figs. 8 to 14 illustrate the isochrons that are based on the experimental data. Figs. 8, 12 and 14 contain isochrons fitted according to the model of McIntyre et al. using the error parameters: X (variance of unspiked determinations) =  $1.95 \times 10^{-6}$ , Y (variance of spiked determinations) =  $10.7 \times 10^{-6}$ , CONX (constant of variance of  $^{87}Rb/^{86}Sr$ ) =  $38.13 \times 10^{-6}$  (Green et al., 1968). Figs. 9, 10, 11 and 13 show isochrons fitted to the data points with a modification of the York programme written in APL by Dr. H. Baadsgaard. In more recent work it is considered that the error limits in this laboratory are better than those established by the writer and others during 1967 and used in the original Fortran IV McIntyre programme. For this reason the value of the variance of unspiked runs has been reduced to  $0.4 \times 10^{-6}$  and that of spiked runs to  $1.0 \times 10^{-6}$ . The error limits quoted on the diagrams are those of the respective methods. Where X-ray fluorescence methods have been used for Sr determination,





Table 18. Rb-Sr analytical data for isochron plot, Yellowknife (meta) volcanics

| Sample No. | Total Rb<br>(p.p.m.) | Common Sr<br>(p.p.m.) | $\frac{^{87}\text{Sr}}{^{87}\text{Sr} + ^{87}\text{Rb}}$ | $\frac{^{87}\text{Rb}}{^{86}\text{Sr}}$<br>(atomic ratio) | $\frac{^{87}\text{Sr}}{^{86}\text{Sr}}$<br>Spiked | (atomic ratio)<br>Unspiked |
|------------|----------------------|-----------------------|--|---|---|----------------------------|
| DCG 75     | 86.9                 | 119.0                 | 0.114  | 2.109   | 0.7790  | 0.7801                     |
| DCG 74     | 77.4                 | 181.9                 | 0.070  | 1.229   | 0.7470  | 0.7489                     |
| DCG 115    | 67.3                 | 203.3                 | 0.052  | 0.956   | 0.7382  | 0.7369                     |
| DCG 37     | 46.2                 | 229.2                 | 0.034  | 0.583   | 0.7232  | 0.7242                     |
| DCG 139    | 12.7                 | 91.8                  | 0.023  | 0.400   | 0.7173  | 0.7162                     |
| DCG 137    | 4.7                  | 103.2                 | 0.011  | 0.131   | -   | 0.7076                     |





Table 19. Rb-Sr analytical data for isochron plot, Cameron River (meta) volcanics

| Sample No. | Total Rb<br>(p.p.m.) | Total Sr<br>(p.p.m.) | $\frac{^{87}\text{Sr}}{^{87}\text{Sr}} \frac{\text{Rad}}{\text{N}}$ | $\frac{^{87}\text{Rb}}{^{86}\text{Sr}}$<br>(atomic ratio) | $\frac{^{87}\text{Sr}}{^{86}\text{Sr}}$<br>Spiked | (atomic ratio)<br>Unspiked |
|------------|----------------------|----------------------|---|---|---|----------------------------|
| E 8        | 182.67               | $72.5 \pm 1.0$       |   | 7.453   | -   | 0.9758                     |
| E 3        | 121.75               | $82.5 \pm 1.0$       |   | 4.328   | -   | 0.880*                     |
| E 7        | 81.16                | $205 \pm 3.0$        |   | 1.147   | -   | 0.756*                     |
| E15        | 36.95                | $174 \pm 3.0$        |   | 0.613   | -   | 0.7204*                    |
| E16        | 0.65                 | $266 \pm 5.0$        |   | 0.007   | -   | 0.7104*                    |

\* Previous unpublished results, O. Van Breeman and H. Baadsgaard



Table 20. Rb-Sr analytical data for isochron plot, Yellowknife Group (meta) sediments

| Sample No. | Total Rb<br>(p.p.m.) | Total Sr<br>(p.p.m.) | $\frac{^{87}\text{Sr}}{^{87}\text{Sr}} \frac{\text{Rad}}{\text{N}}$ | $\frac{^{87}\text{Rb}}{^{86}\text{Sr}}$<br>(atomic ratio) | $\frac{^{87}\text{Sr}}{^{86}\text{Sr}}$<br>Spiked | (atomic ratio)<br>Unspiked |
|------------|----------------------|----------------------|---|---|---|----------------------------|
| DCG 311    | 110.88               | 198 ± 3              |   | 1.622   | -   | 0.7648                     |
| DCG 313    | 130.84               | 122 ± 2              |   | 3.146   | -   | 0.7630                     |
| DCG 312    | 151.08               | 168 ± 2              |   | 2.605   | -   | 0.7517                     |
| DCG 310    | 89.63                | 166 ± 2              |   | 1.562   | -   | 0.7365                     |
| DCG 309    | 77.79                | 180 ± 3              |   | 1.249   | -   | 0.7322                     |
| DCG 314    | 69.57                | 259.0                | 0.03  | 0.775   | 0.7327  | 0.7278                     |





Table 21. Rb-Sr analytical data for isochron plot, South-east granodiorite

| Sample No.    | Total Rb<br>(p.p.m.) | Common Sr<br>(p.p.m.) | $\frac{^{87}\text{Sr}}{^{87}\text{Sr} + ^{87}\text{N}}$ | $\frac{^{87}\text{Rb}}{^{86}\text{Sr}}$<br>(atomic ratio) | $\frac{^{87}\text{Sr}}{^{86}\text{Sr}}$<br>Spiked | (atomic ratio)<br>Unspiked |
|---------------|----------------------|-----------------------|---|---|---|----------------------------|
| DCG 127       | 103.29**             | 44.945**              | 0.382**   | 6.719**   | 0.9544**  | -                          |
| O.V.B. (1965) | 82.00*               | 309.3*                | 0.025*  | 0.769*  | -   | 0.7285*                    |
| DCG 126       | 64.08                | 320 $\pm$ 5           | 0.02  | 0.578   | -   | 0.7212                     |
| DCG 307       | 58.45                | 361.89                | 0.015   | 0.465   | 0.7257  | 0.7166                     |
| DCG 122       | 41.17                | 258 $\pm$ 4           | 0.01  | 0.461   | -   | 0.7208                     |
| DCG 124       | 24.30                | 320 $\pm$ 5           | 0.01  | 0.219   | -   | 0.7072                     |
| DCG 120       | 22.48                | 400 $\pm$ 5           | 0.01  | 0.161   | -   | 0.7077                     |

\* Previous results, Van Breeman (1965)      \*\* Provisional results, pending retermination,  
as sample inhomogeneity is suspected.





Table 22.

Rb-Sr analytical data for isochron plot, Western granodiorite

| Sample No. | Total Rb<br>(p.p.m.) | Common Sr<br>(p.p.m.) | $\frac{^{87}\text{Sr}}{^{87}\text{Sr} + ^{87}\text{N}}$ | $\frac{^{87}\text{Rb}}{^{86}\text{Sr}}$<br>(atomic ratio) | $\frac{^{87}\text{Sr}}{^{86}\text{Sr}}$<br>Spiked | (atomic ratio)<br>Unspiked |
|------------|----------------------|-----------------------|---|---|---|----------------------------|
| DCG 50     | 195.4                | 30.0                  | 0.952   | 18.840  | 1.392*  | 1.3887                     |
| DCG 8      | 141.7                | 51.7                  | 0.394   | 7.917   | 0.9904  | 0.9893                     |
| DCG 33     | 144.3                | 126.3                 | 0.166   | 3.300   | 0.829*  | -                          |
| DCG 5      | 113.4                | 139.6                 | 0.098   | 2.302   | 0.7884  | 0.7875                     |
| DCG 11     | 73.8                 | 238.7                 | 0.036   | 0.893   | 0.7370  | -                          |
| DCG 48     | 53.7                 | 303.4                 | 0.016   | 0.511   | 0.7220  | 0.7227                     |

\* Chart data only, remainder recorded on integrating digital voltmeter.



Table 23. Rb-Sr analytical data for isochron plot, Ross Lake granodiorite

| Sample No. | Total Rb<br>(p.p.m.) | Common Sr<br>(p.p.m.) | $\frac{87\text{Sr}}{87\text{Sr} + 87\text{N}}$ | $\frac{87\text{Rb}}{86\text{Sr}}$<br>(atomic ratio) | $\frac{87\text{Sr}}{86\text{Sr}}$<br>Spiked | (atomic ratio)<br>Unspiked |
|------------|----------------------|-----------------------|--|---|---|----------------------------|
| DCG 161    | 99.35                | 44.5 ± 1.0            | 0.32   | 6.600   | -   | 0.9447                     |
| DCG 250    | 94.12                | 41.788                | 0.33   | 6.575   | 0.9413                                      | 0.9393                     |
| DCG 245    | 357.5                | 186.62                | 0.29   | 5.514   | 0.9082                                      | 0.9062                     |
| DCG 259    | 124.5                | 125.50                | 0.11   | 3.315   | 0.8131                                      | 0.8208                     |
| DCG 158    | 39.95                | 82.866                | 0.08   | 1.391   | 0.756                                       | -                          |
| DCG 157    | 48.28                | 102.56                | 0.08   | 1.359   | 0.760                                       | -                          |





Table 24.

Rb-Sr analytical data for mineral isochron plot, Prosperous Lake granite

| Mineral      | Total Rb<br>(p.p.m.) | $^{87}\text{Sr}/^{86}\text{Sr}$<br>(atomic ratio) | $^{87}\text{Sr}$ Rad<br>(p.p.m.) | $\text{Sr}^{\text{N}}$ (p.p.m.) | $^{87}\text{Rb}/^{86}\text{Sr}$<br>(atomic ratio) |
|--------------|----------------------|---|----------------------------------|---------------------------------|---|
| Biotite      | 1555                 | $18.27 \pm .02^*$                                 | 14.646                           | 8.6                             | 485   |
| Muscovite    | 685.0                | $8.99 \pm .01$                                    | 6.758                            | 8.4                             | 225   |
| Microcline   | 673.2                | $1.116 \pm .003$                                  | 6.314                            | 163.2                           | 11.14   |
| (Whole rock) | 291.4                | $1.088 \pm .003$                                  | 2.717                            | 75.6                            | 10.323  |
| Plagioclase  | 52.1                 | $0.763 \pm .002$                                  | 0.501                            | 99.2                            | 1.306   |
| Apatite      | -                    | $0.709 \pm .001$                                  | -                                | 40.0                            | -   |

\* Estimated error





Table 25.

Lead isotope analytical data, zircons

| Specimen                        | Pb isotope ratios, unspiked |                    | Pb isotope ratios, Pb <sup>208</sup> spiked |                    |
|---------------------------------|-----------------------------|--------------------|---|--------------------|
|                                 | 207/206                     | 208/206            | 207/206                                     | 208/206            |
| <u>Western Granodiorite:</u>    |                             |                    |   |                    |
| 1. Fort Rae                     | 0.17779<br>±.00009          | 0.15100<br>±.00006 | 705 ± 2                                     | 0.17937<br>±.00013 |
| 2. DCG 5 (fine fraction)        | 0.17896<br>±.00012          | 0.15054<br>±.00004 | 1072 ± 2                                    | 0.17997<br>±.00009 |
| 3. DCG 5 (coarse fraction)      | 0.17818<br>±.00013          | 0.15610<br>±.00014 | 945 ± 5                                     | 0.1787<br>±.0001   |
| 4. F-82 (Stock Lake stock)      | 0.17662<br>±.00012          | 0.20185<br>±.00006 | 1426 ± 6                                    | 0.17869<br>±.00012 |
| <u>Ross Lake Granodiorite:</u>  |                             |                    |   |                    |
| 5. DCG 259                      | 0.18130<br>±.00010          | 0.15466<br>±.00009 | 1910 ± 8                                    | 0.18309<br>±.00013 |
| <u>South-east Granodiorite:</u> |                             |                    |   |                    |
| 6. F-52 (Wool Bay)              | 0.18391<br>±.00007          | 0.14184<br>±.00008 | 860 ± 4                                     | 0.18750<br>±.00013 |
| 7. F-10A                        | 0.19724<br>±.00017          | 0.2923<br>±.0003   | 494 ± 2                                     | 0.19930<br>±.00014 |
| 8. F-10B                        | 0.19467<br>±.00008          | 0.22067<br>±.00019 | 534 ± 3                                     | 0.19728<br>±.00011 |
| 9. F-11 (cuts F-10)             | 0.1812<br>±.0002            | 0.13801<br>±.00008 | 1230 ± 10                                   | 0.18155<br>±.00015 |



Table 25 contd.

| Specimen                               | Pb isotope ratios, unspiked |                    | Pb isotope ratios, Pb <sup>208</sup> spiked |                   |
|--|-----------------------------|--------------------|---|-------------------|
|  | 207/206                     | 208/206            | 207/206                                     | 208/206           |
| 10. F-13                               | 0.17849<br>±.00014          | 0.13513<br>±.00009 | 2037 ± 30                                   | 1.2595<br>±.00009 |
| 11. DCG 120                            | 0.28214<br>±.00015          | 0.45642<br>±.00024 | 116.7 ± 0.5                                 | 8.328<br>±.005    |
| <u>Yellowknife Group:</u>              |                             |                    |   |                   |
| 12. <u>Conglomerate</u> DCG 116        | 0.17628<br>±.00014          | 0.13379<br>±.00011 | 2024 ± 8                                    | 0.7503<br>±.0006  |
| 13. F-24                               | 0.3053<br>±.0002            | 0.5192<br>±.0004   | 92.5 ± 0.5                                  | 2.7831<br>±.0021  |
| 14. <u>Sediments</u> (Group B) F-44    | 0.23059<br>±.00015          | 0.3651<br>±.0001   | 191 ± 1                                     | 2.452<br>±.002    |
| 15. <u>Volcanics</u> (Group A) DCG 206 | 0.19230<br>±.00020          | 0.17085<br>±.00014 | 785 ± 2                                     | 0.8841<br>±.0007  |





Table 26.

Uranium-lead data and radiometric dates

| Specimen       | U     |             | Radiogenic Pb |             |        | U-Pb dates m.y.                        |  |  |
|----------------|-------|-------------|---------------|-------------|--------|--|--|--|
|                | 235   | ppm.<br>238 | 208           | ppm.<br>207 | 206    | <sup>238</sup> U/<br><sup>206</sup> Pb | <sup>235</sup> U/<br><sup>207</sup> Pb | <sup>207</sup> U/<br><sup>206</sup> Pb |
| Fort Rae       | 8.606 | 1201.4      | 31.138        | 47.341      | 295.29 | 1625*                                  | 2040**                                 | 2490*                                  |
| DCG 5 (fine)   | 3.614 | 504.44      | 21.071        | 29.192      | 173.89 | 2180                                   | 2390                                   | 2565                                   |
| DCG 5 (coarse) | 4.229 | 590.41      | 23.976        | 32.236      | 194.83 | 2100                                   | 2330                                   | 2540                                   |
| F-82           | 5.990 | 836.18      | 51.717        | 48.067      | 285.27 | 2160                                   | 2380                                   | 2575                                   |
| DCG 259        | 5.085 | 709.87      | 32.670        | 41.260      | 235.05 | 2110                                   | 2390                                   | 2640                                   |
| F-52           | 4.256 | 594.14      | 12.187        | 19.839      | 116.78 | 1330                                   | 1890                                   | 2590                                   |
| F-10A          | 2.715 | 379.08      | 15.288        | 11.375      | 65.967 | 1190                                   | 1800                                   | 2610                                   |
| F-10B          | 2.779 | 387.91      | 12.760        | 13.058      | 76.062 | 1330                                   | 1900                                   | 2605                                   |
| F-11           | 2.962 | 413.52      | 14.061        | 21.484      | 125.12 | 1950                                   | 2290                                   | 2605                                   |
| F-13           | 3.403 | 475.03      | 19.704        | 28.395      | 164.05 | 2185                                   | 2420                                   | 2620                                   |
| DCG 120        | 2.131 | 297.46      | 15.568        | 14.400      | 82.157 | 1800                                   | 2220                                   | 2640                                   |
| DCG 116        | 6.577 | 918.18      | 33.910        | 48.774      | 285.51 | 1995                                   | 2310                                   | 2595                                   |
| F-24           | 6.965 | 972.25      | 20.614        | 19.312      | 114.16 | 830                                    | 1460                                   | 2575                                   |
| F-44           | 5.543 | 773.79      | 24.105        | 19.527      | 118.69 | 1060                                   | 1660                                   | 2530                                   |
| DCG 206        | 6.478 | 904.40      | 40.768        | 55.514      | 314.33 | 2195                                   | 2440                                   | 2650                                   |

\* rounded to nearest 5.m.y.

\*\* " " " 10 m.y.

NOTE: Common lead correction (generally small) is based on Russell-Farquhar normal model lead of same age as <sup>207</sup>Pb/<sup>206</sup>Pb age. Composition of laboratory contaminant lead is 1 : 20.2 : 17.05 : 40.05.





a value of CONX of  $50 \times 10^{-6}$  has been used and the variance of unspiked  $^{87}\text{Sr}/^{86}\text{Sr}$  ratios is estimated at  $4 \times 10^{-6}$ . Insufficient duplicate determinations have been made to determine these parameters more precisely, but the above estimates are believed to be generous estimates of the experimental precision.

#### U-Pb Data

Tables 25 and 26 show the analytical data from uranium and lead isotopic determinations carried out on 15 samples. The results are given in terms of the observed unspiked lead isotope ratios, the isotopic ratios for spiked samples and the calculated U-Pb dates.

If errors are assigned to the dates on the basis of measurement precision alone, the error limits on the quoted dates are within  $\pm 10$  m.y. in each case. These are well within the limits quoted by Stieff et al. (1959) who incorporate estimates of the precision of the various decay constants.



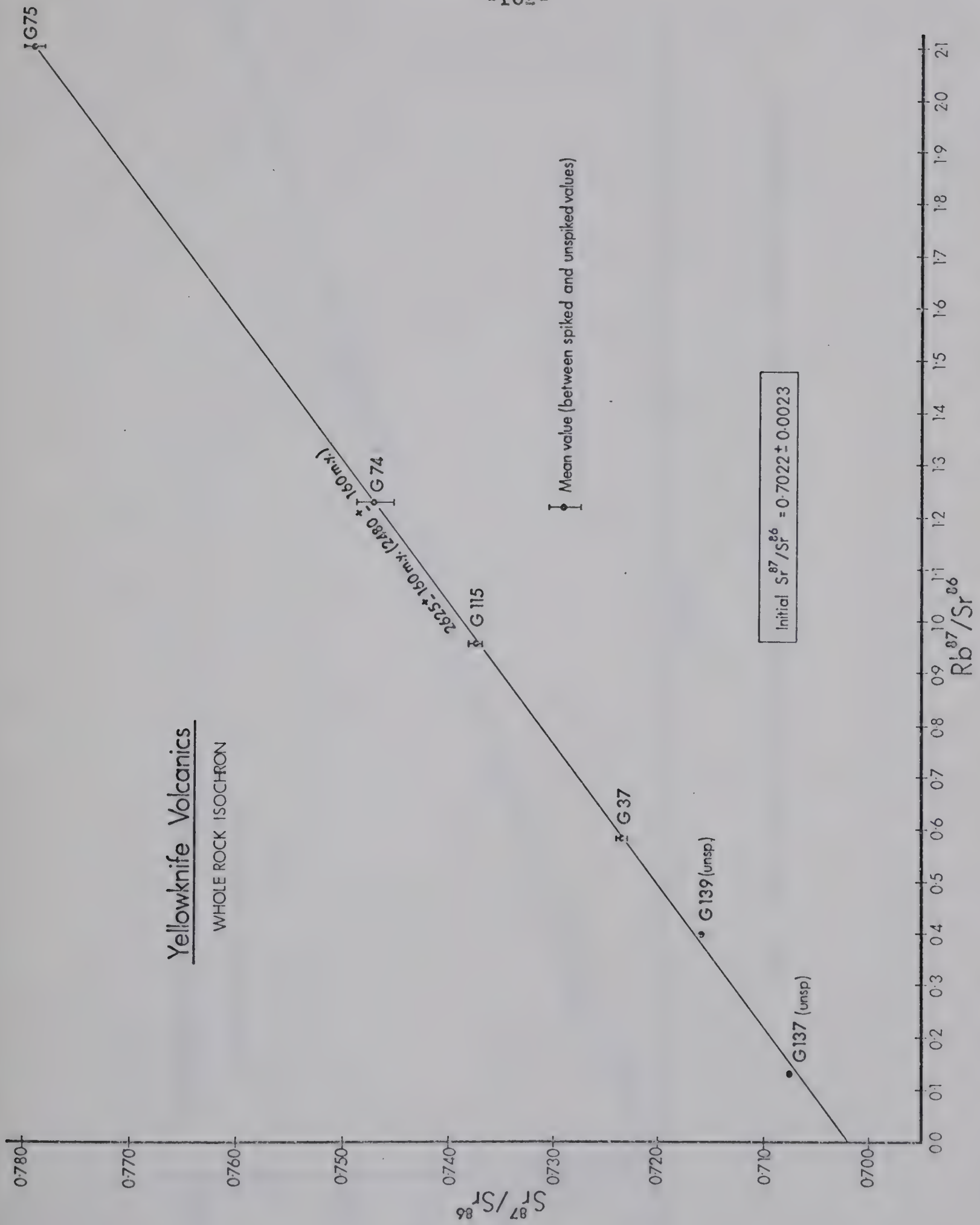


Fig. 8. Rb-Sr whole rock isochron plot, Yellowknife (meta-) volcanics

Note: age using alternative 47 b.y. half life is given in parentheses.





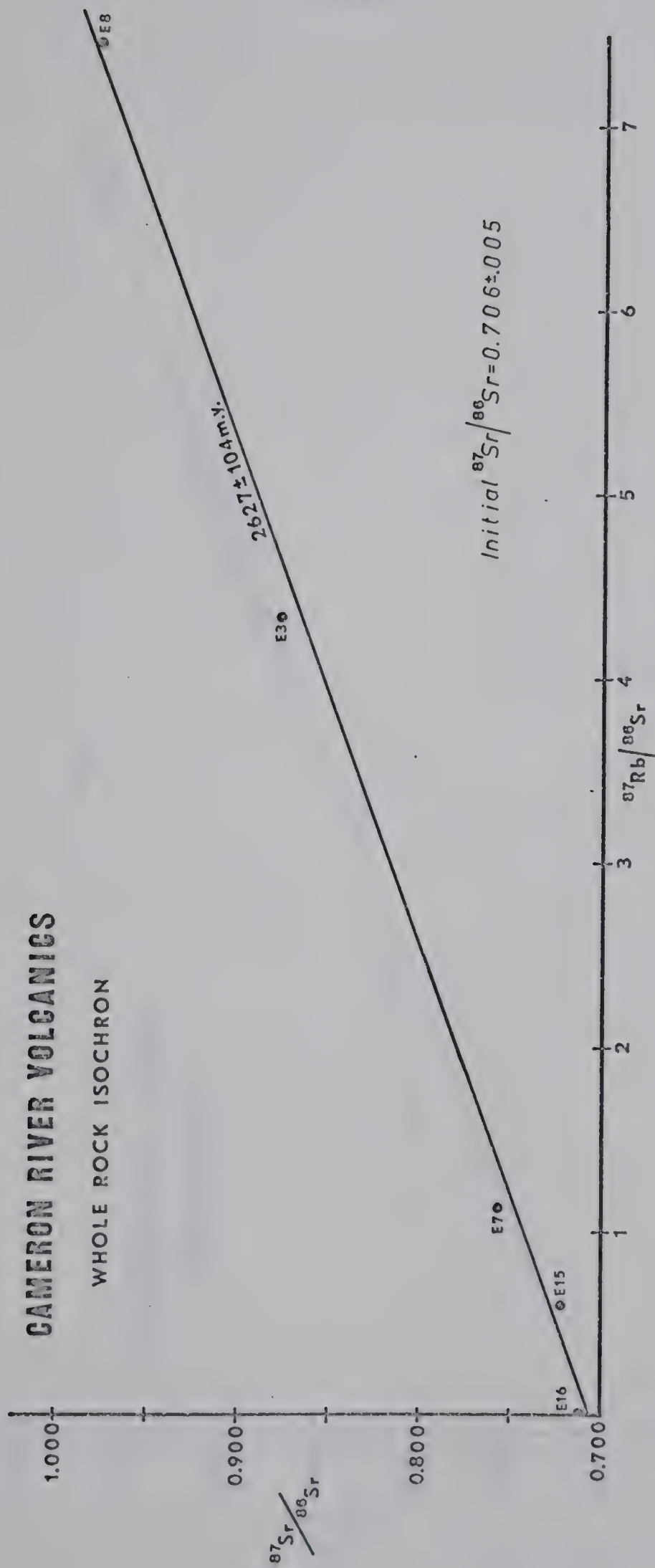


Fig.9. Rb-Sr whole rock isochron plot, Cameron River (meta-) volcanics





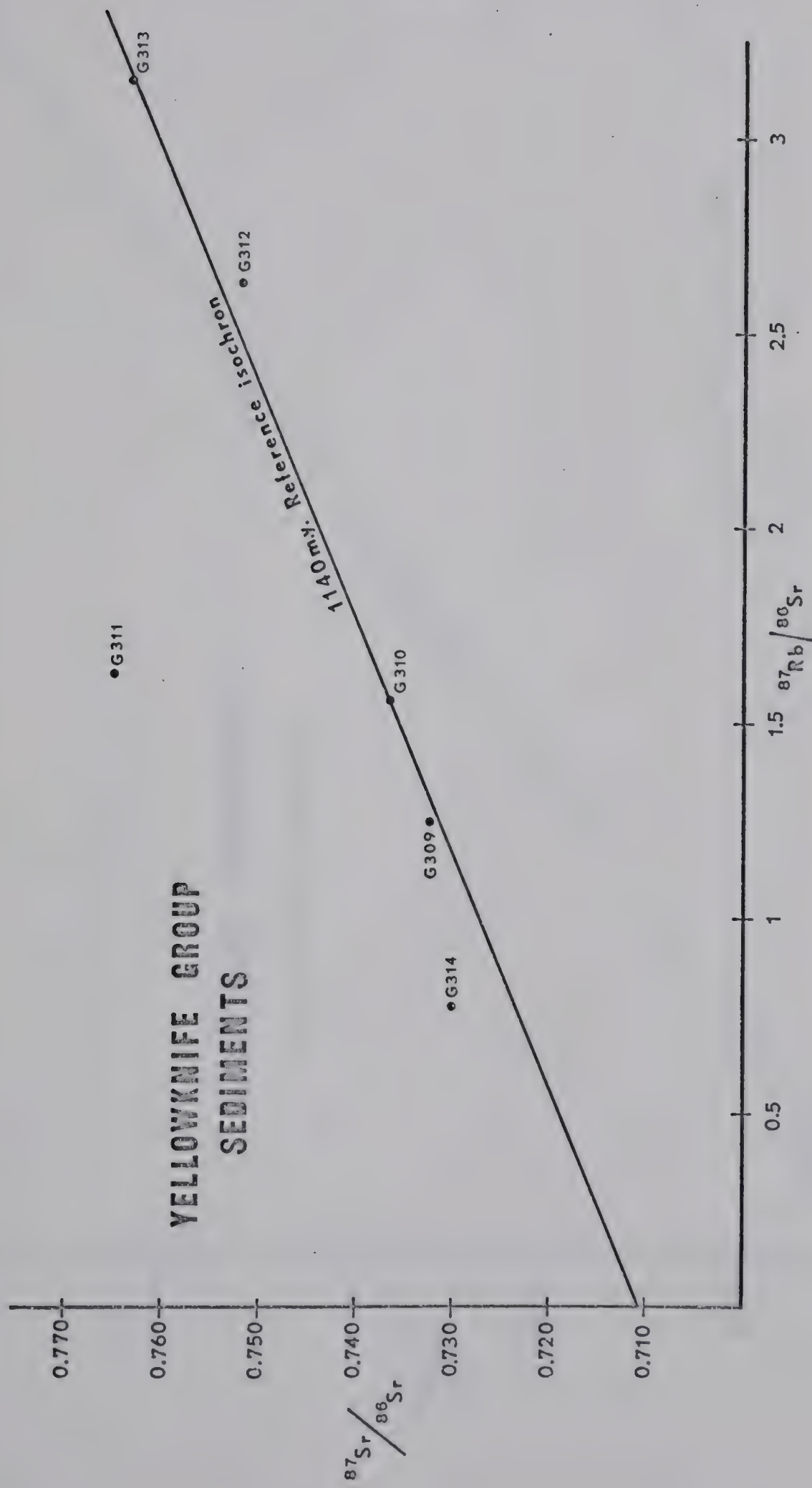


Fig.10. Rb-Sr whole rock isochron plot, Yellowknife Group (meta-) sediments



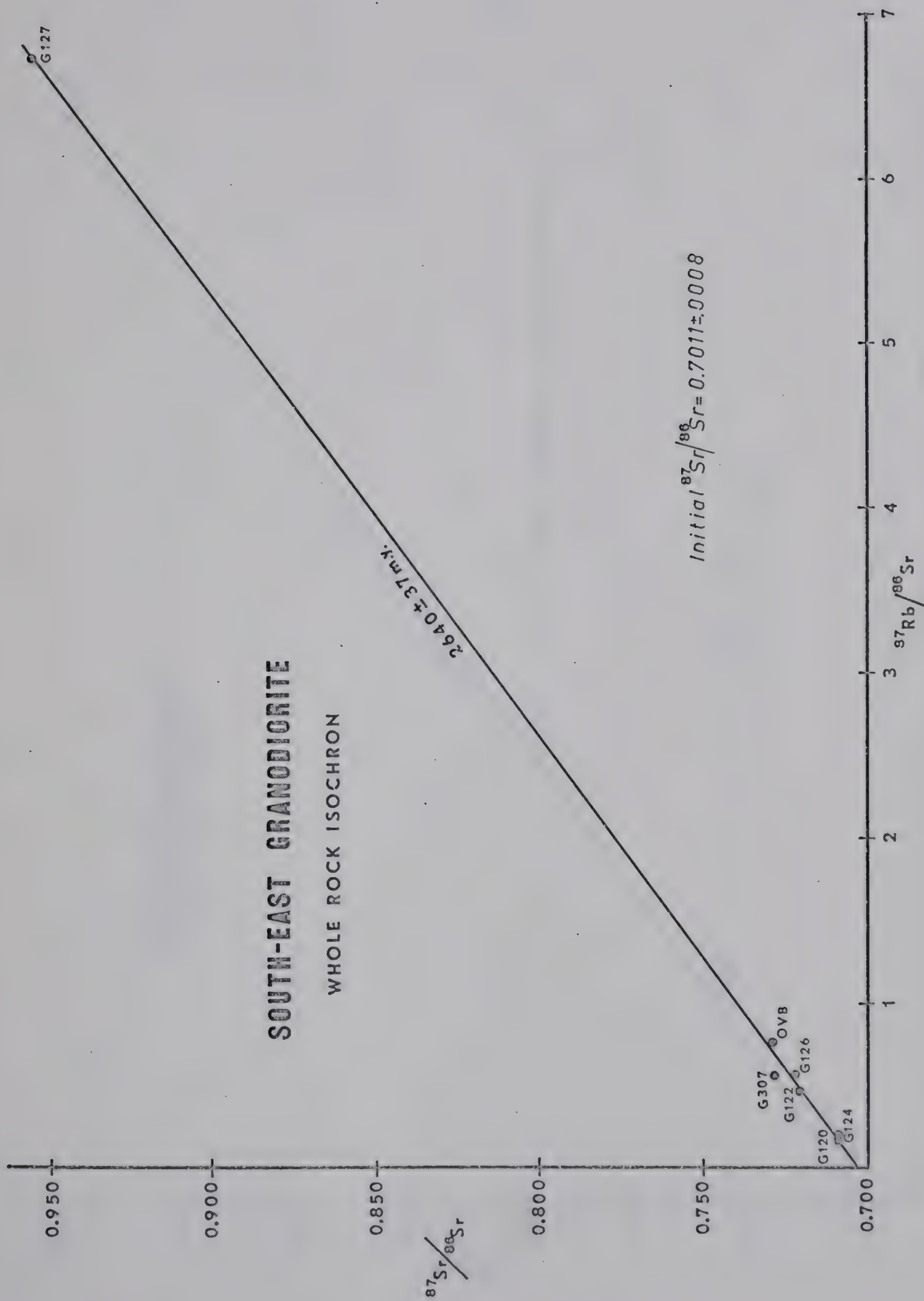


Fig.11. Rb-Sr whole rock isochron plot, South-east granodiorite





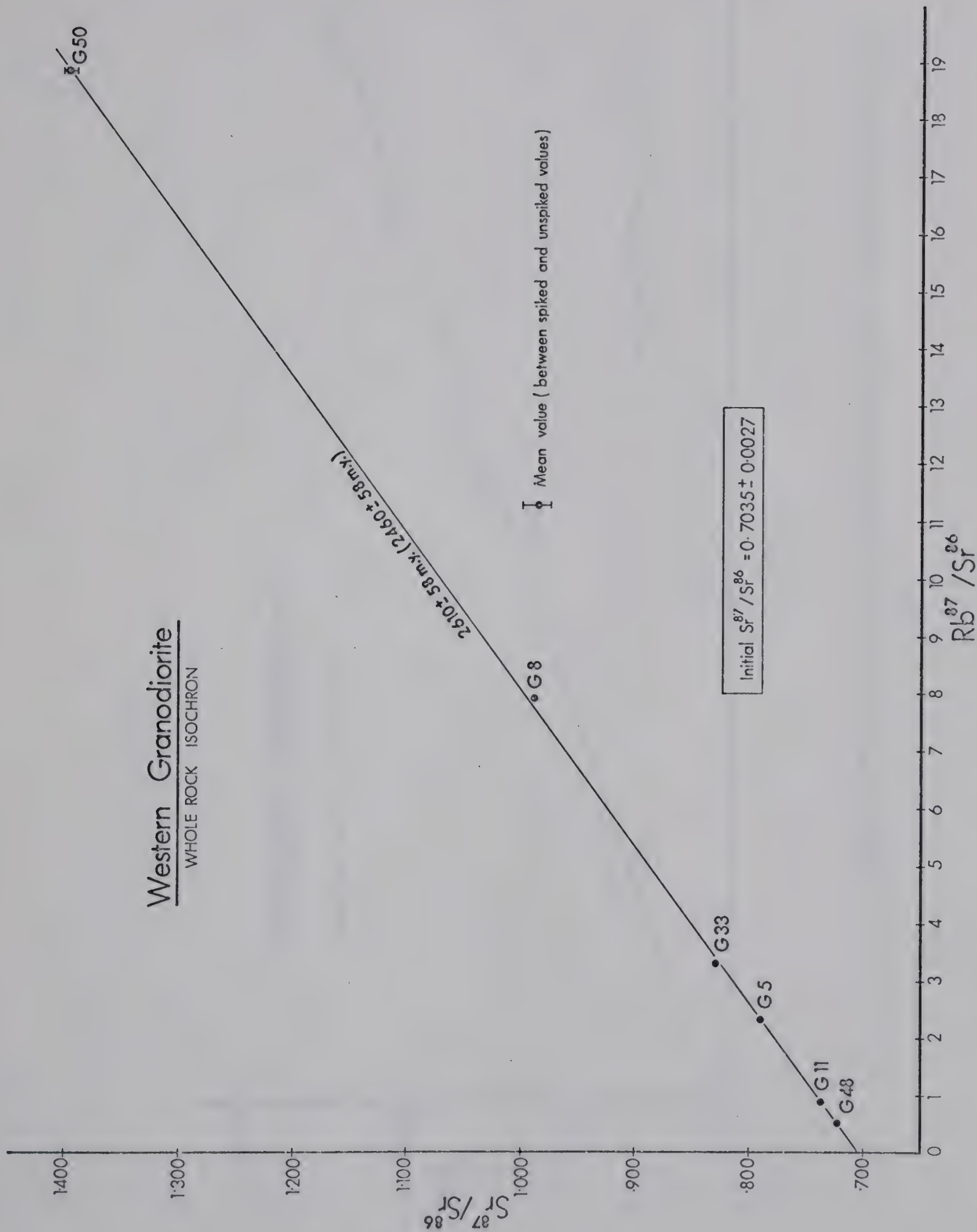


Fig.12. Rb-Sr whole rock isochron plot, Western granodiorite  
Note: age using alternative 47 b.y. half life is given in parentheses.





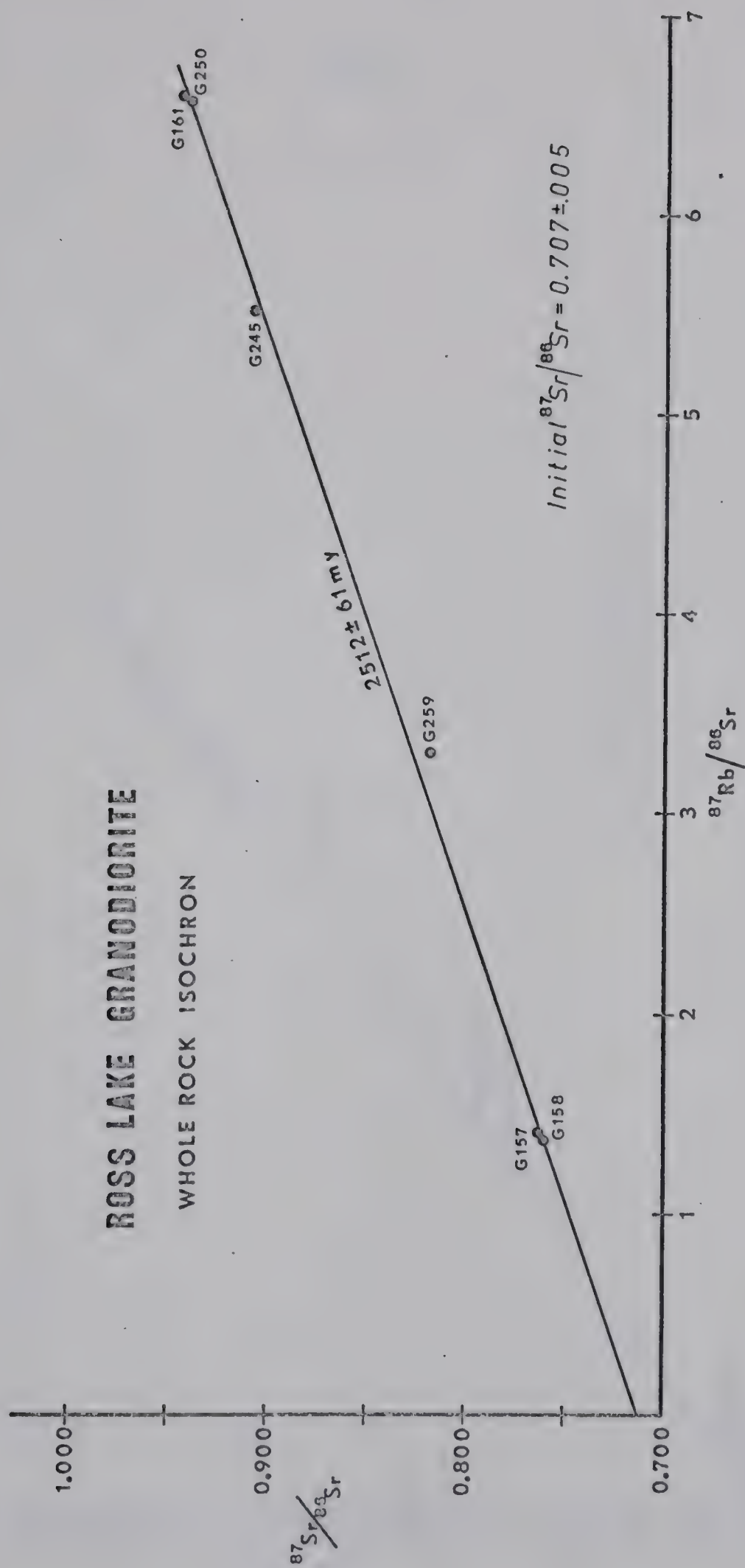


Fig.13. Rb-Sr whole rock isochron plot, Ross Lake granodiorite



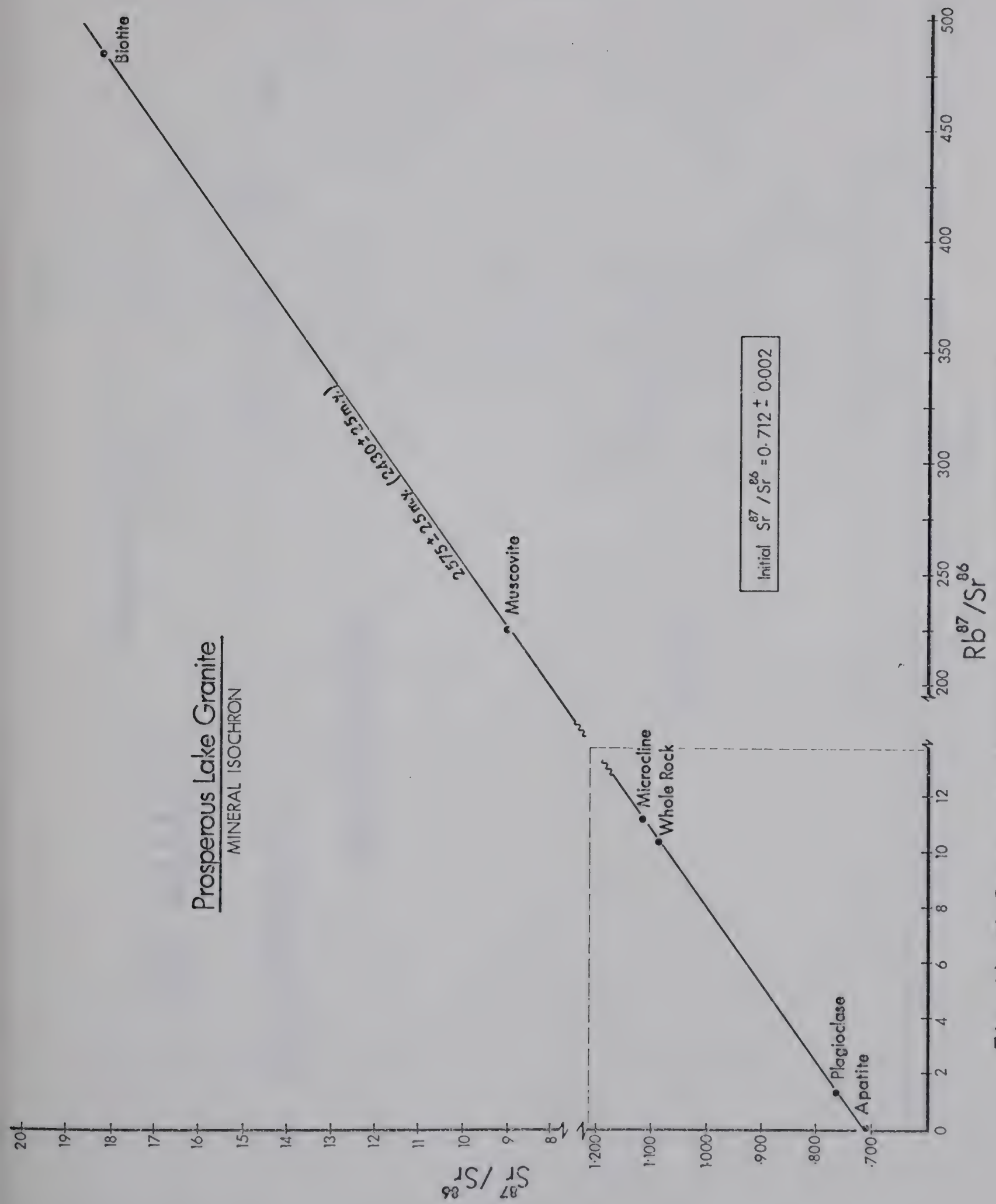


Fig. 14. Rb-Sr mineral isochron, Prosperous Lake granite

Note: age using alternative 47 b.y. half life is given in parentheses.





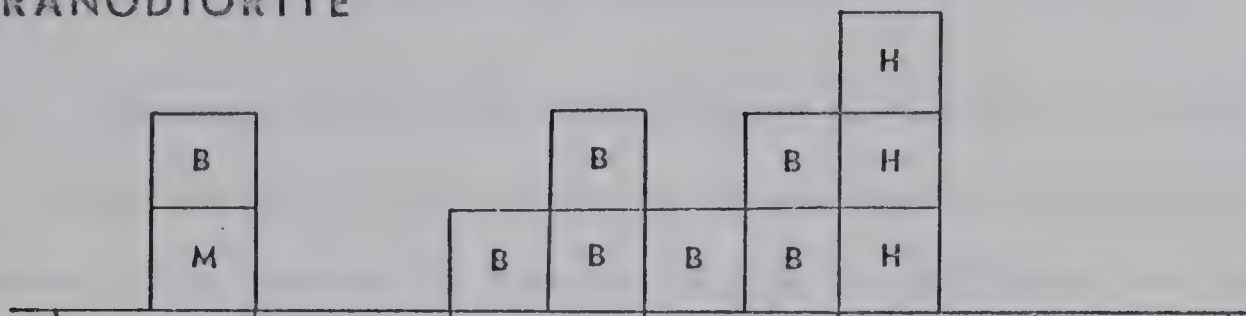




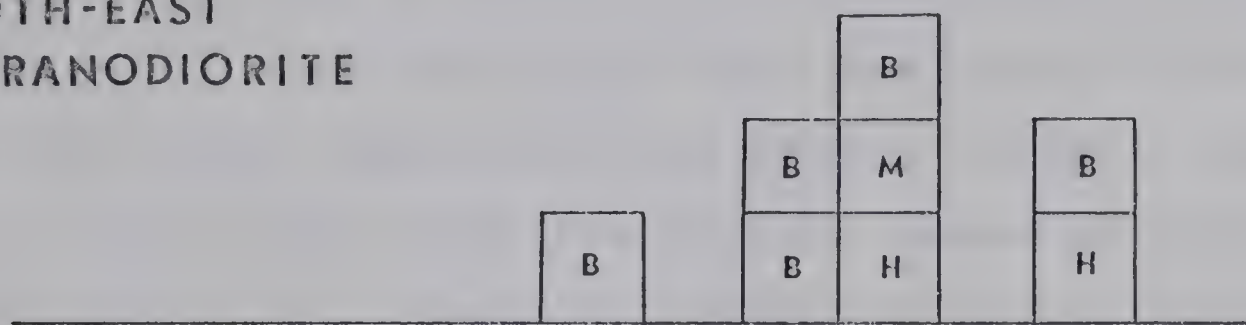


# K-Ar DATES

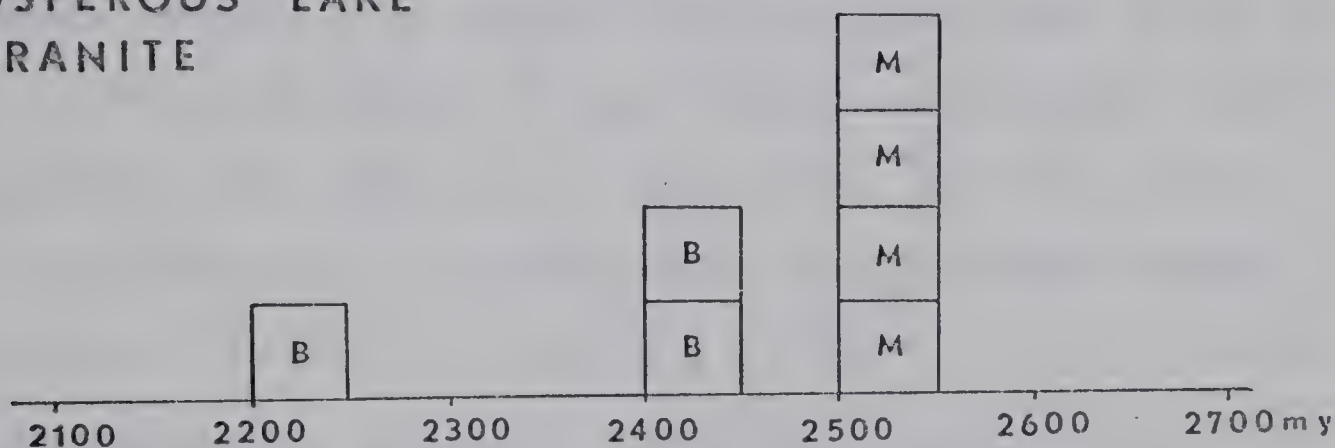
## WESTERN GRANODIORITE



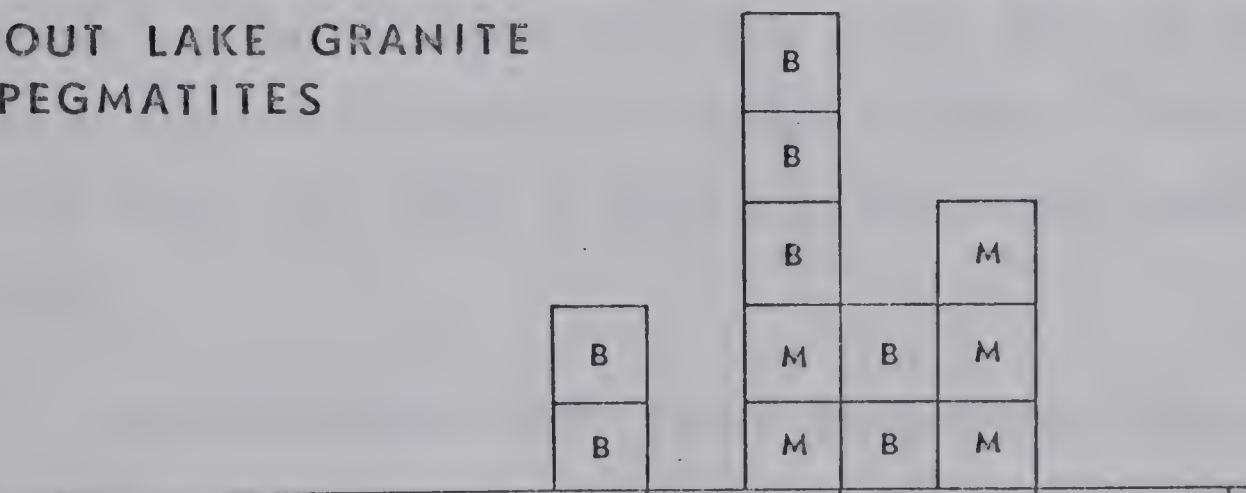
## SOUTH-EAST GRANODIORITE



## PROSPEROUS LAKE GRANITE



## REDOUT LAKE GRANITE & PEGMATITES



## ROSS LAKE GRANODIORITE

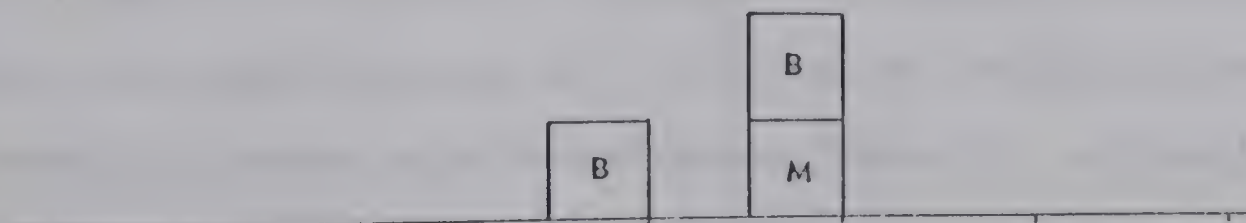


Fig.16. K-Ar dates, Yellowknife subprovince, in terms of rock units



CHAPTER IV

INTERPRETATION OF RADIOMETRIC DATA

Reconnaissance K-Ar geochronology of the Slave province carried out by the Geological Survey of Canada clearly established a close correlation between the Kenoran orogeny in the Slave province and the type Kenoran orogeny of the Superior province (Stockwell, 1964). Stockwell (p. 5-6) found that mica K-Ar dates from the major orogenic events affecting the Canadian Shield were normally distributed, and on this basis proposed that the MM (mean minus one standard deviation) could be used to define a time-stratigraphic boundary at the end of an orogeny. The probable duration of an orogeny is defined by Stockwell as the interval between the MM and MP values. If these concepts are accepted, the K-Ar data recorded in this thesis from a small part of the Slave province amply confirm Stockwell's correlation with the type Kenoran orogeny; e.g. MM = 2,407 m.y., M = 2,463 m.y. and MP = 2,519 m.y. The 30 mica K-Ar determinations used in the present statistical evaluation include five G.S.C. dates from the Yellowknife subprovince (G.S.C. 61-67, 61-64, 60-49, 61-68 and 61-66), four by Burwash and Baadsgaard (1962) and three recently reported by Green et al. (1968) in addition to new analyses included in this thesis.

Although Moorbath (1967) regards the plotting of K-Ar histograms as futile unless the analytical dates are related to the true age of a geological event, some pertinent comments may be drawn from an examination of Figs. 15 and 16. In general, K-Ar dates on hornblende are the oldest, muscovites are slightly younger and biotite may be considerably younger. Where coexisting mineral pairs are available (Table 17), a situation arises





in which K-Ar dates on biotite and coexisting muscovite or hornblende often lie outside the error limits of the analytical procedures. Such discordance has been termed "updating", "partial updating" or "overprinting". It is obvious that the oldest apparent K-Ar dates from a given rock unit will most nearly approach the time of crystallisation of that unit. Inspection of the individual histograms (Fig. 16) suggests that the Southeast granodiorite may be as old as 2,650 m.y., Redout Lake granite and pegmatites 2,600 m.y. and other units as old as 2,550 m.y.

Grain size plays an important role. The oldest dates on micas are from coarse-grained, pegmatitic minerals and the youngest from massive, even-grained granodiorites. Such discordance is commonly attributed to the influence of a later thermal event. This may take the form of a separate thermal pulse or the closure of an entire metamorphic episode as cooling occurs.

The difference in dates between micas and hornblendes is clearly explicable in terms of the considerable difference in activation energies for argon loss from the respective minerals. It should be noted that the apparent difference in retentivity of radiogenic argon between muscovite and biotite may be more apparent than real as simple diffusion theory (volume or lattice diffusion) shows that the fractional loss of  $^{40}\text{Ar}$  from a crystal is inversely proportional to the significant diffusion dimension. This effect was investigated by Hart (1964) and found to be valid for anisotropic crystals such as micas. Most muscovite samples come from large pegmatitic books while biotites vary considerably in grain size.

The nature of the later thermal event is controversial. In Chapter II (Metamorphism) reference was made to a pervasive retrogressive hydrothermal episode associated with the Prosperous Lake granite and causing





extensive chloritization of biotite. This event may be responsible for the invariably younger dates recorded on chloritized biotites from this body. Muscovites appear to be unaffected and give sharply defined dates of 2,500 to 2,550 m.y.

The western border of the Western granodiorite also shows clear evidence of "updating" caused by the encroachment of the Hudsonian event onto the Yellowknife craton. Sample DCG 233 contains relatively large flakes of biotite and fresh books of muscovite which give dates of  $1,970 \pm 25$  m.y. and  $2,190 \pm 28$  m.y. respectively. This sample was collected more than five miles from the nearest granitic body that is regarded as Proterozoic. The result is similar to the dates quoted by Wanless (in Leech et al., 1963) which were obtained from bi-mica granites close to the Archaean-Snare Group unconformity between Basler and Arseno Lakes (Ross and McGlynn, 1965). Apart from these two cases where a later event is clearly established, loss of radiogenic argon could also occur as a result of cataclasis near the large transcurrent faults of the Yellowknife Bay area. The thermal effects of the extensive diabase dyke swarms apparently are not important (Leech, 1966).

Recent papers (Armstrong, 1966, Harper, 1967 and Moorbath, 1967) emphasise the importance of an appreciation of the mobility of radiogenic daughter nuclides under the pressure - temperature conditions of orogenesis. In these considerations more importance is placed on the termination of a continuous  $^{40}\text{Ar}$  diffusion process consequent upon uplift or slow cooling rather than the implied relatively rapid closure and subsequent opening of the system required by the "updating" hypothesis. There is some evidence that high level granitic rocks (emplaced in the epizone) may cool very rapidly. Larsen (1945) has calculated that a time of as short as one million years is required for a large batholith of the mesozone to cool from  $800^{\circ}\text{C}$  to  $200^{\circ}\text{C}$ . (This figure is misquoted in Hamilton, 1965,





where the evaluation of Lovering, 1955, is confused with Larsen's original figure). The thermal history would be very much more complicated in a combined regional metamorphic and intrusive epoch.

Baadsgaard et al. (1961) report K-Ar dates as young as 18 m.y. from quartz diorite plutons near Chilliwack, British Columbia. Examples such as this, together with dates as young as 11 m.y. from the Alps (Jager, 1966) and less than 5 m.y. from the New Zealand Alps (Hurley et al., 1962) emphasise how closely biotite K-Ar dates reflect the time of erosion and sedimentation in a newly formed mountain belt rather than the time of crystallisation of a mineral phase at depth.

To explain the results quoted in the previous paragraph in terms of "updating", it would be necessary to postulate a major thermal pulse in the upper Pliocene or Pleistocene. There is no evidence for such an event in the Southern Island of New Zealand or in the Swiss Alps and only minor evidence of reheating in the third case, attested by the Pleistocene volcanics of the Garibaldi Group of southern B.C. Gabrielse and Reesor (1964) demonstrate the range of mica K-Ar apparent dates which characterise the Cordillera of southern B.C. It is a sobering thought to consider the demonstration by J. V. Ross (1966) that a very similar range of histogram peaks may be obtained by plotting an equal number of values (to which are attached error limits) from a table of random numbers.

Although the apparent bias between K-Ar dates has been considered (see above) to be partly a function of grain size, Jager (1966) and Harper (1967) suggest that system closure to  $^{40}\text{Ar}$  loss in muscovite occurs before that in the biotite lattice. This effect is explicable on





crystallographic grounds as muscovite forms stable, fully ordered  $2M_1$  polymorphs while stacking disorder is common in the other micas (Smith and Yoder, 1956).

Despite a discrepancy between experimentally determined activation energies (summarized by Fechtg and Kalbitzer, 1966) and those deduced on geological grounds (e.g. Hurley et al., 1962), reasonable limits may be set to the temperatures at which minerals become effectively closed systems to  $^{40}\text{Ar}$  loss in nature. Moorbath (1967) suggests between  $150^\circ\text{C}$  -  $200^\circ\text{C}$  for biotite and between  $200^\circ\text{C}$  and  $300^\circ\text{C}$  for muscovite.

The function  $\log D$  vs.  $1/T$  (or  $\log D/a^2$  vs  $1/T$ ) is generally non-linear for sheet silicate lattices and there are consequently at least two values of the activation energy ( $E$ ) in the diffusion equation:

$$D = D_0 e^{-E/RT} \quad \begin{array}{l} \text{where } D = \text{diffusion constant (cm}^2/\text{sec.)} \\ \text{and } T = \text{absolute temperature} \end{array}$$

Since laboratory values of the diffusion parameter  $D/a^2$  (where  $a$  is the effective radius of diffusion) for micas are generally smaller than  $10^{-29} \text{ sec}^{-1}$  and volume diffusion at relatively high temperatures is the rate-controlling step (neglecting gross lattice imperfections), it is reasonable to assume that the effective activation energy is somewhat higher than that obtained by the indirect measurement of Hurley et al. (1962). For these reasons, biotite is effectively closed to  $^{40}\text{Ar}$  diffusion at a temperature somewhat above that encountered in deep drill holes entering the basement beneath the Western Canadian sedimentary basin (Burwash et al. 1962).

It is difficult to decide whether the scatter in biotite K-Ar dates from the Yellowknife area is the result of "updating" or represents progressive closure in response to gradual cooling of the entire area. That the Slave Province (Yellowknife craton) was exposed at the surface before deposition of the Great Slave group was established by Stockwell in





1936 and confirmed by the radiometric dating of Burwash and Baadsgaard (1962). These latter authors suggest (p. 27) that peneplanation may have required a time span of 100 m.y. and deposition of the Great Slave group a similar length of time. Since a syenite dyke dated at 2200 m.y. (K-Ar, biotite) cuts the Great Slave group, it is likely that some part of the Yellowknife craton was exposed at the surface at least 2,300 m.y. ago. Practically all the fresh mica K-Ar dates fall in the range 2,350 to 2,600 m.y. and there is no evidence of a younger mineral-forming event to account for this spread of values. Since the majority of the minerals dated by the K-Ar method are relatively fine-grained biotites, it is reasonable to expect a negatively skewed distribution of biotite dates on a histogram if progressive closure is effective, and a positively skewed distribution (cf. Baadsgaard and Godfrey, 1967, Fig. 5) if "updating" is effective. The histogram shown in Fig. 15 is slightly negatively skewed but there are insufficient data to give an unequivocal answer.

In all probability, the Yellowknife craton has undergone a multi-stage thermal history in which dates from the least retentive fine-grained biotites do represent the termination of a regional diffusion episode. However, coarse-grained micas form a spectrum of dates lying between the oldest and youngest major intrusive events. Pegmatitic muscovites are particularly retentive and suggest that the final hydrothermal metamorphism was insufficient to expel any substantial amount of radiogenic  $^{40}\text{Ar}$  from the muscovite lattice.

No K-Ar data are available from the Yellowknife Group rocks in the thesis area, but a recent K-Ar determination on a muscovite from a conglomerate boulder near the top of the volcanic section at Point Lake,





200 miles north of Yellowknife, yielded a date of  $2,660 \pm 75$  m.y. (G.S.C. 65-64, Wanless et al., 1967).

The foregoing discussion illustrates some of the problems that are encountered in attempting to elucidate the geochronological history of an area by means of K-Ar dates alone.

Turning to rubidium - strontium methods, the bulk of the data has been derived from whole rock samples. Analytical dates from this method have been proven to approximate the true age of crystallisation (Compston et al., 1960, Nicholaysen, 1961). From this point onwards in the discussion, the term "age" will appear more frequently as the analytical methods allow a crystallisation or recrystallisation episode to be defined.

Rb-Sr isochrons were obtained from the oldest exposed rock units, the Yellowknife Group metavolcanics (Figs. 8 and 9) in the Yellowknife Bay and Cameron River areas. In spite of the metamorphism of this series of rocks, the whole rock isochrons represent a reasonable fit to the analytical data. In the case of the less metamorphosed Yellowknife area, the fitted line falls within experimental error limits to give a Model 1 result using the statistical assessment of McIntyre et al., 1966). The scatter in analytical data for the Cameron River area shown in Fig. 9 is probably due to a combination of experimental and geological factors. In this case, the strontium concentration of samples was measured by means of X-ray fluorescence and only the most radiogenic sample was re-analysed for isotopic composition of strontium. The remaining unspiked  $^{87}\text{Sr}/^{86}\text{Sr}$  data are those recorded by Mr. O. Van Breeman in 1964-1965 (pers. comm. H. Baadsgaard). The samples from the Cameron River area were originally collected by Edie (1949) and because of the substantial alteration and





metamorphism of this series of metavolcanics, the writer was not able to collect more suitable samples specifically for Rb-Sr work. Rubidium compositions were determined by isotope dilution and substantially confirmed the X-ray fluorescence values obtained by Van Breeman.

The Rb-Sr isochron ages for the two areas of metavolcanics,  $2,625 \pm 160$  m.y. and  $2,627 \pm 104$  m.y. are not statistically distinct from those of the batholiths which intrude them. However, the mean values of the isochron slopes are consistently greater than that of the intruding plutonic bodies, lending support to the classic concept of Archaean metavolcanics intruded by large granitic bodies. The initial  $^{87}\text{Sr}/^{86}\text{Sr}$  ratio obtained from the well-defined Yellowknife area isochron ( $0.7022 \pm .0023$ ) is consistent with a subcrustal origin. The initial ratio of the Cameron River samples ( $0.706 \pm .005$ ) is less well defined and does not allow any firm conclusion to be drawn as to the source.

The results are slightly older than dates (regarded as minimum dates), obtained by Fairbairn et al. (1967) on Precambrian metavolcanics from the Kirkland Lake area of Ontario, but are entirely compatible with the single K-Ar date mentioned previously (G.S.C. 65-64, 2,660 m.y.) and with Rb-Sr isochron dates reported from the Archaean metasediments of the Canadian Shield by Fairbairn et al. (1967,  $2,619 \pm 58$  m.y.) and Hart et al. (1963, 2,655 m.y.). A zircon sample from the porphyritic dacite horizon gave a  $^{207}\text{Pb}/^{206}\text{Pb}$  date of 2,650 m.y. (Table 26).

Compilation of the available data suggests that the age of the Yellowknife Group metavolcanics may be placed in the range 2,625-2,650 m.y. with considerable confidence. The Rb-Sr isochron age is younger than the model lead date (2,900 m.y.) obtained by Robertson and Cumming (1966) on sulphides from veins in the metavolcanics. Although the bulk of the data





presented by Robertson and Cumming fall on a long period anomalous lead line intersecting the growth curve at approximately 2,900 m.y. (revised to 2,860 m.y. in Robertson, 1966), some results may be interpreted as falling on a short period anomalous lead line consistent with lead evolution in a low U-Th environment ending at a younger date ( $2,500 \pm 100$  m.y.) (D. K. Robertson, personal communication, December, 1967). Insufficient samples have been analysed to define the short period lead line (Robertson, 1966) and work is in progress to clarify this problem.

A discrepancy between model lead ages and ages obtained by other methods is not uncommon, e.g. Butte district (Murthy and Patterson, 1961). If the granodiorites are not the source of the ore-bearing fluids, the metamorphism accompanying the intrusion of the granodiorites at least provided the thermal energy for the distribution of sulphides and native metals into ore deposits (Boyle, 1961). In either event, it may be concluded that the outpouring of volcanics took place only slightly before the intrusion of the granodiorite batholiths. Because of the agreement between the K-Ar and Rb-Sr data for the granodiorites, an age of 2,625-2,650 m.y. is considered more probable for the Yellowknife Group volcanics.

It was hoped that the Rb-Sr whole rock method could also be applied to the Yellowknife Group metasediments. Recent work by Fairbairn, et al. (op. cit.) suggests that Archaean metagreywackes may be successfully dated. Despite careful sampling of the clay rich upper parts of graded beds by Mr. J. Henderson, the results (Fig. 10) give a single apparent isochron plus two other markedly divergent points. This isochron is not interpretable at the present time as the Yellowknife Group metasediments are at least 2,575 m.y. old (the Rb-Sr mineral isochron age of the Prosperous Lake granite). It may be surmised that relatively recent loss of radiogenic





$^{87}\text{Sr}$  has taken place, but further work is required to clarify the meaning of this result. One zircon  $^{207}\text{Pb}/^{206}\text{Pb}$  date (Table 26) imposes a minimum age of 2,530 m.y. on this unit.

Unfortunately, the Rb-Sr ratios of the granitoid pebbles and boulders in the "unclassified conglomerate" horizon are too low to allow meaningful Rb-Sr data to be obtained. Folinsbee et al. (1956) obtained a minimum K-Ar date of 1,440 m.y. from an albite separated from a granite boulder. At the time, Folinsbee stated that "the 1,440 m.y. age is 1,000 m.y. less than the minimum figure which would be geologically reasonable".

The Yellowknife Group rocks are intruded by five major plutonic bodies. Two of these have been considered to be older than at least part of the Yellowknife Group (Baragar, 1966 - Ross Lake granodiorite, and Folinsbee et al., 1968 - South-east granodiorite).

A Rb-Sr whole rock isochron (Fig. 11) and the U-Pb data on zircons (Fig. 17) from the South-east granodiorite confirm that this batholith is as old as 2,640 m.y. A lower limit is imposed by the Yellowknife Group metavolcanics which are intruded by the South-east granodiorite. Together with the mineral isochron data of Van Breeman, 1965 (2,590 m.y.,  $^{87}\text{Rb} \lambda = 1.39 \times 10^{-11}/\text{year}$ ), the extrapolated upper concordia intercept age of  $2,618 \pm 20$  m.y. (Fig. 17) represents the most reasonable estimate of the age of the South-east granodiorite. The initial  $^{87}\text{Sr}/^{86}\text{Sr}$  ratio of  $0.7011 \pm 0.0008$  is indicative of an origin within the upper mantle.

On the basis of all three radiometric methods, the weight of evidence favours the conclusion of Folinsbee et al. (1968) that this batholith was emplaced prior to the deposition of the "unclassified conglomerate" horizon. Additional support is found in Fig. 17 where zircons separated from two conglomerate boulders plot just above the





# ZIRCONS from YELLOWKNIFE AREA

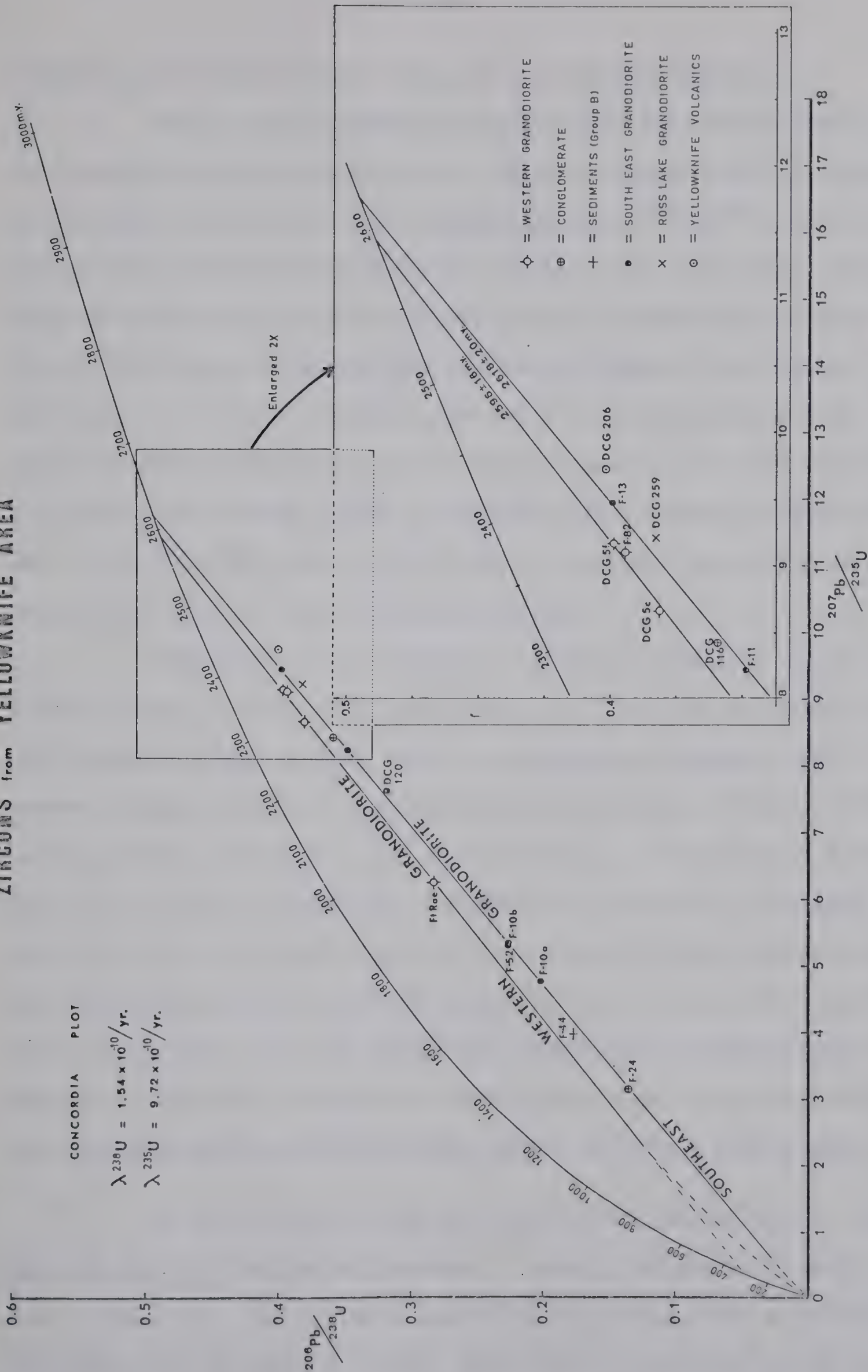


Fig.17. Concordia plot of zircons from six rock units, Yellowknife area





concordia chord defined by the South-east granodiorite samples.

There is less evidence on which to base the relative ages of the Cameron River metavolcanics and the Ross Lake granodiorite. A single zircon sample from the Ross Lake granodiorite has a  $^{207}\text{Pb}/^{206}\text{Pb}$  age of  $2,640 \pm 10$  m.y. but K-Ar and Rb-Sr whole rock isochron ages are younger. The Rb-Sr whole rock isochron shown in Fig. 13 has an apparent age of  $2,512 \pm 60$  m.y. The scatter of points lies outside experimental error and the close proximity to the Redout Lake pegmatites (which are clearly younger on geological grounds) suggests that the analysed samples have been affected to a small, but variable, extent by the pervasive K-feldspar metasomatism. The initial  $^{87}\text{Sr}/^{86}\text{Sr}$  ratio ( $0.707 \pm .003$ ) is somewhat higher than that of the plutonic bodies of the Yellowknife Bay area.

Additional work is required to firmly substantiate the interpretation given in Chapter II, particularly as it has been suggested that this granodiorite may be older than the metavolcanics (Baragar, 1966). The present evidence supports the alternative interpretation of Fortier (1947) and the present writer but is not as unequivocal as is desirable. A younger limit to the age of the Ross Lake granodiorite is imposed by K-Ar dates (up to 2,550 m.y.) on large muscovite books from the Redout Lake granite. These K-Ar dates on coarse muscovites probably give a reasonable approximation to the true age of the Redout Lake granite and associated pegmatites. Samples of the Redout Lake granite showed insufficient variation in Rb/Sr ratio to allow their use for the determination of a whole rock isochron.

In the Yellowknife Bay area, the Western granodiorite is well dated by all three radiometric methods. A sharply defined Rb-Sr whole rock isochron (Fig. 12) yields an age of  $2,610 \pm 58$  m.y. with an initial  $^{87}\text{Sr}/^{86}\text{Sr}$  ratio of  $0.7035 \pm 0.0027$ . This result is confirmed by the zircon





concordia plot which gives an upper intercept age of  $2,596 \pm 16$  m.y. (Fig. 17). The geological interpretation of the lower intersection of the concordia chord is more difficult. There is some evidence in the northern Yukon (Baadsgaard et al., 1961b) for a mid-Palaeozoic event which could have effected episodic lead loss. However, it is probable that a combination of recent leaching and episodic loss of lead during the Hudsonian orogeny has produced the result for the Fort Rae sample (which largely controls the slope of the chord representing the Western granodiorite). The discordancy line falls below that calculated by Tilton (1960) for continuous Pb loss by volume diffusion.

Together with the Redout Lake granite and pegmatites, the Prosperous Lake granite and its associated pegmatites are the youngest plutonic bodies in the area. There is insufficient variation in Rb-Sr ratios in samples of these bodies to allow the construction of a whole rock isochron plot. For this reason, the mineral isochron plot (Fig. 14 - based on unheated samples) produced by Dr. H. Baadsgaard in the course of thermal migration experiments has been utilised. Since the biotite data strongly control the isochron gradient, it is necessary to assess the remaining minerals in order to be certain that whole rock, feldspar and muscovite fractions are each registering the same isotopic event. The biotite date (2,550 m.y.) falls within the 95% confidence limits obtained on regression analysis of the remaining points ( $2,575 \pm 25$  m.y.). The initial  $^{87}\text{Sr}/^{86}\text{Sr}$  ratio is  $0.712 \pm 0.002$ . Such a relatively high initial ratio may point to the inheritance of excess radiogenic  $^{87}\text{Sr}$  from the surrounding metasediments or to later complete internal rearrangement on a scale larger than that of the whole rock sample. The second alternative is unlikely as there is no evidence from K-Ar dates of a thermal





event of sufficient intensity to cause complete mixing of radiogenic and common strontium.

It has been suggested that the Western granodiorite originated by the granitization of a large mass of sediments that lay below the greenstone belt (Boyle, 1961). Because of the relatively low abundance of radiogenic strontium during the Archean, the effect of incorporation of radiogenic strontium on the initial ratio is less than its effect on younger rocks. Modal analysis of nine selected samples (Table 5) indicates that the average composition of the main mass of the Western granodiorite is close to the quartz diorite(tonalite)-granodiorite boundary. According to Winkler (1965), almost complete anatexis of argillaceous sediments at temperatures of greater than  $740^{\circ}\text{C}$  and  $\text{P}_{\text{H}_2\text{O}}$  above 2,000 bars is required to produce a melt of this composition. If these conditions were fulfilled, then the Rb-Sr whole rock data would record the time of metamorphism, and the initial  $^{87}\text{Sr}/^{86}\text{Sr}$  ratio would reflect a metasedimentary provenance. It seems unlikely that the necessary conditions of temperature and pressure required for extensive remobilization of a hypothetical pre-volcanic sedimentary terrain were realized at this time. Additional evidence comes from Western granodiorite zircon separates, which appear to be drawn from a single population of hyacinth colour and lack any overgrowths or sign of multiple parentage.

The Prosperous Lake granite (Tables 11, 12), on the other hand, occupies the centre of a wide aureole of knotted schists, which reach the sillimanite-cordierite-muscovite-almandine subfacies in the zone nearest the granite. Although affected by a retrogressive hydrothermal phase (Folinsbee, 1942), the association andalusite + cordierite + plagioclase +





muscovite is characteristic of the assemblage expected from relatively K-poor, Al-rich argillites.

The metamorphic history of the area has been discussed in Chapter II (Metamorphism) where it is suggested that the temperature - pressure conditions reach the intersection of the orthoclase - muscovite boundary with the granite solidus curve; i.e. approximately 700°C and 4 Kb. pressure (c.f. Winkler, 1965, Fig. 28). If partial anatexis of the surrounding metasediments was responsible for the increase in original  $^{87}\text{Sr}/^{86}\text{Sr}$  shown by the Prosperous Lake granite in comparison with the other major igneous bodies of the area, it is necessary to ascertain the Rb-Sr ratio of the metasediments at the time of anatexis and to estimate whether sufficient time had elapsed in order to allow them to accumulate sufficient radiogenic  $^{87}\text{Sr}$ . The sediments are younger than the volcanics but older than the Western granodiorite. Thus, between 35 and 50 m.y. are available in which the sediments could accumulate radiogenic strontium. The Rb-Sr ratio of the sediments is not known accurately. The Prosperous Lake granite has a  $^{87}\text{Rb}/^{86}\text{Sr}$  ratio of approximately 11.5.

$$(^{87}\text{Sr}/^{86}\text{Sr})_i = (^{87}\text{Sr}/^{86}\text{Sr})_x - (^{87}\text{Rb}(e^{\lambda t} - 1)/^{86}\text{Sr})$$

$$0.703 \cong 0.712 - 11.5 \lambda t,$$

and since  $e^{\lambda t} - 1 = t$ ,

therefore  $t = 56$  m.y.

Thus the high initial ratio of the Prosperous Lake granite mineral isochron is compatible with its origin by partial anatexis of the surrounding metasediments during the process of emplacement.





## CHAPTER V

### COMPARISON WITH OTHER AREAS

This discussion of other Archaean areas is not exhaustive and serves only to underline the similarities and differences between the thesis area and other well known Archaean areas. Much of the material is drawn from informal discussions and from abstracts of the presently unpublished proceedings of a conference on the "Geochronology of Precambrian Stratified Rocks", held at the University of Alberta during June, 1967.

Two other areas on the North American continent yield Early Precambrian (Archaean) ages. The most recent compilation of subsurface data by Goldich et al. (1966) indicates that the ancient rocks of Wyoming and Montana are connected to the Archaean rocks of Minnesota and the remainder of the Superior Province.

The oldest mineral dates in North America are from the Morton Gneiss and Montevideo Granite Gneiss exposed in the Minnesota River valley. Catanzaro (1963) and Stern et al. (1966) show that fresh zircon samples plot along a chord on the concordia plot yielding an upper intersect age of 3,540 m.y. and a lower intercept age of 1,840 m.y. The lower intercept is indicative of episodic lead loss during the Penokean event (1,700-1,800 m.y.) for which there is clear evidence in K-Ar dates from the Granite Falls - Montevideo region.

One of the most detailed contributions to the geochronology of the southern part of the Superior Province is that of Goldich et al. (1961). The major contribution, as far as the Early Precambrian is concerned, is the relegation of the Laurentian to an early phase of the more important Algoman (Kenoran) orogeny and clarification of the relationship





between the Timiskaming and the Ontarian (Keewatin, in part) Series. Almost all the K-Ar and Rb-Sr mineral dates reported by Goldich et al. range from 2,600 to 2,300 m.y. They fall into three groups; the oldest, circa. 2,600 m.y. are equated with the Laurentian folding and igneous activity, the second group, circa. 2,540 m.y. may represent the main Algoman orogeny and a third group, 2,300-2,400 m.y., are thought to represent postkinematic granites. Good evidence for a major unconformity between the Keewatin and Timiskaming Series is known only from along the Minnesota-Ontario boundary.

Although large areas of the Superior Province are shown on regional maps as "granite and gneiss", there is little evidence that the gneisses represent rejuvenated original acidic crust. Purdy and York (1965) found no isotopic evidence to support the concept of Gross and Ferguson (1965), amongst others, who suggested that the gneisses were the remains of an ancient crust over which Keewatin lavas were erupted. It is possible, however, that the Kenoran metamorphism was so severe that the Rb-Sr isochron records only the time of metamorphism. Remelting of older basement and its subsequent rise into a sedimentary succession has created mantled gneiss domes in other areas of the world. These are not described from the Canadian Shield with the possible exception of the Rainy Lake area of Ontario.

In the Beartooth Mountains of Montana detrital zircon concentrates from the metasedimentary gneisses give discordant ages of greater than 3,100 m.y. An episode of metamorphism and pegmatite formation is dated by Rb-Sr methods at 2,700 m.y. (Gast et al. 1958). Published mineral dates from central Wyoming range from 2,200 to 2,600 m.y. A recent





comprehensive study of the Louis Lake granodiorite in Wyoming gives a Rb-Sr age of  $2,650 \pm 100$  m.y. ( $(^{87}\text{Sr}/^{86}\text{Sr})_i = 0.703 \pm .001$ ) while cogenetic zircon fractions form a linear array with an upper intersection on the concordia plot of  $2,675 \pm 15$  m.y. (Naylor et al. 1968). The lower intercept ( $100 \pm 80$  m.y.) is lower than the  $500 \pm$  m.y. intercept predicted by continuous diffusion models. If this represents Laramide disturbance (as suggested in similar work by Silver, et al., 1963) then the Rb-Sr mineral data do not show the effects of the younger event. A similar conclusion was drawn independently by the writer in Chapter IV. Archaean ages are also found in the Black Hills of South Dakota.

Goldich et al. (1966) regard the zircon ages of greater than 3,000 m.y. from the Minnesota River valley as sufficient evidence to reject Wilson's (1949) concept of continental growth of the Canadian Shield around the Superior Province nucleus. For this reason, the search for remnants of an older crust has been pursued with some vigour in Canada. No proven radiometric dates older than 2,700 m.y. have been found at the present time and any evidence of an older crust relies on lead model dates such as those of the Manitouwadge galena deposit (Ostic et al., 1963) and the Yellowknife area (Robertson, 1966) and the "pebble batholiths" described by Bass (1961).

Miller's (1911) binary classification of Archaean formations into a predominantly volcanic series, the Keewatin, overlain, in some cases unconformably, by a predominantly sedimentary series, the "Timiskaming, is still followed by the Ontario Department of Mines. In general terms, the binary classification may be applied to all Archaean formations of the Shield. In 1939, Wilson used the terms "Keewatin-type" and "Timiskaming-type" to designate the dominantly volcanic and dominantly sedimentary





sequences of the Archaean. In these terms, stratigraphic rather than lithologic similarity is implied. Goldich et al. (1961) raised the Timiskaming to the status of a system - Timiskamian System - typified by the Knife Lake Group.

Although a two-fold division of Archaean rocks on the basis of lithology alone is inadequate in detail, it is a valid regional concept. The nature of the contact between the two divisions is similarly controversial. Both problems are not restricted to the Canadian Archaean but have been discussed in Scandinavia, Europe, South Africa and Australia.

The Pre-Karelian (Saamian) basement of the Baltic Shield was strongly affected by the Svecofenno - Karelidic orogeny about 1,800-1,900 m.y. ago. However, Archaean basement is recognised in eastern Fennoscandia, Lapland and the Finnmark area of northern Norway. Most of the pre-Karelian dates fall in the range 2,600-2,800 m.y. but some dates of 3,000-3,400 m.y. are found in the Kola Penninsula (Kuovo and Simonen, 1967, Kratz et al. 1967). Holmes (1965, p. 368) correlates the Palomas Greenstones of the Kola Penninsula with Keewatin greenstones of North America. In West Greenland, infracrustal gneisses and granulites yield K-Ar dates of 2,490-2,710 m.y. (Larsen and Moller, 1967) although the more important Ketilidian orogeny (1,500-1,800 m.y.) has largely "updated" micas from the infracrustal rocks. A similar situation exists in the British Isles where a small area of Scourian granulite facies rocks yield dates of greater than 2,600 m.y. Pegmatites intruding the Scourian rocks are now dated at 2,460 m.y. (Lambert et al., 1967).

In the Ukrainian Shield, Semenenko (1967) recognises two cycles within the earliest division of the Precambrian (Precambrian I). In the geosynclinal assemblage of formations, an earlier cycle (Konkian)





operative within the period 3,500 to 3,100 m.y. and a later (Aulian) cycle, operative within the period 3,100 to 2,700 m.y., are distinguished.

Recent work by the M.I.T. group and the University of Sao Paulo in Brazil carried out with a view to verification of the hypothesis of continental drift (Hurley et al., 1967), suggests that the Imataca complex of Venezuela (approximately 3,000 m.y.) has a counterpart on the West African Shield in Sierra Leone and western Liberia. It is particularly interesting to note the antiquity of the Venezuelan iron ores. These correspond to the Archaean iron ore formations in Minnesota (Soudan member) and those of the Ukraine and are generally older than the major Lower Proterozoic iron ore formations of Minnesota and Western Australia.

In central Africa, the Swaziland System contains a well preserved Archaean sequence which yields Rb-Sr isochrons as old as 2,970 m.y. (Fig. Tree shales). Here the sequence of rock types is similar to that of other Archaean areas, i.e. volcanics (including the Dominion Reef System) and banded cherts with serpentized ultramafics are overlain by greywackes and shales with subordinate tuffs and banded cherts. The volcanic - sedimentary sequence is intruded by pegmatites which give ages of 2,900 to 3,400 m.y. (Allsopp et al., 1967).

Archaean rocks in India include the Penninsula Gneiss in Bangalore ( $2,635 \pm 45$  m.y.) and the Dharwars (schists) which appear to be somewhat older (2,800-3,000 m.y. - Crawford and Compston, 1967). Charnokites and granites near Madras also give Archaean ages. In the Central Highlands of Ceylon, khondalites (garnet sillimanite schists) may be as old as 2,850 m.y.

The Precambrian Shield forms two large blocks in Australia. The Yilgarn block in southwest Western Australia contains granitic gneisses





and metasediments with ages in the range 2,700 to 3,000 m.y. (Compston and Arriens, 1967). The Kalgoorlie goldfields belt was studied by Turek, 1966 and yielded well-defined Rb-Sr isochrons for several pre-granite volcanic and sedimentary units which range around 2,665 m.y. The age of granite emplacement is closely defined as  $2,612 \pm 13$  m.y. Turek also studied the earliest post-granite dyke set in the area ( $2,420 \pm 30$  m.y.) and found that an isochron defined by gold-bearing whole rock samples ( $2,400 \pm 30$  m.y.) correlated with the emplacement of these E - W mafic dykes. Recent work from this area has disclosed a conglomerate (Kurrawong conglomerate) bearing 3,000 m.y. granitic boulders at the base of the Upper Sequence of Horwitz and Sofoulis, 1965.

This area has many similarities to the Yellowknife district but the division into upper and lower divisions is not nearly as distinct. Detailed mapping has shown that basic pillow lavas occur in both units and that they interfinger with the sediments. Both upper and lower units are folded considerably and are intruded by granites and rare element-bearing pegmatites. The structural configuration is of basins and domes resulting from two superimposed fold trends and the grade of regional metamorphism is upper greenschist to lower amphibolite facies.

Archaean rocks are also found in the Pilbara block in northwest Western Australia. Here, massive granites and lithia pegmatites dated at 3,000 to 3,050 m.y. intrude greenstones and metasediments of the Pilbara System. There appears to be no equivalents of the 2,600 m.y. granites of the Kalgoorlie area.



## CHAPTER VI

### TECTONIC HISTORY OF THE YELLOWKNIFE DISTRICT

A possible model for the tectonic evolution of the Yellowknife area is discussed in this chapter. Such a synthesis draws not only on the geochronology but also on the regional structure, sedimentary and volcanic parameters, metamorphic evolution and plutonic history. It is inevitable that a few contradictions are introduced but it is thought that the synthesis given represents a reasonable basis on which to plan further work.

In order to establish a basis on which to develop the arguments that are used, a short outline of the proposed tectonic history is given. Each of the major points in this outline is then discussed in a sequence which corresponds to the development in time of the various facets of the tectonic cycle.

It is considered that the area is representative of a discrete orogenic addition to the earth's crust and may be treated as the result of one complete tectonic cycle.

#### Outline

Outpouring of a thickness of as much as 40,000 feet of submarine volcanics onto the oceanic crust marked the commencement of the eugeosynclinal phase of the tectonic cycle. The chemical character of the volcanics, with some calc-alkaline affinities, is similar to that of Cenozoic oceanic island arcs. Unconformably overlying the volcanics is a thin sequence of conglomerate and quartzite that passes, with apparent conformity, into an accumulation of graded quartz greywackes and minor





shales. The unconformity between Divisions A and B of the Yellowknife Group is of local character and of temporally minor extent. Further, the character of the clastic fragments forming the "unclassified conglomerate" horizon does not suggest an earlier completed tectonic cycle. Anticipating a conclusion reached later in the chapter, it may be stated that potassic granites and high grade metamorphic rocks represent the closing stages of a tectonic cycle. There is no evidence that these rocks are represented in the "unclassified conglomerate". If a substantial body of older sialic crust existed at the time of deposition of this unit, it is likely that representatives of this crust would be found. Rather, the fragments are of local provenance, derived chiefly from the volcanic rocks of Division A, but locally from the potash-deficient South-east granodiorite.

This results in the superficially paradoxical picture of a deformed volcanic - sedimentary accumulation containing fragments from plutonic masses emplaced during the same orogeny that was responsible for the deformation. Such complexity is a common feature of Phanerozoic orogenic belts (e.g. Read, 1955, p. 424). A combination of radiometric methods makes it possible to determine a sequence of igneous and metamorphic events within an orogeny.

Although the metavolcanic pebbles did not receive detailed attention, it is not improbable that mild predepositional regional metamorphism may have taken place prior to the erosion of part of the volcanic pile. Read (1955) has used the term 'orogenic metamorphism' to describe the pervasive greenschist facies metamorphism commonly associated with early orogenic metavolcanics and metasediments.

Experimental studies show that differentiation under temperature-pressure conditions prevailing in the upper mantle is able to





produce magmas of the calc-alkaline suite by fractional melting of eclogite at depths of as much as 150 km. or by fractionation of alumina-rich edenitic hornblende at approximately 40 km. Ringwood and Green (1966) suggest that the gabbro-eclogite transformation may form a "tectonic engine".

Calc-alkaline magmas generated in this manner moved upwards and invaded the deforming volcanic-sedimentary assemblage. Early plutons are almost synchronous with the initial Kenoran deformation and possibly contribute to the clastic sediments forming the upper part of the Yellowknife Group.

The continued accession of magma into the deformed Yellowknife Group metavolcanics and metasediments in the form of late kinematic batholiths caused an abnormally high thermal gradient in the orogenic belt. As the orogeny developed, the metamorphism passed gradually into higher grade metamorphic facies (described in Chapter II) as a result of the higher thermal gradients experienced in the culminating stages of the orogeny.

Low  $^{87}\text{Sr}/^{86}\text{Sr}$  original ratios from Rb-Sr whole rock isochrons indicate that the major synkinematic - late kinematic bodies rose from the upper mantle without any significant anatectic contribution from the crust. On the other hand, the younger Prosperous Lake granite appears to have incorporated radiogenic  $^{87}\text{Sr}$  from the surrounding metasediments.

The new sialic segment was slowly uplifted, became stabilised and erosion commenced. The oldest set of diabase dykes mark the final stage of the first tectonic cycle involving the Slave Province.

Thus there is no need to postulate an extensive pre-existing sialic segment in the Yellowknife area although it is possible that small





older segments may, in time, be found. It seems likely that if ancient segments did exist, they were not sufficiently substantial to allow the accumulation of miogeosynclinal sediments.

#### Nature of the volcanic sequence

The association of calc-alkaline rocks with tectonically active zones is suggestive of a close relationship between the genesis of calc-alkaline rocks and the fundamental mechanism of orogenesis.

Baragar (1966) describes the Yellowknife volcanics as of tholeiitic character modified by the superposition of calc-alkaline characteristics by sialic wall-rock contamination. The writer prefers to exchange Baragar's priorities and regard the partially calc-alkaline character as fundamental and the tholeiitic properties as superimposed. This transposition is in harmony with Baragar's observation that the short range iron enrichment (which forms the basis for the tholeiitic trend in the sills) takes place in a high level magma chamber but the MgO/FeO (total) ratio, the "most conspicuous indicator of basaltic differentiation, shows no overall variation".

Although Baragar (1966, p. 26) claims that the metamorphism of the Yellowknife Group rocks was essentially isochemical, Boyle (1961, p. 67) suggests that there has been some migration of potash and soda during metamorphism. Without complete analyses (including the CO<sub>2</sub> content), it is difficult to evaluate the relation between normative and modal anorthite content used by Baragar to substantiate the isochemical nature of the metamorphism. In a similar manner, Wilson et al. (1965) have used Larsen variation diagrams and silica variation diagrams to assess the possibility of migration of cations during metamorphism and agree that





substantial migration is unlikely. This point is particularly important since the statistical differences in principal oxides (excepting  $\text{TiO}_2$ ) between oceanic and circumoceanic lavas are not readily distinguished if the analysed rocks contain more than 1%  $\text{H}_2\text{O}$  (Chayes, 1964). The low totals in Table II of Baragar (1966) suggest that  $\text{H}_2\text{O}$  may have formed as much as 3% of these ancient lavas.

Nevertheless, the chemical character of the Yellowknife lavas is strongly akin to the circumoceanic (calc-alkaline) Tertiary and Quaternary lavas from the Mariana Islands and the Aleutian chain. Gorshkov (1962) and Coats (1962) reject the concept that the calc-alkaline rocks of these areas originate from contamination of oceanic magmas by sial from an adjacent continental mass, since geophysical evidence shows that these areas are surrounded by oceanic crust. It is concluded since tholeiite (once considered specifically characteristic of continental areas) is also characteristic of areas floored by oceanic crust, circumoceanic (or calc-alkaline) lavas need not be specific indicators of crustal contamination.

#### Character of the "unclassified conglomerate" and Division B sediments

The poorly sorted conglomerate of the Sub Islands in Yellowknife Bay contains relatively well rounded boulders in a matrix of coarse sand grade. Interbedded with the conglomerate are cross-bedded quartzites containing isolated pebbles of granite and metavolcanics. To the north, on the west shore of Yellowknife Bay, the conglomerate is very much more deformed with a marked near-vertical schistosity which tends to bend around the larger boulders. In spite of the attention paid to the granitoid boulders, the majority of clasts are from the metavolcanics and metagabbros





of Division A of the Yellowknife Group. Vein quartz pebbles are not uncommon.

It has been demonstrated in Chapter II that the conglomerate and overlying quartzite horizons were involved in the Kenoran deformation. For this reason, the suggestion of Henderson and Brown (1952) that the rocks are much younger than the Yellowknife Group is not valid. The problem of the apparent difference in sedimentary character between the well sorted quartzites and the overlying greywackes remain, however. The abundant development of cross-bedding and predominance of sandy sediments and conglomerates indicates that deposition took place in a high energy environment adjacent to a coastline formed largely of meta-volcanic rocks. It is not improbable that greywacke sediments would accumulate in the deeper parts of the same basin under the influence of turbidity currents.

Of more importance is the problem of quartz provenance. It is necessary to establish a source for the substantial amount of quartz which contributed to the clastic fraction of the Yellowknife Group B sediments. Brief examination in the field tends to confirm the statement by Donaldson and Jackson (1965) that Archaean greywackes are richer in quartz than some Phanerozoic greywacke sequences. The high content of clastic quartz in the North Spirit Lake area prompted Donaldson and Jackson to postulate the existence of older granitoid rocks removed from the Archaean volcanics by one or more orogenic cycles. It should be noted that the chemical and modal analyses of the leucophanerites (Donaldson and Jackson, p. 634-635) bear a remarkable resemblance to the Kenoran quartz diorites which intrude the sedimentary sequence. The absence of feldspar in many of the North Spirit Lake greywackes and the comparative





maturity of the quartz clasts are possible indicators of a second cycle origin, but both characters may equally well represent a distant provenance.

There is no reason to suspect that the intrusion of synkinematic plutons took place at exactly the same time throughout the Superior and Slave Provinces. Evidence from other orogenic belts indicates that tectonic evolution occurs in both space and time. Two well-known examples of a temporal overlap between volcanism, the appearance of diorite plutons and flysch sedimentation are those of the Ordovician of the British Isles (Read, 1961) and the Tasman geosyncline of eastern Australia (Snelling, 1960). This observation helps resolve some aspects of the conflicting interpretations of Donaldson and Jackson (op. cit.) and Boutcher et al. (1966).

Recent work by Henderson (1968) confirms that the parallel drawn by Pettijohn (1943) between the sedimentary-volcanic belts of the Superior Province and classical eugeosynclines may be extended to the Slave Province. The prolific occurrence of graded bedding and turbidity current features in Division B rocks led Henderson to compare the sedimentary succession with classical flysch deposits of Europe.

#### Island arc formation and determination of the age of the Yellowknife Group volcanics

The combination of pillowed metabasalts, polymictic conglomerates and greywacke-type sedimentation is characteristic of eugeosynclinal environments forming the pre-tectonic to early tectonic portion of an orogenic cycle. Folinsbee et al. (1968) suggest that this portion of the evolution of the Yellowknife area may be explained in terms of the development





of an island arc. Coats (1962) illustrates a possible mechanism which is compatible with seismic evidence from the Pacific basin (Benioff, 1954). This model explains the creation of a sima-floored island arc as the result of extrusion of magma adjacent to the apex of a crust-mantle wedge formed by the development of a low angle thrust plane in response to the downward motion of a convection cell.

The analytical precision of the Rb-Sr isochron and zircon data do not permit one to distinguish between the probable age of the Yellowknife volcanics given by a  $^{207}\text{Pb}/^{206}\text{Pb}$  age on a single zircon sample (2650 m.y.) and that given by the Rb-Sr isochrons (2625 m.y.). Turek (1967) considers that the Rb-Sr isochrons from the pre-granite units at Kalgoorlie, Western Australia, represent the result of a low grade regional metamorphic episode and do not give the true age of intrusion. If the mild metamorphism suffered by the Yellowknife Group volcanics chosen to define the isochron was essentially isochemical, then there is no reason to suspect disturbance of the Rb-Sr system on a whole rock sample basis. For this reason the age of extrusion is probably no more than 2650 m.y.

#### A possible model for derivation of the calk-alkaline suite

Recent experimental work at the Australian National University has resulted in several papers on the origin of igneous rocks from the upper part of the mantle. In spite of the simplified nature of the initial compositional ranges, the products of high temperature - high pressure experiments give a valuable insight into possible stability fields of minerals under conditions experienced in the upper part of the mantle.

Ringwood and Green (1966) propose a possible 'tectonic engine'





based on experimental investigation of the gabbro-eclogite transformation. The following summary is that of Green (T. H.) and Ringwood (1966).

"According to this model, it is envisaged that in present or possible future active orogenic regions of the earth's crust such as island arcs, some oceanic rises, oceanic rift systems and continental margins, large piles of basalt have developed as the first stage in the cycle of orogenic activity and continental growth. As long as active basaltic activity persists, the geotherms in the particular region remain high. However, with cessation of volcanic activity the geotherms fall and the deeper regions of the basaltic pile begin to transform to eclogite. The eclogite ( $\rho = 3.45 \text{ gm/cm}^3$ ) is denser than the ultramafic upper mantle ( $\rho = 3.3 \text{ gm/cm}^3$ ) so that it begins to sink into the mantle. In the early stages, sinking is relatively slow, and results in formation of a geosyncline. At a later stage, sinking becomes catastrophic, leading to severe crustal deformation and folding of the geosyncline. Eventually, the sinking eclogite bodies reach a level in the mantle (probably at depths of 100-150 km) where the temperature is sufficiently high to cause partial melting of the eclogite. Magmas thus produced rise upward and intrude the folded geosyncline. It is proposed that these magmas may represent the calc-alkaline suite".

The validity of this model rests on the feasibility of transforming basalt into eclogite under near-anhydrous conditions in the upper part of the oceanic crust. It is necessary to assume that this condition is able to be met as no field evidence from the Yellowknife area is able to confirm or deny the possibility.

In this model, as first proposed, the lack of variation in  $\text{MgO/FeO}$  (total) ratio is attributed to the presence of Fe-rich garnet





in the residuum left after fractional melting of eclogite under conditions of high pressure. A complementary two stage model (Green and Ringwood, 1968) allows access of water to the volcanic pile. Under conditions of approximately 10 Kb (30-40 km depth), where  $P_{H_2O} < P$  load, the stability field of subsilicic amphiboles is greatly enlarged with the result that a persilicic liquid is formed on fractionation. A point in favour of both these models is that the mass ratio of residual phases to liquid is approximately unity compared with ratios of at least two in conventional Bowen-type fractionation.

Access of water to the volcanic pile appears to be a more reasonable hypothesis than that requiring almost dry transformation to eclogite so that the 1968 model is preferred because of its simplicity. Geophysical evidence suggests that a drop in seismic velocity (e.g. Hess, 1962) occurs in the upper mantle beneath areas of rising convection cells and also on the upper side of the "Benioff earthquake zone". This decrease in seismic velocity is attributed to serpentization of the volcanic pile. It is readily explained by means of water from the hydrosphere introduced into the mantle by the sinking limb of a convection cell.

The presence of a potash-bearing phase such as amphibole in the crystal residuum explains to some extent the low potash content of the calc-alkaline diorite plutons. At this point it is germane to quote the conclusion reached independently by the writer and also by Tougarinov (pers. comm. in Marmo, 1967) that true granite compositions were probably not attained until potassium was concentrated in the upper lithosphere by passage through a sedimentary cycle.





Onset of plutonism within the Kenoran orogeny

Although a gneissic character is typical of synkinematic granites, there are substantial bodies of comparatively homogeneous quartz diorite composition that form early batholiths in the Precambrian shields of Russia, Asia, Finland and West Africa. (It may not be entirely coincidence that these areas are also amongst the most ancient segments of the earth's crust). While these bodies are discordant in detail, synkinematic granitoid rocks are approximately concordant with the regional strike of the country rocks. Such "granites" are placed in the 'mesozone' of Buddington (1959) or termed 'harmonious granites' by Walton (1955).

Two granitic bodies in the area under investigation may fall into the category of synkinematic masses. The Ross Lake body is foliated and on the basis of a single  $^{207}\text{Pb}/^{206}\text{Pb}$  age is approximately the same age as the volcanics which it probably intrudes. The radiometric evidence strongly suggests that the intrusion of the South-east granodiorite was approximately synchronous with the onset of deformation and possibly antedates the deposition of the upper part of the Yellowknife Group sediments.

The relative homogeneity of these bodies suggests that they passed through a molten stage in their evolution and have moved upwards into the lower part of the Yellowknife Group as plutonism commenced. The homogeneity and uniquely igneous appearance of the zircon population from the South-east granodiorite gives no evidence of a sedimentogeneous origin. This possibility is not excluded for the Ross Lake granodiorite although overgrowths were not recorded in two separates from one large sample of this body. Hamilton (1948) has studied the zircons from the Ross Lake granodiorite in more detail and also reports a lack of overgrowths.

Chemically, the border zones of both the South-east granodiorite





and Ross Lake granodiorite are characterised by a lack of potash. This observation has been previously expressed in a positive sense by the use of the term 'sodic' but the two expressions may not be mutually exclusive. Low potash quartz diorites are typical of the early stages of modern island arc plutonism (Matsuda, 1962). The consistently high percentage of CaO in quartz diorites practically ensures that the plagioclase cannot be more sodic than oligoclase. Albite granites (such as those described by Moore, 1954, from the Porcupine area) are regarded by Bass (1961) as of restricted distribution. Further, albite bearing granites are almost invariably late kinematic bodies (Marmo, 1967). Additional support for this concept comes from the common association of economic mineralization with albite granites. It is probable that late kinematic granites are intruded under hydrothermal conditions, a concept that is in harmony with the plagioclase - epidote relationship which is used as an indicator of metamorphic grade.

The Western granodiorite carries an abundance of epidote and the K-feldspar in this (and other late kinematic bodies) is highly triclinic microcline. Together with the extensive stoping and wall-rock assimilation, these are considered to be features of a disharmonious, late kinematic body. The age of emplacement, 2595 to 2610 m.y., is consistent with such a view. Zircon samples from this unit are completely free from overgrowths and lack any sign of multiple parentage.

#### Strontium isotope initial ratios

It has been suggested that the Western granodiorite and Southeast granodiorite originated by the granitisation of a large mass of sediments that lay stratigraphically below the metavolcanics of the Yellowknife





Group (Boyle, 1961). The original  $^{87}\text{Sr}/^{86}\text{Sr}$  ratios (0.701 and 0.7035) of well defined Rb-Sr isochrons add some support to the argument that the granitic rocks are largely derived from the mantle and represent a significant addition of new material to the embryonic crust. This conclusion must be qualified by the assumptions that the Rb/Sr ratios of the hypothetical sediments were compatible with those of existing Archaean sediments and that sufficient time elapsed (about 50 m.y.) between accumulation of the hypothetical sediments and their suggested anatexis.

The initial  $^{87}\text{Sr}/^{86}\text{Sr}$  ratios recorded from the plutons in question are not distinct from those recorded by other workers in Archaean terrains (c.f. Peterman et al., 1967). A strong case is made in a later section of this chapter for incorporation of radiogenic  $^{87}\text{Sr}$  into the Prosperous Lake granite because the  $^{87}\text{Sr}/^{86}\text{Sr}$  initial ratio (0.712) of the mineral isochron is significantly higher than those of the earlier batholiths.

#### Late kinematic granites and pegmatites

Heat associated with the continued accession of magma in the form of synkinematic - late kinematic batholiths was the major cause of the increased thermal gradient at the culminating point of the orogeny. The metamorphic gradients inferred by the occurrence of the andalusite-sillimanite facies are more extreme than may be attributed to simple geothermal heat conducted from the mantle. If the geothermal gradient was as high as  $150^{\circ}\text{C}/\text{Km}$  (less than an Hercynian geothermal suggested by Schuiling, 1960, i.e.  $200^{\circ}\text{C}/\text{Km}$ , and approximately the same as that deduced for the Buchan metamorphism on the Banffshire coast, Johnson, 1963), there is an excellent possibility of anatexis at a depth of about 4 Kms. Marmo





(1967, p. 75) points out that simple recrystallisation of argillaceous sediments results in a quartz diorite or granodiorite composition, but that regional metamorphism results in an expulsion of the mobile phases (chiefly potassium and water) into a tectonically receptive phase.

The  $^{87}\text{Sr}/^{86}\text{Sr}$  initial ratio of the mineral isochron of the Prosperous Lake granite (0.712) points to the inheritance of radiogenic  $^{87}\text{Sr}$  from the surrounding sediments. It seems probable that the accession of volatiles, including K, Rb and radiogenic  $^{87}\text{Sr}$  into the pluton (or group of plutons) caused both an increase in mobility and changed the composition towards that of a true granite. In such a manner, it appears to be essential that additional potassium (and Rb) be made available from the process of sedimentary 'differentiation' before true granites may form as part of the tectonic cycle.

It has been shown previously that the granitic composition of part of the Ross Lake granodiorite is due to the metasomatic introduction of potassium from the younger Redout Lake granite pluton which it entirely surrounds. This has caused disturbance of the K-Ar and Rb-Sr whole rock systems for a distance of over one mile from the contact of the two bodies and supports the conclusion of Marmo (1967, p. 55) that highly triclinic microcline is invariably a late component in synkinematic "granites".

Addition of water to the rising plutons probably causes separation of a gas phase which is in equilibrium with the liquid and solid phases of the magma. The gaseous phase accommodates the volatile halides of the rare elements and allows their ultimate deposition in complex pegmatites. Elements such as beryllium, lithium and tantalum do not substitute for common elements in the crystal lattices of minerals forming





from a liquid melt. Because of complex ionic charge and ionic radius considerations they are excluded from major crystalline phases. Although one would expect tantalum to be "captured" by titanium-bearing minerals and collected in the earliest crystallising fraction, the tantalum group of elements appear to act as the centres of complex anions.

#### Final stages of the tectonic cycle

At the end of late kinematic plutonic activity, the last and possibly longest stage begins. Uplift of the newly created sialic segment occurs as a result of isostatic readjustment. This isostatic readjustment is largely dependent on the magnitude of the downbulge developed in the Mohorovicic discontinuity. Wollenburg and Smith (1964) suggest that the amount of radioactive heat in silicic batholiths retards cooling and causes partial melting of the mantle at the base of the batholith. The magnitude of the root may therefore be a function of the radioactivity (and indirectly the composition) of the members of the plutonic series. This seems to be demonstrated in the Coast Range of British Columbia where the more silicic batholiths tend to reach higher elevations than the less silicic bodies. Since it has been shown that the plutons involved in Archaean orogenies are lacking in potassium, there is no necessity to postulate the existence of a large root beneath the orogenic belt.

In addition, there is evidence for a progressive increase in the depth of ocean basins through geological time if the hydrosphere is almost entirely of volcanic origin (Rubey, 1955). This suggests that the thickness of the first sialic segment was less than that of later segments and is consistent with the minor importance of load pressure in the metamorphic history of the orogen.





Combining both these factors and assuming that the rate of uplift is directly proportional to the displacement from isostatic equilibrium, it is clear that relatively slow uplift is probable. For this reason, a suggested cooling interval of as much as 150 m.y. is not unreasonable.

After stabilisation of the newly created sialic segment, intrusion of post orogenic diabase dykes concludes the tectonic cycle. At the same time, erosion of the new segment contributed to marginal shelf-type sediments (Snare Group) which in turn pass into the deeper water sediments. Both the sedimentary margins and the edge of the craton itself were involved in the next tectonic cycle (Hudsonian) of the Canadian Shield.

#### General comments on the tectonic cycle

The tectonic cycle proposed here differs considerably from the classic Alpine - type orogeny but fits most of the parameters which Zwart (1967) would attribute to an Hercynotype orogenic belt, i.e. low pressure metamorphism, a relatively thin metamorphic zone, abundant granites (*sensu lato*), a broad orogen, small uplift and no nappe structures.

Because of the ensimatic nature of the eugeosyncline, meta-volcanics are abundant but the ophiolites and serpentinites which characterise an Alpinotype orogenic belt are absent.





## SUMMARY AND CONCLUSIONS

Two areas within the Slave Province have been studied with the aid of K-Ar, Rb-Sr and U-Pb geochronology. A combination of the radiometric methods permits the sequence of events in the Kenoran orogeny to be established and placed in the framework of a single tectonic cycle.

Yellowknife Group volcanics with mixed calc-alkaline and tholeiitic affinities were poured out on a thin oceanic-type crust. No isotopic evidence was found for contamination of the volcanics by extensive early Archaean sialic segments. Rb-Sr isochrons and U-Pb zircon data indicate that the outpouring of a thickness of as much as 40,000 feet of marine volcanics took place approximately 2650 m.y. ago.

As the volcanic pile reached its maximum development, deformation began almost immediately, possibly as a result of transformation of the lower part of the pile to eclogite. Under conditions of moderate pressure ( $\approx 10\text{kb}$ ) near the top of the mantle, fractionation of subsilicic hornblende presents a possible means of forming calc-alkaline magmas. Synkinematic potash-deficient quartz diorite to granodiorite plutons rose into the deforming volcanic pile and may have been exposed before deposition of at least part of the Yellowknife Group sediments. An age of between 2620 and 2640 m.y. is indicated by all three radiometric methods for the syntectonic South-east and Ross Lake granodiorites.

The "unclassified conglomerate" was deposited in a high energy environment adjacent to the coastline of an emerging volcanic island arc. Large clastic fragments are of local derivation. In contrast, a significant contribution of quartz from the near synchronous quartz diorite masses is likely in the deeper water eugeosynclinal basins where the Yellowknife Group sediments were deposited.





Kenoran deformation continued and major syn-late kinematic batholiths such as the Western granodiorite were emplaced about 2590-2610 m.y. ago. Strontium isotope initial ratios indicate that these and preceding bodies were derived from the mantle. As the calc-alkaline magmas continued to invade the deforming volcanic-sedimentary assemblage, the increased amount of heat from these bodies caused partial anatexis of the Yellowknife Group metasediments. Radiogenic  $^{87}\text{Sr}$ , potassium and water from the sedimentary pile moved into the rising plutons and caused a change in composition towards that of true granite. The culmination of late kinematic plutonic activity took place approximately 2575 m.y. ago with the emplacement of the Prosperous Lake granite, Redout Lake granite and associated pegmatites.

Regional metamorphism associated with the major Kenoran plutons is of the andalusite-sillimanite or Abukama facies reflecting the relative unimportance of load pressure in the Kenoran deformation.

Because the new sialic segment was relatively thin (perhaps 10-15 km.) compared with the present thickness of the Canadian Shield, the divergence from isostatic equilibrium imposed by the new segment was comparatively small. For this reason, uplift of the newly formed crust was relatively slow.

During the gradual uplift, K-Ar systems in three different minerals, hornblende, muscovite and biotite, closed in sequential order of their argon retentivities. Hornblende K-Ar dates (2500-2650 m.y.) most closely approach the true age of crystallisation of the igneous bodies in this orogenic belt, coarse-grained muscovite dates (2450-2600 m.y.) also approach the time of crystallisation. Fine-grained biotites are susceptible both to continuous argon loss until their closure at approximately





150°C and to subsequent "updating" by later events.

Examination of the K-Ar histograms suggests that effective argon closure of biotites occurred between 2350 and 2400 m.y. Younger biotite dates are attributed to Hudsonian "updating" along the western margin of the area or to the extensive Proterozoic transcurrent faulting concentrated around Yellowknife Bay.

The oldest set of Proterozoic diabase dykes (2200-2400 m.y.) are post-orogenic features and mark the end of the tectonic cycle.

Despite the uncertainties inherent in the determination of the decay constants, there is good agreement between ages determined by the three radiometric methods. Perhaps this is to be expected, as the K-Ar and Rb-Sr decay constants are based on "geological" estimates derived by comparison with the relatively precise determination of uranium decay constants on cogenetic minerals.

Zircon concordia plots appear to be the most promising method of distinguishing between synkinematic and late-kinematic plutonic episodes in an orogeny. Discordant U-Pb dates are explained on the basis of a Pb loss pattern, possibly related to recent leaching (South-east granodiorite) or to a disturbance of the lead system some 320 m.y. ago (Western granodiorite). There does not seem to be any evidence which requires the adoption of a continuous diffusion model.

Unless particularly rubidium-rich whole rock samples are available, it is difficult to achieve sufficient precision to separate individual events within an orogeny on the basis of Rb-Sr isochron plots. In view of the strong geochemical diadochy between K and Rb and the suggestion that K is not a prominent component of the lithosphere until a stage of sedimentary differentiation takes place, it is unlikely that Rb is an important component





of Archaean rocks.

K-Ar dating is most valuable in establishing the thermal history of an area in conjunction with estimates of the time of primary crystallisation obtained by other methods, but may not be the most satisfactory basis on which to establish time-stratigraphic boundaries. This study largely confirms the conclusions reached by Jolliffe (1942, 1946) and Henderson (1939, 1941) on the basis of field geology, particularly in regard to the relatively brief time span involved in the emplacement of the major plutonic bodies of the area.

The area merits further work along at least two lines; (a) determination of the time of gold mineralization and (b) further mineralogical study of the metamorphic history. The range in time of the mineralization is broad but Rb-Sr isochrons on the tan coloured sericitic alteration associated with the mineralized quartz veins could be of considerable value. Correlation of such a study with existing and future common lead studies is imperative. The reinterpretation of the metamorphic history offered in this thesis should be tested by further mineralogical and petrological studies.





REFERENCES CITED

- Aldrich, L. T., and Wetherill, G. W. (1958): Geochronology by radioactive decay. *Ann. Rev. Nucl. Sci.*, 8, pp. 257-298.
- Aldrich, L. T., Wetherill, G. W., Tilton, G. R., and Davis, G. L. (1956): Half Life of  $\text{Rb}^{87}$ , *Phys. Rev.*, 103, pp. 1045-1047.
- Allsopp, H. L., Ulrych, T. J., and Nicolaysen, L. O. (1967): Dating some significant events in the history of the Swaziland by the Rb-Sr isochron method: *Abst.* in *Geochronology of Precambrian stratified rocks* (R. A. Burwash and R. D. Morton, *Eds.*), University of Alberta, Edmonton, June, 1967, pp. 21-22.
- Armstrong, R. L. (1966): K-Ar Dating of Plutonic and Volcanic Rocks in Orogenic Belts: *In*: Schaeffer, O. A., and Zahringer, J., (*Eds.*) *Potassium-Argon Dating*, Springer, Berlin, pp. 117-133.
- Aston, F. W. (1933): The Isotopic Composition and Atomic weight of Lead from Different Sources: *Proc. Roy. Soc. (London)*, A140, pp. 535-543.
- Baadsgaard, H. (1965): Geochronology: *Medd. Dansk. Geol. Forening.*, 16, pp. 1-48.
- Baadsgaard, H., Folinsbee, R. E., and Lipson, J. (1961a): Potassium-Argon dates of biotites from Cordilleran granites: *Bull. Geol. Soc. Amer.* 72, pp. 689-702.
- 
- (1961b): Caledonian or Acadian Granites of the Northern Yukon Territory: *Geology of the Arctic*, University of Toronto Press, Toronto.
- Baadsgaard, H., and Godfrey, J. D. (1967): Geochronology of the Canadian Shield in Northeastern Alberta: I. Andrew Lake Area. *Can. J. Earth Sci.*, 4, pp. 541-563.
- Baadsgaard, H., Lipson, J., and Folinsbee, R. E. (1961): The leakage of radiogenic argon from sanidine: *Geochim. Cosmochim. Acta.* 25, pp. 147-157.
- Badgely, P. C. (1965): *Structural and tectonic principles*, Harper and Row, New York.
- Bainbridge, K. T., and Nier, A. O. (1950): Prelim. Ref. No. 9, *Nucl. Sci. Ser. Nat. Res. Coun. U.S.*, Washington.
- Banks, P. O., and Silver, L. T. (1966): Evaluation of the Decay Constant of Uranium 235 from Lead Isotope Ratios: *J. Geophys. Res.*, 71, pp. 4037-4046.
- Baragar, W. R. A. (1966): Geochemistry of the Yellowknife volcanic rocks: *Can. J. Earth Sci.*, 3, pp. 9-30.
- Bass, M. N. (1961): Regional Tectonics of part of the Southern Canadian Shield. *J. Geol.* 69, pp. 668-702.





- Bell, J. M. (1929): Great Slave Lake: Proc. Trans. Roy. Soc., Can., 3rd ser., 23, pp. 5-38.
- Benioff, H. (1954): Orogenesis and Deep Crustal Structure: Additional Evidence from Seismology: Bull. Geol. Soc. Amer., 65, pp. 465-500.
- Boltwood, B. B. (1907): On the ultimate Disintegration Products of the Radioactive Elements: Pt. II The Disintegration Products of Uranium: Amer. J. Sci., 23, pp. 77-88.
- Boutcher, S. M. A., Edhorn, A. S., and Moorhouse, W. W. (1966): Archaean conglomerates and lithic sandstones of Lake Timiskaming, Ontario: Proc. Geol. Assoc. Can., 17, pp. 21-42.
- Boyle, R. W. (1961): The geology, geochemistry, and origin of the gold deposits of the Yellowknife district: Can. Dept. Mines Tech. Surv. Geol. Surv. Can. Mem. 310.
- Brown, I. C. (1949): Structure of the Yellowknife gold belt, Northwest Territories: Unpublished Ph.D. thesis, Harvard University, Boston.
- \_\_\_\_\_ (1955): Late Faults in the Yellowknife Area: Proc. Geol. Assoc. Can., 7, pp. 123-138.
- Bryan, W. H., and Jones, O. A. (1962): The Bedded Cherts of the Neranleigh-Fernvale Group of South-Eastern Queensland: Proc. Roy. Soc. Qd., 62, pp. 17-36.
- Buddington, A. F. (1935): High-temperature mineral associates at shallow to moderate depths: Econ. Geol. 30, pp. 205-222.
- \_\_\_\_\_ (1959): Granite emplacement with special reference to North America: Bull. Geol. Soc. Amer., 70, pp. 671-747.
- Burwash, R. A., and Baadsgaard, H. (1962): Yellowknife-Nonacho age and structural relations: Roy. Soc. Canada Spec. Pub. 4, pp. 22-29.
- Burwash, R. A., Baadsgaard, H., Campbell, F. A., Cumming, G. L., and Folinsbee, R. E. (1963): Potassium-argon dates of diabase dyke systems, District of MacKenzie, N.W.T.: Trans. Can. Inst. Mining Met., 67, pp. 303-307.
- Burwash, R. A., Baadsgaard, H., and Peterman, Z. E. (1962): Precambrian K-Ar dates from the Western Canada Sedimentary Basin: J. Geophys. Res., 67, pp. 1617-1625.
- Campbell, N. (1948): West Bay Fault, in Structural geology of Canadian ore deposits: Can. Inst. Mining Met. Jubilee Volume, pp. 244-259.
- Catanzaro, E. J. (1963): Zircon ages in southwestern Minnesota: J. Geophys. Res., 68, pp. 2045-2048.





- Catanzaro, E. J., Murphy, T. J., Shields, W. R., and Garner, E. L. (1968): Absolute isotopic abundance ratios of three lead isotope standards; (Abst.) Program, 49th Annual Meeting, Am. Geophys. Union, Washington, D.C., April, 1968.
- Chayes, F. (1964): A petrographic distinction between Cenozoic volcanics in and around the open oceans: J. Geophys. Res., 69, pp. 1573-1588.
- Coats, R. R. (1962): Magma type and crustal structure in the Aleutian Arc: In The crust of the Pacific Basin, Geophysical Monograph No. 6 (G. A. MacDonald and H. Kuno Eds.) Am. Geophys. Union, pp. 92-109.
- Coleman, L. C. (1957): Mineralogy of the Giant Yellowknife Gold Mine, Yellowknife, N.W.T.: Econ. Geol., 52, pp. 400-425.
- Compston, W., Jeffrey, P. M., and Riley, G. H. (1960): Age of emplacement of granites: Nature, 186, pp. 702-703.
- Compston, W., and Arriens, P. A. (1967): The Precambrian geochronology of Australia: Abst. in Geochronology of Precambrian stratified rocks (R. A. Burwash and R. D. Morton, Eds.) University of Alberta, Edmonton, June, 1967, pp. 27-29.
- Compston, W., McDougall, I., and Heier, K. S. (1968): Geochemical comparison of the Mesozoic basaltic rocks of Antarctica, South Africa, South America and Tasmania: Geochim. Cosmochim. Acta, 32, pp. 129-149.
- Compston, W., and Pidgeon, R. T. (1962): Rubidium-strontium dating of shales by the total rock method: J. Geophys. Res., 67, pp. 3493-3502.
- Crawford, A. R., and Compston, W. (1967): New Rb-Sr age determinations for the Precambrian of S. India and Ceylon: Abst. in Geochronology of Precambrian stratified rocks (R. A. Burwash and R. D. Morton, Eds.) University of Alberta, Edmonton, June, 1967, p. 33.
- Dadson, A. S., and Bateman, J. D. (1948): Giant Yellowknife Mine, in Structural Geology of Canadian Ore Deposits: Can. Inst. Mining Met., Jubilee Volume, pp. 273-283.
- Damon, P. E., and Kulp, J. L. (1958): Excess helium and argon in beryl and other minerals: Am. Mineralogist, 43, pp. 1117-1140.
- Davis, E. F. (1918): The Radiolarian Cherts of the Franciscan Group: Bull. Dep. Geol. Univ. Calif., II, pp. 235-432.
- Deer, W. A. (1950): The diorites and associated rocks of the Glen Tilt Complex, Perthshire; II. Diorites and Appinites: Geol. Mag. 87, pp. 181-195.





- De la Cruz, N. N. (1967): Chemical and isotopic variations within the Ordovician Kinnekulle A<sub>1</sub> bentonite, Kinnekulle, Sweden.: M.Sc. thesis, University of Alberta (unpublished).
- Donaldson, J. A., and Jackson, G. D. (1965): Archaean sedimentary rocks of North Spirit Lake area, Northwestern Ontario: Can. J. Earth Sci., 2, pp. 622-647.
- Edie, R. W. (1949): Petrography and Petrology of the Cameron River Volcanic Belt, District of MacKenzie, N.W.T.: M.Sc. thesis, Univ. of Alta. (unpublished).
- Eskola, P. (1939): Die Entstehung der Gesteine: Springer, Berlin.
- \_\_\_\_\_ (1941): Erkki Mikkola und der heutige Stand der Praekambrischen Geologie in Finnland: Geol. Rund. 32, pp. 452-483.
- Fairbairn, H. W., Hurley, P. M., Knight, C. J., and Pinson, W. H. (1967): Rb-Sr whole rock isochron ages of volcanics and sediments in the Precambrian of Ontario: Abst. in Geochronology of Precambrian stratified rocks (R. A. Burwash and R. D. Morton, Eds.) University of Alberta, Edmonton, June, 1967, pp. 37-38.
- Fairbairn, H. W., and Pinson, W. H., Jr. (1967): Rb-Sr Isochron Ages of Metasediments in the Canadian Shield: M.I.T. 1381-15. Fifteenth Annual Progress Report for 1967, U.S. Atomic Energy Commission, Contract AT (30-1) - 1381.
- Farrar, E., MacIntyre, R. M., York, D., and Kenyon, W. J. (1964): A simple mass spectrometer for the analysis of argon at ultra-high vacuum: Nature, 204, pp. 531-533.
- Faul, H., (Ed.) (1954): Nuclear Geology: John Wiley and Sons, New York.
- Faure, G., and Hurley, P. M. (1963): The isotopic composition of Sr in oceanic and continental basalts: Application to the origin of igneous rocks: J. Petrol. 4, pp. 31-50.
- Fechteg, H., and Kalbitzer, S. (1966): The diffusion of argon in potassium-bearing solids: In: Schaeffer, O. A. and Zahringer, J., (Eds.) Potassium-Argon Dating: Springer, Berlin, pp. 68-107.
- Flynn, K. F., and Glendenin, L. E. (1959): Half-life and Beta Spectrum of Rb<sup>87</sup>: Phys. Rev. 116, pp. 744-748.
- Folinsbee, R. E. (1942): Zone Facies of Metamorphism in Relation to the Ore Deposits of the Yellowknife-Beaulieu Region: Ph.D. thesis, University of Minnesota. (unpublished).
- \_\_\_\_\_ (1947): Preliminary map, Lac de Gras, Northwest Territories: Geol. Surv. Canada, Paper 47-5.
- \_\_\_\_\_ (1955): Archaean Monazite in Beach Concentrates, Yellowknife Geologic Province, Northwest Territories, Canada: Trans. Roy. Soc. Canada, 3rd Ser., 49, pp. 7-24.





- Folinsbee, R. E., Baadsgaard, H., Cumming, G. L., and Green, D. C. (1968): A very Ancient Island Arc: Amer. Geophys. Union Mono. No. 12, (in press).
- Folinsbee, R. E., Lipson, J., and Reynolds, J. H. (1956): Potassium-argon dating: Geochim. Cosmochim. Acta, 10, pp. 60-68.
- Fortier, Y. O. (1947): Ross Lake, Northwest Territories: Geol. Surv. Canada, Paper 47-16.
- Fyfe, W. S., Turner, F. J., and Verhoogen, J. (1958): Metamorphic Reactions and Metamorphic Facies: Geol. Soc. Amer. Mem. 73.
- Gabrielse, H., and Reesor, J. (1964): Geochronology of Plutonic rocks in two areas of the Canadian Cordillera: Roy. Soc. Canada Spec. Publ. No. 8, pp. 96-138.
- Gast, P. W. (1965): Terrestrial ratio of potassium to rubidium and the composition of the Earth's mantle: Science, 147, pp. 858-860.
- Gast, P. W., Kulp, J. L., and Long, L. E. (1958): Absolute Age of Early Precambrian Rocks in the Bighorn Basin of Wyoming and Montana, and Southeastern Manitoba: Trans. Am. Geophys. Union 39, pp. 322-334.
- Gerling, E. K., Kol'tsova, T. V., Petrov, B. V., and Zul'fikarova, Z. L. (1965): On the suitability of amphiboles for age determination by the K-Ar method: (Trans.) Geokhimiya, 2, pp. 219-226.
- Gill, J. E. (1948): Mountain building in the Canadian Precambrian Shield: Abst. 18th Int. Geol. Congress, London, Pt. XIII, pp. 97-104.
- \_\_\_\_\_ (1949): Natural divisions of the Canadian Shield: Trans. Roy. Soc. Canada, 3rd Ser., 43, pp. 61-69.
- Goldich, S. S., Nier, A. O., Baadsgaard, H., Hoffman, J. H., and Krueger, H. W. (1961): The Precambrian geology and geochronology of Minnesota: Minn. Geol. Surv. Bull. 41, pp. 1-193.
- Goldich, S. S., Lidiak, E. G., Hedge, C. E., and Walthall, F. G. (1966): Geochronology of the Midcontinent Region, United States; Pt. 2. Northern Area: J. Geophys. Res., 71, pp. 5389-5408.
- Gorshkov, G. S. (1962): Petrochemical features of volcanism in relation to the types of earth's crust; In The Crust of the Pacific Basin, Geophysical Monograph No. 6 (G. A. MacDonald and H. Kuno Eds.) Am. Geophys. Union, pp. 110-115.
- Green, D. C., Baadsgaard, H., and Cumming, G. L. (1968): Geochronology of the Yellowknife area, Northwest Territories, Canada: Can. J. Earth Sci., 5, (in press).





- Green, T. H., and Ringwood, A. E. (1966): Origin of the Calc-alkaline igneous suite: In Petrology of the Upper Mantle, Publication 444, Department of Geophysics and Geochemistry; Aust. Nat. Univ., Canberra, pp. 105-117.
- 
- \_\_\_\_\_ (1968): Crystallisation of basalt and andesite under high pressure hydrous conditions: Earth Planet Sci. Letters, 3, pp. 481-489.
- Gross, W. H., Ferguson, S. A. (1965): The anatomy of an Archaean greenstone belt: Can. Mining Met. Bull., 58, pp. 940-941.
- Hamilton, E. I. (1965): Applied Geochronology: Academic Press Inc. (London) Ltd.
- Hamilton, J. D. (1948): Correlation Problem of the Granodiorites of Yellowknife and Ross Lake, N.W.T.: B.Sc. thesis, Queen's University, Kingston. (unpublished).
- Harper, C. T. (1967): On the interpretation of potassium-argon ages from Precambrian shields and Phanerozoic orogens: Earth Planet. Sci. Letters, 3, pp. 128-132.
- Hart, S. R. (1961): The use of amphiboles and pyroxenes for K-Ar dating: J. Geophys. Res., 66, pp. 2995-3001.
- 
- \_\_\_\_\_ (1964): The petrology and isotopic-mineral age relations of a contact zone in the Front Range, Colorado: J. Geol., 72, pp. 493-525.
- Hart, S. R., Aldrich, L. T., Davis, G. L., Tilton, G. R., Baadsgaard, H., Kuovo, O., and Steiger, R. N. (1963): Geochronology and Isotope Geology; Carnegie Inst. Wash. Ann. Rep. Year Book 62, pp. 267-280.
- Hart, S. R., and Dodd, R. T. (1962): Excess radiogenic argon in pyroxenes: J. Geophys. Res., 67, pp. 2998-2999.
- Hedge, C. E., and Walthall, F. G. (1963): Radiogenic strontium-87 as an index of geological processes: Science, 140, pp. 1214-1217.
- Heier, K. S., Compston, W., and McDougall, I. (1965): Thorium and uranium concentrations, and the isotopic compositions of strontium in the differentiated Tasmanian dolerites: Geochim. Cosmochim. Acta, 29, pp. 643-659.
- Henderson, J. B. (1968): Sedimentology of the Yellowknife Group: Geol. Surv., Canada: Report of activities, Pt. A. Paper 68-1A, p. 138.
- Henderson, J. F. (1939): Beaulieu River Area, Northwest Territories: Geol. Surv., Canada, Pap. 39-1.
- 
- \_\_\_\_\_ (1941): Gordon Lake South, District of MacKenzie, Northwest Territories: Geol. Surv., Canada, Map 645A.





- Henderson, J. F. (1948): The Relation of Gold Deposits to Structure, Yellowknife, N.W.T.: Precambrian, 21, No. 7, pp. 6-11.
- Henderson, J. F., and Brown, I. C. (1949): Yellowknife, Northwest Territories: Geol. Surv., Canada, Paper 50-34.
- \_\_\_\_\_ (1950): Structure of the Yellowknife Greenstone Belt, Northwest Territories: Trans. Can. Inst. Mining Met., 53, pp. 427-434.
- \_\_\_\_\_ (1952): The Yellowknife Greenstone Belt; Geol. Surv., Canada, Paper 52-28.
- Henderson, J. F., and Frazer, N. H. C. (1948): Camlaren Mine: In Structural Geology of Canadian Ore Deposits - a symposium: Can. Inst. Mining. Met., pp. 269-272.
- Hess, H. H. (1962): History of Ocean Basins: Geol. Soc. Amer., Buddington Volume, pp. 599-620.
- Hills, L. S. (1940): A Petrographic Study of a Basic Intrusive Sheet in the Yellowknife Area, Northwest Territories: M.Sc. thesis, McGill University, Montreal. (unpublished).
- Holmes, A. (1913): The Age of the Earth: Harper Brothers, New York.
- \_\_\_\_\_ (1929): Ore-lead and Rock-lead and the Origin of certain Ore deposits: Nature, 124, pp. 477-478.
- \_\_\_\_\_ (1931): Radioactivity and Earth Movements: Trans. Geol. Soc. Glasgow, 18, pp. 559-606.
- \_\_\_\_\_ (1965): Principles of Physical Geology, 2nd Ed.: Thomas Nelson, London.
- Horwitz, R. C., and Sofoulis, J. (1965): Igneous Activity and Sedimentation in the Precambrian between Kalgoorlie and Norseman, Western Australia: Proc. Aust. Inst. Min. and Met., 214, pp. 45-59.
- Hunt, G. (1962): Time of Purcell eruption in southeastern British Columbia and southwestern Alberta: Alberta Soc. Petrol. Geol. J. 10, pp. 438-442.
- Hurley, P. M. (1968): Absolute abundance and distribution of Rb, K and Sr in the Earth: Geochim. Cosmochim. Acta., 32, pp. 273-283.
- Hurley, P. M., and Fairbairn, H. W. (1953): Radiation damage in zircon: A possible age method. Bull., Geol. Soc. Amer. 64, pp. 659-674.
- Hurley, P. M., de Almeida, F. F. M., Melcher, G. C., Cordani, U. G., Rand, J. R., Kawashita, K., Vandoros, P., Pinson, W. H. Jr., and Fairbairn, H. W. (1967): Test of Continental Drift by Comparison of Radiometric Ages. Science, 157, pp. 495-500.





- Hurley, P. M., Hughes, H., Pinson, W. H., and Fairbairn, H. W. (1962): Radiogenic argon and strontium diffusion parameters in biotite at low temperatures from Alpine fault uplift in New Zealand: *Geochim. Cosmochim. Acta*, 26, pp. 67-80.
- Hutchison, R. W. (1955): Regional zonation of pegmatites near Ross Lake, Northwest Territories: *Geol. Surv. Canada Bull.* 34, pp. 1-50.
- Jager, E. (1966): Das alter von Graniten und Gneissen: *Tsch. min. petr. Mitt.* 11, pp. 304-316.
- Johannsen, A. (1931): A Descriptive Petrography of the Igneous Rocks; 1: University of Chicago Press, Chicago.
- Johnson, M. R. W. (1963): Some Time relations of movement and metamorphism in the Scottish Highlands: *Geol. en Minjb.*, 42, pp. 121-142.
- Jolliffe, A. W. (F.) (1936): Yellowknife River Area, Northwest Territories: *Geol. Surv. Canada*, Paper 36-5.
- \_\_\_\_\_ (1942): Yellowknife Bay, District of MacKenzie, Northwest Territories: *Geol. Surv. Canada*, Map 709A.
- \_\_\_\_\_ (1946): Prosperous Lake, District of MacKenzie, Northwest Territories: *Geol. Surv. Canada*, Map 868A.
- \_\_\_\_\_ (1952): The northwestern part of the Canadian Shield: *Congr. Geol. Intern., Compt. Rend.*, 18th, London, 1948, Pt. XIII, Sect. M., pp. 141-149.
- Kanasewich, E. R. (1962): Quantitative Interpretations of Anomalous Lead Isotope Abundances: Ph.D. thesis, University of British Columbia, Vancouver (unpublished).
- Kay, K. (1951): North American geosynclines: *Geol. Soc. Amer. Mem.* 48, pp. 1-143.
- Keevil, N.B., Jolliffe, A. W., and Larsen, E. S. (1942): Distribution of helium and radioactivity in rocks: Pt. IV. Helium age investigations of diabase and granodiorite from Yellowknife, Northwest Territories, Canada: *Amer. J. Sci.*, 4th Series, 240, pp. 831-846.
- Kelly, J. A. (1964): The petrography and petrology of the Stock Lake stock, Yellowknife, N.W.T., Canada: M.Sc. thesis, Montana State University, Bozeman (unpublished).
- Kirsten, T. (1966): Determination of Radiogenic Argon; In: Schaeffer, O. A. and Zahringer, J., (eds.), *Potassium-Argon Dating*: Springer, Berlin, pp. 7-39.
- Knopf, A. (1957): The Boulder Batholith of Montana: *Amer. J. Sci.*, 255, pp. 81-103.
- Kratz, K. O., Gerling, E. K., and Lobach-Zhuchenko, S. B. (1967): The isotopic geology of the Precambrian of the Baltic Shield: Abst. in *Geochronology of Precambrian stratified rocks* (R. A. Burwash and R. D. Morton, Eds.), University of Alberta, Edmonton, June, 1967, pp. 57-58.
- Kretz, R. (1963): Note on some equilibria in which plagioclase and epidote participate: *Amer. Jour. Sci.*, 261, pp. 973-982.





- Kuovo, O., and Simonen, A. (1967): Tectonic Units and Geochronology of the Baltic Shield: Abst. in Geochronology of Precambrian stratified rocks (R. A. Burwash and R. D. Morton, Eds.), University of Alberta, Edmonton, June, 1967, pp. 55-56.
- Lambert, R. St. J., Holland, J. G., and Evans, C. R. (1967): The chronology of the Lewisian complex of the mainland of Scotland and its bearing on the classification of Precambrian time; Abst. in Geochronology of Precambrian stratified rocks (R. A. Burwash, and R. D. Morton, Eds.), University of Alberta, Edmonton, June, 1967, pp. 59-60.
- Lanphere, M. A., and Dalrymple, G. B. (1967): K-Ar and Rb-Sr measurements on P-207, the U.S.G.S. interlaboratory standard muscovite: *Geochim. Cosmoch. Acta*, 31, pp. 1091-1094.
- Larsen, E., Jr. (1945): Time required for the crystallisation of the great batholith of Southern and Lower California: *Amer. J. Sci.* 243-A, pp. 398-416.
- Larsen, E., Jr., Keevil, N. B., and Harrison, H. C. (1952): Method for determining the age of igneous rocks using the accessory minerals; *Bull. Geol. Soc. Amer.* 63, pp. 1045-1052.
- Larsen, O., and Møller, J. (1967): Geochronological studies in West Greenland: Abst. in Geochronology of Precambrian stratified rocks (R. A. Burwash and R. D. Morton, Eds.), University of Alberta, Edmonton, June, 1967, p. 63.
- Leech, A. P. (nee Payne, A. V.) (1965): A reconnaissance: Basic Intrusive Rocks of the Precambrian Shield, Canada: M.Sc. thesis, University of Alberta (unpublished).
- \_\_\_\_\_ (1966): Potassium-argon dates of basic intrusive rocks of the District of MacKenzie, N.W.T.: *Can. J. Earth Sci.*, 3, pp. 389-412.
- Leech, G. B., Lowdon, J. A., Stockwell, C. H., and Wanless, R. K. (1963): Age determinations and geological studies: Pt. 1. Isotopic Ages. Report 4. Can. Dept. Mines Tech. Surv. Geol. Surv. Can. Paper 63-17.
- Leutz, H., Wenninger, H., and Ziegler, K. (1962): Die Halbwertszeit des Rb<sup>87</sup>: *Zeits. für Phys.*, 169, pp. 409-416.
- Lindgren, W. (1900): Granodiorite and other intermediate rocks: *Amer. J. Sci.*, 2, pp. 269-282.
- Lord, C. S. (1942): Snare River and Ingray Lake map areas, Northwest Territories: *Geol. Surv. Canada Mem.* 235.
- Lovering, T. S. (1955): Temperatures in and near intrusions: *Econ. Geol.* 50th Anniv. Volume, pp. 249-281.
- Lowden, J. A. (1961): Age determinations by the Geological Survey of Canada: Report 2. Can. Dept. Mines Tech. Surv. Geol. Surv. Can. Paper 61-17 (see also later papers in this series).





- McDougall, I., and Green, D. H. (1964): Excess radiogenic argon in pyroxenes and isotopic ages of minerals from Norwegian eclogites, Norsk Geol. Tidsskr., 44, pp. 183-196.
- McGlynn, J. C., and Ross, J. V. (1963): Arseno Lake map area, District of MacKenzie; 86B/12: Geol. Surv. Canada, Paper 63-26.
- MacIntyre, R. M., York, D., and Moorhouse, W. W. (1967): Potassium-argon age determinations in the Madoc-Bancroft area in the Grenville Province of the Canadian Shield: Can. J. Earth Sci., 4, pp. 815-828.
- McIntyre, G. A., Brooks, C., Compston, W., and Turek, A. (1966): The statistical assessment of Rb-Sr isochrons. J. Geophys. Res., 71, pp. 5459-5468.
- McKinstry, H. E. (1953): Shears of the Second Order, Amer. J. Sci., 251, pp. 401-414.
- McMullen, C. C., Fritze, K., and Tomlinson, R. H. (1966): The half-life of Rubidium-87: Can. Jour. Phys. 44, pp. 3033-3038.
- Marmo, V. (1967): On granites, a revised study: Bull. Comm. geol. Finlande, 227, pp. 1-83.
- Matsuda, T. (1962): Crustal deformation and igneous activity in the South Fossa Magma, Japan: In The crust of the Pacific Basin, Geophysical Monograph No. 6 (G. A. MacDonald and H. Kuno Eds.) Am. Geophys. Union, pp. 140-150.
- Miller, W. G. (1911): Notes on the Cobalt Area: Eng. Min. Jour., 92, pp. 645-649.
- Mirashiro, A. (1961): Evolution of metamorphic belts: J. Petrol. 2, pp. 277-311.
- Moorbath, S. (1967): Recent advances in the application and interpretation of radiometric age data: Earth-Sci. Rev., 3, pp. 111-133.
- Moorbath, S., and Bell, J. D. (1965): Strontium isotope abundance studies and Rb-Sr age determinations on Tertiary igneous rocks from the Isle of Skye, N-W Scotland: J. Petrol. 6, pp. 37-68.
- Moore, E. S. (1954): Porphyries of the Porcupine Area, Ontario: Trans. Roy. Soc. Can. Ser. 3, Sect. IV, 48, pp. 41-57.
- Moore, J. C. G. (1956): Courageous-Matthews Lake, District of MacKenzie, Northwest Territories: Geol. Surv. Canada Mem. 283.
- Murthy, V. R., and Patterson, C. C. (1961): Lead isotopes in ores and rocks of Butte, Montana: Econ. Geol., 56, pp. 59-67.





- Naylor, R. S., Steiger, R. H., and Wasserburg, G. J. (1968): U-Th-Pb and Rb-Sr Systematics in a  $2.7 \times 10^9$ -yr Plutonic Complex: (Abst.) Program, 49th Annual Meeting. Am. Geophys. Union, Washington D.C., April, 1968, pp. 347-348.
- Nicolaysen, L. O. (1961): Graphic interpretation of discordant age measurements on metamorphic rocks: Ann. N.Y. Acad. Sci., 91, pp. 198-206.
- Nier, A. O. (1938): Variations in the Relative Abundances of the Isotopes of Common Lead from Various Sources, J. Amer. Chem. Soc. 60, pp. 1571-1576.
- \_\_\_\_\_ (1950): A Redetermination of the Relative Abundances of the Isotopes of Neon, Krypton, Rubidium, Xenon, and Mercury. Phys. Rev. 72, pp. 450-454.
- \_\_\_\_\_ (1950): A Redetermination of the Relative Abundances of the Isotopes of Carbon, Nitrogen, Oxygen, Argon, and Potassium: Phys. Rev. 77, pp. 789-793.
- Nockolds, S. R. (1954): Average Chemical Compositions of some Igneous Rocks: Bull. Geol. Soc. Amer., 65, pp. 1007-1032.
- Ostic, R. G., Russell, R. D., and Reynolds, P. H. (1963): A new calculation for the age of the earth from abundances of lead isotopes: Nature, 199, pp. 1150-1152.
- Payne, A. V., Baadsgaard, H., Burwash, R. A., Cumming, G. L., Evans, C. R., and Folinsbee, R. E. (1965): A line of evidence supporting continental drift. Intern. Union Geol. Sci. Upper Mantle Symp. New Dehli, 1964. Ed. C. H. Smith and T. Sorgenfrei, Copenhagen, pp. 83-93.
- Peterman, Z. E. (1962): Precambrian basement of Saskatchewan and Manitoba: Ph.D. thesis, University of Alberta (unpublished).
- Peterman, Z. E., Hedge, C. E., Coleman, R. G., and Snavely, P. D., Jr. (1967):  $^{87}\text{Sr}/^{86}\text{Sr}$  ratios in some eugeosynclinal sedimentary rocks and their bearing on the origin of granitic magma in orogenic belts: Earth Planet. Sci. Letters, 2, pp. 433-439.
- Pettijohn, F. J. (1943): Archaeian sedimentation: Bull. Geol. Soc. Amer., 54, pp. 925-972.
- Purdy, J., and York, D. (1965): A geochronometric study of the Superior Province near Red Lake, Northwestern Ontario: Can. J. Earth Sci., 3, pp. 277-286.
- Ramberg, H. (1952): The Origin of Metamorphic and Metasomatic Rocks: University of Chicago Press, Chicago.
- Rankama, K. (1954): Isotope Geology: Interscience, New York.





- Read, H. H. (1952): Metamorphism and migmatization in the Ythan Valley, Aberdeenshire: Trans. Edinburgh Geol. Soc., 15, pp. 265-279.
- \_\_\_\_\_ (1955): Granite Series in Mobile Belts: Geol. Soc. Amer. Spec. Paper 62, pp. 409-429.
- \_\_\_\_\_ (1961): Aspects of Caledonian magmatism in Britain: Lpool. Manchr. Geol. J., 2, pp. 653-683.
- Robertson, D. K. (1966): Isotope analysis for lead and sulphur from the Great Slave Lake area: M.Sc. thesis, University of Alberta (unpublished).
- Robertson, D. K., and Cumming, G. L. (1966): Isotope Analyses for Lead and Sulphur from the Great Slave Lake Area: (Abst.) Program, 47th Annual Meeting Am. Geophys. Union, Washington D.C., April, 1966, p. 206.
- Ross, J. V. (1966): A Note on histogram analysis of isotopic age data: Can. J. Earth Sci., 3, pp. 259-262.
- Ross, J. V., and McGlynn, J. C. (1963): Concentric folding of cover and basement at Basler Lake, N.W.T.: J. Geol. 71, pp. 644-653.
- \_\_\_\_\_ (1965): Snare-Yellowknife Relations, District of MacKenzie, N.W.T., Canada: Can. J. Earth Sci., 2, pp. 118-180.
- Rubey, W. W. (1955): Development of the hydrosphere and atmosphere - with special reference to the probable composition of the early atmosphere. Geol. Soc. Amer. Spec. Paper 62, pp. 631-650.
- Russell, R. D., and Cumming, G. L. (1955): Lead isotope abundances: (Abstr.) Program, 36th Annual Meeting, Am. Geophys. Union, Washington, D.C., May, 1955, p. 526.
- Russell, R. D., and Farquhar, R. M. (1960): Dating galenas by means of their isotopic constitutions - II; Geochim. Cosmochim. Acta, 19, pp. 41-52.
- Russell, R. D., Farquhar, R. M., Cumming, G. L., and Wilson, J. T. (1954): Dating galenas by means of their isotopic constitutions: Trans. Am. Geophys. Union, 35, pp. 301-309.
- Schuiling, R. D. (1960): Le dome gneissic de l'Argout: Mem. Geol. Soc. France, 91, pp. 1-58.
- Sederholm, J. J. (1931): On the sub-Bothnian unconformity and on Archaean rocks formed by secular weathering: Bull. Comm. geol. Finlande, 95, 81 p.





- Semenenko, N. P. (1967): Geochronology of the Precambrian of the Ukrainian Shield: Abst. in Geochronology of Precambrian stratified rocks (R. A. Burwash and R. D. Morton, Eds.) University of Alberta, Edmonton, June, 1967, p. 83-85.
- Silver, L. T., and Deutsch, S. (1961): Uranium-lead method on zircons: New York Acad. Sciences Annals, 91, pp. 279-283.
- Silver, L. T., McKinney, C. R., Deutsch, S., and Bolinger, J. (1963): Precambrian age determinations in the western San Gabriel Mountains, California: J. Geol., 71, pp. 196-214.
- Smith, J. V., and Yoder, H. S. (1956): Experimental and theoretical studies of the mica polymorphs: Min. Mag., 31, pp. 209-235.
- Snelling, N. J. (1960): The geology and petrology of the Murrumbidgee batholith: Quart. J. Geol. Soc. Lond., 116, pp. 187-217.
- Stern, T. W., Goldich, S. S., and Newell, M. F. (1966): Effects of weathering on the U-Pb ages of zircon from the Morton Gneiss, Minnesota: Earth Planet. Sci. Letters, 1, pp. 369-371.
- Stieff, L. R., Stern, T. W., Oshiro, S., and Senftle, F. E. (1959): Tables for the Calculation of Lead Isotope Ages: U.S. Geol. Surv. Prof. Paper 334A.
- Stockwell, G. H. (1936): Eastern portion of Great Slave Lake, N.W.T.: Geol. Surv. Canada, Map 377A.
- \_\_\_\_\_ (1964): Age Determinations and Geological Studies. Pt. II Geological Studies, 4th Report on Structural Provinces, Orogenies, and Time Classification of Rocks of the Canadian Precambrian Shield. Can. Dept. Mines Tech. Surv. Can. Paper 64-17.
- \_\_\_\_\_ (ed.) (1957): Geology and Economic Minerals of Canada, Dept. Mines Tech. Surv. Geol. Surv. Can. Econ. Geol. Ser. 1.
- Sutton, J. (1963): Some recent advances in our understanding of the controls of metamorphism; In Controls of Metamorphism, Pitcher, W. S., and Flinn, G. W. Eds., Oliver and Boyd, London.
- Tilley, C. E. (1924): Metamorphic zones in the southern Highlands of Scotland, Geol. Soc. London Quart. Jour., 81, pp. 100-125.
- Tilton, G. R., Patterson, C., Brown, H., Inghram, M., Hayden, R., Hess, D., and Larsen, E. (1955): Isotopic composition and distribution of lead, uranium and thorium in a Precambrian granite: Bull. Geol. Soc. Amer., 66, pp. 1131-1148.
- Tilton, G. R. (1960): Volume diffusion as a mechanism for discordant lead ages: J. Geophys. Res., 65, pp. 2933-2945.
- Turek, A. (1966): Rubidium-strontium isotope studies in the Kalgoorlie-Norseman area, Western Australia. Ph.D. thesis, Aust. Nat. Univ., Canberra (unpublished).





- Turek, A. (1967): Geochronology of the Kalgoorlie-Norseman area, Western Australia, Abst. in Geochronology of Precambrian stratified rocks (R. A. Burwash and R. D. Morton, Eds.) University of Alberta, Edmonton, June, 1967, p.
- Turner, F. J. (1937): The metamorphic and plutonic rocks of Lake Manapouri, Fiordland, New Zealand: Trans. Roy. Soc. New Zealand, 67, pp. 83-100.
- Turner, F. J., and Verhoogen, J. (1960): Igneous and metamorphic petrology: McGraw-Hill, New York.
- Tyler, S. A., Marsden, R. W., Grant, F. F., and Thiel, G. A. (1940): Studies of the Lake Superior Precambrian by accessory mineral methods: Bull. Geol. Soc. Amer., 51, pp. 1429-1538.
- Van Breeman, O. (1965): Thermally induced relocation of strontium and rubidium in a granodiorite: M.Sc. thesis, University of Alberta (unpublished).
- Walton, M. (1955): The emplacement of granite: Amer. J. Sci., 253, pp. 1-18.
- Wanless, R. K., Stevens, R. D., Lachance, G. R., and Edmonds, C. M. (1957): Age determinations and Geological Studies, K-Ar Isotopic Ages, Rep. 7. Can. Dept. Mines Tech. Surv. Geol. Surv. Can. Paper 66-17.
- Wasserburg, G. J. (1963): Diffusion processes in lead-uranium systems. J. Geophys. Res., 68, pp. 4823-4846.
- Wasserburg, G. J., Hayden, R. J., and Jensen, K. J. (1956):  $A^{40}/K^{40}$  dating of igneous rocks and sediments, Geochim. Cosmoch. Acta, 10, pp. 153-165.
- Waters, A. C. (1938): Petrology of the contact breccias of the Chelan Batholith: Bull. Geol. Soc. Amer., 49, pp. 763-794.
- Wetherill, G. W. (1956): Discordant uranium-lead ages: Trans. Am. Geophys. Union, 37, pp. 320-326.
- Whitney, P. R., and Hurley, P. M. (1964): The problem of inherited radiogenic strontium in sedimentary age determinations: Geochim. Cosmochim. Acta, 28, pp. 425-436.
- Wilson, G. A. (1949): A petrographic study of some late basic dykes of the Yellowknife greenstone belt: B.Sc. thesis, Queen's University, Kingston, (unpublished).
- Wilson, H. D. B., Andrews, P., Moxham, R. L., and Ramlal, K. (1965): Archaean volcanism in the Canadian Shield: Can. J. Earth Sci., 2, pp. 161-175.
- Wilson, J. T. (1949a): Some major structures of the Canadian Shield: Trans. Can. Inst. Mining Met., 52, pp. 231-242.





Wilson, J. T. (1949b): The origin of continents and Precambrian history: Trans. Roy. Soc. Can. 43, Sect. IV, pp. 157-184.

Wilson, M. E. (1939): The Canadian Shield: In Geologie der Erde, Geology of North America I, Berlin.

\_\_\_\_\_ (1941): Precambrian: Geol. Soc. Amer. (50th Anniversary volume), pp. 271-305.

Winkler, H. G. F. (1965): Petrogenesis of Metamorphic Rocks: Springer-Verlag, New York.

Wollenburg, H. A., and Smith, A. R. (1964): Radioactivity and radiogenic heat in the Sierra Nevada plutons: J. Geophys. Res., 69, pp. 3471-3478.

York, D. (1966): Least-squares fitting of a straight line: Can. Jour. Phys., 44, pp. 1079-1086.

Zwart, H. J. (1962): On the determination of polymetamorphic mineral associations and its application to the Bosost area (Central Pyrenees): Geol. Rundsch., 52, pp. 38-65.

\_\_\_\_\_ (1967): The Duality of Orogenic Belts: Geol. en Mijnb., 46, pp. 283-309.





APPENDIX 1

Petrography of dated samples: (locations are tabulated in Appendix 2).

DCG 3. A medium-grained granodiorite with xenomorphic-granular texture. Quartz (31.3%) shows moderate undulatory extinction and contains few inclusions, microcline (5.4%) is unaltered, plagioclase (46.6%, An<sub>28</sub>-An<sub>23</sub>) showing slight oscillatory zoning is incipiently altered to a fine white clay mineral (montmorillonite), the alteration being concentrated along cleavage planes. Myrmekite is relatively common near microcline - plagioclase boundaries. Biotite (6.7%  $\gamma = 1.646 \pm .001$ ,  $\alpha$  = straw yellow,  $\beta = \gamma$  = dark green-brown) is slightly chloritized and hornblende (6.5%,  $\alpha$  = yellow brown,  $\beta$  = dark olive-green,  $\gamma$  = deep blue-green; abs.  $\gamma \geq \beta > \alpha$ ) is unaltered. Epidote, magnetite, garnet, sphene and apatite are minor accessory minerals.

The biotite concentrate (60-120 U.S. standard mesh) contains 5% chlorite, 3% hornblende and approx. 1% quartz. The hornblende concentrate (60-120 mesh) contains less than 2% biotite,  $< 1\%$  quartz and traces of epidote.

DCG 5. A coarse-grained porphyritic adamellite with hypidiomorphic-granular texture. Quartz (21.5%) is unaltered, has marked undulatory extinction and traces of minute, dusty inclusions. K-feldspar (34.6%) is in the form of a stringlet microperthite showing blotchy extinction but is only slightly altered to sericite. Plagioclase (34.4%, An<sub>27</sub>) is extensively altered to a pale brown clay mineral and occurs as subhedral crystals often poikilitically enclosed in K-feldspar. In the latter case the plagioclase phenocrysts are rimmed by albite. Fresh biotite (8.6%,  $\alpha$  = straw-yellow,  $\beta = \gamma$  = dark green) and hornblende ( $\alpha$  = yellow





brown,  $\beta$  = dark olive green,  $\gamma$  = dark green-brown) occur together in heterogeneous clusters and it is in these clusters that the accessory minerals apatite, opaque oxides, epidote and zircon are found. Pleochroic haloes mark the loci of zircon inclusions in biotite flakes.

Although the thin section shows a preponderance of biotite, the crushed rock (60-120 mesh) gave a clean separation of hornblende with 3% epidote and traces of quartz and biotite as impurities. Zircons are relatively large (up to 1-2 mms.) well crystallised pale purple hyacinths with lll terminations and zoned in terms of a small amount of included dust particles. A coarse and a fine separation of zircon was made on the least magnetic fraction.

DCG 8. A pink leucogranite (aplite) dyke which intrudes the Western granodiorite. The texture is saccharoidal with approx. equigranular phenocrysts of quartz and alkali feldspar reaching a maximum of 1 mm. diameter. Two types of alkali feldspar are present, a soda orthoclase ( $X^a = -11^\circ$ ) with fleck sericite alteration and a fresh microcline micropertthite. Together they form 41.5% of the thin-section. Other minerals include quartz (36.3%), plagioclase (15.3% -  $An_{20}$ ), chlorite (after biotite?), muscovite (4.7%), opaque oxides (1.1%), apatite (0.1%) and a trace of zircon.

DCG 11. A coarse-grained, biotite-bearing granodiorite with hypidiomorphic texture. Quartz (26.6%) occupies an intergranular position and shows undulatory extinction. K-feldspar (11.0%) is fresh, occurs in intergranular spaces and has exceptionally fine tartan twin lamellae. Plagioclase phenocrysts (53%,  $An_{30}-An_{25}$ ) may be as much as 6 mm. in length, they are slightly zoned in an oscillatory manner and





have thin albite rims. Zoning is accentuated by differential sericitization. Biotite (6.8%) flakes are slightly chloritized, some biotite occurs in clumps where it is associated with clinozoisite (0.8%) and sphene (0.1%). Granular sphene appears to be a concomitant deuteric product of the slight chloritization of biotite. Accessory minerals include muscovite (0.8%), opaque oxides (0.9%) and traces of apatite and zircon.

DCG 33. A fine to medium-grained quartz diorite with allotriomorphic-granular texture. Quartz (33.4%) is slightly strained and contains very few inclusions. K-feldspar (5.7%) occurs interstitially as microcline. The plagioclase (52.4%, An<sub>26</sub>-An<sub>22</sub>) phenocrysts are slightly zoned, the inner (calcic) portion being extensively altered to sericitic muscovite, while the outer rim is unaltered. Myrmekitic intergrowths are common. Biotite (5.9%,  $\gamma = 1.648$ ,  $\alpha$  = pale yellow,  $\beta = \gamma$  = medium brown) is slightly altered to chlorite and is dotted with inclusions of apatite and zircon. Primary muscovite forms approx. 1% while accessory minerals are apatite, opaque oxides and sphene.

The biotite concentrate (60-120 mesh) contains less than 5% chlorite and less than 1% quartz as impurities.

DCG 37. A fine-grained meta-andesite, slightly schistose, consisting of a finely recrystallised aggregate of sodic plagioclase, chlorite, antigorite, epidote, quartz, opaque oxides and sphene.

DCG 44. A medium-grained granodiorite with hypidiomorphic-granular texture. Quartz (38.6%) is moderately strained and contains rare dusty trains of inclusions. Microcline (11.2%) is only slightly altered to a pale brown clay mineral while plagioclase (37.6%, An<sub>27</sub>) is more strongly altered, often in concentric zones and patches. Myrmekite forms





5% of the thin section. Biotite (5.0%,  $\gamma = 1.646$ ,  $\alpha$  = light yellow,  $\beta = \gamma$  = light red-brown) occurs as fresh flakes or may be completely altered to chlorite. Accessories include primary muscovite, apatite, magnetite and zircon.

A biotite concentrate of 98%+ purity was obtained from the crushed rock (60-120 mesh), minor impurities are chlorite and quartz.

DCG 48. A medium-grained quartz diorite with hypidiomorphic-granular texture. Quartz (5.2%) is moderately strained, fresh microcline (5.2%) occurs as interstitial string perthite, euhedral plagioclase (57.6%,  $An_{27}-An_6$ ) shows strong concentric zoning, alternate more calcic zones are marked by late hydrothermal alteration products, fleck mica (?paragonite), zoisite and a pale brown clay mineral. Biotite (8.5%,  $\gamma = 1.645$ ,  $\alpha$  = pale yellow-green,  $\beta = \gamma$  = dark green) occurs as ragged flakes, partly converted to chlorite and muscovite, magnetite, haematite, pyrite, apatite, epidote, sphene and zircons are accessory minerals.

The biotite concentrate (60-120 mesh) contains 2% epidote, 2% chlorite and less than 1% quartz.

DCG 50. A medium-grained adamellite with poikilitic-granular texture. Quartz (36.6%) forms small anhedral, often set in poikilitic plates of K-feldspar (34.0%). K-feldspar varies from relatively fresh microcline to simply twinned orthoclase, generally sericitized. Plagioclase (27.0%,  $An_{27}$ ) is commonly sericitized but also occurs as small subhedra. Biotite (1.0%) is altered to chlorite along cleavages and sericite, muscovite, allanite, opaque oxides and apatite are minor accessory minerals.

DCG 55. An amphibolite xenolith within the Western





granodiorite with panidiomorphic - granular texture. Hornblende (approx. 65%,  $\alpha$  = pale yellow-brown,  $\beta$  = khaki green,  $\gamma$  = blue-green, abs.  $\beta > \gamma > \alpha$ ,  $\gamma^{\wedge} Z = 22^{\circ}$ ,  $2V_x = 80^{\circ}$ ) occurs as subhedral to euhedral grains between 0.5 and 3 mms. in length, granular quartz (approx. 10%), fresh plagioclase (approx. 15%,  $An_{30}$ ) and microcline (approx. 5%) are minor components. Accessories include opaque oxides and biotite. Several thin veins of granular epidote traverse the thin section, in one case the epidote vein is associated with a light brown carbonate.

The hornblende concentrate (80-120 mesh) contains 15% epidote, less than 1% biotite and a trace of quartz.

DCG 59. A porphyritic quartz diorite with subhedral hornblende phenocrysts up to 2 cms. in length in a hypidiomorphic-granular groundmass. Quartz (approx. 15%) is moderately strained, microcline forms less than 2% of the thin section and plagioclase (approx. 45%) is extensively altered to a light brown clay mineral. Hornblende (approx. 25%) is consistently altered to biotite along cleavage planes, and to epidote in patches. This secondary biotite is identical in optical properties ( $\gamma = 1.637$ ,  $\alpha$  = pale straw,  $\beta = \gamma$  = medium brown) to the primary biotite (approx. 10%) which forms ragged flakes in the groundmass dotted with magnetite, haematite and rare zircon inclusions. Accessory minerals are opaque oxides, apatite and epidote.

The biotite concentrate (40-115 mesh) contains 5% hornblende and 2% chlorite.

DCG 74. A porphyritic metadacite with large phenocrysts of andesine set in a finely recrystallised matrix of quartz, untwinned plagioclase (?albite), chlorite, epidote, calcite, biotite and opaque oxides.





Clumps of biotite and calcite have vague, pseudomorphous outlines.

Sphene and deep green prochlorite are other secondary minerals.

DCG 75 (DCG 206). A porphyritic metadacite with twinned phenocrysts of primary plagioclase (andesine) up to 15 mm. in length set in a finely granular recrystallised matrix of untwinned plagioclase (?albite), chlorite, epidote and quartz. Plagioclase phenocrysts are slightly zoned and may have sponge-like inclusions of epidote and opaque oxides. The groundmass includes as much as 5% of fresh biotite flakes; these are clearly of secondary origin, but there is no trace of a parental mafic mineral. Minor accessory minerals are calcite, apatite, opaque oxides and zircon.

Zircons (DCG 206) from this rock are well crystallised, have elongation ratios of 2-4, are pale brown to pink in colour, between 0.5 mm. and 2 mm. in length and slightly zoned. They contain occasional inclusions of ?magnetite and are irregularly fractured.

DCG 115. A pale grey sericitized medium-grained metadacite. Phenocrysts of quartz and plagioclase (andesine) are less than 5 mm. in diameter and the outlines of a former mafic mineral (?hornblende) are recognised by the distinctive shape of epidote - prochlorite - magnetite pseudomorphs. Primary phenocrysts are of blocky shape and extensively altered to sericite. The groundmass is completely recrystallised and consists of albite, quartz, calcite and sericite with minor apatite and opaque oxide accessory minerals.

DCG 118. A fine to medium-grained contaminated diorite with allotriomorphic-granular texture from the margin of the South-east grano-diorite. Quartz (approx. 5%) is a minor interstitial component, K-feldspar





is absent. Plagioclase (approx. 50%,  $An_{34}$ ) is generally fresh but contains inclusions of epidote. Clinozoisite (approx. 5%) forms elongated prisms up to 3 mms. in length and grades into granular, slightly pleochroic pale green epidote (approx. 20%) which is thought to be of xenocrystal origin (see Chapter 11 - contaminated rocks). Hornblende (approx. 10%,  $\alpha$  = yellow-brown,  $\beta = \gamma$  = olive green to olive brown) is altered to biotite (approx. 10%,  $\gamma = 1.642$ ,  $\alpha$  = pale yellow,  $\beta = \gamma$  = deep red-brown) and chlorite. Apatite, sphene, zircon and magnetite are accessory minerals.

The crushed rock gave concentrates of biotite with 5% epidote, 1% quartz and less than 2% chlorite as impurities and a pure hornblende with only a trace of epidote.

DCG 120. A medium-grained diorite (see analysis, South-east granodiorite) with hypidiomorphic-granular texture. Quartz (12.0%) is only slightly strained, microcline (0.6%) is a minor constituent. Plagioclase (56.8%,  $An_{26}$ ) is slightly zoned, has ubiquitous patchy extinction and is slightly altered to a pale brown clay mineral, particularly along cleavage planes. Hornblende (15.2%,  $\alpha$  = yellow-brown,  $\beta$  = olive green,  $\gamma$  = dark blue-green) is partly converted to biotite (11.6%,  $\gamma = 1.637$ ,  $\alpha$  = pale yellow,  $\beta = \gamma$  = medium red-brown) which in turn is slightly altered to chlorite. Pleochroic haloes around zircon inclusions are marked in some fresh biotite flakes. Epidote (2.2%) and opaque oxides (1.1%) also contribute to mafic clusters. Zircon and apatite are the main accessory minerals.

The biotite concentrate (40-80 mesh) from this rock contains 3% of hornblende and less than 2% chlorite as impurities and the hornblende concentrate (80-200 mesh) contains 10% epidote, less than 1% biotite and a trace of quartz as impurities. The zircons from this rock are pale pink





hyacinths, well crystallised and free from inclusions.

DCG 122. A porphyritic hornblende diorite with hypidiomorpho-granular texture. Quartz (approx. 15%) forms irregular, intergranular anhedral, plagioclase (approx. 45%) is heavily sericitized, it is often poikilitically enclosed by fresh hornblende (approx. 30%,  $\alpha$  = light yellow,  $\beta$  = dark green,  $\gamma$  = dark khaki green). Biotite (slightly chloritized) and epidote form the remainder of the thin section. Apatite needles with extreme elongations are particularly common. Opaque oxides are closely associated with the mafic constituents.

DCG 124. A coarse grained diorite with hypidiomorpho-granular texture. Quartz (approx. 8%) occurs as moderately strained intergranular anhedral, free from inclusions. Plagioclase (approx. 60%,  $An_{32}-An_{20}$ ) forms large subhedral phenocrysts, often formed of several individuals and showing oscillatory and patch zoning. Plagioclase is slightly sericitized. Biotite (approx. 15%,  $\gamma = 1.639$ ,  $\alpha$  = pale yellow,  $\beta = \gamma$  = medium brown) is very slightly altered to chlorite and associated with hornblende (approx. 15%,  $\alpha$  = yellow,  $\beta$  = deep green,  $\gamma$  = greyish blue-green (?bleached) in mafic clusters accompanied by opaque oxides (approx. 2%). Apatite and a trace of zircon are accessory minerals.

The biotite concentrate (35-115 mesh) from the rock contains less than 5% hornblende and less than 3% chlorite as impurities and the hornblende separate (60-120 mesh) contains less than 1% quartz and no biotite.

DCG 127. Pale green muscovite in books up to 1" in diameter and  $\frac{1}{4}$ " thick gave a clean concentrate of greater than 98% purity, the only contaminants being quartz grains with a light iron oxide dust coating.





The pegmatite which carries the muscovite is probably related to the South-east granodiorite.

DCG 129. A medium-green granodiorite with hypidiomorphic-granular texture. Quartz (29.8%) is moderately strained and is moderately free from inclusions. Microcline (14.4%) is fresh and occupies an interstitial position between subhedral plagioclase laths. Plagioclase (36.0%,  $An_{30}-An_{24}$ ) is concentrically zoned but in contrast to previously described rocks, the slight pervasive alteration is not confined to bands of a particular composition. Biotite (16.8%,  $\gamma = 1.635$ ,  $\alpha$  = pale yellow,  $\beta = \gamma$  = deep red-brown) is slightly altered to chlorite (0.6%) with anomalous blue interference colours. Epidote, muscovite, apatite, pyrrhotite, magnetite, haematite and sphene are accessory minerals.

The biotite concentrate from the crushed rocks (45-120 mesh) contains less than 1% chlorite as an impurity.

DCG 137. A porphyritic dacite or rhyodacite with multiply twinned plagioclase ( $An_{35}$ ) and embayed quartz phenocrysts up to 10 mms. in diameter set in a finely recrystallised felsic groundmass which contains occasional patches of calcite. Zircon is a relatively common accessory mineral but insufficient of this sample was collected to allow separation of zircon.

DCG 139. A porphyritic dacite with relatively fresh plagioclase ( $An_{40}$ ) and embayed quartz phenocrysts up to 4 mms. in diameter in a completely recrystallised felsic groundmass. Glomeroporphyritic clusters of plagioclase ( $An_{50}$ ) laths are also common. The groundmass contains quartz, albite and minor epidote and nests and veins of quartz, calcite and ankerite are scattered through the thin section. Opaque oxides and apatite are





accessory minerals.

DCG 157. A medium grained, slightly porphyritic adamellite with a slight foliation. The texture is xenomorphic-granular with simply twinned orthoclase cryptoperthite (approx. 20%) and quartz (approx. 30%) in a poorly defined groundmass of altered plagioclase (25%), quartz (approx. 10%), microcline (approx. 5%) and biotite flakes (approx. 5%). Accessory minerals include apatite, opaque oxides and muscovite. The plagioclase (approx. An<sub>20</sub>) is heavily altered to sericite and both feldspars are riddled with muscovite flakes. Myrmekite is common.

DCG 158. A porphyritic adamellite, somewhat fresher than the previous specimen. Quartz (approx. 30%) occurs as granular aggregates in the groundmass and as rare anhedral phenocrysts. Microcline microperthite (approx. 15%) forms ragged phenocrysts of string perthite and plagioclase (approx. 30%, An<sub>18</sub>-An<sub>5</sub>) is clearly zoned. Commonly the albite rim is in turn rimmed by fresh microcline (10%) with distinct tartan twinning. Microcline (5%) also accompanies quartz in the fine-grained granular groundmass. Biotite (approx. 7%), commonly chloritized, and opaque oxides (approx. 3%) are clustered together in irregular patches. The larger feldspar phenocrysts are extensively sericitized and myrmekite is particularly common.

DCG 161. A porphyritic adamellite with a slightly gneissic foliation. In thin section the rock shows a considerable amount of granulation in the groundmass quartz (approx. 30%) leading to what is described as mortar texture. Large anhedral microcline phenocrysts (approx. 40%) up to 10 mms. in length are dotted with quartz inclusions and are generally fresh. Biotite (approx. 5%) and muscovite (2%) flakes are concentrated in





bands parallel to the foliation. Plagioclase (20%+) occurs as small anhedral- the composition is  $An_{28}-An_{23}$  and no albite was observed. Most plagioclase is fresh but may be altered to sericite along cleavage planes. Accessory minerals include opaque oxides and apatite. No zircons were extracted from a large crushed sample.

DCG 204. A medium to coarse grained adamellite with hypidio-morphic-granular texture. Quartz (37.4%) shows slight undulatory extinction, microcline (25.9%) is in the form of patch perthite, plagioclase (21.7%,  $An_{13}$ ) is slightly altered to a fine white clay mineral and has inclusions of albite ( $An_3$ ), quartz, microcline and biotite. Biotite flakes (1.7%,  $\alpha$  = pale yellow,  $\beta = \gamma$  = brown) are invariably altered along cleavages to a brown-green chlorite and opaque oxides while muscovite (12.5%) is fresh and free from inclusions. Apatite, opaque oxides and garnet are accessory minerals.

The muscovite concentrate from the crushed rock (45-120 mesh) contains approx. 1% quartz and a trace of biotite, the biotite concentrate is pure but shows incipient chloritization.

DCG 233. A slightly porphyritic medium-grained adamellite with xenomorphic - granular texture. Quartz (approx. 25%) is slightly strained, microcline (approx. 35%) forms fresh subhedra 5 mms. in diameter which often enclose idiomorphic plagioclase phenocrysts in a poikilitic manner. Plagioclase (approx. 25%) is zoned, the outer sodic zoned ( $Ab_5$ ) are fresh while the inner portions ( $An_{25}$ ) are superficially altered to a pale brown clay mineral. Biotite (approx. 10%) is moderately chloritized. Fresh muscovite, opaque oxides and apatite are minor accessories.

The crushed rock (60-120 mesh) gave a concentrate of muscovite





with 3% quartz and less than 1% chlorite as impurities and biotite with 10% chlorite and 1% quartz as impurities.

DCG 244. A discordant pegmatite from Peg. 84 claim which contains perthite, muscovite, biotite and beryl. The biotite concentrate (35-120 mesh) contains less than 2% quartz as an impurity and the muscovite concentrate (35-80 mesh) contains only a trace of K-feldspar. Both concentrates were obtained by hand-picking of individual mica books.

DCG 245. A medium-grained granodiorite with hypidiomorphic-granular texture. Quartz (approx. 35%) is free from inclusions and moderately strained. K-feldspar (approx. 5%) is in the form of untwinned orthoclase and minor microcline, relatively fresh. Plagioclase (approx. 40%, An<sub>24</sub>) is extensively altered to light brown clay minerals and poikilitically encloses many sharp flakes of white mica of average size 0.2 mm. x 0.08 mm. Fresh biotite (approx. 15%) occurs in ragged clumps. Sphene, muscovite, apatite and opaque oxides are accessory minerals.

A biotite concentrate from the crushed rock contained a trace of sphene and approx. 7% of plagioclase with a light iron dusting and many muscovite inclusions as impurities.

DCG 246. A discordant pegmatite from Peg. 97 claim which contains perthite, muscovite, biotite, cleavelandite and tapiolite. The biotite concentrate (35-120 mesh) shows slight incipient chloritization and less than 5% quartz as an impurity and the muscovite concentrate (35-60 mesh) shows no impurities. Minerals for separation were hand picked.

DCG 253. A biotite schist from a shear zone in wall rock





adjacent to a concordant pegmatite. Some tremolite needles are also present, apparently as a replacement of the original biotite, the lineations formed by tremolite lie in the plane of the dragfolded cleavage flakes of the original biotite. A biotite separate (35-60 mesh) has less than 3% of chlorite as a contaminant.

DCG 254. Similar to DCG 253, the biotite concentrate (35-60 mesh) contains 2% tremolite, and less than 1% quartz and chlorite as impurities.

DCG 256. A concordant pegmatite (Peg. 50 claim) from which clean muscovite was hand-picked. The muscovite concentrate (35-120 mesh) contains less than 1% quartz as an impurity.

DCG 257. The muscovite from this sample (Peg. 91 claim) was hand-picked and the sieved concentrate (35-80 mesh) contained less than 1% quartz as an impurity.

DCG 258. A medium-grained adamellite with hypidiomorphic-granular texture. Quartz (approx. 20%) occurs as large anhedral up to 5 mms. in diameter with strained extinction, microcline microperthite (approx. 30%) forms subhedral plates poikilitically enclosing small euhedral or subhedral plagioclase laths. Plagioclase (approx. 35%) is zoned ( $An_{22}-An_3$ ) with the calcic cores outlined with slight sericitic alteration. Fresh muscovite is developed along 001 and 010 cleavage planes in some instances. Biotite (8%) occurs as slightly chloritized flakes containing occasional zircons with accompanying pleochroic haloes. Muscovite (5%) and opaque oxides (2%) are accessory minerals.

A clean biotite concentrate with a trace of chlorite was





separated from the 60-120 mesh fraction of the crushed rock.

DCG 259. A coarse-grained porphyritic granite with hypidiomorphic-granular texture. Quartz (approx. 25%) occurs as large, subhedral, slightly strained grains with very few inclusions. Microcline microperthite (approx. 40%) forms large, fresh poikilitic phenocrysts up to 10 mms. in diameter with numerous inclusions of quartz. Plagioclase (approx. 10%) is subordinate and occurs as small, zoned ( $An_{32}-An_{22}$ ), intergranular laths, commonly slightly sericitized. Biotite (15%,  $\alpha$  = straw yellow,  $\beta = \gamma$  = dark grey-brown) contains many pleochroic haloes from included zircon crystals. Muscovite (5%) is closely associated with biotite, some epidote and opaque oxides (2%).

A biotite concentrate (40-120 mesh) contains less than 5% iron stained quartz and less than 1% epidote as impurities. Hyacinth zircons range from clear to dusty forms up to 0.5 mms. in length with elongation ratios of between 2 and 4.

DCG 307. A coarse-grained diorite with hypidiomorphic-granular texture. Quartz (approx. 20%) shows strained extinction and is virtually free from inclusions, plagioclase (approx. 45%,  $An_{27}-An_{18}$ ) shows normal and oscillatory zoning and has slight sericitic alteration. Hornblende (approx. 15%,  $\alpha$  = straw yellow,  $\beta$  = pale blue-green,  $\gamma$  = deep blue-green) and biotite (approx. 15%,  $\alpha$  = pale yellow,  $\beta = \gamma$  = red-brown) are closely associated. Some biotite is altered to pale green penninite (approx. 3%) with anomalous blue interference colours. Apatite, opaque oxides and zircon are accessory minerals.

A biotite concentrate (45-120 mesh) contains 10% hornblende, 5% chlorite and 2% quartz.





APPENDIX 2SAMPLE INDEX

| <u>Sample No.</u> | <u>Latitude</u> | <u>Longitude</u> |
|-------------------|-----------------|------------------|
| DCG 1             | 62°46'48" N     | 115°57'05" E     |
| 2                 | 62°49'00" N     | 115°56'30" E     |
| 3                 | 62°37'32" N     | 115°13'00" E     |
| 4                 | 62°37'32" N     | 115°13'00" E     |
| 5                 | 62°37'32" N     | 115°13'00" E     |
| 6                 | 62°28'25" N     | 114°26'20" E     |
| 7                 | 62°28'25" N     | 114°26'20" E     |
| 8                 | 62°28'25" N     | 114°26'25" E     |
| 9                 | 62°28'25" N     | 114°26'25" E     |
| 10                | 62°28'25" N     | 114°26'25" E     |
| 11                | 62°28'32" N     | 114°28'00" E     |
| 12                | 62°27'48" N     | 114°30'40" E     |
| 13                | 62°27'40" N     | 114°31'35" E     |
| 14                | 62°27'40" N     | 114°31'35" E     |
| 15                | 62°27'30" N     | 114°32'00" E     |
| 16                | 62°27'25" N     | 114°32'20" E     |
| 17                | 62°27'20" N     | 114°33'15" E     |
| 18                | 62°27'30" N     | 114°36'20" E     |
| 19                | 62°28'10" N     | 114°39'00" E     |
| 20                | 62°28'35" N     | 114°43'45" E     |
| 21                | 62°26'24" N     | 114°24'00" E     |
| 22                | 62°34'14" N     | 114°21'38" E     |
| 23                | 62°34'56" N     | 114°21'02" E     |





| <u>Sample No.</u> | <u>Latitude</u> | <u>Longitude</u> |
|-------------------|-----------------|------------------|
| DCG 24            | 62°35'13" N     | 114°21'20" E     |
| 25                | 62°35'12" N     | 114°21'22" E     |
| 26                | 62°35'42" N     | 114°21'28" E     |
| 27                | 62°35'44" N     | 114°21'31" E     |
| 28                | 62°35'45" N     | 114°21'33" E     |
| 29                | 62°35'38" N     | 114°21'45" E     |
| 30                | 62°35'36" N     | 114°21'57" E     |
| 31                | 62°35'38" N     | 114°22'01" E     |
| 32                | 62°35'33" N     | 114°22'05" E     |
| 33                | 62°35'33" N     | 114°22'11" E     |
| 34                | 62°35'31" N     | 114°22'33" E     |
| 35                | 62°35'25" N     | 114°22'37" E     |
| 36                | 62°30'31" N     | 114°21'35" E     |
| 37                | 62°30'24" N     | 114°21'38" E     |
| 38                | 62°28'16" N     | 114°24'52" E     |
| 39                | 62°28'19" N     | 114°24'53" E     |
| 40                | 62°28'24" N     | 114°25'07" E     |
| 41                | 62°28'34" N     | 114°25'22" E     |
| 42                | 62°28'36" N     | 114°25'24" E     |
| 43                | 62°28'43" N     | 114°25'14" E     |
| 44                | 62°28'41" N     | 114°25'04" E     |
| 45                | 62°28'39" N     | 114°24'58" E     |
| 46                | 62°28'17" N     | 114°24'57" E     |
| 47                | 62°25'16" N     | 114°25'02" E     |
| 48                | 62°25'20" N     | 114°25'45" E     |
| 49                | 62°25'24" N     | 114°25'46" E     |



| <u>Sample No.</u> | <u>Latitude</u> | <u>Longitude</u> |
|-------------------|-----------------|------------------|
| DCG 50            | 62°28'13" N     | 114°23'14" E     |
| 51                | 62°28'48" N     | 114°25'42" E     |
| 52                | 62°28'50" N     | 114°26'01" E     |
| 53                | 62°28'43" N     | 114°26'11" E     |
| 54                | 62°28'43" N     | 114°26'11" E     |
| 55                | 62°28'43" N     | 114°26'11" E     |
| 56                | 62°28'43" N     | 114°26'11" E     |
| 57                | 62°28'43" N     | 114°26'11" E     |
| 58                | 62°28'51" N     | 114°27'26" E     |
| 59                | 62°29'18" N     | 114°28'40" E     |
| 60                | 62°29'25" N     | 114°28'36" E     |
| 61                | 62°29'20" N     | 114°28'58" E     |
| 62                | 62°35'36" N     | 114°21'57" E     |
| 63                | 62°35'36" N     | 114°21'57" E     |
| 64                | 62°35'18" N     | 114°22'42" E     |
| 65                | 62°35'18" N     | 114°22'42" E     |
| 66                | 62°35'18" N     | 114°22'42" E     |
| 67                | 62°35'18" N     | 114°22'42" E     |
| 68                | 62°35'18" N     | 114°22'42" E     |
| 69                | 62°35'18" N     | 114°22'42" E     |
| 70                | 62°28'08" N     | 114°24'42" E     |
| 71                | 62°27'36" N     | 114°24'48" E     |
| 72                | 62°27'05" N     | 114°24'21" E     |
| 73                | 62°26'18" N     | 114°22'30" E     |
| 74                | 62°27'34" N     | 114°22'25" E     |
| 75                | 62°27'30" N     | 114°22'35" E     |





| <u>Sample No.</u> | <u>Latitude</u> | <u>Longitude</u> |
|-------------------|-----------------|------------------|
| DCG 76            | 62°26'18" N     | 114°22'35" E     |
| 100               | 62°29'50" N     | 114°20'19" E     |
| 101               | 62°29'50" N     | 114°20'19" E     |
| 102               | 62°29'50" N     | 114°20'19" E     |
| 103               | 62°29'50" N     | 114°20'19" E     |
| 104               | 62°29'50" N     | 114°20'19" E     |
| 105               | 62°29'50" N     | 114°20'19" E     |
| 106               | 62°29'50" N     | 114°20'19" E     |
| 107               | 62°29'50" N     | 114°20'19" E     |
| 108               | 62°29'50" N     | 114°20'19" E     |
| 109               | 62°29'50" N     | 114°20'19" E     |
| 110               | 62°29'50" N     | 114°20'19" E     |
| 111               | 62°29'50" N     | 114°20'19" E     |
| 112               | 62°29'50" N     | 114°20'19" E     |
| 113               | 62°29'50" N     | 114°20'19" E     |
| 114               | 62°33'48" N     | 114°19'12" E     |
| 115               | 62°33'59" N     | 114°19'10" E     |
| 116               | 62°21'48" N     | 114°22'16" E     |
| 117               | 62°18'59" N     | 114°14'38" E     |
| 118               | 62°18'59" N     | 114°14'38" E     |
| 119               | 62°18'59" N     | 114°14'38" E     |
| 120               | 62°18'59" N     | 114°14'39" E     |
| 121               | 62°18'59" N     | 114°14'39" E     |
| 122               | 62°18'59" N     | 114°14'39" E     |
| 123               | 62°18'57" N     | 114°14'48" E     |
| 124               | 62°18'56" N     | 114°14'49" E     |





| <u>Sample No.</u> | <u>Latitude</u>       | <u>Longitude</u>       |
|-------------------|-----------------------|------------------------|
| DCG 125           | 62°18'53" N           | 114°14'48" E           |
| 126               | 62°20'43" N           | 114°16'32" E           |
| 127               | 62°21'47" N           | 114°16'34" E           |
| 128               | 62°34'21" N           | 114°11'48" E           |
| 129               | 62°36'52" N           | 114°14'12" E           |
| 130               | 62°36'52" N           | 114°14'12" E           |
| 131               | 62°36'47" N           | 114°14'10" E           |
| 132               | 62°36'44" N           | 114°14'11" E           |
| 133               | 62°36'44" N           | 114°08'39" E           |
| 134               | 62°36'26" N           | 114°08'38" E           |
| 135               | 62°36'26" N           | 114°08'38" E           |
| 136               | 62°36'26" N           | 114°08'38" E           |
| 137               | 62°34'06" N           | 114°19'18" E           |
| 138               | 62°34'07" N           | 114°19'18" E           |
| 139               | 62°34'07" N           | 114°19'18" E           |
| 140               | 62°34'05" N           | 114°19'27" E           |
| 141               | 62°34'05" N           | 114°19'27" E           |
| 142               | 62°34'26" N           | 114°18'48" E           |
| 143               | 62°34'12" N           | 114°18'02" E           |
| 144               | 62°34'09" N           | 114°17'23" E           |
| 145               | 62°47'45" N (approx.) | 113°12' 0" E (approx.) |
| 146               | 62°47'30" N "         | 113°12' 0" E "         |
| 147               | 62°47'30" N "         | 113°12'30" E "         |
| 148               | 62°47'30" N "         | 113°12'30" E "         |
| 149               | 62°47'15" N "         | 113°12'30" E "         |
| 150               | 62°47'15" N "         | 113°12' 0" E "         |



| <u>Sample No.</u> | <u>Latitude</u>       | <u>Longitude</u>       |
|-------------------|-----------------------|------------------------|
| DCG 151           | 62°47'15" N (approx.) | 113°11'45" E (approx.) |
| 152               | 62°47'15" N "         | 113°11'40" E "         |
| 153               | 62°47'15" N "         | 113°11'40" E "         |
| 154               | 62°47'15" N "         | 113°11'15" E "         |
| 155               | 62°47'15" N "         | 113°11'10" E "         |
| 156               | 62°47'15" N "         | 113°11'00" E "         |
| 157               | 62°47'15" N "         | 113°11'00" E "         |
| 158               | 62°47'15" N "         | 113°10'45" E "         |
| 159               | 62°47'15" N "         | 113°10'40" E "         |
| 160               | 62°47'15" N "         | 113°10'40" E "         |
| 161               | 62°47'15" N "         | 113°10'40" E "         |
| 162               | 62°26'18" N "         | 114°22'30" E "         |
| 201               | 62°31'15" N           | 114°19'10" E           |
| 202               | 62°30'20" N           | 114°15'55" E           |
| 203               | 62°32'12" N           | 114° 8'30" E           |
| 204               | 62°33'00" N           | 114° 6'00" E           |
| 205               | 62°29'50" N           | 114°16'10" E           |
| 206               | 62°27'34" N           | 114°22'25" E           |
| 207               | 62°38'48" N           | 114°16'35" E           |
| 208 A & B         | 62°37'48" N           | 114°17'20" E           |
| 209               | 62°34'50" N           | 114°21'12" E           |
| 210               | 62°35'00" N           | 114°20'48" E           |
| 211               | 62°35'00" N           | 114°20'48" E           |
| 212               | 62°27'28" N           | 114°21'40" E           |
| 213               | 62°34'58" N           | 114°20'48" E           |
| 214               | 62°34'43" N           | 114°21'28" E           |





| <u>Sample No.</u> | <u>Latitude</u> | <u>Longitude</u> |
|-------------------|-----------------|------------------|
| DCG 215           | 62°34'50" N     | 114°20'25" E     |
| 216               | 62°34'48" N     | 114°20'25" E     |
| 217               | 62°35'25" N     | 114°22'37" E     |
| 218               | 62°35'25" N     | 114°22'37" E     |
| 219               | 62°35'25" N     | 114°22'37" E     |
| 220               | 62°35'25" N     | 114°22'37" E     |
| 221               | 62°35'31" N     | 114°22'33" E     |
| 222               | 62°35'33" N     | 114°22'01" E     |
| 223               | 62°35'33" N     | 114°22'01" E     |
| 224               | 62°34'48" N     | 114°20'22" E     |
| 225               | 62°31'00" N     | 114°54'00" E     |
| 226               | 62°35'00" N     | 115°11'00" E     |
| 227               | 62°40'10" N     | 115°22'30" E     |
| 228               | 62°42'00" N     | 115°33'30" E     |
| 229               | 62°44'30" N     | 115°44'30" E     |
| 230               | 62°44'25" N     | 115°45'00" E     |
| 231               | 62°44'30" N     | 115°46'00" E     |
| 232               | 62°45'00" N     | 115°47'00" E     |
| 233               | 62°45'00" N     | 115°47'00" E     |
| 234               | 62°50'15" N     | 116°03'30" E     |
| 235               | 62°50'15" N     | 116°03'30" E     |
| 236               | 62°50'12" N     | 116°03'30" E     |
| 237               | 62°32'42" N     | 114°19'33" E     |
| 238               | 62°32'38" N     | 114°19'00" E     |
| 239               | 62°34'12" N     | 114°18'10" E     |
| 240               | 62°34'10" N     | 114°17'58" E     |





| <u>Sample No.</u> | <u>Latitude</u> | <u>Longitude</u> |
|-------------------|-----------------|------------------|
| DCG 241           | 62°34'20" N     | 114°17'56" E     |
| 242               | 62°34'23" N     | 114°17'50" E     |
| 243               | 62°34'23" N     | 114°17'50" E     |
| 244               | 62°44'24" N     | 113°07'00" E     |
| 245               | 62°44'24" N     | 113°07'00" E     |
| 246               | 62°44'15" N     | 113°06'45" E     |
| 247               | 62°43'50" N     | 113°08'15" E     |
| 248               | 62°43'52" N     | 113°08'18" E     |
| 249               | 62°44'24" N     | 113°08'30" E     |
| 250               | 62°44'22" N     | 113°08'35" E     |
| 251               | 62°44'24" N     | 113°08'40" E     |
| 252               | 62°44'22" N     | 113°08'45" E     |
| 253               | 62°44'32" N     | 113°04'10" E     |
| 254               | 62°44'33" N     | 113°04'30" E     |
| 255               | 62°44'33" N     | 113°04'30" E     |
| 256               | 62°44'32" N     | 113°04'15" E     |
| 257               | 62°44'25" N     | 113°06'42" E     |
| 258               | 62°45'30" N     | 113°03'20" E     |
| 259               | 62°45'45" N     | 113°03'20" E     |
| 300               | 62°44'40" N     | 113°03'10" E     |
| 301               | 62°44'42" N     | 113°03'10" E     |
| 302               | 62°44'44" N     | 113°03'10" E     |
| 303               | 62°44'48" N     | 113°03'10" E     |
| 304               | 62°44'50" N     | 113°03'10" E     |
| 305               | 62°45'00" N     | 113°03'10" E     |
| 306               | 62°44'44" N     | 113°03'12" E     |



| <u>Sample No.</u> | <u>Latitude</u> | <u>Longitude</u> |
|-------------------|-----------------|------------------|
| DCG 307           | 62°25'40" N     | 114°13'15" E     |
| 308               | 62°32'40" N     | 114°21'25" E     |
| 309               | 62°25'32" N     | 114°18'38" E     |
| 310               | 62°26'12" N     | 114°18'05" E     |
| 311               | 62°27'27" N     | 114°19'20" E     |
| 312               | 62°24'50" N     | 114°17'30" E     |
| 313               | 62°29'35" N     | 114°18'00" E     |
| 314               | 62°24'50" N     | 114°19'05" E     |





APPENDIX 3Chemical Procedures

The analytical procedures for K, Rb and Sr are well established, but are listed here in descriptive form. The U and Pb methods have been discussed previously.

Potassium

(Double leach method)

1. Weigh out (accurately) 0.25 gm. of mica or 1.0 gm. of hornblende into a cleaned Pt. dish.
2. Moisten with distilled water, add 3 ml. 1:1  $H_2SO_4$  and 10 ml. 40% HF.
3. Evaporate slowly to dryness, increasing temperature to fume off  $SO_3$ .
4. Ignite over Tyrrell burner, then heat strongly for 1 hour on Meker burner.
5. Moisten residue with 10 ml. warm distilled water and transfer to a 50 ml. beaker.
6. Leach for 30 minutes on a steam bath, decant through 7 cm. blue band filter paper and repeat leach twice. The filtrate is collected in a 150 ml. beaker.
7. Transfer residue to filter paper and wash three times with warm distilled water.
8. Transfer residue back to Pt dish, add 2 ml. 1:1  $H_2SO_4$  and repeat steps 3 to 7 (inclusive).

The entire filtrate is retained and used for estimation of potassium with sodium tetraphenylboron solution or by flame photometry (hornblendes).

Potassium tetraphenylboron Precipitation

1. Warm the filtrate from the previous stage to approximately 70°C.





2. Add filtered sodium tetraphenylboron solution in drops until precipitation of  $\text{KB}(\text{C}_6\text{H}_5)_4$  is complete.
3. Allow to stand for at least 2 hours.
4. Check for complete precipitation with a few drops of  $\text{NaB}(\text{C}_6\text{H}_5)_4$  solution.
5. Filter through a weighed, finely fritted glass filter.
6. Dry the precipitate for at least an hour at  $105^\circ\text{C}$ .
7. Cool the fritted glass filter and precipitate in a dessicator and weigh.
8. Calculate %  $\text{K}_2\text{O}$  (+  $\text{Rb}_2\text{O}$ ,  $\text{Ca}_2\text{O}$ ) from the following formula:

$$\% \text{K}_2\text{O} = \frac{\text{wt. KB}(\text{C}_6\text{H}_5)_4 \times 0.1314 \times 100}{\text{sample wt.}}$$

#### Flame photometry

The filtrate from the double leach is made up to 100 ml.

This solution is aspirated directly into a Perkin - Elmer flame photometer.

Comparison with a calibration curve established with standard solutions allows the concentration in p.p.m. to be read directly. The concentration in p.p.m. is converted to %  $\text{K}_2\text{O}$  with the following formula:

$$\% \text{K}_2\text{O} = \frac{\text{p.p.m.} \times 10^{-4}}{\text{sample wt.}}$$

#### Rubidium

1. Clean crucible in hot conc.  $\text{HNO}_3$ , rinse, ignite at  $900^\circ\text{C}$  for  $\frac{1}{2}$  hour, replace in hot conc.  $\text{HNO}_3$  for two hours, rinse in demineralized water, ignite, cool and weigh.
2. Accurately weigh out sufficient sample to give approximately 15 gm. total Rb. This amount is determined by the Rb spike composition and a spiked ratio of  $^{87}\text{Rb}/^{85}\text{Rb}$  of approximately 2.0 is convenient for



mass spectrometric measurement.

3. Treat sample with a few drops of demineralized water, add 5 drops conc.  $\text{H}_2\text{SO}_4$ , 5 ml. HF and 5 ml. demineralized water. At this stage the Rb spike solution is added quantitatively.
4. Slowly evaporate to dryness at  $300^\circ\text{C}$ .
5. Fume off  $\text{SO}_3$  at  $500\text{--}600^\circ\text{C}$ . in fume cupboard.
6. Ignite for  $\frac{1}{2}$  hour at  $900^\circ\text{C}$ .
7. Cool and take up in 2 or 3 ml. demineralized water.
8. Centrifuge, if necessary, to remove cloudiness.
9. Transfer to small silica glass vial, evaporate to dryness and cover with Parafilm until ready to load onto the mass spectrometer filament.

Strontium (spiked determination - unspiked similar but delete addition of spike solution in step 2).

1. On a cleaned Pt. crucible lid accurately weigh out sufficient sample to give a  $^{88}\text{Sr}/^{86}\text{Sr}$  ratio of approximately 2.0 if the sample is rich in  $^{88}\text{Sr}$  or a  $^{87}\text{Sr}/^{86}\text{Sr}$  ratio of approximately 1.0 (if the sample is rich in  $^{87}\text{Sr}$ ).
2. Transfer sample quantitatively to a cleaned Teflon beaker and add the mixed  $^{84}\text{Sr}/^{86}\text{Sr}$  spike solution. The spike solution contains approximately 10 micrograms of total Sr. The spike container is rinsed into the Teflon beaker with dil. HCl and 10 ml. of 1:1 redistilled  $\text{HNO}_3$  and 10 ml. of 40% HF added.
3. Evaporate to dryness at  $100\text{--}120^\circ\text{C}$ . under an enclosure with slightly positive air pressure.
4. Moisten the residue with demineralized  $\text{H}_2\text{O}$  and add 5 ml. of 1:1  $\text{HNO}_3$ .
5. Evaporate to dryness at  $120^\circ\text{C}$ . and bake at  $250^\circ\text{C}$ , also under protective enclosure.





6. Moisten the residue with demineralized  $H_2O$  and add 5 ml. of redistilled 1:1 HCl. Evaporate to dryness and bake under the protective enclosure.
7. Take up the residue in a minimum amount (1-2 ml.) of 2.5 N redistilled HCl and transfer to a centrifuge tube.
8. Centrifuge thoroughly and carefully add the supernatant liquid to the top of a prepared ion exchange column (Dowex 50-X8, 200-400 mesh).
9. Allow to soak in, wash in twice with approximately 1 ml. of 2.5 N HCl.
10. Add the remainder of the 2.5 N HCl up to the point at which Sr elution commences and allow to run through.
11. Place a cleaned 20 ml. beaker under the column and elute out the Sr fraction.
12. Evaporate to dryness under a protective enclosure and cover with Parafilm until ready to load onto the mass spectrometer filament.

#### Lead and Uranium

The techniques used for separation of these elements from the zircon solution are described in the body of the thesis (Chapter III). All glassware was cleaned in hot 10% NaOH, rinsed in distilled water, then further cleaned with hot conc.  $HNO_3$ , washed with triple distilled (3D) water and wrapped in Parafilm until required.

A dithizone stock solution is made up with 10 mg. of diphenylthiocarbazone (M.W. 256.32) per 100 ml. washed  $CHCl_3$ . 1 mm. of stock solution is equivalent to approximately 40 micrograms Pb. The solution is diluted 1:10 with freshly washed chloroform for the final Pb extraction stage.





Chloroform is freshly washed with 3D water to remove HCl (or decomposition products, chiefly chlorine) from the preliminary cleaning. The chloroform should be kept away from sunlight.

Potassium cyanide solution contains 2 gm./100 ml. and is made directly from lead-free analytical grade reagent. The solution is made 3% in  $\text{NH}_3$  for storage and use. Hydrochloric acid is purified by distillation of the constant boiling azeotrope in a fused silica still.

Triple distilled (3D) water is prepared by passing normal laboratory distilled water through a cation exchange water softener, followed by slow distillation in a silica still.

Borax flux is prepared by treating a 10% solution of hydrated sodium tetraborate ( $\text{Na}_2\text{B}_4\text{O}_7 \cdot 10 \text{H}_2\text{O}$ ) with a small amount of dithizone solution to extract lead and other heavy metals. The aqueous phase is then washed with cleaned chloroform, transferred to a clean platinum dish and evaporated to a syrup. This is very slowly dried and then ignited strongly to an anhydrous glass. The glass is cracked out of the platinum dish and broken into convenient sized fragments for use as a flux.

The saturated  $\text{NH}_4\text{NO}_3$  solution is made by dissolving 800 gm. of  $\text{NH}_4\text{NO}_3$  in 500 ml.  $\text{H}_2\text{O}$ (3D). The solution is warmed, filtered and may be further cleaned with 15 ml. of washed hexone. The saturated aluminium nitrate solution contains 75 ml. conc.  $\text{HNO}_3$ , and is purified by extraction with hexone just before use.



APPENDIX 4K-Ar, Rb-Sr and U-Pb calculations

Analytical data are transcribed onto the calculation sheets illustrated in Tables 27 to 29. Although many of the calculations were carried out by hand in the first instance, all data has been recalculated by the computer programmes listed in Appendix 5.

Samples of the calculations are given because they form the basis on which the computer programmes were written. Brief explanatory notes are given on the sample tables where they are required.

The following additional data is necessary in order to complete the calculation sheets:

$$\text{p.p.m. } ^{40}\text{K} = 1.0106 \times \% \text{K}_2\text{O}$$

$$\text{p.p.m. } ^{40}\text{Ar} = 1.7846 \times 10^3 \times \text{cc. } ^{40}\text{Ar/gm. (at S.T.P.)}$$

Argon spike composition:

$$^{36}\text{Ar}/^{38}\text{Ar} = 0.000105, \quad ^{40}\text{Ar}/^{38}\text{Ar} = 0.00354$$

Strontium isotope abundances in weight % for various initial  $^{87}\text{Sr}/^{86}\text{Sr}$  ratios are now calculated by means of an APL programme MA which sets up a matrix varying  $(^{87}\text{Sr}/^{86}\text{Sr})_i$  in steps of 0.001 from 0.695 to 0.725. In the original Fortran IV programme (AGE) the most commonly used values were:

| $(^{87}\text{Sr}/^{86}\text{Sr})_i$ | $^{84}\text{Sr}$<br>wt. % | $^{86}\text{Sr}$<br>wt. % | $^{87}\text{Sr}$<br>wt. % | $^{88}\text{Sr}$<br>wt. % |
|-------------------------------------|---------------------------|---------------------------|---------------------------|---------------------------|
| 0.702                               | 0.00536                   | 0.09678                   | 0.06873                   | 0.82913                   |
| 0.712                               | 0.00536                   | 0.09668                   | 0.06964                   | 0.82832                   |

The relative isotopic abundances of natural uranium nuclides are:

$$\begin{aligned} \frac{^{238}\text{U}}{^{235}\text{U}} &= 139.56 \text{ (weight ratio)} \\ &= 137.8 \text{ (atomic ratio)} \end{aligned}$$





## POTASSIUM-ARGON

Table 27

|                       |            |                                   |
|-----------------------|------------|-----------------------------------|
| Run No. 742           | AK No. 712 | Description: Muscovite + 115 mesh |
|                       |            | DCG 127 Pegmatitic vein in        |
| Sample Wt. 1.7137 gm. |            | South-east granodiorite           |
| Spike No. A-406       |            |                                   |

## I. Preparation

|  |   |  |
|--|---|--|
| <input checked="" type="checkbox"/> Flux (..ll..... $\times$ Sample Wt.) | <input checked="" type="checkbox"/> Getter      | <input checked="" type="checkbox"/> Leak testing |
| <input checked="" type="checkbox"/> Sample (+ filter)                    | <input checked="" type="checkbox"/> Steel Balls | <input checked="" type="checkbox"/> Pumps        |
| <input checked="" type="checkbox"/> Spike                                | <input checked="" type="checkbox"/> C-trap      | <input checked="" type="checkbox"/> Heaters      |

Outgassing 6 pm Thurs. 18 hrs.      Torching: 1 x around sample, 5 mins

## II. Fusion

|  |   |   |
|--|---|---|
| <input checked="" type="checkbox"/> Cool flux    | <input checked="" type="checkbox"/> Drop sample                                       | <input checked="" type="checkbox"/> Introduce Spike Argon |
| <input checked="" type="checkbox"/> Seal F-train | <input checked="" type="checkbox"/> Start fusion <sup>60</sup> (55v)<br>to 90V - 3 pm | <input checked="" type="checkbox"/> Trap H <sub>2</sub> O |

### III. Transfer

|   |  |  |
|---|--|--|
| <input checked="" type="checkbox"/> H <sub>2</sub> O trapped with liq. N <sub>2</sub> | <input checked="" type="checkbox"/> Break seal                                 | <input checked="" type="checkbox"/> Seal off P-train |
| <input checked="" type="checkbox"/> Seal off from pumps                               | <input checked="" type="checkbox"/> Short cleanup to TG <sub>1</sub> =160..... | <input checked="" type="checkbox"/> Heat C-trap      |
| <input checked="" type="checkbox"/> Drop furnaces from Ni-crucible                    | <input checked="" type="checkbox"/> Liq. N <sub>2</sub> on C-trap, 30 min.     |  |

#### IV. Purification

☒ Preliminary cleanup to TG<sub>1</sub>=113

☒ Gettered 5 min. to TG<sub>1</sub>=173 ☒ Sample trapped out 20 minutes

$$TG_{\max} = 177$$

## V. Notes

Melt  $\rightarrow$  complete, no residue





Run 742 AK 712 % K<sub>2</sub>O 9.097  
 Sample Muscovite Sample wt. 1.7137 - .03 Rb<sub>2</sub>O  
 Spike No. A 406 cc. STPAr<sup>38</sup>  $0.9593 \times 10^{-4}$  9.067  
 $^{40}\text{K} = 9.067 \times 1.0106 \text{ ppm}$   
 $= 9.163 \text{ ppm}$

|      | Peak height   | Scale factor | Total argon | Residual argon | Corr. for M.D.  |
|------|---------------|--------------|-------------|----------------|---|
| 40 — | 7.97 x 30,000 | =            | 239100      | - 84.9         | = 239015.1 x 1.000 = 239015   |
| 38 — | 8.165 x 1000  | =            | 8165        | - 0.9          | = 8164.1 x 1.0162 = 8296.4<br>(negligible air argon correction)   |
| 36 — | 0.11 x 30     | =            | 3.3         | - 0.6          | (spike <sup>36</sup> Ar) — — — — —<br>= 2.7 x 1.0324 = 2.79 - .87<br>= 1.92<br>(spike <sup>38</sup> Ar) |

$$^{40}\text{Ar}^* = 239015 - (1.92 \times 295.5 + 8296.4 \times 0.00354)$$

$$= \underline{238418.3}$$

$$\frac{\text{Ar}^{38}}{\text{Ar}^{40}} = \frac{8296.4}{238418.3} = 0.034797$$

$$\text{Ar}^{40} = \frac{.9593 \times 10^{-4}}{1.7137 \times .034797} = 16.0871 \times 10^{-4} \times 1.7846 \times 10^3 = 2.8709 \text{ p.p.m.}$$

$$\text{K}^{40} = \underline{9.163} \text{ p.p.m.}$$

$$\frac{\text{Ar}^{40}}{\text{K}^{40}} = .3133$$

$$t = \frac{4.341}{4.307} \times 10^9 \log \left[ 1 + 0.3133 \times \frac{9.068}{(9.07)} \right] = 2540 \text{ million years.}$$

$$\% \text{ radiogenic } ^{40}\text{Ar} = \frac{238418}{239015} \times 100$$

$$= \underline{99.8\%}$$

$$\lambda_e = 0.585 \times 10^{-10} / \text{yr}$$

$$\lambda_\beta = 4.72 \times 10^{-10} / \text{yr}$$

$$^{40}\text{K}/\text{K} = 0.000119 \text{ (Nier, 1950)}$$



## DEPARTMENT OF GEOLOGY, GEOCHEMISTRY

Table 28.

UNIVERSITY OF ALBERTA

## RUBIDIUM-STRONTIUM

Rb-Sr No. \_\_\_\_\_ Sample No. DCG 37

DESCRIPTION: Whole rock, Yellowknife Group volcanics, W. of B shaft,  
Giant Property, Brock horizon.

X-R-F

## SAMPLE PREPARATION

Rb/Sr = .18

Sample weight - gm

Sr spike No. 62 Set IV, Total Sr. <sup>XRF</sup> 240 ppm

Rb spike No. 40 Set III, Total Rb 40 ppm

HF 10 ml. HNO<sub>3</sub>  $\frac{10 + 5 \text{ ml.}}{5 \text{ ml HCl}}$ 

|  | Total Sample<br>(unspiked) | Sr-spiked | Rb-spiked |     |
|--|----------------------------|-----------|-----------|-----|
| Wt. Pt. lid and sample   | 5.1561                     | 5.186334  | 26.7814   | gm. |
| Wt. Pt. lid alone  | 5.0915                     | 5.091360  | 76.3101   | gm. |
| Wt. sample   | .0646                      | .094974   | 0.4713    | gm. |
| Wt. of sample Sr-spiked = 0.094974      Wt. of sample Rb-spiked 0.4713 |                            |           |           |     |

## RUBIDIUM

$$(^{87}/_{85}) \text{ meas.} = 1.5077 \pm .0011 \quad \text{ug Rb}_{\text{sp}}^{87} = \text{_____} \times \text{_____} = 18.192$$

$$\text{ug Rb}_{\text{N}}^{85} = 2.540 \text{ ug Rb}_{\text{N}}^{87} \quad \text{ug Rb}_{\text{sp}}^{85} = \text{_____} \times \text{_____} = 0.139$$

$$(^{87}/_{85}) \text{ meas.} \times ^{87}/_{85} = \frac{\text{ug Rb}_{\text{sp}}^{87} + \text{ug Rb}_{\text{N}}^{87}}{\text{ug Rb}_{\text{sp}}^{85} + \text{ug Rb}_{\text{N}}^{85}} = 1.5432 = \frac{18.192 + x}{0.139 + 2.54x}$$

$$0.2145 + 3.9197x = 18.192 + x$$

$$\text{ug Rb}_{\text{N}}^{87} = 6.1573$$

$$\text{ppm Rb}^{87} = \frac{\text{ug Rb}^{87}}{\text{wt. sample}} = 13.064$$





## STRONTIUM

## Measured Atomic Ratios:

$$\begin{aligned}
 \text{Spiked} & : \quad {}^{88}\text{Sr}/{}^{86}\text{Sr} = 2.4884 \pm .0008 \quad {}^{87}\text{Sr}/{}^{86}\text{Sr} = 0.24775 \pm .00021 \quad {}^{84}\text{Sr}/{}^{86}\text{Sr} = 0.62389 \pm .00025 \\
 \text{Unspiked} & : \quad 1/{}^{88}\text{Sr}/{}^{86}\text{Sr} = .1184 \pm .0001 \quad {}^{87}\text{Sr}/{}^{86}\text{Sr} = .7273 \pm .0006 \\
 \text{Normalized} & : \quad 1/{}^{88}\text{Sr}/{}^{86}\text{Sr} = 0.1194 \quad {}^{87}\text{Sr}/{}^{86}\text{Sr} = .7242 \pm .0006
 \end{aligned}$$

$${}^{88}\text{Sr}/{}^{86}\text{Sr} \times ({}^{88}\text{Sr}/{}^{86}\text{Sr})_{\text{meas.}} (\text{Sr}_{\text{sp}}^{86} + 0.09678) = 0.8291\text{N} + \text{Sr}_{\text{sp}}^{88}$$

$${}^{88}\text{Sr}/{}^{86}\text{Sr} \times 2.4884 (5.624 + 0.09678\text{N}) = 0.8291\text{N} + 1.417$$

$$2.5463 (5.624 + 0.09678\text{N}) = 0.8291\text{N} + 1.417 \quad \text{N} = 22.1453; \text{ from this value}$$

of N, provisional values (a) of  ${}^{86}\text{Sr}$  and  ${}^{84}\text{Sr}$  are found and a provisional value of  ${}^{84}\text{Sr}/{}^{86}\text{Sr}$  calculated. Comparison of this value with the measured ratio yields the mass discrimination which is then applied to the measured  ${}^{88}\text{Sr}/{}^{86}\text{Sr}$  ratio and the calculation repeated until the iterative cycle closes.

$$\text{N} = 21.7751 \text{ ug} / .094874 \text{ gm. sample}$$

| Isotope   | $\text{Sr}^{\text{N}}, \text{ug}$ | $\text{Sr}_{\text{sp}}, \text{ug}$ | $\text{Sr}^{\text{N}} + \text{Sr}_{\text{sp}}, \text{ug}$ |  |
|---|-----------------------------------|------------------------------------|---|--|
| For $({}^{87}\text{Sr}/{}^{86}\text{Sr}) = 0.702$ |                                   |                                    |   |  |
| 82.91 wt. % 88                                    | 18.054                            | 1.417                              | 19.471  | Normal Sr = $2.107 / .094974$<br>= <u>22.185 ppm</u> |
| 6.873 wt. % 87                                    | 1.4966                            | 0.3856                             | 1.882   |  |
| 9.678 wt. % 86                                    | (a) 2.107 (final value)           | 5.624                              | 7.731   |  |
|   | 2.143                             |                                    | 7.767   |  |
| 0.536 wt. % 84                                    | (a) 0.1167 (final value)          | 3.120                              | 3.2367  |  |
|   | 0.119                             |                                    | 3.239   |  |

$$\begin{aligned}
 ({}^{84}\text{Sr}/{}^{86}\text{Sr})_{\text{calc.}} &= 0.4170 \quad ({}^{84}\text{Sr}/{}^{86}\text{Sr})_{\text{meas.}} = .4239 \times \frac{84}{86} = .4140 \quad \text{M.D.} = .72\% \\
 \text{wt. ratio } 0.4187 \text{ (final value)} &\quad \text{at ratio} \quad - 1.11\% \text{ (final value)}
 \end{aligned}$$





SPIKED:

$$\text{Sr}^{87*} = \frac{87}{86} \times \left( \frac{87}{86} \right)_{\text{meas.}} \times (\text{Sr}_N^{86} + \text{Sr}_{\text{sp}}^{86}) - (\text{Sr}_N^{87} - \text{Sr}_{\text{sp}}^{87})$$

(corrected)

$$\text{Sr}^{87*} = \frac{87}{86} \times .24775 \times .9944 \times 7.731 - 1.8822 = 0.0446 \text{ ug}$$

$$\text{Sr}^{87*} = .4693 \text{ ppm} \quad \text{Calculated } \frac{^{84}\text{Sr}}{^{86}\text{Sr}} = \frac{1.4966 + 0.0446}{2.107}$$

$$= .7314 \text{ (wt. ratio)}$$

$$= .7231 \text{ (at. ratio)}$$

UNSPIKED:

normalized

$$\text{Sr}_N^{87*} = \frac{87}{86} \times \left( \frac{87}{86} \right)_{\text{meas.}} \times \text{Sr}_N^{87} - \text{Sr}_N^{87}$$

$$\text{Sr}_N^{87} = 0.06873 \times \text{ppm Sr}^N \times \text{wt. unspiked sample} = 1.0181 \text{ ug}$$

$$\text{Sr}_N^{86} = 0.09678 \times \text{ppm Sr}^N \times \text{wt. unspiked sample} = 1.4336 \text{ ug}$$

$$\text{Sr}^{87*} = \left( \frac{87}{86} \times .7242 \times 1.4336 \right) - 1.0181 = 0.0322 \text{ ug}$$

$$\text{Normal Sr} = \frac{21.7751}{0.094974}$$

$$\text{Sr}^{87*} = .4982 \text{ ppm} \quad = \underline{229.3 \text{ ppm.}}$$

$$\frac{^{87}\text{Sr}^*}{^{87}\text{Sr}_N} = \frac{0.0322}{1.0181} = \underline{0.032}$$

$$\frac{^{87}\text{Rb}}{^{86}\text{Sr}} = \frac{13.064}{22.185} \times \frac{86}{87} = 0.582 \text{ (at. ratio)} \quad \text{Total Rb} = 13.064$$

$$\quad \quad \quad + 33.183$$

$$\quad \quad \quad \underline{46.247 \text{ ppm}}$$



Table 29

Department of Geology  
University of AlbertaU/Pb Calculation Sheet

Sample ... ZIRCON ..... (U/Pb No) ..... DCG 116 ..... (Field No)

Wt of sample ... 0.4970 ..... gm + wt of borax ... 3.2756 ..... gm

diluted to ... 100 ..... ml

Contaminant lead:-

common lead 1 : 13.5 : 15 : 33.5 (..... my) - cogenetic mineral

blank lead 1 : 20.2 : 17.05 : 40.05

URANIUM (assumes negligible  $U^{238}$  blank)  
 $\frac{U^{238}}{U^{235}}_{sp}$ meas  $U^{238}/U^{235} = 2.061 \pm 0.003$ 

$$U^{238} = \frac{\frac{238}{235} (\text{meas } \frac{U^{238}}{U^{235}}) (\mu g U^{235}_{sp}) - U^{238}_{sp}}{1 - (\text{meas } \frac{U^{238}}{U^{235}}) / 137.8} = \frac{\frac{238}{235} (2.061) \times (4.287) - (0.003)}{1 - (2.061) / 137.8}$$

= 9.0811 .....  $\mu g$ 

$$\text{ppm } U^{238} = \frac{100}{1.99} \times \frac{\mu g U^{238}}{\text{smp wt (gms)}}$$

 $U^{238} = 918.18$  ..... ppm $\div 139.56$  $U^{235} = 6.579$  ..... ppm

THORIUM (assumes negligible Th blank)

meas  $Th^{232}/Th^{230} = N/A \pm$ 

$$Th^{232} = \frac{232}{230} (\text{meas } \frac{Th^{232}}{Th^{230}}) (\mu g Th^{230}_{sp}) - \mu g Th^{232}_{sp} = \frac{232}{230} ( ) \times ( ) - ( )$$

= .....  $\mu g$ 

$$\text{ppm } Th^{232} = \frac{100}{1.99} \times \frac{\mu g Th^{232}}{\text{smp wt}}$$

 $Th^{232} =$  ..... ppm





LEADMeasured ratios:-

$$\text{Pb IR} \quad \frac{^{206}\text{Pb}}{^{204}\text{Pb}} = 2024 \pm 8 \quad \frac{^{207}\text{Pb}}{^{206}\text{Pb}} = 0.17628 \pm .00014 \quad \frac{^{208}\text{Pb}}{^{206}\text{Pb}} = 0.13379 \pm .00011$$

$$\text{Pb ID} \quad \frac{^{206}\text{Pb}}{^{204}\text{Pb}} = 1637 \pm 5 \quad \frac{^{207}\text{Pb}}{^{206}\text{Pb}} = 0.17745 \pm .00012 \quad \frac{^{208}\text{Pb}}{^{206}\text{Pb}} = 0.7503 \pm .0006$$

$$\text{Compute } ^{204}\text{Pb} = 1.00 \quad \text{Pb IR} \longrightarrow 1 : 2024 : 356.8 : 270.8$$

$$\text{subtract common lead (2600 m.y.)} \longrightarrow \begin{array}{r} 1 : 13.5 : 15 : 33.5 \\ (14.0) : (15.2) : (34.0) \end{array} \text{---(after correction)}$$

$$\begin{array}{r} 2010.5 : 341.8 : 237.3 \\ (2010) : (341.6) : (236.8) \end{array} \text{ (radiogenic + spike lead)}$$

$$\frac{\text{Pb}^{207} \text{ corr}}{\text{Pb}^{206} \text{ IR}} = \frac{(.16995)}{.17001}$$

$$\frac{\text{Pb}^{208} \text{ corr}}{\text{Pb}^{206} \text{ IR}} = \frac{(.11781)}{.11803}$$

$$\text{Pb ID} \longrightarrow 1 : 1637 : 290.5 : 1228.2$$

$$\text{subtract common lead (.....m.y.)} \longrightarrow \begin{array}{r} 1 : 13.5 : 15.0 : 33.5 \\ (14.0) : (15.2) : (34.0) \end{array}$$

$$\begin{array}{r} 1623.5 : 275.5 : 1194.7 \\ 1623 : 275.3 : 1194.2 \end{array} \text{ (radiogenic + spike lead)}$$

$$\frac{\text{Pb}^{206} \text{ corr}}{\text{Pb}^{208} \text{ ID}} = \frac{(1.35902)}{1.35887}$$

$$\text{Spike composition} \quad \text{Pb}^{208} = 22.180 \mu\text{g} \quad \text{Pb}^{207} = .011 \mu\text{g}$$

$$\text{Pb}^{206} = 0.0485 \mu\text{g} \quad \text{Pb}^{204} = \text{---} \mu\text{g}$$

Pb<sup>206</sup>:-

$$\text{Pb}_{\text{rad}}^{206} = \frac{\frac{^{206}\text{Pb}}{^{208}\text{Pb}} \left( \frac{\text{Pb}^{206} \text{ corr}}{\text{Pb}^{208} \text{ ID}} \right) \times \mu\text{g Pb}_{\text{sp}}^{208} - \mu\text{g Pb}_{\text{sp}}^{206}}{1 - \left( \frac{\text{Pb}^{206} \text{ corr}}{\text{Pb}^{208} \text{ ID}} \right) \times \left( \frac{\text{Pb}^{208} \text{ corr}}{\text{Pb}^{206} \text{ IR}} \right)} = \frac{\frac{^{206}\text{Pb}}{^{208}\text{Pb}} (1.35887) \times (22.180) - (.0485) (35.486)}{1 - (1.35887) \times (.11803)} = 35.4984 \mu\text{g}$$

$$\text{Pb}_{\text{rad}}^{206} (\text{IR}) = \mu\text{g Pb}_{\text{rad}}^{206} (\text{ID}) \times \frac{\text{aliquot IR}}{\text{aliquot ID}} = (35.498) \times \frac{50}{25} = 70.9968 \mu\text{g (IR)}$$

$$\text{Pb}_{\text{rad}}^{206} = \frac{\text{ml dil vol}}{\text{ml aliquot}} \times \frac{\mu\text{g Pb}^{206} (\text{IR})}{\text{smpl wt}} = \frac{100}{50} \times \frac{(70.9726)}{.4970} \text{ ppm} = 285.70 \text{ ppm}$$





Page 3

Contaminant lead:

$$\begin{aligned}
 \text{Pb}_{\text{com}}^{204} &= \frac{\mu\text{g Pb}_{\text{rad}}^{206} + \mu\text{g Pb}_{\text{bl}}^{206} - \mu\text{g Pb}_{\text{bl}}^{204} \times \frac{206}{204} \left( \frac{\text{Pb}^{206}}{\text{Pb}^{204}} \right)_{\text{IR}}}{\frac{206}{204} \left( \frac{\text{Pb}^{206}}{\text{Pb}^{204}} \right)_{\text{IR}} - \frac{206}{204} \left( \frac{\text{Pb}^{206}}{\text{Pb}^{204}} \right)_{\text{com}}} \\
 &= \frac{(70.997) + (.0579) - (.00284) \times \frac{206}{204} (2024)}{\frac{206}{204} (2024) - \frac{206}{204} (13.5)} = \dots 0.03214 \dots \mu\text{g}
 \end{aligned}$$

|                          |  |  |
|--------------------------|--|--|
| Full Blank: (take 1/5)   | $\text{Pb}^{208} = \dots 0.5793 \dots \mu\text{g}$ | $\text{Pb}^{206} = \dots 0.2894 \dots \mu\text{g}$ |
| 1 : 20.2 : 17.05 : 40.05 | $\text{Pb}^{207} = \dots 0.2454 \dots \mu\text{g}$ | $\text{Pb}^{204} = \dots 0.0142 \dots \mu\text{g}$ |

$$\mu\text{g Pb}_{\text{com}}^{204} / \mu\text{g Pb}_{\text{bl}}^{204} = \dots 11.3 \dots$$

$$\dots 11.3 \dots \times \dots 2600 \dots \text{m.y. common Pb} = \dots 11.3 : 152.55 : 169.5 : 378.55$$

$$\text{blank Pb} = 1.00 : 20.2 : 17.05 : 40.05$$

$$\text{Total contaminant Pb} = \frac{12.3 \quad 172.75 \quad 186.55 \quad 418.6}{\dots}$$

$$\text{contaminant lead composition} \quad 1.00 : 14.0 : 15.2 : 34.0$$

If contaminant lead differs substantially from the assumed common already used in computation, repeat computation using corrected values. (return to page 2)

$$\begin{aligned}
 \text{Pb}_{\text{rad}}^{208} &= \text{ppm Pb}_{\text{rad}}^{206} \times \frac{208}{206} \left( \frac{\text{Pb}^{208}}{\text{Pb}^{206}} \right)_{\text{IR}}^{\text{corr}} \\
 &= \dots 285.60 \dots \times \frac{208}{206} \times \dots 11781 \dots = \dots 33.973 \dots \text{ppm}
 \end{aligned}$$

$$\begin{aligned}
 \text{Pb}_{\text{rad}}^{207} &= \text{ppm Pb}_{\text{rad}}^{206} \times \frac{207}{206} \left( \frac{\text{Pb}^{207}}{\text{Pb}^{206}} \right)_{\text{IR}}^{\text{corr}} \\
 &= \dots 285.60 \dots \times \frac{207}{206} \times \dots 16995 \dots = \dots 48.773 \dots \text{ppm}
 \end{aligned}$$



Page 4

Check of ID vs IR :

ID:

$$\begin{aligned}
 \text{Pb}_{\text{rad}}^{207} &= \frac{\text{ug Pb}_{\text{rad}}^{206} + \text{ug Pb}_{\text{sp}}^{206}}{\frac{206}{207} \left( \frac{\text{Pb}^{206}_{\text{corr}}}{\text{Pb}^{207}_{\text{ID}}} \right)} - \text{ug Pb}_{\text{sp}}^{207} \\
 &= \frac{35.4863 + .0485}{\frac{206}{207} \times 5.895} - .011 = \dots 6.046 \dots \text{ug} \\
 &= 48.66 \text{ ppm}
 \end{aligned}$$

$$\begin{aligned}
 \text{Pb}_{\text{rad}}^{208} &= \frac{\text{ug Pb}_{\text{rad}}^{206} + \text{ug Pb}_{\text{sp}}^{206}}{\frac{206}{208} \left( \frac{\text{Pb}^{206}_{\text{corr}}}{\text{Pb}^{208}_{\text{ID}}} \right)} - \text{ug Pb}_{\text{sp}}^{208} \\
 &= \frac{35.4863 + .0485}{\frac{206}{208} \times 1.3590} - 22.18 = \dots 4.222 \dots \text{ug} \\
 &= 33.977 \text{ ppm}
 \end{aligned}$$

$$\text{Atomic Ratio } \frac{\text{Pb}}{\text{U}} = \frac{\text{ppm Pb}}{\text{ppm U}} \times \frac{\text{mass of U isotope}}{\text{mass of Pb isotope}}$$

| Nuclide           | ppm       |  | (0.3593)*  | Date m.y. |
|-------------------|-----------|--|------------|-----------|
| U <sup>238</sup>  | 918.18    | $\frac{238}{206} \times \frac{285.60}{918.18}$ | = 0.3594   | 1995      |
| U <sup>235</sup>  | 6.579     | $\frac{235}{207} \times \frac{48.773}{6.579}$  | = 8.416    | 2310      |
| Th <sup>232</sup> | (33.910)* | $\frac{232}{208} \times \dots$                 | = .....    | .....     |
| Pb <sup>208</sup> | 33.973    |  |            |           |
| Pb <sup>207</sup> | 48.773    |  | (0.17001)* |           |
| Pb <sup>206</sup> | 285.60    | $\frac{207}{206} \text{corr} = \dots$          | 0.16995    | 2595      |

\*Computer calculated values.

$$\lambda_1^{238}\text{U} = 1.56 \times 10^{-10}/\text{yr}$$

$$\lambda_2^{235}\text{U} = 9.72 \times 10^{-10}/\text{yr}$$





The composition of common lead used in the preliminary calculations carried out by hand was an approximate average of the results recorded by Robertson (1966) for common leads extracted from veins in the Yellowknife metavolcanics; viz.,  $^{206}\text{Pb}/^{204}\text{Pb} = 13.5$ ,  $^{207}\text{Pb}/^{204}\text{Pb} = 15.0$  and  $^{208}\text{Pb}/^{204}\text{Pb} = 33.5$ .

When the calculations were repeated with the computer, the speed of this process made it possible to use an iterative procedure (APL programme UPBCOMP) to substitute the composition of conformable common lead of the same age (on the Russell - Farquhar model, Russell and Farquhar, 1960, Kanasewich, 1962) as the  $^{207}\text{Pb}/^{206}\text{Pb}$  age of the analysed zircon. An example of both sets of results is given in Table 29. Because of the favourable  $^{206}\text{Pb}/^{204}\text{Pb}$  ratio of almost all the zircon samples, the results are indistinguishable within experimental error.

The APL programme PBCOM is used to give a listing of the ratios  $^{206}\text{Pb}/^{204}\text{Pb}$ ,  $^{207}\text{Pb}/^{204}\text{Pb}$  and  $^{208}\text{Pb}/^{204}\text{Pb}$  for concordant common leads on the Russell-Farquhar model according to the following initial data.

|  |  |
|--|--|
| $t_0 = 4.56 \times 10^{-9} \text{ yrs.}$ |  |
| $V_0 = 0.0654$                           | $X = a_0 - 137.8 V (e^{\lambda t_0} - e^{\lambda t_1})$          |
| $137.8 V_0 = 9.012$                      | $Y = b_0 - V (e^{\lambda' t_0} - e^{\lambda' t_1})$              |
| $W_0 = 38.21$                            | $Z = c_0 - W (e^{\lambda'' t_0} - e^{\lambda'' t_1})$            |
| $a_0 = 9.50$                             | $\lambda^{238}\text{U} = 1.537 \times 10^{-10} / \text{year}$    |
| $b_0 = 10.36$                            | $\lambda'^{235}\text{U} = 9.722 \times 10^{-10} / \text{year}$   |
| $c_0 = 29.49$                            | $\lambda''^{232}\text{Th} = 0.499 \times 10^{-10} / \text{year}$ |

APL programmes MA, UPBCOMP and PBCOM were written by Dr. H. Baadsgaard and complete details of these brief programmes are available in the Department of Geology, University of Alberta.





APPENDIX 5Computer Programmes

Four Fortran IV computer programmes were written or modified from existing programmes for this thesis. All programmes were initially written for the I.B.M. 7040 computer but were subsequently converted to run on the I.B.M. 360/67 installation. The only programme which is entirely original is AGE which was written to carry out the iterative computation illustrated in Table 28.

AGE - (U. of A. No. 450015)

Input consists of seven I.B.M. cards on which are punched:

(1) the sample number, (2) the measured spiked  $^{88}\text{Sr}/^{86}\text{Sr}$ ,  $^{87}\text{Sr}/^{86}\text{Sr}$  and  $^{84}\text{Sr}/^{86}\text{Sr}$  ratios, (3) the measured unspiked  $^{86}\text{Sr}/^{88}\text{Sr}$  and  $^{87}\text{Sr}/^{86}\text{Sr}$  ratios, (4) the strontium spike composition, (5) the sample weights for Sr and Rb spiked analyses, (6) the measured  $^{87}\text{Rb}/^{85}\text{Rb}$  ratios and (7) the Rb spike composition. In addition, the appropriate weight percentages of  $^{84}\text{Sr}$ ,  $^{86}\text{Sr}$ ,  $^{87}\text{Sr}$  and  $^{88}\text{Sr}$  for the initial  $^{87}\text{Sr}/^{86}\text{Sr}$  ratio assumed in the computation are prepunched for inclusion in the programme.

The operation is rapid and there is no limit to the number of data sets which may be processed in one computer run. Output consists of a listing of the input data in order to detect possible punching errors, the computed  $^{87}\text{Sr}/^{86}\text{Sr}$  ratio, amounts of radiogenic  $^{87}\text{Sr}$  (spiked and unspiked), p.p.m. Rb, p.p.m. common Sr, Sr mass discrimination,  $^{87}\text{Rb}/^{86}\text{Sr}$  ratio (atomic ratio), normalized unspiked  $^{87}\text{Sr}/^{86}\text{Sr}$  and the computed ages (with both commonly used decay constants).

This programme is now replaced in routine use by APL programme RBSRCOMP which carries out the same computations.





ISOCH (option LINYX) - (U. of A. No. 450012)

This programme is basically the programme written by McIntyre et al. (1966). It was introduced to the writer by Dr. W. Compston of the Australian National University. In its original form (MS-0250) it was written for the C.D.C. 3600 computer at Canberra. When introduced to this University, it was modified to run on the I.B.M. 7040 computer by Dr. Compston and subsequently modified to some extent by the writer for the I.B.M. 360/67 installation. Further changes were made at the suggestion of Dr. P. Arriens (A.N.U.).

The programme uses independent estimates of the variance in  $^{87}\text{Sr}/^{86}\text{Sr}$  and  $^{87}\text{Rb}/^{86}\text{Sr}$  ratios to compute a Rb-Sr isochron age and  $^{87}\text{Sr}/^{86}\text{Sr}$  initial ratio. Turek (1966, pp. C-6 to C-8) describes the programme in detail and the following description is taken, in part, from his thesis, supplemented by notes from Dr. Compston.

The independently determined estimates of variance for the horizontal and vertical ordinates respectively,  $\text{CONX}$ ,  $\text{VAR}(Y)_{\text{sp}}$  and  $\text{VAR}(Y)_{\text{unsp}}$  are punched on the first header card. (The latter two estimates are abbreviated to "Y" and "X" in Green et al., 1968). These estimates are discussed in Chapter III (Results) and their derivation is shown in Appendix 6. The second header card is a title card. The data cards are arranged in increasing values of  $^{87}\text{Rb}/^{86}\text{Sr}$ . Each data card contains the  $^{87}\text{Rb}/^{86}\text{Sr}$  ratio, the  $^{87}\text{Sr}/^{86}\text{Sr}$  ratio and an indication as to whether the data is from an unspiked or spiked Sr run and whether duplicate analyses are recorded.

An estimate of the approximate slope of the isochron (B) is made from the extreme points.

$$Y_i = A + B X_i \quad (A = (^{87}\text{Sr}/^{86}\text{Sr})_i)$$





The line of best fit is then obtained by minimizing the expression:  $F U = \sum W_i (Y_i - A - B X_i)^2$ , where  $Y_i$ ,  $X_i$  are the means of  $^{87}\text{Sr}/^{86}\text{Sr}$  and  $^{87}\text{Rb}/^{86}\text{Sr}$  ratios over  $ND_i$  replicate assays from a rock specimen.  $W$  is a weighting factor:

$$W_i = 1/(\text{Var}(Y)_i - B^2 \text{VAR}(X)_i),$$

where  $\text{VAR}(Y)_i$  is the known replicate variance (assumed to be uniform) of  $^{87}\text{Sr}/^{86}\text{Sr}$  measurements (either spiked or unspiked) divided by the number of replicate assays.  $\text{VAR}(X) = C.X_i^2$ , where  $C$  is determined by least squares weighting. For a normal distribution this weighting is proportional to the variance squared, i.e., to  $(^{87}\text{Rb}/^{86}\text{Sr})^4$ . This takes account of the non-uniform variance of  $^{87}\text{Rb}/^{86}\text{Sr}$  measurements.

The expression to be minimized ( $F U = \sum W_i (Y_i - A - B X_i)^2$ ) is solved by forming a cubic equation (see McIntyre et al., 1966) and determining  $A$  and  $B$  by iteration. The term  $FU$  has an expectation of  $N-2$  if all the errors are within experimental variance (where  $N$  is the number of rock sample points in the isochron plot). The computer programme forms the best straight line and calculates  $FU/(N-2) = \text{MSWD} = \text{mean square of weighted deviates}$ .

If the variance is within experimental error, the  $\text{MSWD}$  is  $\leq 1$  and the calculation stops (Model 1). If the  $\text{MSWD}$  is significantly greater than unity, the computation proceeds on to three other stages which attempt to describe the type of geological variation. In Model 2, variance in  $^{87}\text{Sr}/^{86}\text{Sr}$  is distributed proportionally to the  $^{87}\text{Rb}/^{86}\text{Sr}$  ratio, in Model 3, variance in  $^{87}\text{Sr}/^{86}\text{Sr}$  is distributed independently of the  $^{87}\text{Rb}/^{86}\text{Sr}$  ratio. Model 2 indicates that open system behaviour or redistribution of radiogenic  $^{87}\text{Sr}$  is suspected and Model 3 is applicable to samples with differing initial ratios. The computer programme chooses one of these alternatives





on the basis of the smaller MSWD for the favoured model. Model 4, in practice, suggests that more samples are required in order to obtain an unequivocal result. The output follows the format of McIntyre et al. (1966).

York (1966) deals with the problem in a very similar manner, first solving a "least-squares cubic" equation by substituting an approximate value of the slope. It should be noted that  $\omega$  in York's programme is equivalent to  $1/\text{VAR}$  in the programme of McIntyre et al.

APL programme RBSRISOCHRON is essentially based on York's programme. Experimental data for  $^{87}\text{Rb}/^{86}\text{Sr}$  (either spiked or unspiked) form an input matrix and the estimates of experimental variance are fed directly into the programme for later inversion to give  $W$ . The output gives the slope and initial ratio with estimates of the uncertainties, the value of MSWD, the centre of gravity of the data and the age with 68% confidence limits.

#### KARG - (U. of A. No. 450025)

This programme was written by Mr. R. K. O'Nions. It is based on the relative error equation given by Kirsten (1966, p. 32) and calculates the date and the analytical and total uncertainties for K-Ar data.

The total relative error which results from relative errors in decay constants and  $^{40}\text{Ar}^*/^{40}\text{K}$  ratios is given by partial differentiation of the K-Ar decay equation:

$$\frac{\Delta t}{t} = \frac{\Delta \lambda}{\lambda} + \frac{1 - e^{-\lambda t}}{\lambda t} \cdot \frac{\Delta(^{40}\text{Ar}^*/^{40}\text{K})}{^{40}\text{Ar}^*/^{40}\text{K}} + \frac{1 - e^{-\lambda t}}{\lambda t} \cdot \frac{\lambda_\beta(\Delta \lambda_e - \frac{\Delta \lambda_\beta}{\lambda_\beta})}{\lambda(\lambda e^{-\lambda t} - \lambda_\beta)}$$

The analytical error is given by the second term alone;

$$\frac{\Delta(^{40}\text{Ar}^*/^{40}\text{K})}{^{40}\text{Ar}^*/^{40}\text{K}}$$





and is calculated from the following estimates of the experimental precision:

|             |                      |       |    |  |
|-------------|----------------------|-------|----|--|
| all samples | $^{40}\text{Ar}$     | $\pm$ | 1% | (Baadsgaard, 1965)   |
| micas       | $\text{K}_2\text{O}$ | $\pm$ | 1% | (16, based on duplicate determinations by the writer, Mr. R. K. O'Nions, Mrs. A. Leech and Mr. A. Stelmach)  |
| hornblendes | $\text{K}_2\text{O}$ | $\pm$ | 3% | (16, O'Nions obtained a standard deviation of 2.8% for a series of 9 duplicate determinations by the potassium tetraphenylboron precipitation technique. Experience in this laboratory and others suggests that the flame photometric method gives a similar precision). |

Input for this programme is by means of a single card for each sample. This card contains the sample number, p.p.m.  $^{40}\text{Ar}$  and wt. %  $\text{K}_2\text{O}$ . The output gives the sample number, p.p.m.  $^{40}\text{K}$ ,  $^{40}\text{Ar}/^{40}\text{K}$  ratio, the age in millions of years, the analytical error and the total uncertainty.

The programme is used to provide a check on the dates read from a prepared table of  $^{40}\text{Ar}/^{40}\text{K}$  ratios in addition to the analytical uncertainty (16). Prepared tables of  $^{40}\text{Ar}/^{40}\text{K}$  ratios versus dates form a separate sub-programme and are used also to convert data from other sources (which may be based on slightly different decay constants) to the decay constants currently adopted.

#### CIPWNORM - (U. of A. No. 450021)

This programme was initiated by Mr. W. Morgan of Townsville University College, Queensland, Australia. In its original form, it was written in Fortran II for punch card input and output. The output format was completely rewritten to take advantage of the speed of the I.B.M. 360 on-line printer.

The programme computes a slightly shortened version of the C.I.P.W. norm. Normative minerals chromite, fluorite,  $\text{NaCl}$ ,  $\text{Na}_2\text{SO}_4$ , pyrite and zircon are not calculated.





Details and listings of all the programmes referred to in this appendix are deposited in the Department of Geology, University of Alberta, from which they may be obtained on application.





APPENDIX 6Error analysisK-Ar

Experimental errors introduced in potassium and argon analyses form the basis for the calculation of analytical error and total uncertainty in Appendix 5 (Fortran IV programme KARG). With increasing age, the influence of analytical error on the experimentally determined date decreases because of the exponential term in the second term of the relative error equation quoted in Appendix 5. For this reason, the relative errors in Archaean rocks are well within the uncertainties introduced by the precision of the decay constants.

Analytical errors ( $\pm 1\%$ ) on micas range from  $\pm 26$  to  $\pm 28$  m.y. and the total uncertainties between 80 and 90 m.y. while analytical errors on hornblendes are higher,  $\pm 41$  to  $\pm 57$  m.y. and the total uncertainty is as much as 226 m.y. On this basis, the 50 m.y. interval adopted in the histograms (Figs. 15 and 16) is a reasonable choice.

Rb-Sr

Errors in the Rb-Sr isochrons are treated at considerable length both in the text and in Appendix 5. To restate the problem briefly, it is desired to use regression analysis to draw a line of best fit through the experimental data, giving appropriate weight to the various data coordinate values and to determine whether the scatter in points is within analytical error or may be accounted for with a geological explanation. Computer programmes ISOCH and RBSRISOCHRON fulfill this function and determine error limits at the  $2\%$  and  $1\%$  limits respectively. It should be noted that the somewhat larger errors developed in the treatment of the isochron for the Yellowknife volcanics compared with the errors



quoted for the less precise isochron drawn for the Cameron River volcanics are a result of this difference in the level of confidence expressed in the error limits.

The data used to compute the values of variance for the Fortran IV programme ISOCH used in Green et al. (1968) are given below:

Note: Variance =  $(\sigma)^2$ , where  $\sigma$  = standard deviation

Variance between duplicates (1 degree of freedom) =  $(\text{Dupl.}_1 - \text{Dupl.}_2)^2 / 2$

### $^{87}\text{Sr}/^{86}\text{Sr}$ variance

VAR(Y) - unspiked

0.36 x  $10^{-6}$   
 0.16 x  $10^{-6}$   
 2.56 x  $10^{-6}$   
 2.56 x  $10^{-6}$   
 6.76 x  $10^{-6}$   
 2.56 x  $10^{-6}$   
2.49 x  $10^{-6}$

Measured values of  $^{87}\text{Sr}/^{86}\text{Sr}$ : 1.087, 1.086, 1.086, 1.088,  
 1.089, 1.089, 1.088, (1.079)

Mean = 1.0864

VAR(Y) for 6 samples of the Prosperous Lake granite (one sample rejected).

2.25 x  $10^{-6}$   
 0.36 x  $10^{-6}$   
 0.06 x  $10^{-6}$   
0.87 x  $10^{-6}$

Measured values of  $^{87}\text{Sr}/^{86}\text{Sr}$ : 0.8722, 0.8737; 0.7801,  
 0.7807; 0.77090, 0.77084

VAR(Y) for 3 duplicate samples, DCG 8, DCG 75 and N 14

These values are pooled to give a value of VAR(Y)<sub>unsp</sub> =  $1.95 \times 10^{-6}$

VAR(Y) - spiked

34.81 x  $10^{-6}$   
 .01 x  $10^{-6}$   
 .81 x  $10^{-6}$   
 9.61 x  $10^{-6}$   
 16.81 x  $10^{-6}$   
 4.41 x  $10^{-6}$   
 8.41 x  $10^{-6}$   
10.70 x  $10^{-6}$

Calculated values of  $^{87}\text{Sr}/^{86}\text{Sr}$ : 1.086, 1.080, 1.081, 1.077  
 1.076, 1.078, 1.083

Mean = 1.0801

VAR(Y) for 7 samples of the Prosperous Lake granite

The value of VAR(Y)<sub>sp</sub> =  $10.70 \times 10^{-6}$  is adopted.





$^{87}\text{Rb}/^{86}\text{Sr}$  variance

$$\text{CONX} = \text{VAR}(X) / (^{87}\text{Rb}/^{86}\text{Sr})^2$$

| VAR(X)               | CONX                                     |  |
|----------------------|--|--|
| $4.0 \times 10^{-6}$ | $195.6 \times 10^{-6}$                   | $^{87}\text{Rb}/^{86}\text{Sr}$ values: 0.144, 0.142 -DCG 137<br>(before Rb spike redetermination) |
| $1.0 \times 10^{-2}$ | $74.6 \times 10^{-6}$                    |  |
| $3.6 \times 10^{-5}$ | $.29 \times 10^{-6}$                     | 11.521, 11.621 -N 17   |
| $4.0 \times 10^{-6}$ | $.03 \times 10^{-6}$                     | 11.129, 11.133, 11.144 -N 41   |
| $8.1 \times 10^{-5}$ | $.65 \times 10^{-6}$                     | 40.349, 40.375, 40.439 -N 6  |
| $1.5 \times 10^{-3}$ | $.93 \times 10^{-6}$                     |  |
| $1.7 \times 10^{-4}$ | $.10 \times 10^{-6}$                     |  |
| $2.6 \times 10^{-3}$ | $1.59 \times 10^{-6}$                    |  |
|                      | <u><math>34.22 \times 10^{-6}</math></u> | CONX for 4 samples, 2 in duplicate, 2 in triplicate.   |

| VAR(X)               | CONX                                     |  |
|----------------------|--|--|
| $5.8 \times 10^{-3}$ | $47.51 \times 10^{-6}$                   | Measured values of $^{87}\text{Rb}/^{86}\text{Sr}$ : 10.9977, 10.9882,<br>10.9829, 11.1496, 11.077 |
| $7.3 \times 10^{-3}$ | $60.07 \times 10^{-6}$                   |  |
| $5.7 \times 10^{-3}$ | $46.56 \times 10^{-6}$                   | Mean = 11.0391   |
| $8.8 \times 10^{-6}$ | $.07 \times 10^{-6}$                     |  |
| $8.3 \times 10^{-3}$ | $67.72 \times 10^{-6}$                   |  |
|                      | <u><math>44.39 \times 10^{-6}</math></u> | CONX for 1 sample of the Prosperous Lake granite,<br>analysed 5 times.                             |

These values are pooled to give a value of CONX =  $38.13 \times 10^{-6}$

Further work is presently in progress to substantiate the claim made in Chapter III (Results) that the variance values are better than the values quoted by Green et al. (1968).

As uncertainties in the slope of the line (b) are related to the number of samples by a relation of the form:

$$\sigma_b^2 = \frac{1}{n-2} \frac{\sum_i W_i (bU_i - V_i)^2}{\sum_i W_i U_i^2}, \quad (\text{York, 1966}),$$

an increase in the number of samples (n) reduces the uncertainty in the slope. For this reason, a minimum of 6 samples should be analysed in order to apply rigorous statistical analysis.





U-Pb

Because of the generally excellent analytical precision of the mass spectrometer runs and the relatively high  $^{206}\text{Pb}/^{204}\text{Pb}$  ratios, the Pb/Pb and U/Pb dates from the zircon samples have low error limits. The APL programme UPBCOMP made it possible to recompute the analytical data using  $V + 1\sigma$  or  $V - 1\sigma$  (where V represents the measured value) in appropriate positions in the calculation. The resulting Pb/Pb and U/Pb dates differed by less than 10 m.y. from those recorded initially. In spite of this unsophisticated treatment, the data is seen to be of very satisfactory quality.

An internal check is provided by comparison of the amount of radiogenic  $^{207}\text{Pb}$  indicated by spiked and unspiked runs. The percentage difference,

$$\% \text{ diff.} = 100 \left\{ 1 - \left( \frac{\text{ug } ^{207}\text{Pb}^* \text{ unsp.}}{\text{ug } ^{207}\text{Pb}^* \text{ sp.}} \right) \right\},$$

is particularly sensitive. The value of this expression is greater than 1.5% only on the two occasions when lower quality chart data was obtained for one of the mass spectrometer measurements. The percentage difference between the two values for radiogenic  $^{207}\text{Pb}$  content is unrelated to the  $^{206}\text{Pb}/^{204}\text{Pb}$  measurements, suggesting that the measurement errors are random and attributable to experimental error alone.

The chords of the zircon concordia plot (Fig. 17) were fitted to the experimental points with a standard regression line. Since variation on the x axis ( $^{206}\text{Pb}/^{238}\text{U}$ ) is much greater than that on the y axis ( $^{207}\text{Pb}/^{235}\text{U}$ ), regression of x upon y was performed. The slopes of the chords are given by the following equations:

$$\begin{aligned} x &= 23.930 y - 0.0760 & (1) - \text{South-east granodiorite} \\ x &= 25.508 y - 1.0018 & (2) - \text{Western granodiorite} \end{aligned}$$





$$\text{i.e. } ^{207}\text{Pb}/^{235}\text{U} = 23.930 (^{206}\text{Pb}/^{238}\text{U}) - 0.0760 \quad (1)$$

$$\text{and } ^{207}\text{Pb}/^{235}\text{U} = 25.508 (^{206}\text{Pb}/^{238}\text{U}) - 1.0018 \quad (2)$$

Since the standard deviations of the slopes are:

$$\sigma_1 = .073 \text{ and } \sigma_2 = .065, \text{ respectively, } (\sigma = \sqrt{(\frac{(\text{true } x - \text{calc. } x)^2}{n-2})}$$

it is possible to test whether the slopes are distinct:

$$\begin{aligned} \sigma_D &= \sqrt{\frac{\sigma_1^2}{n_1} - \frac{\sigma_2^2}{n_2}} \\ &= .044 \end{aligned}$$

It is clear that the slopes are distinct at the 95% confidence level.

Although the  $^{207}\text{Pb}/^{206}\text{Pb}$  ages of these two bodies are distinct (Table 26), the upper concordia intersections are not distinct at the 95% confidence level ( $\approx 2\sigma$ ). This is a result of the upward convergence of the concordia chords. Intercept ages and error limits were established by simultaneous solution of the decay equations controlling the concordia plot and the equation representing the concordia chord. This is most simply carried out by trial and error. The initial intersection age is first established, the slope is increased by  $2\sigma$  and the process repeated. The resulting error limits overlap although there is a better than even chance that the ages are distinct.









**B29887**